# Optimized Clean Hydrogen Production using Nuclear Small Modular Reactor and Concentrated Solar Power as a Renewable Energy Source

by

Mustafa Ciftcioglu

A thesis submitted to the
School of Graduate and Postdoctoral Studies in partial
fulfillment of the requirements for the degree of

**Master of Applied Science in Nuclear Engineering**

Faculty of Engineering and Applied Science

University of Ontario Institute Technology

Oshawa, Ontario, Canada
December 2022

**THESIS EXAMINATION INFORMATION**

Submitted by: **Mustafa Ciftcioglu**

**Master of Applied Science in The Faculty of Energy Systems and Nuclear Science**

Thesis title: Optimized Clean Hydrogen Production using Nuclear Small Modular Reactor and Concentrated Solar Power as a Renewable Energy Source

An oral defense of this thesis took place on December 2, 2022 in front of the following examining committee:

**Examining Committee:**

| | |
|---|---|
| Chair of Examining Committee | Jennifer McKellar |
| Research Supervisors | Akira Tokuhiro |
| Research Co-supervisor | Filippo Genco |
| Examining Committee Member | Dan Hoornweg |
| Thesis Examiner | Salam Ali |

The above committee determined that the thesis is acceptable in form and content and that a satisfactory knowledge of the field covered by the thesis was demonstrated by the candidate during an oral examination. A signed copy of the Certificate of Approval is available from the School of Graduate and Postdoctoral Studies.

**ABSTRACT**

According to current predictions, hydrogen will serve as a key fuel and energy source by decreasing greenhouse gas (GHG) emissions. In this research an integral Pressurized Water Reactor-type Small Modular Reactor (iPWR-type SMR), connected to a molten-salt based Concentrated Solar Power (CSP) plant, producing electricity and hydrogen is investigated specifically, by modeling and simulations of a Nuclear-Renewable Hybrid Energy System (N-RHES). Optimization of design and functional variables/parameters, as complexity in system engineering, are considered as scenarios. The major results of this research is that multi-objective optimization provides recommended, operational scenarios to obtain preferred results in spite of variability of sunshine in terms of objectives, which are maximizing total profit and total heat equivalent. This research carried out based on modeling and simulations on MATLAB and Genetic Algorithms (GAs) for optimization is key for real life applications. Moreover, in terms of SMR safety-in-design, important time slots are given and explained in this thesis.

**Keywords**: Hydrogen Production; Small Modular Reactors; Renewable Energy; Thermo-chemical Cycles; Multi-objective Optimization; Complexity.

## AUTHOR'S DECLARATION

I hereby declare that this thesis consists of original work of which I have authored. This is a true copy of the thesis, including any required final revisions, as accepted by my examiners.

I authorize the University of Ontario Institute of Technology (Ontario Tech University) to lend this thesis to other institutions or individuals for the purpose of scholarly research. I further authorize University of Ontario Institute of Technology (Ontario Tech University) to reproduce this thesis by photocopying or by other means, in total or in part, at the request of other institutions or individuals for the purpose of scholarly research. I understand that my thesis will be made electronically available to the public.

The research work in this thesis that was performed in compliance with the regulations of Research Ethics Board/Animal Care Committee under **REB Certificate number/Animal care certificate file number**. (Does not apply. No animals were used in the course of this research.)

Mustafa Ciftcioglu YOUR NAME

## STATEMENT OF CONTRIBUTIONS

The research focuses on optimized clean hydrogen and electricity production with an approach of Nuclear-Renewable Hybrid Energy (N-RHES) system. A review paper on this issue was prepared and published in a scientific international journal, Major Trends in Energy Policy and Nuclear Power, ATW [1].

Results, obtained from N-RHES, designed and modeled using MATLAB and LabVIEW, and including simulated values were published and presented at the 4$^{th}$ International Conference on Generation IV and Small Reactors (G4SR-4) in Toronto, Canada (October 3-6, 2022) [2].

This research contributes to the development of a coupled SMR - hydrogen production system, and indicates the importance of optimizing complex systems such as N-RHES by giving optimized results.

**ACKNOWLEDGEMENTS**

I would like to say a special thank you to my supervisor, Professor Akira Tokuhiro from whom I learned a lot thank to his personality and humanity. His support, guidance and overall insights in this field have made this an inspiring experience for me. I also want to thank him very much for his help with licensing and software used in this research work.

In addition to this, I would like to thank my valuable co-supervisor, Professor Filippo Genco, who showed the best way to solve the problem and his support I felt at every stage of this thesis at Ontario Tech University.

I want to express my gratitude to Dr. Alper Kerem for encouraging me in my academic life.

I would also like to thank my friend Gurur Furkan Sarılmaz, who motivated me while living abroad and helped me with this thesis.

Last but not least, I am grateful to the Republic of Türkiye for contribution to my academic life.

**TABLE OF CONTENTS**

**ABSTRACT** ..... **iii**

**STATEMENT OF CONTRIBUTIONS** ..... **v**

**ACKNOWLEDGEMENTS** ..... **vi**

**TABLE OF CONTENTS** ..... **vii**

**LIST OF TABLES** ..... **xi**

**LIST OF FIGURES** ..... **xii**

**LIST OF ABBREVIATIONS AND SYMBOLS** ..... **xv**

**Chapter 1. Introduction** ..... **1**

1.1 Background ..... 1

1.2 Motivation ..... 6

1.3 Research Objectives ..... 9

1.4 Scope of the Research ..... 11

1.5 Thesis Organization ..... 11

**Chapter 2. Literature Review** ..... **13**

2.1 Nuclear Power Plant (NPP) ..... 13

2.2 Generation-IV Nuclear Reactors ..... 14

2.3 Small Modular Reactors (SMRs) ..... 16

2.4 Renewable Energy ..... 18

2.4.1 Solar Photovoltaic (PV) ..... 21

2.4.2 Concentrated Solar Power (CSP) ..... 21

2.4.3 Wind Energy ..... 22

2.5 Hydrogen ..... 23

2.5.1 Hydrogen's Future in Relation to Gasoline ..... 24
2.6 Nuclear Hydrogen Production ..... 24
2.6.1 SMR Design & Engineering & Production of $H_2$ from a Co-located Plant ..... 27
2.7 Thermochemical Cycles for Hydrogen Production ..... 30
2.7.1 Copper-Chlorine (Cu-Cl) Cycle ..... 31
2.7.2 Sulfur-Iodine (S-I) Cycle ..... 32
2.8 High Temperature Electrolysis (HTE) ..... 33
2.9 Comparison of The Potential Methods ..... 36
2.10 Technology Readiness Level ..... 37
2.11 Optimization ..... 39
2.12 Complexity and Multi-objective Optimization ..... 39
2.13 Multi-objective Optimization Methods ..... 41
2.13.1 Priori Articulation of Preference Methods ..... 41
2.13.2 Posteriori Articulation of Preference Methods ..... 41
2.13.3 No Articulation of Preference Methods ..... 42
2.14 Genetic Algorithm ..... 43
2.14.1 Fundamental Theorem of Genetic Algorithms ..... 43
2.14.2 Basics of Genetic Algorithm ..... 45
2.14.2.1 Coding Solutions ..... 47
2.14.2.2 Creating the First Population ..... 47
2.14.2.3 Calculation of Conformity Value ..... 48
2.14.2.4 Application of the Multiplication Process ..... 48
2.14.2.5 Application of the Crossover Operation ..... 49

2.14.2.6 Application of the Mutation Process .....49
2.14.3 General Application Areas.....50
2.14.3.1 Optimization.....50
**Chapter 3. Mathematical Modeling of the N-RHES .....51**
3.1 Assumptions .....51
3.2 LabVIEW .....52
3.3 MATLAB .....53
3.4 System Advisor Model (SAM).....54
3.4.1 Performance Models.....56
3.4.2 Financial Models.....57
3.5 Prototypic iPWR-type SMR / Thermodynamic Side.....60
3.5.1 Validation of Rankine Cycle.....66
3.6 Concentrated Solar Power (CSP).....69
3.6.1 Validation of CSP.....74
3.7 Cu-Cl Thermochemical Hydrogen Generation Cycle.....75
3.8 Thermochemical Heat Pump .....76
3.9 Nuclear-Renewable Hybrid Energy System (N-RHES) .....77
3.9.1 Application of MATLAB for N-RHES.....86
3.9.1.1 Multi-objective Optimization.....95
**Chapter 4. Results.....98**
4.1 Results of NRHES based on Multi-objective Optimization.....103
4.2 Consideration of NPP Electricity Requirement.....111
4.3 Consideration of SMR Safety-in-design .....114

**Chapter 5. Conclusion ..... 119**

5.1 Conclusion ..... 119

5.2 Future Works ..... 124

**References ..... 125**

**Appendices ..... 142**

**Appendix A. Matlab Code** ..... 142

**A1. Main function of N-RHES** ..... 142

**A2. Multi-objective optimization and date range selection code** ..... 149

**A3. Pareto graphs code** ..... 154

**Appendix B. What's Best validation with MATLAB on a HX problem** ..... 156

**B1. Optimization coding** ..... 165

Appendix C. Published Papers and Presentation. ..... 174

## LIST OF TABLES

### Chapter 1

### Chapter 2

Table 2.1: The information of six distinct nuclear reactors [1].....14

Table 2.2: An overview of the prices for generating hydrogen utilizing various technologies that have been published in the literature. Note that CCUS is carbon capture use and storage [1].....26

Table 2.3: A breakdown about using alkaline electrolysis for per kg of hydrogen [1]. ....27

### Chapter 3

Table 3.1: Technical specifications for the prototypic Integral PWR-type SMR. .....61

Table 3.2: Rankine cycle simulation inputs and outputs. .....63

Table 3.3: Comparative results for the question taken from a reference book [181]. .....68

Table 3.4: CSP Plant parameters [2].....71

Table 3.5: Design point solar data [2]. .....72

Table 3.6: An indication of hourly based data of CSP for one year [2]. .....72

Table 3.7: Net electricity amount in kWh depending on TES capacity for a year [2]. .....73

### Chapter 4

Table 4.1: Hydrogen production in kg per given seasonal day (as shown), for four alternative NPP and CSP percentage contributions (scenarios) [2]. .....100

Table 4.2: Production of electricity in kWh for four distinct NPP and CSP percentage contributions on a specific seasonal day (scenarios) [2].....100

Table 4.3: Comparative results.....104

Table 4.4: Comparison of the results. .....106

## LIST OF FIGURES

### Chapter 1

Figure 1.1: The most preferred methods of generating hydrogen from energy sources [1]. .....3

Figure 1.2: Methods for producing hydrogen using the most popular color schemes [1]...4

Figure 1.3: An illustration of the integrated scope. .....11

### Chapter 2

Figure 2.1: SMRs for non-electric applications [1]. .....18

Figure 2.2: An indication of renewable energy sources [1]. .....19

Figure 2.3: Hydrogen production methods with renewable energy [1]. .....20

Figure 2.4: Nuclear hydrogen generation scheme [1]. .....31

Figure 2.5: HTE mechanism [1]. .....35

Figure 2.6: Comparison of the common nuclear hydrogen production methods, namely, Cu-Cl and S-I cycles, HTE [1]. .....37

Figure 2.7: A demonstration of TRLs [1]. .....38

Figure 2.8: TRL of various N-RHES hydrogen production systems in accordance with maximum temperature requirements (a) and hydrogen production cost (b) [1]. .....38

Figure 2.9: Algorithm of "Genetic Algorithm". .....46

Figure 2.10: An example of Genetic Algorithms. .....47

### Chapter 3

Figure 3.1: SAM main window displaying a concentrated solar power system's results summary. .....56

Figure 3.2: Rankine cycle schematic and T-s diagram, respectively. .....65

Figure 3.3: System level model of an iPWR type SMR with prototypic Rankine energy conversion cycle, as modeled using LabVIEW [2]. .....66

Figure 3.4: Simulation results indication. .....68

Figure 3.5: A schematic of the CSP Plant [2]. .....70

Figure 3.6: CSP simulation on SAM. .....74

Figure 3.7: Thermochemical heat pump working mechanism. .....77

Figure 3.8: A schematic of N-RHES [2].....79

Figure 3.9: Control panel/LabVIEW GUI of NPP and CSP to produce hydrogen and electricity [2]. .....80

Figure 3.10: Showing the outcomes of a simulation of the 24-hour total electricity generation (MWh) and $H_2$ production (kg) from a combined NPP and CSP source [2]...81

Figure 3.11: The coding of the hydrogen produced in the Cu-Cl cycle with the use of this heat pump on LabVIEW. .....84

Figure 3.12: Coding of hydrogen and electricity outputs via NPP. .....85

Figure 3.13: An indication of 24-hour period electricity production in kWh by employing 50% of NPP and 50% of CSP, (January 1st). .....90

Figure 3.14: An indication of 24-hour period hydrogen production in kg by employing 50% of NPP and 50% of CSP sources, (January 1st). .....91

Figure 3.15: An indication of 24-hour period total hydrogen production in kg by employing 50% of NPP and 50% of CSP sources, (January 1st). .....92

Figure 3.16: An indication of 24-hour period total electricity production in kWh by employing 50% of NPP and 50% of CSP sources, (January 1$^{st}$ is selected as an example to show a trend). .....93

Figure 3.17: GUI of GA on MATLAB.....96

Figure 3.18: An indication of multi-objective Genetic Algorithm Pareto Front (objective-1: total profit in USD and objective-2: total heat equivalent in kJ).....97

**Chapter 4**

Figure 4.1: A seasonal comparison of hydrogen generation based on a certain percentage of NPP, CSP, or both reliance [2].....101

Figure 4.2: A comparison of seasonal and source-based variations in power production (NPP, CPS or combination) [2]. .....102

Figure 4.3: Applying MOGA for N-RHES (JUN-15, between 00:00am and 1:00am)...104

Figure 4.4: An optimized result for August 1$^{st}$ between 9:00am and 10:00am. .....105

Figure 4.5: Hydrogen production amounts depending on three scenarios (optimized N-RHES for max. profit, 25%NPP-25%CSP and 50%NPP-50%CSP) on August 1st. .....108

Figure 4.6: Electricity production amounts depending on three scenarios (optimized N-RHES for max. profit, 25%NPP-25%CSP and 50%NPP-50%CSP) on August 1st. .....109

Figure 4.7: Total Profit (objective-1) comparison based on scenarios, optimized N-RHES for maximum profit, 25%NPP-25%CSP and 50%NPP-50%CSP on August 1st. .....110

Figure 4.8: Total Heat Equivalent (objective-2) comparison based on scenarios, optimized N-RHES for maximum total heat equivalent, 25%NPP-25%CSP and 50%NPP-50%CSP on August 1st.....111

Figure 4.9: Indication of hourly required $H_2$ amount to meet NPP electricity demand on August 1$^{st}$. .....113

Figure 4.10: NPP electricity requirement while NPP power decreases from 100% to 0% in 4 hours.....115

Figure 4.11: Hydrogen production amount via N-RHES while NPP power decreases from 100% to 0% in 4 hours.....116

Figure 4.12: Electricity production amount while NPP power decreases from 100% to 0% in 4 hours.....117

Figure 4.13: NPP electricity requirement is met by hydrogen-powered electricity generators while NPP power decreases from 100% to 0% in 4 hours.....118

## LIST OF ABBREVIATIONS AND SYMBOLS

| | |
|---|---|
| A | Adenine |
| ANL | Argonne National Laboratory |
| AP | Acidification |
| API | Application Programming Interface |
| BWR | Boiling Water Reactor |
| C | Cytosine |
| CANDU | Canada Deuterium Uranium |
| CCS | Carbon Capture and Storage |
| CCUS | Carbon Capture Use and Storage |
| $CO_2$ | Carbon dioxide |
| CSP | Concentrated Solar Power |
| Cu-Cl | Copper-Chlorine |
| DNA | Deoxyribonucleic Acid |
| DOE | Department Of Energy |
| DR | Dish Receiver |
| EFF | Efficiency |

| | |
|---|---|
| FR | Fresnel Reflectors |
| G | Guanine |
| GA | Genetic Algorithm |
| GEN-IV | Generation-IV |
| GFR | Gas-Cooled Fast Reactor |
| GHG | Greenhouse Gas |
| GIF | Generation-IV International Forum |
| GUI | Graphical User Interface |
| GWP | Global Warming Potential |
| $H_2$ | Hydrogen |
| HHV | Higher Heating Value |
| HOEP | Hourly Ontario Electricity Price |
| HTE | High Temperature Electrolysis |
| HTSE | High Temperature Steam Electrolysis |
| HX | Heat Exchanger |
| IAEA | International Atomic Energy Agency |
| INL | Idaho National Laboratory |

| | |
|---|---|
| iPWR | Integral Pressurized Water Reactor |
| LCOE | Levelized Cost Of Energy |
| LFR | Lead-Cooled Fast Reactor |
| LWR | Light Water Reactor |
| MMR | Micro Modular Reactor |
| MOGA | Multi Objective Genetic Algorithm |
| MSFR | Molten Salt-Cooled Fast Reactor |
| NGNP | Next Generation Nuclear Plant |
| NPP | Nuclear Power Plant |
| NREL | National Renewable Energy Laboratory |
| N-RHES | Nuclear-Renewable Hybrid Energy System |
| OBJ | Objective |
| PCHE | Printed Circuit Heat Exchangers |
| PPA | Power Purchase Agreement |
| PRA | Probabilistic Risk Assessment |
| PSA | Probabilistic Safety Assessments |
| PSS | Passive Safety System |

| | |
|---|---|
| PT | Parabolic Trough |
| PV | Photovoltaic |
| PWR | Pressurized Water Reactor |
| R&D | Research and Development |
| RPV | Reactor Pressure Vessel |
| SAM | System Advisor Model |
| SCC | Social Cost of Carbon |
| SCWR | Supercritical-Water-Cooled Reactor |
| SDK | Software Development Kit |
| SFR | Sodium-Cooled Fast Reactor |
| S-I | Sulfur-Iodine |
| SMRs | Small Modular Reactors |
| T | Thymine |
| TES | Thermal Energy Storage |
| TOD | Time-Of-Delivery |
| TRL | Technology Readiness Level |
| VHTR | Very High Temperature Reactor |

## Nomenclature

### Symbol

| | |
|---|---|
| ® | Registered Trendmark |
| $\Delta T$ | Temperature difference |
| $p_c$ | Crossover possibility |
| $P_m$ | Mutation probability |
| $T$ | Temperature |
| $H$ | Enthalpy |
| $V$ | Specific volume |
| $w_{p,\,in}$ | Inlet pump work |
| $Wnet$ | Net work |
| $S$ | Entropy |
| $h_f$ | Enthalpy for saturated liquid |
| $h_{fg}$ | Enthalpy for evaporation (latent heat) |
| $h_s$ | Enthalpy isentropic point |
| $h_a$ | Enthalpy for actual point |
| $q_{in}$ | Heat inlet |
| $q_{out}$ | Heat outlet |
| $n_p$ | Pump efficiency |
| $n_{Turbine}$ | Turbine efficiency |

| | |
|---|---|
| $n_{Total}$ | total efficiency |
| $T_{Cu\text{-}Cl,\ max}$ | Max temperature required for Cu-Cl cycle |
| $T_{NPP,max}$ | Max temperature provided by Nuclear Power Plant [°C] |
| $E_1$ | Electricity required for producing per mol H2/s for Cu-Cl, 25W. |
| $\eta_1$ | Nuclear Power Plant Rankine cycle efficiency |
| $A_1$ | Heat energy amount for electricity required to producing 1 mol H2 via NPP [W] |
| $B_1$ | Heat energy required for Cu-Cl cycle to produce one mol H2 [W] |
| $C_1$ | Total heat energy required for producing one mol H2 via NPP [W] |
| $D_1$ | Heat energy consumed by heat pump [W] |

**Subscript**

| | |
|---|---|
| $E$ | Electrical |
| $Th$ | Thermal |
| $_c$ | Crossover |
| $F$ | Fluid |

# Chapter 1. Introduction

## 1.1 Background

The need for energy is increasing as the world's population and economy expand and people move from rural to urban areas [1, 3]. People need more energy in urban areas than in the countryside. Fossil fuels (hydrocarbons) are the primary source of today's electricity production in the world [4]. The consistent use of hydrocarbon-based energy caused considerable increases in the atmospheric concentrations of $CO_2$ and greenhouse gases, which has been identified as the main contributors to global warming [5]. In order to reduce global warming and maintain a clean environment, sustainable and renewable energy sources are essential [6-9]. Renewable energy sources have an important role to protect our world by decreasing greenhouse gases emissions. However, producing energy from renewables has some drawbacks. Finding electric energy at a highly competitive price from renewable energy sources can be difficult. In fact, the variety and irregularity of these kinds of energy sources is one of their noticeable characteristics [10]. To solve these issues, it is thus required to put into practise effective and technical solutions. To give a clear example, large-scale storage systems have been suggested and developed to satisfy market demand in order to deal with the volatility and discontinuity of renewable energy sources [11]. Storage devices can decouple supply and demand (hourly, daily, and seasonally) by transferring generated energy on various time intervals [12].

When it comes to storing energy, hydrogen is a good energy carrier [13-16]. For instance, hydrogen can be used to produce electricity or heating in remote areas. Additionally, hydrogen is already a commodity that is used as a feedstock in many industrial processes, including refineries and the production of methanol and ammonia

[17]. Due to its portability, hydrogen-based energy storage devices are becoming more important for large-scale energy storage [13, 18, 19]. The demand for pure hydrogen has drastically increased, going from less than 20 Mt in 1975 to more than 70 Mt in 2018 [20]. Despite the fact that it has only recently started to show promise [21], the majority of the recent studies have come to the conclusion that a fully hydrogen-dependent economy is unachievable or at least still disputable [13, 22]. This is despite the fact that many researchers support the use of hydrogen as an energy carrier for the reasons just mentioned [23]. Whatever the challenges, clean hydrogen generation is the trend to lower $CO_2$ emissions and meet the world's energy need [5, 14, 24-26] particularly in the sectors of transportation and energy conversion into electricity. Therefore, it can be said that hydrogen is a key issue for decreasing greenhouse gas emissions and transitioning to a low-carbon future.

As depicted in Fig. 1.1, hydrogen can be created by a variety of energy sources, including coal, natural gas, nuclear, biomass, solar, wind [27]. To supply the majority of the present hydrogen demand, fossil fuels like natural gas, oil, and coal are still used since they are currently the most affordable source, with costs ranging from 1 to US$ 3 per kilogram of hydrogen generated [28-30].

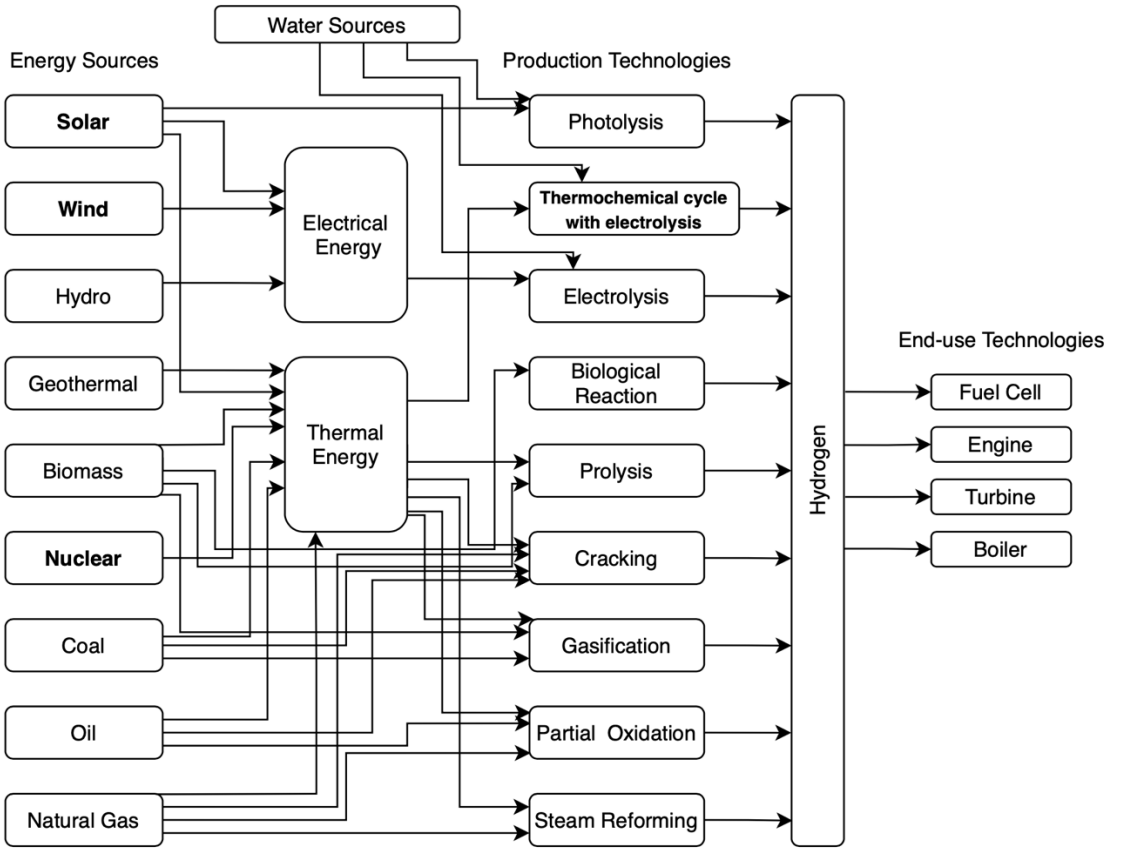


Figure 1.1: The most preferred methods of generating hydrogen from energy sources [1].

Hydrogen can be categorised based on the type of energy source and the technologies mentioned above. It is becoming more and more popular to characterise hydrogen generating technology using a color-coded system. The process of producing hydrogen is depicted in Figure 1.2 using different colours [1]. The principal colours under consideration are listed below [31]:

• Grey (or brown/black) hydrogen that emits carbon dioxide and is created from fossil fuels, mostly coal and natural gas;

• Blue hydrogen, which eliminates the majority of the process' GHG emissions by mixing grey hydrogen with carbon capture and storage (CCS);

• Turquoise hydrogen, which is created from the pyrolysis of a fossil fuel and leaves behind solid carbon;

• Green hydrogen, which is created when electrolysers fueled by renewable energy (and occasionally, other bioenergy-based processes like biomethane reforming or solid biomass gasification) are used to make hydrogen;

• Yellow (or purple) hydrogen, which is created by nuclear-powered electrolysers.

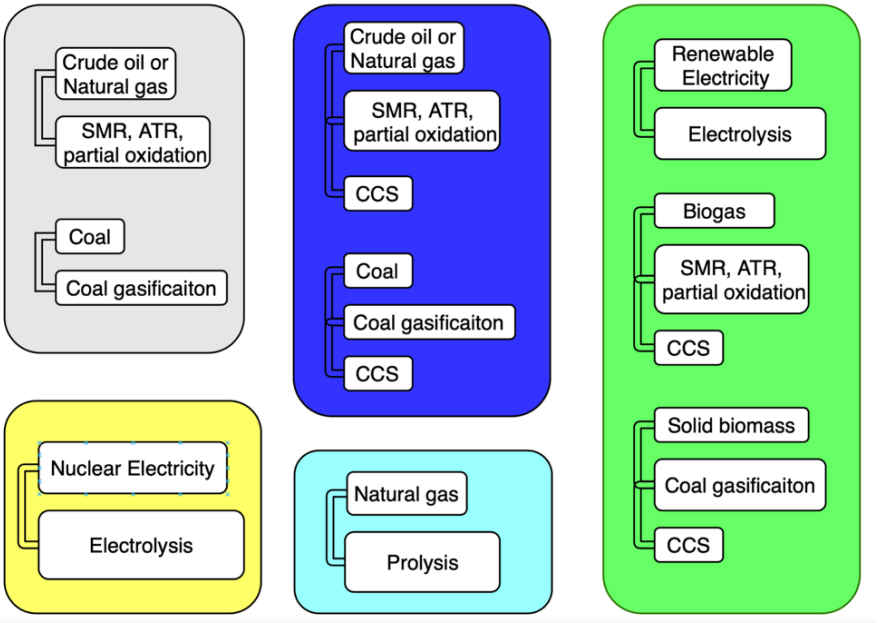


Figure 1.2: Methods for producing hydrogen using the most popular color schemes [1].

Among the methods described in the literature that can generate heat and electricity as well as manufacture hydrogen from water by the same nuclear power reactor are traditional water electrolysis, steam reforming, steam electrolysis at high temperatures, hybrid, and thermochemical cycles [27, 31]. The Nuclear-Renewable Hybrid Energy System (N-RHES) is one of the appealing technologies. In addition to producing cheap power, the N-RHES can also produce hydrogen [32-34].

Provided that N-RHES is used to produce hydrogen, thermochemical cycles can be preferred, since thermochemical cycles require mostly heat energy. As a result of

combining N-RHES and thermochemical cycles such as Cu-Cl, hydrogen produced is effectively clean. Moreover, another advantage of this hybridization is that .nuclear power plants can continue producing maximum power even if the electricity demand decreases.

Since N-RHES is complex system, it must be improved to be more effective [33]. Since practically all real-world optimization problems are framed utilizing several competing objectives, multi-objective optimization in the N-RHES shows to be a particularly difficult element of optimization process. The typical solution to such issues is to merge several goals into a single goal, but the best strategy attempts to address the multi-objective optimization problem in the actual world and not always is effective. Numerous processes in complex systems can be optimized using artificial intelligence and Algorithms [8, 24, 35-39]. Furthermore, the Lindo® What's Best (or comparable) tool can be utilized for linear, integer, and nonlinear optimization [40, 41]. With specified constructions and parameters, the tool offers the best response as indicated by [40]. As a result, one of this research purposes is to investigate and report on the recent methods that have been put forth to produce hydrogen using nuclear and renewable energy sources. In addition to this, to reduce greenhouse gas emissions and meet the world's current energy needs, fossil-based energy sources must be replaced with clean energy sources.

This study gives a comprehensive review of methods for producing clean hydrogen using nuclear energy via mostly focused on water-based methods. Additionally, it includes a description of small modular reactors, including their temperature ranges and prospective application areas. Details about hydrogen production, including its potential applications across several industries are also provided. The cost, efficiency, global warming potential (GWP), and other characteristics of two hydrogen production technologies as the thermochemical cycles and electrolysis are compared in the sections that follows. This

research then, identifies the technology readiness level of these two hydrogen production technologies. The ultimate objective of this research is to optimise each stage of the hybrid system to produce preferred results while taking complexity and multi-objectivity into account.

### 1.2 Motivation

As the world's population and economy grow and more people relocate to the city centers, the demand for energy is rising [3]. The main source of energy in the world today is fossil fuels (hydrocarbons), however due to their geographic availability and ease of extraction, their supply is decreasing and is restricted [4, 18]. It has been shown that the primary cause of global warming is the persistent use of hydrocarbon-based energy, which significantly increased the atmospheric quantities of $CO_2$ and greenhouse gases [5]. Sustainable and renewable energy sources are essential to overcome global warming and preserve the ecosystem [6-9]. Therefore, as mentioned in the background, one of the possible and promising solutions is to operate a N-RHES to decrease the greenhouse gases emission of the world by producing clean hydrogen. Utilizing renewable energy in addition to nuclear energy has an important role in not only decreasing greenhouse gases emission but also producing clean hydrogen. Although renewable energy sources are clean, the energy generated via renewable sources has fluctuations depending on the climate conditions. In order to compensate for that, nuclear power plants are envisioned as they provide stable energy without interruptions for long periods of time. It is obviously concluded then that nuclear power plants and renewable energy sources may work harmoniously together.

When N-RHES is optimized it can be more efficient as it has complexity [33]. Multi-objective optimization in the N-RHES is a particularly challenging aspect of

optimization processes since almost all real-world optimization issues are formulated using multiple competing objectives. The common approach to such challenges is to combine many objectives into a single objective, however the optimal approach tries to solve the multi-objective optimization complexity of the real world. Artificial intelligence and Algorithms can be used to optimize a variety of processes in complex systems [24]. Additionally, linear, integer, and non-linear optimization can be done using a variety of software such as Lindo® What's Best or MATLAB [41]. These software provide the best results when used with defined restrictions and variables [40].

Instead of just creating electricity, nuclear power plants are more effective at producing heat energy. Furthermore, nuclear energy can be used to generate hydrogen since high temperature electrolysis and thermochemical cycles need power and operate at temperatures between 500 and 830°C, meaning they need more heat energy than electricity [17, 42, 43].

Compared to conventional large reactors, SMRs are nuclear fission reactors that are significantly smaller, less powerful, but significantly less expensive. They are manufactured in factory settings and delivered to the installation site as prefabricated modules while using the most modern technologies in terms of passive safety although many of them are not in operation nowadays. Therefore, small modular reactors are considered to be safer than currently in use conventional designs (PWR, BWR, and CANDU) and need less time to construct on-site while improving containment effectiveness, decreasing above all fabrication costs [44, 45]. They are designed to use totally passive safety features that can operate without human involvement increases safety [46, 47]. Compared to conventional nuclear reactors, SMRs require fewer workers and operators [48]. Due to their capacity to overcome the majority of the financial and safety

constraints prohibiting the widespread global building of large conventional reactors, SMRs are currently being designed and suggested as key players for future nuclear power expansion [49].

Small Modular Reactors (SMRs) have significant and evident advantages over conventional large nuclear power plants (NPPs of 1 $GW_e$). These advantages allow sophisticated SMRs to be used for more than just power generation. For instance , they can be employed to generate compounds needed in the petroleum industry, hydrogen, desalinated water, liquid transportation fuels, and others [50].

The design of Small Modular Reactors (SMRs) with advanced characteristics is projected to be simpler [51], their cost to be lower due to mass production, and their physical footprint to be smaller [52, 53]. SMRs also offer higher standards of security, safety, and non-proliferation [52, 54]. The modularizing construction method, which was formerly employed to construct large reactors, has been applied in manufacturing for a long time [55]. Modularization offers a lower initial capital investment, scalability, and siting flexibility in locations where conventional large reactors are neither practical nor required [53].

One of the most important products of the modern oil and petrochemical industry is hydrogen. Innovative fuel cell applications have recently increased the importance of hydrogen [37]. Different feedstocks, routes, and technologies, including a variety of processes, technologies, and energy sources, such as fossil fuels and renewable energy sources, can be used to produce hydrogen on a large scale [32, 42, 56, 57].

Green hydrogen production is more expensive than fossil fuel-based hydrogen production [58]. Green hydrogen costs currently between US$ 2.5 and $7.39/kg-$H_2$, which is more expensive than black, blue, and grey hydrogen. 180 MJ of power, 26.2 MJ of heat

energy, and 11.5 kg of water are needed for low-temperature electrolysis to perform at 60°C and 0.1 MPa in order to produce 1 kg of hydrogen. Based on the price of heat and electrical energies per unit, the cost to produce 1 kilogram of hydrogen is US$ 5.92 [4]. The cost of $CO_2$-free aqua hydrogen is US$ 0.23 per kg of hydrogen, according to [58, 59].

To conclude, the major motivation of this research is to study the most recent techniques for producing clean hydrogen using nuclear and renewable energy sources to decrease greenhouse gases emission of the world and by doing that, improving the hybrid system's performance at each stage while taking complexity and multiple objectives into account. Moreover, to provide a thorough analysis of techniques for producing clean hydrogen using nuclear and renewable energy, with a main emphasis on water-based techniques.

### 1.3 Research Objectives

The research's objectivities are;

1- Developing a simplified NPP thermodynamic simulation on LabVIEW.

   To obtain information about electrical and heat power output in MW or kWh for electricity by designing iPWR-type SMR depending on some parameters, which are open-ended, such as minimum or maximum pressure point, maximum temperature and similar.

2- Demonstrating a CSP on the well-known and well-benchmarked NREL SAM software.

   Concentrated Solar Power (CSP) Plant has been chosen in this research, as it is capable of producing not only electricity, but also large amount of heat energy. To obtain data about how much electricity or heat energy produced via CSP, System Advisor Model (SAM) software is selected. On SAM, a CSP plant is

modeled based on several parameters of both the geometry of the CSP and location, time of the year and similar providing enough information for , producing hydrogen and electricity.

3- Coupling LabVIEW/MATLAB and SAM software.

   As one of this research's objectivities is to investigate how capable nuclear-renewable hybrid energy system is to produce hydrogen and electricity: all information about NPP outputs from the simulation on LabVIEW and CSP outputs from the simulation on SAM are then fed to the thermodynamic cycle taking care of hydrogen production.

4- Developing a hybrid system that can generate both hydrogen and electricity with desired power rates.

   In this case it is necessary to develop a hybrid system where power rates of heat energies from the NPP and CSP can be adjusted to produce clean hydrogen and electricity. This allows to be flexible and more efficient when the electricity demand changes or to have more benefit depending on the electricity or hydrogen price to be sold at that point in time.

5- Optimizing the hybrid system to find out most effective way to use the hybrid system.

   Optimization is essential part of this research. Since hybrid systems are complex, with a high number of inputs and outputs, to obtain more benefit from a hybrid system it is necessary to optimize the system by using single or/and multi-objective optimization methods.

## 1.4 Scope of the Research

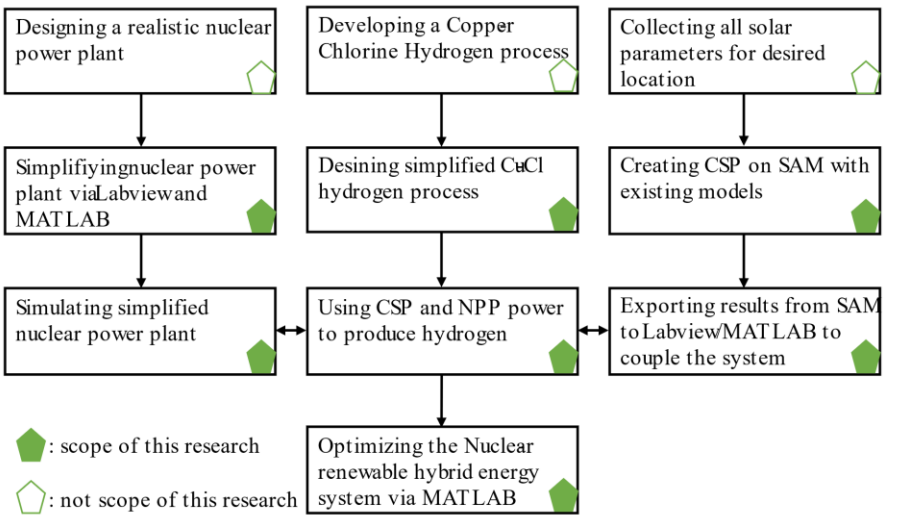


Figure 1.3: An illustration of the integrated scope.

This study is divided into four main sections: building a thermodynamics simulation of NPP in LABVIEW, modeling a CSP power plant in SAM and integrating it with LABVIEW, producing electricity or hydrogen with the integrated hybrid system in LABVIEW (using Copper Chlorine cycle) , and finally optimizing the resulting N-RHES. Figure 1.3 provides a graphic overview of integrated scope.

## 1.5 Thesis Organization

There are five chapters in this thesis, and they are arranged as follows:

Chapter 1 gives information about the research, motivations for nuclear-renewable hybrid energy system (N-RHES) to produce hydrogen and electricity, multiple objectives of the research and organization of the thesis.

Chapter 2 includes a literature review about nuclear hydrogen production with renewable energy sources and, optimization for nuclear-renewable hybrid energy systems.

Chapter 3 contains information about mathematical modeling of the nuclear-renewable hybrid energy system to produce optimized hydrogen and electricity, and refers to the validations and simulations of the N-RHES on LabVIEW, MATLAB and System Advisor Model (SAM).

Chapter 4 demonstrates results in terms of producing optimized clean hydrogen and electricity of the N-RHES.

Chapter 5 focuses on conclusion based on the results of different scenarios of the N-RHES. Finally, future development of the research is discussed.

## Chapter 2. Literature Review

This chapter contains a literature review giving information about how to obtain clean and optimized hydrogen production by using energy coming from nuclear and renewable sources. Furthermore, it gives detailed information about hydrogen and clean hydrogen production methods, comparison of these methods considering technology readiness levels (TRLs). Last but not least, information about optimization takes part in this literature review.

### 2.1 Nuclear Power Plant (NPP)

Nuclear (fission) processes in nuclear power plants provide heat energy almost without releasing carbon dioxide. As is typical of thermal power plants, heat is used to produce steam, which powers a steam turbine connected to an electricity generator. 11.5% of the world's electricity consumption is met by the 440 nuclear power reactors that are currently in operation [60, 61]. Compared to a paper [62], it is seen that 13.5% of the world`s electricity was met by NPPs between 2010 and 2013. In the preceding 50 years, nuclear power plants have decreased $CO_2$ emissions by 60 gigatons [63]. Table 2.1 summarises data for six different nuclear reactors in terms of coolant type, neutron spectrum, capacity (MWe), fuel cycle, and outlet temperature (°C).

Table 2.1: The information of six distinct nuclear reactors [1].

| | SWCR | GFR | LFR | MSR | SFR | VHTR |
|---|---|---|---|---|---|---|
| Coolant | Water | Helium | Lead/Lead-Bismuth | Fluoride Salts | Sodium | Helium |
| Neutron Spectrum | Thermal/Fast | Fast | Fast | Thermal/Fast | Fast | Thermal |
| Capacity (MWe) | 300-1500 | 1-200 | 20-1000 | 800-700 | 50-1600 | 250-300 |
| Fuel Cycle | Open/Closed | Closed | Closed | Open | Closed | Open |
| Outlet temperature (°C) | 510-625 | 850 | 480-570 | 700-800 | 500-550 | 900-1000 |
| Reference | [64, 65] | [65-67] | [65, 68] | [65, 68] | [65, 68] | [69, 70] |

Nuclear reactors can produce hydrogen due to their excellent thermal energy capabilities [71, 72]. Hydrogen can be produced using a range of technologies and techniques from fossil fuels, renewable energy sources, and nuclear energy [21, 73, 74]. One of fascinating technologies is the nuclear-renewable hybrid energy system (N-RHES) [4]. Both hydrogen and inexpensive electricity can be produced by the N-RHES [32, 75]. The same nuclear power reactor can produce heat and electricity while also producing hydrogen from water using various methods [75], which are water electrolysis, steam reforming, steam electrolysis at high temperatures, hybrid, and thermochemical cycles are just a few of the methods covered in the literature [6, 76, 77].

Nuclear power reactors are divided into three categories based on their capacity: small, medium, and large reactors [78]. Small modular reactors (SMRs), a promising technology nowadays, are the subject of next sections of this study.

### 2.2 Generation-IV Nuclear Reactors

The US DOE was the first to propose the concept of six Generation-IV reactors, and under the auspices of the Generation-IV International Forum (GIF), several nations

have proposed the creation of one or more GEN-IV designs. Initially, it was planned for two to three concepts to be chosen and built before 2030: US showed interest in the Next Generation Nuclear Plant (NGNP) as a type of VHTR as part of the Generation-IV initiatives, along with interest in a hydrogen production plant (INL) [79]. Additionally, Patterson [67] claims that studies were conducted in the (State of) Hawaii to produce liquid fuel from biomass by hosting a VHTR plant. Due to the possibility of downsizing turbine components and the availability of printed circuit heat exchangers (PCHE), the use of $CO_2$ gas in the VHTR also attracted attention in supercritical phenomena ($CO_2$, light water) and higher overall plant efficiency. In collaboration with ANL, Song et al. reported on testing a PCHE in a supercritical $CO_2$ Brayton cycle [80]. Then, Tokuhiro et al. used a high-temperature gas circulator (to simulate a VHTR) and an intelligent control system (applied neural networks) to extract energy from 950 °C to 50 °C [81].

It is commonly known that traditional nuclear reactors do not have particularly high thermal efficiencies, mostly because of restrictions on moderator temperatures. Because of this, more than two thirds of the thermal energy generated by traditional nuclear reactors is lost to waste and the environment. The temperature difference ($\Delta T$ between maximum and lowest Rankine cycle points) must be raised to improve the efficiency of nuclear reactors, for instance by raising coolant temperature. Thermodynamic efficiency can be enhanced in this way [82].

Six different nuclear reactor types, including the Gas-Cooled Fast Reactor (GFR), Very High-Temperature Reactor (VHTR), Lead-Cooled Fast Reactor (LFR), Molten Salt-Cooled Fast Thermal Reactor (MSFR), Supercritical-Water-Cooled Reactor (SCWR), and Sodium-Cooled Fast Reactor (SFR), have been developed as part of Generation-IV nuclear reactors. Aiming for improved cycle efficiency, high temperature steam electrolysis, high

temperature thermo-chemical cycling, or hybrid water separation for hydrogen production, Gen-IV reactors are being developed all around the world. For instance, the SCWR (Canada's Gen-IV design) may be set to produce hydrogen via the Cu-Cl thermo-chemical cycle and has a greater net thermal efficiency of 45% [83]. The anticipated SCWR technology will produce the higher temperatures required by this cycle. Due to supercritical thermophysical characteristics gains, SCWR can operate at temperatures and pressures up to 500°C and 28 MPa, which explains why it has a better efficiency. The most promising nuclear technology, according to Atomic Energy of Canada Limited, is the SCWR concept that can employ Cu-Cl to produce hydrogen [84]. Generation-IV nuclear reactors have increased safety and reliability, sustainability, resistance to proliferation, and physical protection in addition to greater efficiency [85].

Temperature differences ($\Delta T$) or heat energy at high temperatures are crucial for producing hydrogen, which highlights the significance of generation-IV nuclear reactors [82, 86]. In terms of temperature difference, concentrated solar power (CSP) technologies can be recommended for use with Generation-IV nuclear reactors, such as SCWR, to raise the temperature difference and thereby contribute to the hydrogen economy. CSPs are actually capable of meeting the high-temperature requirement as reported in the literature [32, 87, 88].

### 2.3 Small Modular Reactors (SMRs)

SMRs are nuclear fission reactors that are considerably smaller, less powerful, and less expensive than traditional large reactors. They can be built in a factory and delivered to a site prepared for installation in prefabricated modules. Therefore, modular reactors reduce the amount of time needed for construction on-site, increase containment effectiveness, lower fabrication costs, and are thought to be safer than currently used

conventional designs (PWR, BWR, and CANDU) [44, 45, 89]. Increased safety is achieved by using entirely passive safety components that can function without human intervention [46, 47]. SMRs require less employees than traditional nuclear reactors [48]. SMRs are currently being designed and proposed due to their ability to get through the majority of the financial and safety barriers preventing the widespread global construction of large conventional reactors [49].

The International Atomic Energy Agency (IAEA) defines small reactors as those that generate equivalent electric power of less than 300 Megawatts ($MW_e$) [90], while medium modular reactors are defined as those that generate equivalent electric power of between 300 $MW_e$ and 700 $MW_e$ [78, 91].

Scaled-down versions of earlier designs to fully revolutionary Generation-IV designs are all included in SMR designs. Recently, concepts for thermal-neutron reactors, fast-neutron reactors, molten salt-cooled reactors, and gas-cooled reactors have all been put forth [92].

The advantages of Small Modular Reactors (SMRs) over traditional large nuclear power plants (NPPs of 1 $GW_e$) are substantial and obvious. Sophisticated SMRs can be utilized for more than just power generation thanks in part to these benefits. As shown in Figure 2.1 [1] (when co-located), they can also be utilized to produce hydrogen, desalinated water, liquid transportation fuels, and some compounds required in the petroleum sector [50].

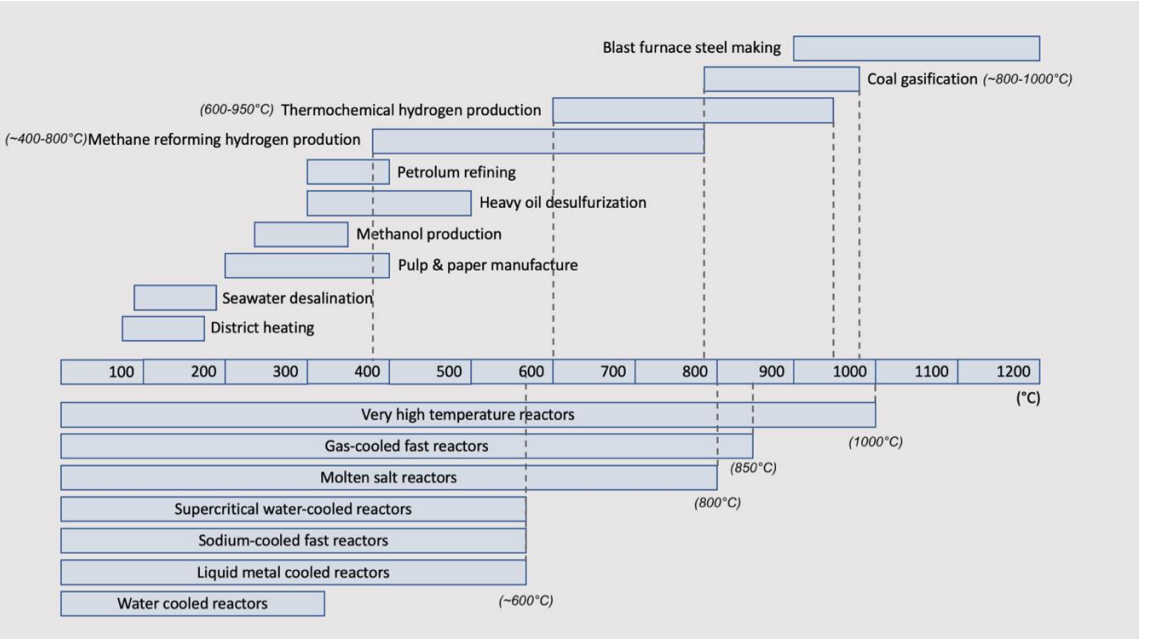


Figure 2.1: SMRs for non-electric applications [1].

Small Modular Reactors (SMRs) with advanced features are anticipated to have a more simply design [51], reduced cost as a result of mass production, and a smaller physical footprint [52, 53]. Additionally, SMRs have superior levels of security, safety, and anti-proliferation [52-54]. The manufacturing sector has long used the modularizing construction technique, which was previously used to build large reactors [55]. Modularizations, on the other hand, offer a lower initial capital investment, scalability, and site flexibility in regions where conventional large reactors are neither viable or necessary [53]**.**

The next sections examine renewable energy with focus on hybridization of nuclear-renewable hybrid systems to produce hydrogen.

## 2.4 Renewable Energy

Traditional energy production from fossil fuels (coal, oil, and natural gas) has been successful in fostering worldwide economic development and continues to be a major

contributor to meeting global energy demands [7, 21]. However, as a result of growing population and increased energy demand brought on by higher living standards, the world's primary energy consumption is rising [3]. The majority of the greenhouse gas emissions reductions needed between now and 2050 to maintain the rise in the world's average surface temperature below 2°C are made possible by renewable energy [7]. As a result, the importance of renewable energy sources has started to grow in order to fulfil the increasing global energy demand and to minimise $CO_2$ emissions in terms of environmental issues [14]. By utilising renewable energy sources, which lower greenhouse gas emissions and guarantee dependable, timely, and cost-effective energy delivery, we can minimise future extreme weather and climate effects [93]. Deployment here is the key factor.

Renewable resources, such as carbon-neutral sources including sunlight, wind, rain, tides, waves, and geothermal heat, are those that naturally regenerate on a human timescale [94]. Although most renewable energy sources are sustainable, some, particularly biomass, are not and are finite (potentially eroding other feedstocks) [6]. A breakdown [1] of renewable energy sources is shown in Fig. 2.2 [95]. Thanks to renewable energy technology, renewable energy sources can be converted into useful energy types as electricity, fuels, hydrogen, and heat [96].

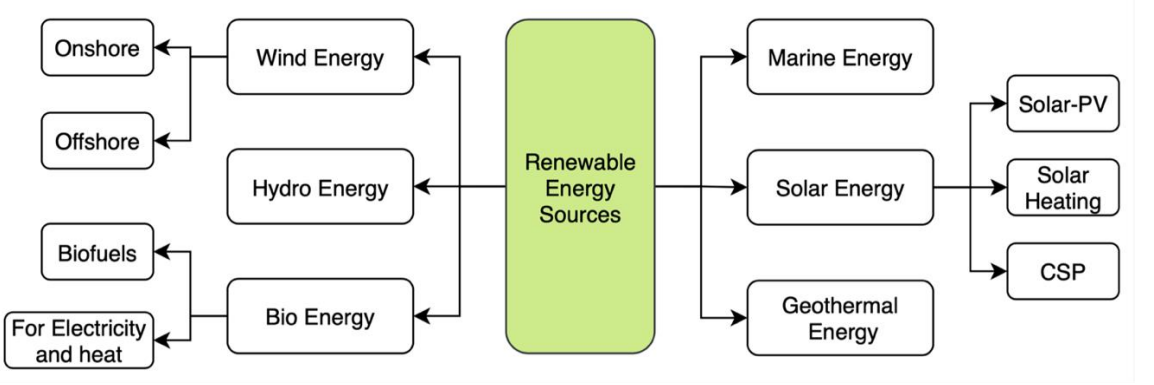


Figure 2.2: An indication of renewable energy sources [1].

It may be feasible to reduce and eliminate greenhouse gas emissions while meeting global energy demands by locating more dependable, sustainable, and diversified energy sources. As a result, hydrogen is superior to conventional fuels in many ways and can be used to lessen pollution and dependent on imported oil [5, 97, 98]. Although hydrogen is not a major energy source, it can be separated from other elements using an energy source to transform it into a desirable energy carrier [23, 88, 99]. Fig. 2.3 [1] illustrates various renewable energy methods for producing hydrogen [6, 21, 88]. Fuel cells use hydrogen as a clean energy source since it only produces water when it combines with oxygen, leaving no carbon dioxide as a by-product [99].

The following benefits of hydrogen are listed as direct or indirect benefits [21];

- Assist a country with paucity of oil and in reducing its imports.
- Assist in achieving a longer-term sustainability way better than it is possible with the use of present energy sources.
- Modify the prognosis for the environment by enabling emission reduction.

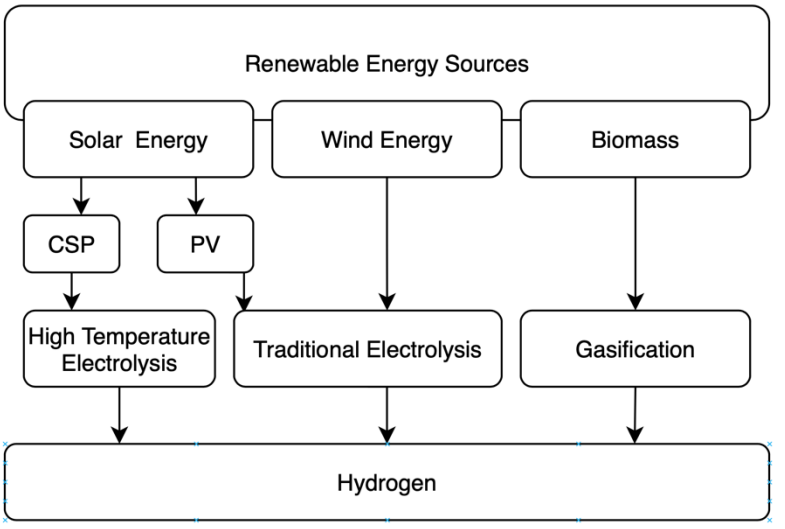


Figure 2.3: Hydrogen production methods with renewable energy [1].

### 2.4.1 Solar Photovoltaic (PV)

An expensive technique of hydrogen generation, solar electrolysis has a cost of hydrogen that is approximately 25 times higher than alternatives using fossil fuels. On the other hand, it is anticipated that the cost of solar PV would decrease much further, having already decreased from 25 to 6 times [21, 100]. Then, more work is required to make this hybrid system truly competitive on the market in terms of cost and coupling efficiency.

### 2.4.2 Concentrated Solar Power (CSP)

Concentrated solar power (CSP) plants can generate heat energy that can be used to produce hydrogen [87, 88]. Mirrors in concentrated solar power plants reflect sunlight toward a receiver. A steam turbine is driven by the thermal energy collected in the receiver to produce electricity [101]. This CSP technology is ideal for hydrogen production via Cu-Cl thermochemical cycle as CSP is capable to produce heat energy at the temperature of 530°C, which can meet the requirement of Cu-Cl thermochemical cycle. The literature frequently reports on three different types of CSP technology that can handle very high temperatures. These technologies are divided into groups based on the CSP mirroring equipment. These include the Fresnel Reflectors (FR), Dish Receiver (DR) and Parabolic Trough (PT) [32, 102]. Over 90% of PT systems were operational in 2013 [103], and more recently, more than 60% of CSP systems [104]. The FR system uses many ground-based, flat or slightly curved mirrors positioned at different angles to focus sunlight onto a stationary receiver several metres above the mirror region, which is comparable to the PT collector technology [105]. Solar power towers are a type of solar furnace that receive focused sunlight through a tower. They are sometimes referred to as "central tower" power plants, "heliostat" power plants, or "power towers." It utilises a system of flat, mobile mirrors known as heliostats to concentrate the sun's rays onto a collection tower.

Concentrated solar thermal power is one potential substitute for clean, sustainable energy [106].

Location has a big impact on how much thermal energy is produced by CSP. It can be claimed that CSP is useless in locations with insufficient sunlight. Therefore, it is believed that as the location changes, CSP outputs would also vary. It is known that CSP includes some inputs, including the number of heliostats, which is connected with outcomes. It is possible to obtain the same results with fewer heliostats in an area with more sunlight than it is with more heliostats in an area with less sunlight.

CSP plant accounts for mainly three subsystems, being solar field, thermal storage, and power block. To produce electricity, CSP uses heat energy in the thermal storage. If the thermal energy taking part in the thermal storage is not enough, CSP cannot produce electricity.

When CSP does not produce energy, it requires electrical energy from the grid to keep its main cycle fluid (molten-salt) in a liquid form. This required energy can be met via another energy sources, for instance, via a NPP where N-RHES is employed.

### 2.4.3 Wind Energy

One of the renewable energy sources with the greatest promise for manufacturing pollution-free hydrogen is this method, which electrolyzes wind energy [107]. This method is especially effective for dispersed systems. In addition to the high cost of wind turbines and electrolysers, the optimization of the turbine electrolyser-storage system is a disadvantage of using wind energy to produce hydrogen. Since the cost of producing hydrogen with wind turbines is currently 6–10 times higher than that of fossil fuel alternatives, it is not cost-competitive [21, 100].

## 2.5 Hydrogen

The chemical element hydrogen has the symbol H and the atomic number "1". One of the most prevalent elements in the cosmos, hydrogen ($H_2$) is mostly present in water and organic compounds on the Earth [7]. It is an odorless, colorless, combustible gas [108]. It was determined that October 8$^{th}$ (10/08) should be proclaimed National Hydrogen and Fuel Cell Day in the United States since hydrogen has an atomic weight of 1.008 amu [109].

Numerous industrial sectors, including petrochemicals, agriculture (such as ammonia for fertilizers), food processing, plastics, manufacturing, and, more and more, transportation, heavily rely on hydrogen [110].

Hydrogen is one of the most crucial elements in the petroleum and petrochemical industries. Hydrogen has lately grown in significance due to innovative fuel cell applications [37, 111]. Numerous processes, technologies, and energy sources, such as fossil fuels and renewable energy sources, can be used to manufacture hydrogen, including different feedstocks, routes, and technologies [32, 37, 42, 56, 57].

With over half of all hydrogen produced worldwide coming from steam (methane) reforming of natural gas, this has emerged as the most economical and popular method for producing hydrogen [6, 112, 113]. A considerable quantity of $CO_2$ is released into the environment during the steam-methane reforming of fossil fuels like coal or methane, which produces over 97% of the hydrogen used in the world today [110, 114]. It is estimated that the steam methane reforming process has a global warming potential of 13.7 kg $CO_2$ per kilogram of net hydrogen produced ($CO_2$ makes up 77.6% of the system's global warming potential) [114, 115]. A typical steam methane reforming hydrogen plant that generates $10^6$ $m^3$ of hydrogen per day emits 0.3-0.4 million standard $m^3$ of $CO_2$, which

is typically released into the environment [114]. Potential nuclear-based hydrogen generation techniques are described in section 2.6.

Hydrogen can be used to power a facility (based on Turbogas technology) or for mobile applications by being stored in an integrated system that provides dispersed renewable energy and is coupled to a base-loaded nuclear power grid [116].

### 2.5.1 Hydrogen's Future in Relation to Gasoline

If $CO_2$ emissions are taken into account, efficiency can be significantly reduced to an economic problem that needs to be addressed at the level of the entire value chain. This is noteworthy because hydrogen can be produced with nearly no greenhouse gas emissions and can be used far more effectively in some applications than other fuels. For instance, a hydrogen fuel cell in a car operates at a 60 percent efficiency, compared to a 20 percent efficiency for a gasoline internal combustion engine [20]. Hydrogen has three times more energy (120.1 MJ/kg) per unit of mass than gasoline and also has more energy than natural gas. Therefore, it is thought that hydrogen is a promising fuel for transportation given its high-power density with a concern of hydrogen storing.

By 2030, the cost of gasoline for car owners, after accounting for the efficiency of turning hydrogen into electricity, will be approximately 10 US$/kg-$H_2$. In comparison to the anticipated hydrogen price (US$ 7.5–9.0 per kg $H_2$) in 2030, it suggests that the hydrogen expenses delivered by 2030 will be reasonable [20]. For these reasons, it's feasible that hydrogen will eventually take the place of gasoline in the next years.

## 2.6 Nuclear Hydrogen Production

The growing global energy demand is largely being met by nuclear power plants [117]. The only carbon-free (or low-carbon) possibilities for producing clean hydrogen are

nuclear and renewable energy [118]. Thermochemical reactions using high-temperature reactors may be made possible by electrolysis, which makes use of electricity from intermittent renewable or reliable nuclear sources as well as direct utilization of heat from nuclear energy [66].

Compared to producing hydrogen using fossil fuels, producing green hydrogen is more expensive [58]. According to Table 2.2 [1], green hydrogen is more expensive than black, blue, and grey hydrogen, costing between US $2.5 to $7.39/kg-$H_2$. Table 2.3 [1, 4] provides an overview of the cost of producing green hydrogen using conventional (alkaline) electrolysis. Low-temperature electrolysis at 60 °C and 0.1 MPa requires 180 MJ of power, 26.2 MJ of heat energy, and 11.5 kilogram of water to produce 1 kg of hydrogen. 1 kilogram of hydrogen costs US $5.92 to produce, based on the cost of heat and electrical energies per unit [4]. According to [58], the price of $CO_2$-free aqua hydrogen is US$ 0.23 per kg of hydrogen. Table 2.2 provides information on the price of creating hydrogen using different technologies.

Furthermore, since the cost of producing hydrogen by conventional electrolysis (low temperature electrolysis) plays such an important role in the clean hydrogen economy, using renewable energy sources is a good choice for clean hydrogen production. This is why photovoltaic (PV) panels, a sustainable energy source, were utilized in a study incorporating all key techno-economic criteria to compute the cost of electrolytic hydrogen [119];

- Electricity consumption: 57.85 kWh/kg-$H_2$
- Investment cost: 368 \$/$kW_e$
- Operation life of the electrolyser: 7 years

- Project lifetime: 30 years
- Discount rate: 6%
- Hydrogen capacity production: 250 t/year

The cost of green hydrogen produced through electrolysis, which is more than the cost of other varieties of hydrogen like black, blue, and grey hydrogen, is estimated to be roughly \$7/kg-$H_2$ [119]. It is also shown that the cost of producing hydrogen with a PV energy source is dominated by electricity costs, which account for more than 70% of the total cost.

Another study [120] found that the price of producing hydrogen using low temperature electrolysis is \$6.75 per kg-$H_2$, with parameters of production capacity of 1500 kg/day, capital cost of \$0.96, feedstock cost of \$5.06, and operation and maintenance (O&M) cost of \$0.73.

Table 2.2: An overview of the prices for generating hydrogen utilizing various technologies that have been published in the literature. Note that CCUS is carbon capture use and storage [1].

| | Methods | | | | | | | | |
|---|---|---|---|---|---|---|---|---|---|
| | Black Hydrogen without CCUS | Grey Hydrogen without CCUS | | Blue Hydrogen with CCUS | | Green Hydrogen | | | |
| Energy Source | Coal | Natural Gas | | Coal | Natural Gas | Renewable Electricity | | | |
| Location | Canada | Canada | | Canada | | Canada | | | Europe |
| Hydrogen Cost (US\$/kg-$H_2$) | 1.35 | 1.31 | 0.67-1.05 | 1.60-2.05 | 1.61-1.83 | 7.39 | 2.56-6.84 | 2.28-3.69 | 2.36-8.26 |
| Reference | [58, 121] | [58, 121] | [58, 122] | [58, 121] | | [58, 123] | [58, 124] | [58, 122] | [58, 125] |

Note: Hydrogen prices in €/kg are converted into US\$/kg-$H_2$.

An overview of the prices for generating hydrogen utilizing various technologies that have been published in the literature. Fossil fuel-derived hydrogen generates a substantial amount of emissions, which is detrimental to the environment and the issue of climate change [93]. On the other hand, hydrogen may be produced almost entirely without

the generation of carbon dioxide utilizing electricity from nuclear power plants. Hydrogen may be extracted from ocean water using nuclear energy, a clean energy source [16]. When viewed from this aspect, nuclear power facilities will be essential for the large-scale production of hydrogen in the future [82].

Figure 2.4: Nuclear hydrogen generation scheme [1].Figure 2.4 depicts nuclear energy being used to produce hydrogen. In this scenario, a nuclear power plant transfers heat and electrical energy to a hydrogen production facility so that hydrogen can be produced by separating water [126]. According to the literature [21, 30, 77, 88, 98, 99, 127-134], hydrogen can be produced in a variety of processes, including high temperature steam reforming, coal gasification, traditional water electrolysis, thermo-chemical cycles, hybrid, and high temperature electrolysis.

Table 2.3: A breakdown about using alkaline electrolysis for per kg of hydrogen [1].

| Parameters | | Inputs (/kg $H_2$) | | Outputs (/kg $H_2$) | |
|---|---|---|---|---|---|
| $T_{max}$ (°C) | 60 | Electricity (MJ) | 180 | $H_2$ (kg) | 1 |
| Pressure (MPa) | 0.1 | Heat (MJ) | 26.2 | $O_2$ (kg) | 8 |
| TRL | 9 | Water (kg) | 11.5 | $CO_2$ (kg) | 0 |
| $H_2$ Yield eff. (HHV)** | 29.8 | | | Production cost* | $US 5.92 |

*Production cost (est. $US 2019).
**Assuming a power cycle conversion efficiency of 40%. (HHV: Higher heating value)

Nuclear power plants are more efficient at producing heat than they are at producing electricity. Additionally, nuclear energy can be utilised to produce hydrogen since high temperature electrolysis and thermochemical cycles demand electricity and particularly high temperatures of 500 - 830°C, which implies they require more heat energy than electrical energy [17, 42, 43, 77].

### 2.6.1 SMR Design & Engineering & Production of $H_2$ from a Co-located Plant

Approximately 70 SMR/MMR designs are in various stages of development, according to the IAEA [135]. It is becoming clear that only a small number of the 70

SMR/MMR concepts that are now in various stages of development will be developed to a point where they are ready for construction and commercial application. Here, there are three constraining metrics are relevant: regulator approval (of some sort), large investments and the start of new plant construction. Safety-in-design of the SMR/MMR (here restricted to SMRs) is a given and has to be achieved. Also, according to reactor (SMR) concepts, safety-in-design needs to be considered. When viewed from this angle, the most likely reactor is a light water-cooled, water-moderated (and reflected) design. The reason why is that LWRs – PWRs and BWRs have the most global operational experience. Even though CANDU reactors have unique technical benefits, fewer of them have been installed, are in operation globally, and a CANDU-like SMR is largely conceptual. Since the beginning of the commercial nuclear era, geopolitics (at the level of the Group of Seven) has been crucial in ensuring the sale of reactor ideas. Some of the "players" in the Group of Seven's commercial nuclear energy policy are known to include the United States, Russia, China, France, Korea, and Japan.

Regarding safety in design, passive safety system (PSS) R&D and technology development has attracted attention according to private communications with Akira Tokuhiro [136]. The following is the most recent thinking regarding PSS for integral PWR (iPWR) type SMRs: 1) the application of dynamic PRA/PSA techniques (outside the subject of this study); and 2) the time evolution of any unforeseen event or unforeseen initiating event that has a low to low probability, but a significant impact on the SMR safety-in-design. At the system level, the time evolution – in particular 1 hour, 2 hours, 4 hours, 8 hours, 16 hours, and 24 hours after the accident began, is strongly related to the PSS system's time-response and many other types of SMR safety-in-design events. Therefore, these time "slots" are linked to safety-in-design and need be considered as a

design variable and parameter. It can also be assumed that anything over 4 hours will require reactor shutdown; thus, it is evaluated in two categories as under 4 hours and over 4 hours.

- In terms of the emergency planning zone (EPZ) [137] required for all nuclear power plants, Canadian Nuclear Safety Commission (CNSC) (US, or national) regulations will take precedence, provided that SMRs are co-located with a renewable plant and a hydrogen plant until there is (nuclear and related) regulatory change. One key document in Ontario is termed as the Provincial. The owner/operator of the SMR will be held to further standards by the CNSC.
- SMR (and new reactors) may be anticipated to establish as technical foundation to substantiate the EPZ in accordance with the approval (by the USNRC) of the new technique to evaluating the EPZ [137]. The EPZ might well be built on a hypothetical accident with low probability but significant consequences (radiation emission), where the accident's temporal progression is an important consideration. This is due to the fact that the public cannot be completely evacuated in 24 to 48 hours. Therefore, it is crucial to include safety-in-design of SMRs and new nuclear power plants, which forbids any human interaction (and error), as well as "walk away" passive safety system (PSS) design. Furthermore, it is anticipated that new SMR and reactor designs will remain operator-free for 24 to 48 hours.
- The majority of iPWR type SMRs and distinct SMRs (of all types) with the greatest public safety-in-design data have unique PSS designs. Many rely on gravity-driven one-time coolant inventory addition and naturally occurring convection-driven flows (pressure valve opening). Details about the time evolution of the SMR's PSS are confidential, so no information is available; however, there will be variations

among the several SMR designs [138]. The important point here is the time evolution of the accident, after the accident or event initiation.

- The time response, say 1 hour, 2, 4, 8, 24, or 48 hours after event start, is crucial and connected to the safety-in-design of the SMR at the level of the (nuclear; SMR) safety system. Safety must always be upheld even if the SMR is connected to a renewable energy or hydrogen production facility. The safety of the SMR must not be compromised by any disruption to the hydrogen or renewable energy plant.
- Therefore, if lost for any reason, the SMR design as well as the electrical requirements of the SMR plant must be provided. The issue at hand is whether the SMR's electrical needs can be met by the CSP or by an emergency diesel generator (EDG). As a result of the nuclear plant accident at Fukushima Daiichi in 2011, this is a concern.
- In terms of safety-in-design, the elapsed period after accident onset is thus generally linked to the SMR's design.

## 2.7 Thermochemical Cycles for Hydrogen Production

Many thermochemical hydrogen production cycles based on the basis of employing clean energy sources that do not produce greenhouse gases to thermally split water into oxygen and hydrogen through chemical processes. Approximately 200 thermo-chemical cycles for producing hydrogen in this manner have been documented in the literature [130]. Two thermochemical cycles play a significant part in creating hydrogen according to some criteria, including efficiency, cost analysis, complexity, and industry adaptability: copper-chlorine and sulfur-iodine, which identified as being extremely promising [139]. They are both different from one another in terms of efficiency and general requirements. Utilizing sulfur-iodine (S-I) or copper-chlorine (Cu-Cl) thermo-

chemical cycles, heat rather than electricity acts as the principal energy source for splitting water to produce hydrogen [17]. Chemicals are collected and reused during these cycles [17, 130]. Because the temperature requirements for the sulfur-iodine thermochemical cycle are higher than those for copper-chlorine (approximately 850°C), it can be utilised in conjunction with a Very High Temperature Nuclear Reactor (VHTR) that is gas cooled [16, 64, 140]. On the other hand, the Cu-Cl thermochemical cycle, which needs a lower temperature than the S-I cycle [17], can be favoured with other available energy sources. A schematic for producing hydrogen via nuclear power is depicted in Figure 2.4.

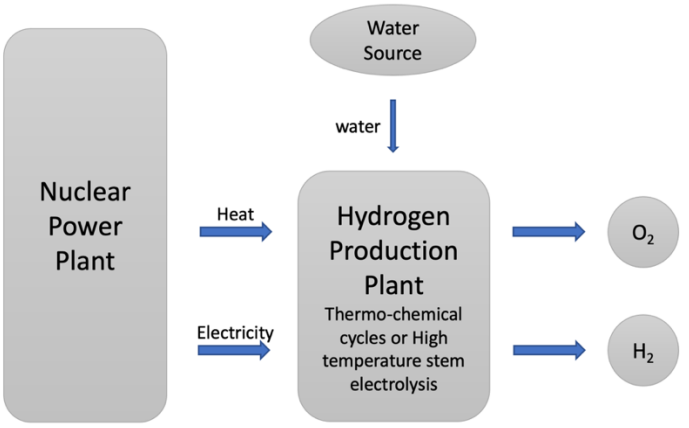


Figure 2.4: Nuclear hydrogen generation scheme [1].

### 2.7.1 Copper-Chlorine (Cu-Cl) Cycle

Seven different types of Cu-Cl cycles exist in the literature [65]. Researchers found that the four-step Cu-Cl cycle, which has a net efficiency of roughly 43% [110], has the highest energetic and exergetic efficiency [141]. Concentrated solar power (CSP) systems or new-generation nuclear reactors can provide the heat needed for Cu-Cl at roughly 530°C [129, 142-144]. The Cu-CI thermochemical cycle may be preferred to create hydrogen because solar and nuclear energy are both clean sources of energy [142].

Hydrolysis, thermolysis, electrolysis, and drying are the four phases in the Cu-Cl cycle [128, 130, 145].

- The hydrolysis-based first step is:

$$2CuCl_2(s) + H_2O(g) \rightarrow Cu_2OCl_2(s) + 2HCl(g) \rightarrow \text{(at 375-400°C [145])} \quad (1)$$

- The decomposition of copper oxychloride occurs in the second step, known as thermolysis, at temperatures of roughly 500–530°C;

$$Cu_2OCl_2(s) \rightarrow ½\ \mathbf{O_2(g)} + 2CuCl(l) \quad (2)$$

- The electrolysis process, the third step;

$$2CuCl(aq) + 2HCl(aq) \rightarrow \mathbf{H_2(g)} + 2CuCl_2(aq) \rightarrow \text{(at 25°C)} \quad (3)$$

- Drying of aqueous cupric chloride occurs in the fourth step at a temperature of 30°C to 80°C;

$$CuCl_2(aq) \rightarrow CuCl_2(s) \quad (4)$$

Super-critical water reactors (SCWRs) can be used to supply the heat required for the Cu-Cl cycle because the temperature required is below 550°C [84, 98]. The Generation-IV SCWR power generation efficiency is 42%, which equates to a net efficiency of approximately 30% for electrolysis-based hydrogen production [110].

### 2.7.2 Sulfur-Iodine (S-I) Cycle

Although there are many different forms of S-I cycles in the literature, the three-step S-I cycle is the most common [140, 146]. S-I cycle efficiency is similar to that of Cu-CI [17].

- Hydrolysis is the first step (exothermic):

$$I_2\ (l+g) + SO_2(g) + H_2O(g) \rightarrow 2HI(g) + H_2SO_4(l) \rightarrow (\text{at } 120°C) \quad (5)$$

- The production of oxygen is the second step (endothermic):

$$H_2SO_4(g) \rightarrow SO_2(g) + H_2O(g) + \tfrac{1}{2}O_2(g) \rightarrow (\text{endothermic at } 850°C) \quad (6)$$

- Hydrogen generation is the third step (endothermic).

$$2HI(g) \rightarrow I2(g) + H_2(g) \rightarrow (\text{at } 450°C) \quad (7)$$

Three chemical reactions are required for this process, together with the utilization of heat and water. In this cycle, the water is divided into oxygen and hydrogen, and the other components are recycled to be used once more. The first procedure, referred to as "catalytic breakdown of sulfuric acid," requires heat of at least 850°C [17, 146]. By limiting pressurization dangers in chemical facilities and lowering high temperature stresses, low pressure also improves safety. This cycle's compatibility with high-temperature nuclear reactors has undergone research, and estimates of the overall process efficiency and hydrogen cost have also been made. According to early predictions, the S-I processes may produce hydrogen with an efficiency of 45% to 55% [98].

**2.8 High Temperature Electrolysis (HTE)**

Hydrogen can also be generated from water via electrolysis [23, 42, 56, 88, 110]. High temperature electrolysis and conventional electrolysis are the two types of electrolysis that have been discussed in the literature [88, 99]. The disparities are brought on by variations in temperature [99]. High temperature electrolysis requires heat at temperatures above 100°C [77], whereas usual electrolysis occurs at temperatures below 100°C [147]. High temperature electrolysis is often referred to as "high temperature steam

electrolysis" because at working temperature, water exists as steam. "High temperature" in this section refers to temperatures more than 600°C [77].

The principle of conventional electrolysis is widely known: pure oxygen is produced on the anode, while hydrogen is produced on the cathode by transferring energy through electrochemical cells inside the water electrolysis unit [77, 148]. 4% of the hydrogen produced worldwide is produced using conventional electrolysis [149]. It implies that the demand for hydrogen in the world cannot be satisfied by conventional electrolysis. Therefore, high temperature electrolysis (HTE) is required for the synthesis of hydrogen on a large scale.

In contrast to conventional electrolysis, high temperature electrolysis (HTE) requires mostly on heat energy rather than electricity to operate. At 2500°C, water undergoes thermolysis to break down into hydrogen and oxygen; no power is needed [150]. The elimination of the rather wasteful process of transferring heat to electricity makes it more efficient than standard electrolysis, but it also necessitates a much higher temperature source. The HTE can use energy from nuclear reactors to produce the heat and electricity needed to create the steam for electrolysis [42]. Nuclear reactors power the HTE by producing heat and electricity, both of which are necessary to generate steam for electrolysis [42, 98].

By adding extra energy to the grid when demand is high and drawing power from the grid when demand is low to produce hydrogen, such HTE facilities can significantly contribute to grid balancing. Over the whole temperature range of 0°C to 2500°C, a combination of electricity and heat is used as the energy input [77]. High temperature steam electrolysis (HTSE) consumes 2.5 [$kWh_e/Nm^3$] and 0.92 [$kWh_t/Nm^3$] of electrical and thermal energy, respectively, at 850°C (a typical temperature) [68, 77]. Nuclear

reactors with Generation-IV Small Modular Reactors are the best option to provide the necessary heat energy since high-temperature electrolysis requires a high-temperature environment, often greater than 600°C [16, 42].

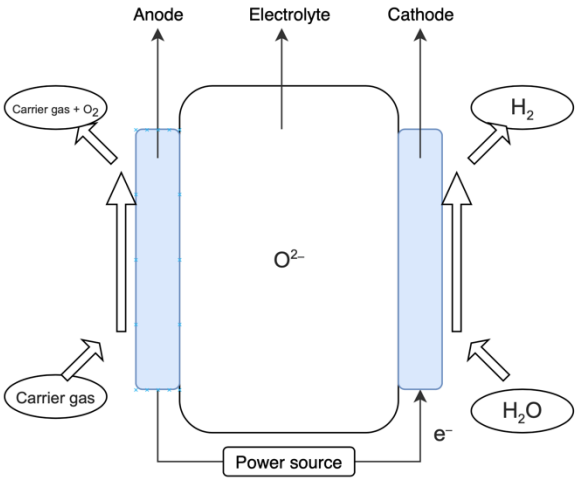


Figure 2.5: HTE mechanism [1].

A cathode (hydrogen electrode), anode (oxygen electrode), and electrolyte make up an electrolysis cell in the HTE mechanism. The cathode is connected to one side of the electrolyte, and the anode to the other. Before entering the electrolysis cell as steam in the HTE process, water is heated by external heat. Applying steam to the cathode of an electrolysis cell causes the steam to break down into hydrogen and oxygen ions, as shown in equation (8). The oxygen ion is then supplied to the anode via the oxygen ion conductivity of the electrolyte after the hydrogen has been extracted as a hydrogen product. The oxygen ion is produced at the anode as the oxygen product, as shown in equation (9). High-temperature electrolysis processes are described by equations (8) and (9), and equation (10) is the result of equations (8) and (9). The process of splitting water into hydrogen and oxygen is shown in equation (10). In Figure 2.5, the HTE's operational mechanism is illustrated.

$$H_2O + 2e^- \rightarrow H_2 + O^{2-} \quad (8)$$

$$O^{2-} \rightarrow \frac{1}{2} O_2 + 2e^- \quad (9)$$

$$H_2O \rightarrow H_2 + \frac{1}{2} O_2 \quad (10)$$

The overall efficiency of the hybrid system (NPP and HTE) is much lower due to nuclear power plant efficiencies of approximately 33% [100], despite the fact that the HTE efficiency of conversion from electricity to hydrogen may reach up to 80%.

**2.9 Comparison of The Potential Methods**

Performance comparison is shown in Figure 2.6 with respect to the potential for global warming (GWP), acidification (AP), social cost of carbon (SCC), cost of hydrogen production, and energy and exergy efficiencies to generate hydrogen (the most popular hydrogen production cycles described in the paragraph above) employing nuclear energy [14, 22]. When Cu-Cl and S-I hydrogen production thermochemical cycles are compared to HTE in terms of energy efficiency and exergy efficiency, cost, GWP, AP and SCC, these two thermochemical cycles are better than HTE. Although these two thermochemical cycles are almost the same specifications in terms of energy efficiency and exergy efficiency, cost, GWP, AP and SCC, the temperature requirement of S-I cycle (850°C) is more than that of Cu-Cl (525°C).

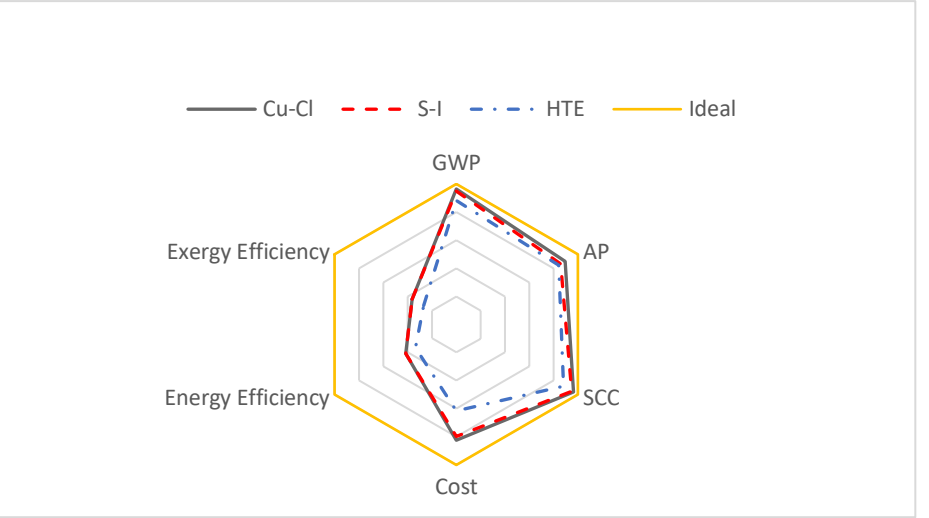


Figure 2.6: Comparison of the common nuclear hydrogen production methods, namely, Cu-Cl and S-I cycles, HTE [1].

## 2.10 Technology Readiness Level

The term "development risk" refers to the degree of vulnerabilities for each new technology that must be examined prior to adoption. A programme for technology development and demonstration that enables timely distribution of N-RHES needs be specified in the technology development strategy. Development risk has been changed into a qualitative composite value based on the preparedness of the subsystems as a result. Instead of focusing on industry-standard processes like waste management or water treatment, the focus is on generic technology-specific components [151].

Each technology has specified its present Technology Readiness Level (TRL) for the major parts of the Nuclear-Renewable Hybrid Energy System (N-RHES) Technology Development Program Plan [4, 152].

When a hybrid system is analyzed in terms of TRL, the system TRL score is determined by the lowest component TRL score. TRLs for N-RHES are depicted in Figure 2.7 in a simplified manner [1].

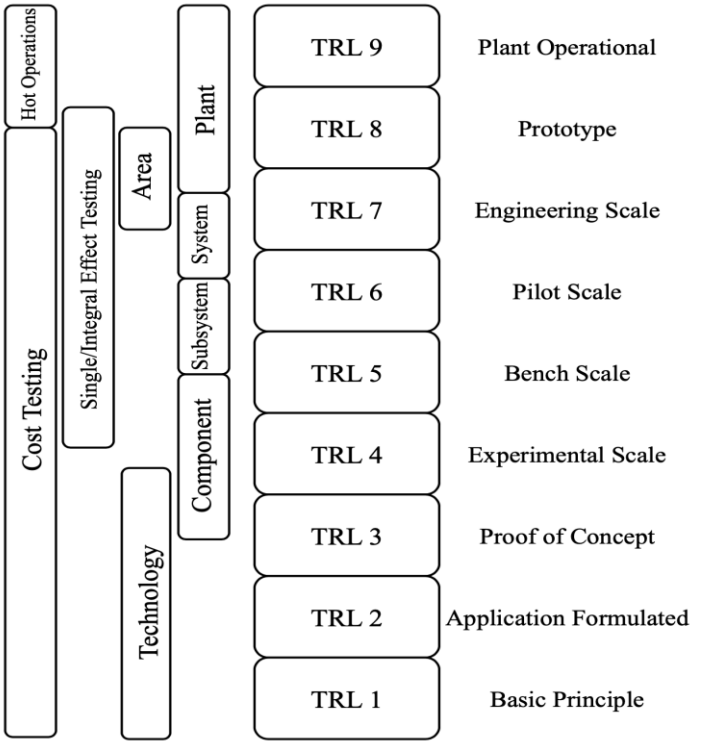


Figure 2.7: A demonstration of TRLs [1].

The TRLs of potential hydrogen production techniques, along with their costs and required maximum temperatures, are shown in Figure 2.8.

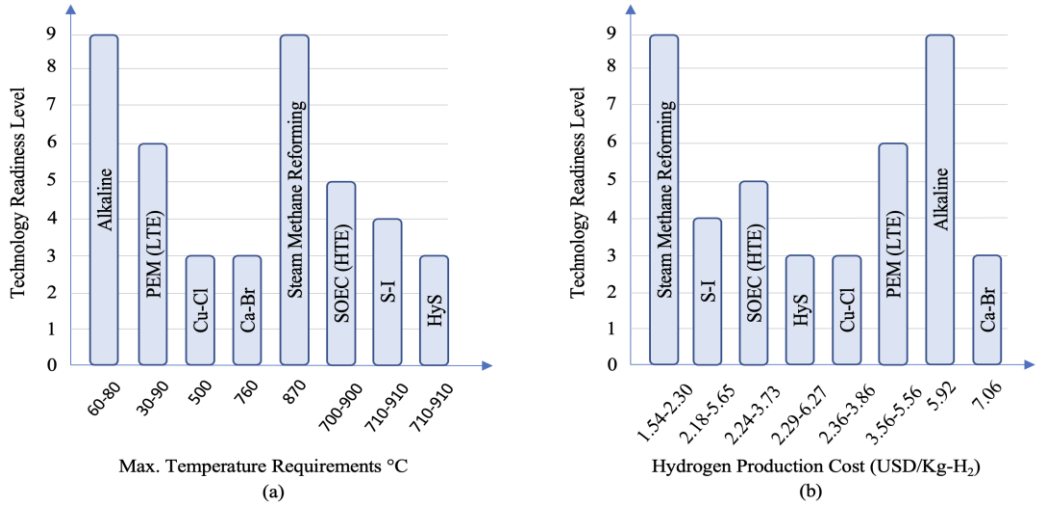


Figure 2.8: TRL of various N-RHES hydrogen production systems in accordance with maximum temperature requirements (a) and hydrogen production cost (b) [1].

The Idaho National Laboratory and three commercial electric companies have been selected to upgrade existing facilities to electrolyze hydrogen without carbon. The primary energy source, as well as for transportation and storage, will be hydrogen. Alkaline electrolysis, or low temperature electrolysis, with a TRL rating of nine is to be used in the project to generate hydrogen that is entirely free of carbon. This research project's main objective is to increase long-term economic competitiveness by demonstrating the competitiveness provided by nuclear power when compared to renewable energy [153]. It makes sense to consider the most compatible subsystems while optimising the key energy sources described above and the hydrogen generation method previously compared. When it comes to multi-objective optimization, Genetic Algorithm is commonly used [154]. As a result, optimization based on Genetic Algorithm is addressed in the following section.

## 2.11 Optimization

The benefits of obtaining the best outputs (results) possible in a specific circumstance is referred to as "optimization process" [8, 33, 38, 39, 155]. In its most basic form, an optimization problem entails choosing input values from a range of viable alternatives and calculating the value of a real function to maximise or minimise it. An important area of applied mathematics is the generalisation of optimization theory and techniques to new formulations. The general goal of optimization, which is applicable to a wide variety of objective functions and domains, is to find the "best available" values of some objective function given a certain input [155].

## 2.12 Complexity and Multi-objective Optimization

Complexity in engineering systems, including design and analysis, refers to multi-tasks with multiple variables. The quantity of variables, parameters, and numerous

objectives in dynamic system behaviour can be used to simply define complexity. For instance, while cost reduction is desired, it is anticipated that the yield (hydrogen), which depends on multiple parameters, will rise. This illustrates the distinction between optimizations with a single and multiple objective optimizations.

It is clear from the literature that several optimization techniques have been used for various areas [57, 117, 125, 131, 156-158]. One of these is Pareto Optimality (Pareto Efficiency), which describes a situation in which no preference criterion can be improved upon without making at least one other criterion worse off or lose its optimal "value" [159, 160]. Pareto optimality, which can be used in nuclear and economic systems, plays a key role in complicated multi-objective optimization issues [143] where trade-off decisions are crucial in determining the "most suitable" system for the underlying conditions rather than necessarily the "best" mathematically. Objective functions can be redefined in accordance with the output required at the time thanks to the complexity's flexibility. For instance, in a hybrid nuclear-renewable hydrogen production facility, more hydrogen can be generated in place of electricity when the price or demand for electricity declines.

Data-driven methodologies have been implemented to improve the outputs in the nuclear technology sector [36]. Artificial intelligence with Algorithms can be applied to optimise a variety of processes in complex systems [33, 117, 131, 161]. For example, linear, integer, and non-linear optimization with the methods of “Solver Decides”, “Backward Analytical”, “Forward Analytical”, “Central Differences”, and “Forward Differences” can be conducted using the Lindo® What's Best tool [40, 41]. It was first released for Lotus, and then later for Microsoft excel [162-164]. With specified configurations and parameters, the tool provides the best result [39].

## 2.13 Multi-objective Optimization Methods

### 2.13.1 Priori Articulation of Preference Methods

By using these techniques, scientists and engineers can pinpoint preferences or goals that can be stated in terms of the relative importance of several goals. The majority of these methods contain parameters together with coefficients, exponents, constraint limitations. Following are priori articulation of preference methods:

- Weighted global criterion method
- Weighted sum method
- Lexicographic method
- Weighted min-max method
- Exponential weighted criterion
- Weighted product method
- Goal programming methods
- Bounded objective function method

The issue of which method is superior arises given the variety of approaches. Sadly, there isn't a simple response to this query. However, it is preferable to use techniques that offer both the conditions required and sufficient for Pareto optimality. The benefits of obtaining just Pareto optimal solutions (that used a formulation which meets a necessary condition) are clear when one is trying to find a single solution.

### 2.13.2 Posteriori Articulation of Preference Methods

It can be challenging for the decision-maker to give an explicit approximation of the preferred function in some circumstances. Consequently, letting the decision maker select from a range of options can be effective. To do this, a form of the Pareto optimum

set is chosen using an Algorithm. These techniques, also referred to as cafeteria or produce first, choose later approaches, require post-articulation of preferences [165]. Followings are posteriori articulation of preference methods:

- Normal boundary intersection (NBI) method
- Normal constraint (NC) method

The aforementioned techniques enable the decision-maker to view the possibilities before choosing. One merely considers which option is the most appealing; one does not consider whether objective function is either more or less essential.

### 2.13.3 No Articulation of Preference Methods

The decision-maker frequently struggles to express his preferences in clear, specific terms. As a result, the techniques listed below do not necessitate the declaration of preferences. The majority of the techniques simplify "2.13.2 Posteriori Articulation of Preference Methods," usually by omitting method parameters. Following are no articulation of preference methods:

- Global criterion methods
- Nash arbitration and objective product method

Despite the fact that this methodology incorporates a variety of strategies, the two fundamental formulations are the objective product and the exponential sum. The formula for the exponential sum is a specific case of the minimum essential and objective sum procedures. A variant of these fundamental scalarization formulations is all that is required for the majority of other ways that do not need for the declaration of preferences.

## 2.14 Genetic Algorithm

The techniques that have been described thus far include multi-objective optimization techniques and original formulations that were resolved using traditional optimization Algorithms (single-objective optimization method). However, methods like Genetic Algorithms are modified to proactively address multi-objective issues. This is the reason why Genetic Algorithm optimization method used in this thesis.

Genetic Algorithms are a search and optimization method based on natural selection principles. Its basic principles were put forward by John Holland [166]. After the basic principles were revealed, many scientific studies about Genetic Algorithms have been published. In addition, many international conferences are held on the theoretical part and applications of Genetic Algorithms. Genetic Algorithms have successful applications in areas such as function optimization, scheduling, mechanical learning, design, and cellular production. Genetic Algorithms, which differ from traditional optimization methods, use their coded form, not the parameter set. Genetic Algorithms operating according to probability rules only need objective function. They scan a specific part of the solution space, not the whole. Thus, they reach a solution in a much shorter time by making an active search [167]. Another important advantage is that they analyze the population of solutions simultaneously and thus do not get stuck with the local best solutions.

### 2.14.1 Fundamental Theorem of Genetic Algorithms

How Genetic Algorithms search is explained by the concept of subsequence. Subsequences are theoretical constructs used to explain the behavior of Genetic Algorithms. A subsequence is a sequence that describes the similarity between certain sets of sequences. Substrings are defined using the (0 , 1 , *) alphabet. For example,

subsequence *H* is for the set of chromosomes with a value of 0 in the first position and 1 in the second and fourth positions.

$$H = 0\ 1\ *\ 1\ *$$

The "*" symbol means that it doesn't matter what value that position of the array takes or not. The array can take the value 0 or 1 at that location. If a sequence x fits the pattern of the substring, the sequence x is said to be "an instance of *H*". Substrings have two properties. These features are given below [167].

**1. Subsequence degree:** The degree of a substring *H* is denoted by *o(H)* and is the number of fixed positions found in the current substring pattern. This number is equal to the sum of the number of values 0 and 1 in the binary alphabet.

**2. Substring length:** The length of a substring *H* is denoted by $\delta(H)$ and is the distance between certain initial and final positions found in the current substring pattern.

The concepts of subsequence degree and subsequence length have an extremely important place in the fundamental theorem of Genetic Algorithms. Sequences with a low subarray degree and a short substring length are called "building blocks". John Holland proposes identifying suitable building blocks in the operation of Genetic Algorithms and combining these building blocks to obtain more suitable building blocks. This idea is known as the building blocks hypothesis. The basic theorem of the Genetic Algorithm is explained as follows [166]:

Subsequences of short length and low rank, showing greater coherence than the population mean, multiply exponentially with the passage of time. This reproduction takes place through genetic processes, and as a result, individuals with superior characteristics

than parents emerge. The increase in the quality of this solution from generation to generation is attributed to two reasons. These reasons can be explained as follows [168]:

- Since the reproductive chances of unsuccessful individuals are reduced, the deterioration becomes more difficult.
- The structure of Genetic Algorithms not only prevents deterioration, but also provides a rapid improvement over time, according to the basic theorem of Genetic Algorithms.

These reasons are better understood when the processing steps of Genetic Algorithms are examined. Due to its nature, Genetic Algorithms eliminate bad individuals, that is, unsuitable solutions, thanks to their operators. These processes continue in a loop until the stopping criterion is met.

### 2.14.2 Basics of Genetic Algorithm

Genetic Algorithms encode each point in a solution space with a binary bit sequence called a chromosome. Each point has a fitness value. Rather than a single point, Genetic Algorithms maintain a set of points as a population. In each generation, the Genetic Algorithm creates a new population using genetic operators such as crossover and mutation. After several generations, the population contains members with better fitness values. This is similar to Darwin's models of evolution based on random mutation and natural selection. Genetic Algorithms include coding solutions, calculating fitness, applying multiplication, crossover and mutation operators [169].

In Figure 2.9 the mechanism of a canonical Genetic Algorithm is depicted. The creation of a population of solutions, identification of the objective function and fitness

function, and use of genetic operators are the main processes. Below is a quick description of these features.

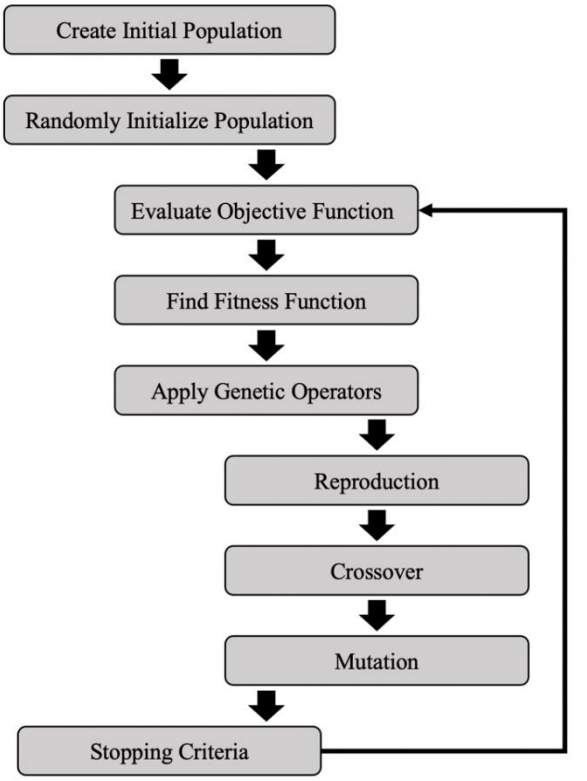


Figure 2.9: Algorithm of "Genetic Algorithm".

In Figure 2.10 a generation is divided into a selection phase and a recombination phase according to the fundamental Genetic Algorithm activities. During selection, strings are assigned to adjacent spaces.

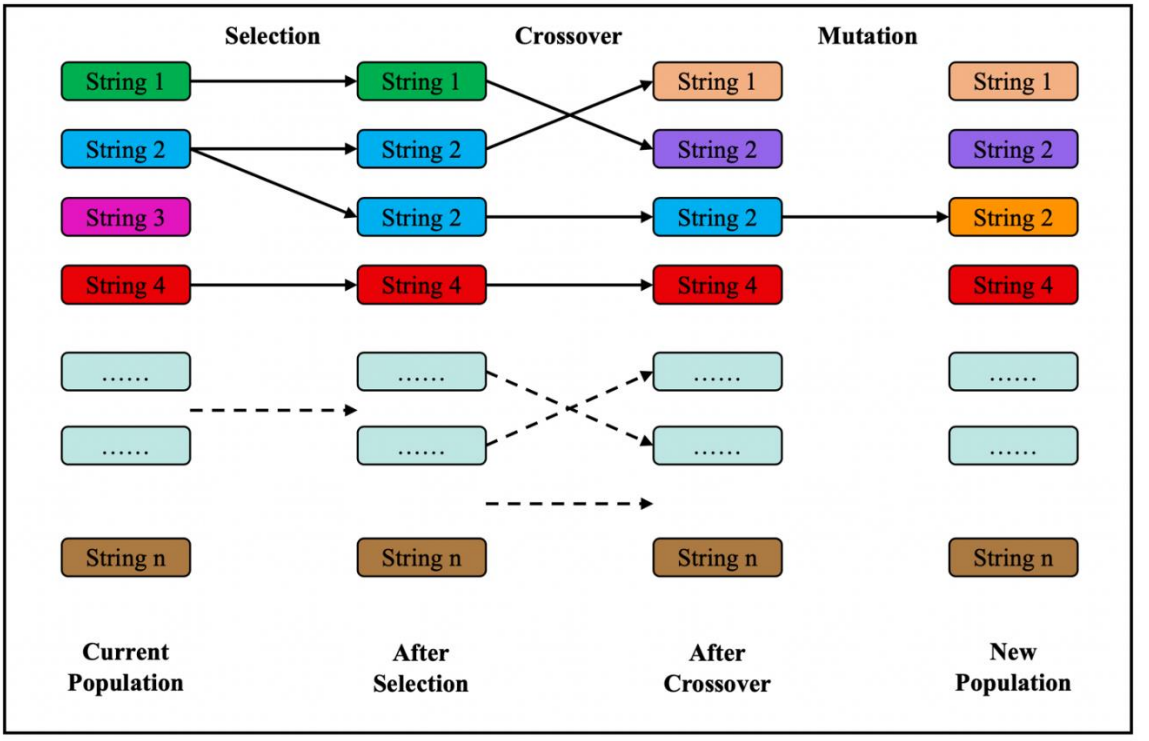


Figure 2.10: An example of Genetic Algorithms.

### 2.14.2.1 Coding Solutions

The first step in developing a Genetic Algorithm for solving a problem is to represent all the solutions as a string of bits with the same dimensions. Each of the sequences represents a random point in the space of possible solutions of the problem [170].The coding of parameters allows the conversion of problem-specific information into the form used by the Genetic Algorithm [169].

### 2.14.2.2 Creating the First Population

A solution group is created in which possible solutions are coded. The solution group is called the population, and the codes of the solutions are called chromosomes. Random number generators can be used to generate the first population in the representation of chromosomes using the binary alphabet. The random number generator is called and the position is set to 0 if the value is less than 0.5, otherwise to 1 [171]. In

problems where the number of individuals and the chromosome length are low, position values can also be determined by flipping a coin. Apart from the binary coding method in Genetic Algorithms, different coding methods are also used depending on the problem to be solved [167].

#### 2.14.2.3 Calculation of Conformity Value

The first step after a generation is created is to calculate the fitness value of each member in the population. For example, for a maximization problem *i*. The fitness value of the member *f(i)* is usually the value of the objective function at that point [169]. There is a fitness function for every problem whose solution is sought. For a given chromosome, the fitness function returns a numerical fitness value that is proportional to the use or ability of the solution represented by that chromosome. This knowledge guides the selection of more suitable solutions in each generation. The higher the fitness value of a solution, the higher the chance of survival and reproduction, and the higher the representation rate in the next generation [172].

#### 2.14.2.4 Application of the Multiplication Process

In the multiplication operator, sequences are copied according to the objective function and individuals who will better pass on good hereditary traits to the next generation are selected. The reproduction operator is an artificial selection. Duplicating sequences according to their fitness values means that sequences with higher fitness values are more likely to contribute to one or more offspring in the next generation. Replication consists of the process of selecting individuals, copying selected individuals into a matching pool, and dividing individuals into groups in pairs in the pool [173].

After the fitness value calculation step, a new population needs be created from the current generation. The selection process decides which families need be involved in order

to produce offspring for the next generation. This is analogous to the survival of the fittest in natural selection. The purpose of this method is to give an opportunity to multiply to values above the mean fitness. The chance of a sequence being copied depends on the fitness value of the sequence calculated with the fitness function [169]. Examples of selection methods are selection methods such as roulette wheel selection, tournament selection and ranking selection.

#### 2.14.2.5 Application of the Crossover Operation

To explore the potential of the current gene pool, the crossover operator is used to create new chromosomes with better traits than the previous generation. Crossover is generally applied to family varieties selected with a probability equal to a given crossover ratio [169].

The crossover operator, which is one of the important parameters affecting the performance of the Genetic Algorithm, corresponds to the crossover in natural populations. Two chromosomes are randomly selected from the new population obtained as a result of the multiplication process and are subjected to the mutual crossover process. In the crossover operation, the integer k is selected in the range of $1 <= k <= L-1$, with the string length L. The array is traversed according to this integer value. The simplest crossover method is the one-point crossover method. Both chromosomes must be of the same gene length for a single point crossover to occur. In two-point crossover, the chromosome is cut from two points and the positions are swapped [173].

#### 2.14.2.6 Application of the Mutation Process

Crossover is used to search for available gene potentials. But if the population does not contain all the necessary encoded information, crossover cannot produce a satisfactory solution. Therefore, an operator capable of generating new chromosomes from existing

chromosomes is required. Mutation performs this task. In artificial genetic systems, the mutation operator provides protection against the loss of a good solution that there is a possibility if may not be obtained again [167]. In problems where the binary coding system is used, the mutation converts one bit value (can be 0 or 1) to the other bit value under a low probability value. In problems where the binary coding system is not used, different mutation methods are used. Whichever method is used, the general purpose of mutation is to provide or maintain genetic diversity [174].

### 2.14.3 General Application Areas

#### 2.14.3.1 Optimization

Genetic Algorithms, a search method, are used to solve optimization problems in different branches of science. Optimization problems in which Genetic Algorithms are applied can be grouped under function optimization and combinatorial optimization.

An important part of Genetic Algorithm research is related to function optimization. Genetic Algorithms are more effective in solving difficult, discontinuous and noise-containing functions than traditional optimization techniques [173]. If the objective function to be optimized is discontinuous, optimization methods based on differentiation cannot be used since the function cannot be differentiated at the discontinuity points. However, since Genetic Algorithms do not require derivative or other auxiliary information for solving problems, they provide a significant advantage over traditional methods, especially in solving such problems [175].

The other applications are as follows;

- Mechanical Learning.
- Economic and Social System Models.

## Chapter 3. Mathematical Modeling of the N-RHES

This chapter gives information about mathematical modeling of the nuclear-renewable hybrid energy system to produce hydrogen and electricity. This N-RHES consists of the merging of three main subsystems which are a prototype iPWR-type SMR, CSP and Cu-Cl thermodynamic cycle. Here, NPP and CSP are capable of producing electricity and/or heat energy to satisfy in part or whole the needs of both the electrical grid and the hydrogen cycle.

A prototype iPWR-type SMR is simulated based on a Rankine cycle working with the real enthalpy values depending on the parameters such as maximum temperature, maximum pressure, minimum pressure [106].

In terms of simulation of CSP, System Advisor Model (SAM) is used in this study. By entering inputs into SAM, a CSP is modelled, afterwards, needed hourly-based data is taken from SAM to transferred into an excel file. 8760 data based on hour of a year is processed on LabVIEW and MATLAB software via the excel file.

When it comes to modeling of this N-RHES, firstly, LabVIEW software is employed. Secondly, to validate data on LabVIEW, MATLAB is used. After getting the same results using both software (for a solved heat exchanger problem), the optimization step, which starts with a single objective optimization and continues with multi-objective optimization based on Genetic Algorithm, comes as the next step of this research.

### 3.1 Assumptions

Assumptions are given in this section.

- As a base load electricity production, 15% of NPP and CSP powers is used to produce electricity. By doing so, continuous electricity demand is met.
- 1 kJ electrical energy = 1 kJ heat energy

- To calculate a realistic overall $H_2$ price depending on the hours of a day:
    - If the hour is between 1:00am to 5:00am, “Hourly Ontario 50 kWh-Electricity Price” is multiplied by the square of “Hourly Ontario 1 kWh Electricity Price”.
    - If the hour is not between 1:00am to 5:00am, “Hourly Ontario 50 kWh Electricity Price” is multiplied by “Hourly Ontario 1 kWh Electricity Price”.

### 3.2 LabVIEW

A graphical programming language called LabVIEW (Laboratory Virtual Instrument Engineering Workbench) is utilized to develop applications by using icons instead of lines of text. LabVIEW employs dataflow programming, which differs from text-based programming languages that use instructions to specify the sequence in which programmes need run. In data flow programming, the VIs and functions are executed in the order that the data flows through the nodes on the block diagram. LabVIEW programmes that represent real instruments are known as virtual instruments, or VIs.

Using a variety of tools and components, a user interface is created in LabVIEW. Front panel is the name given to the user interface. The front panel is first made, and then code is added to control the front panel's items with graphical representations of their functions. This graphic code, also known as block diagram code or G code, is added to the block diagram. A flowchart and a block diagram have certain similarities. A “VI” is made up of a front panel, a block diagram, and graphic code representations.

### 3.3 MATLAB

MATLAB® is a programming software where engineers and/or scientists design and analyze their systems and products which transform to the real world. The MATLAB language, which is a matrix-based language that enables the most natural expression of computer mathematics, is the core of MATLAB®. With the help of a programming language that represents matrix and array mathematics directly, MATLAB® combines a desktop environment tailored for iterative analysis and design processes. The Live Editor allowing writing scripts that mix coding, outputs, and textual information in an interactive notebook is part of it.

By using MATLAB,

- Analysing data
- Developing Algorithms
- Creating models and applications can be carried out.

MATLAB lets engineers and/or scientists take their ideas from research to production by deploying to enterprise applications and embedded devices, as well as integrating with Simulink® and Model-Based Design. Some capabilities of MATLAB are Model-Based Design, Model Deployment, Physical Modeling, Real-Time Simulation and Testing, Systems Engineering, Verification, Validation, and Test.

Numerous applications in industry and academia, such as machine learning and deep learning, control systems, testing and measurement and computational finance, are carried out using MATLAB, which is used by millions of engineers and scientists worldwide.

MATLAB is also employed to solve multi-objective optimization problems thanks to Genetic Algorithm [176]. When employing a kind of approximation for the fitness

function (performance calculations), multi-objective optimization can be done in the MATLAB environment [177, 178].

Firstly, iPWR-type SMR is simulated on MATLAB. As a next step, the outputs of iPWR-type SMR from MATLAB are validated with a reference paper [106]. Moreover, the same results are taken from MATLAB and LabVIEW.

CSP modeled on System Advisor Model (SAM) is validated with a reference paper [106] and data of CSP taken from SAM is transferred to MATLAB.

Data of Cu-Cl thermochemical hydrogen production taken from a refence paper [179] is coded to MATLAB.

After these validation steps, multi-objective optimization based on Genetic Algorithms with the Pareto Front Principle is applied to N-RHES. Afterwards, all results of N-RHES from MATLAB are given in Chapter 4.

### 3.4 System Advisor Model (SAM)

The System Advisor Model (SAM) is designed by the National Renewable Energy Laboratory of the United States Department of Energy (NREL). For people working in the renewable energy industry, SAM is a techno-economic computer model designed to aid in their decision making:

- Project managers and engineers
- Financial and policy analysts
- Technology developers
- Researchers

The following platforms support SAM:

- Desktop software for Linux, Windows, and Mac OS

- Application programming interface (API) with a set of programming tools in the SAM software development kit (SDK)
- A set of documented open-source C++ code repositories

A performance model and a financial model are chosen to represent the project in SAM, and values are assigned to input variables to provide details about the project's location, equipment type, installation and operation costs, and financial and incentive assumptions. Simulations are performed after it is satisfied with the input variable values. Results are then prepared for analysis. A typical analysis accounts for running simulations, examining results, revising inputs, and repeating that process.

The SAM performance models include photovoltaic systems with optional battery storage, concentrated solar power, industrial process heat, solar water heating, wind, geothermal, biomass, and conventional power systems that either directly supply electricity to the power grid or interact with the electric load of a building or facility that is connected to the grid. Off-grid power systems and hybrid power systems with multiple power generation sources are not modeled by SAM. The financial projections apply to either residential and commercial projects that buy and sell electricity at retail rates, or to projects that sell electricity at a price set down in a power purchase agreement (PPA). SAM can simulate both large and small projects, from wind farms to massive concentrating solar power projects, including residential rooftop photovoltaic installations.

Since SAM is an open-source project, anyone can see its source code. Software developers can add their own models and improvements to the project, and researchers can study the code to better understand the model Algorithms. On the SAM website, reference materials defining the model Algorithms can also be downloaded.

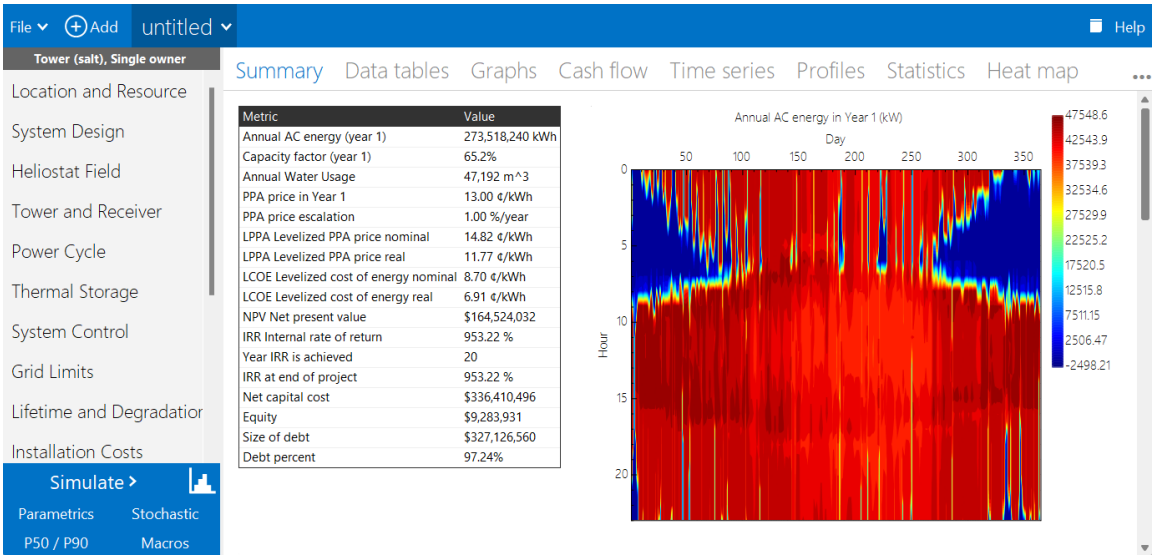


Figure 3.1: SAM main window displaying a concentrated solar power system's results summary.

### 3.4.1 Performance Models

The electric output of a power system is calculated time-by-timestep by SAM's performance models, which produce a set of timeseries data that depicts the system's annual energy generation. The hourly or sub hourly temporal resolution of the data in the weather file determines the simulation timestep.

The performance characteristics of the system can be thoroughly examined by looking at tables and graphs of time series performance data, or for more comprehensive performance evaluations, use performance measures like the system's total annual production and capacity factor.

Performance models for the following technologies are included in the most recent version of SAM. Because it has no restrictions on system size, it can be used to simulate both small residential systems and large utility-scale systems:

- Photovoltaic (PV) with optional electric battery storage
- High concentration PV

- CSP parabolic trough
- CSP power tower (molten salt and direct steam)
- CSP linear Fresnel
- CSP integrated solar combined cycle
- CSP dish-Stirling
- Process heat parabolic trough and linear direct steam
- Conventional thermal (a simple heat rate model)
- Solar water heating for residential or commercial buildings
- Wind power
- Geothermal power and geothermal co-production
- Biomass power

### 3.4.2 Financial Models

Based on a project's cash flows throughout an analysis period you define; SAM's financial models calculate financial metrics for various types of power projects. The series of annual cash flows are calculated by the financial model using the electrical output of the system as determined by the performance model.

The projects that can be used with SAM's financial models include:

- Residential building (retail electricity rates)
- Commercial facility (retail rates)
- Third party ownership
- Power generation (power purchase agreement):
- Single owner
    - Leveraged partnership flip
    - All equity partnership flip

- Sale leaseback

- To determine the levelized cost of energy for any financial structure, the LCOE calculator employs a fixed charge rate, installation costs, and annual operational costs as input.

To decrease a building or facility's reliance on grid electricity, residential and commercial projects generate electricity. They are financed through cash payments or loans, and they recoup their investment expenses through savings from lower electrical service provider purchases. SAM can simulate straightforward flat buy-and-sell prices for electricity, monthly net metering, or intricate rate systems with tiered time-of-use pricing and demand charges. The following metrics are reported by SAM for these projects:

- Levelized cost of energy
- Electricity cost with and without renewable energy system
- Electricity savings
- After-tax net present value
- Payback period

Power purchase agreements (PPAs) for electricity generation offer electricity at a fixed price with an optional annual escalation and time-of-delivery (TOD) factors. In relation to these initiatives, SAM determines:

- Levelized cost of energy
- PPA price (electricity sales price)
- Internal rate of return
- Net present value
- Debt fraction or debt service coverage ratio

SAM can either determine the power price depending on the rate of return you specify or the internal rate of return based on a power price you specify.

SAM determines the levelized cost of energy (LCOE) using cash flows after taxes. The cost of producing electricity over the period of the project, including taxes and incentives, is therefore represented by the LCOE.

The following are the annual cash flows for the project:

- Revenues from electricity sales and incentive payments
- Installation costs
- Operating, maintenance, and replacement costs
- Loan principal and interest payments
- Tax benefits and liabilities (accounting for any tax credits for which the project is eligible)
- Incentive payments
- Project and partner's internal rate of return requirements (for PPA projects)

Numerous incentive payments and tax credits can be accounted for by the financial model, including:

- Investment based incentives
- Capacity-based incentives
- Production-based incentives
- Investment tax credits
- Production tax credits
- Depreciation (Straight-line, custom, bonus)

### 3.5 Prototypic iPWR-type SMR / Thermodynamic Side

In this research, a nuclear power plant with PWR light water technology was preferred. This is the most prevalent, with over 250 used in the power industry and hundreds more in marine shipping. Water is used by PWRs as a coolant and a moderator. Water, the principal coolant, is delivered under high pressure into the reactor core and heated by atomic fission energy. The thermal energy from the heated water is then transferred to a secondary circuit via a steam generator, where it generates steam and transmits it through turbines that turn an electric generator, producing electricity. The primary circuit in large power plants is composed of the reactor pressure vessel (RPV), steam generators, pumps, pressurizer, and connecting pipes [51].

Most contemporary small modular reactor designs have an integrated configuration. The main cooling system parts, including the steam generators, pressurizers, and pumps, are located in integrated reactors inside the RPV. The integrated approach reduces NPP dimensions, eliminates external plumbing and components, and adopts a compact containment enhancing safety.

In this research, a prototypic iPWR-type small modular nuclear reactor is selected as a typical small PWR with integral design. When it comes to Technology Readiness Level (TRL), the components and design of the prototypic iPWR-type SMR have been assessed and this type of SMR will soon be released commercially available. The pressurizer, and steam generators that are the primary parts of the cooling system for iPWR-type SMR are integrated inside the reactor pressure vessel. Additionally, this reactor is operated under natural circulation flow, negating the need for reactor coolant pumps. The steam generator for the prototypical iPWR-type SMR is a helical-coil heat exchanger that is located in the annular space between the hot leg riser and the interior wall

of the reactor vessel. Each reactor has its own high-pressure containment vessel, which is located underwater in a concrete pool covered with stainless steel. The reactor is equipped with a modest 45 $MW_e$ conventional steam turbine generator set designed for prototypical SMR steam generator output conditions. As in every PWR plant, the moisture separator and subsequently the re-heater must be taken into account to minimise erosion and increase thermal efficiency at the final turbine stages. The primary technical information [106] for the single core prototypic iPWR-type SMR plant under consideration is pointed in Table 3.1.

Table 3.1: Technical specifications for the prototypic Integral PWR-type SMR.

| **Parameters** | |
|---|---|
| Live steam flow input (kg/s) | 71.3 |
| Turbine inlet temperature input (ºC) | 255 |
| Turbine inlet pressure input (MPa) | 3.1 |
| Condenser pressure input (MPa) | 0.0063 |
| Exit steam quality output (%) | 80.6 |
| | |
| Nuclear heat input (MW) | 160* |
| Total heat input (MW) | 160** |
| Net electric power output (kW) | 45005 |
| Net electric efficiency output (%) | 28.14 |

*(*Nuclear heat input 159975 kW)*
*(**Total heat input 159975 kW)*

Rankine cycle design parameters shown in Table 3.2 are designed as variables on this simulation. In order to calculate the thermodynamic properties of water for every single point in the Rankine cycle, which changes depending on the parameters turbine inlet temperature, turbine inlet pressure, condenser pressure, the extension named "CoolProp" is added to the LabVIEW. This extension gives a number of thermodynamic properties when at least two thermodynamic properties are known. CoolProp is basically an open-source C++ library that implements [180]:

- Pure and pseudo-pure fluid equations of state and transport properties for 122 components
- Mixture properties using high-accuracy Helmholtz energy formulations
- Correlations of properties of incompressible fluids and brines
- Computationally efficient tabular interpolation
- Highest accuracy psychrometric routines
- User-friendly interface around the full capabilities of NIST REFPROP
- Fast IAPWS-IF97 (Industrial Formulation) for Water/Steam
- Cubic equations of state (SRK, PR)

Table 3.2: Rankine cycle simulation inputs and outputs.

| **Rankine Cycle Simulation** | |
|---|---|
| **Inputs** | |
| Live steam flow (kg/s) | 71.3035 |
| Turbine inlet temperature (°C) | 255 |
| Turbine inlet pressure (MPa) | 3.1 |
| Condenser pressure (MPa) | 0.0063 |
| Total heat input (kW) | 159975 |
| Turbine efficiency (%) | 0.84 |
| Pump efficiency (%) | 0.85 |
| Piping & heat loss correction factor | 0.8285 |
| | |
| **Outputs** | |
| Exit steam quality (%) | 80.0209 |
| Net electric power (kW) | 45592.2 |
| Net electric efficiency (%) | 0.28499 |
| Pump $w_{in}$ (kJ/kg) | 3.66431 |
| Boiler $q_{in}$ (kJ/kg) | 2243.58 |
| Turbine $w_{out}$ (kJ/kg) | 643.075 |
| Condenser $q_{out}$ (kJ/kg) | 1604.16 |
| Enthalpy point1 (kJ/kg) | 130.691 |
| Enthalpy point2 actual (kJ/kg) | 133.730 |
| Enthalpy point3 (kJ/kg) | 2377.20 |
| Enthalpy point4 actual (kJ/kg) | 1735.91 |

Actual enthalpy values of the power cycle of the NPP are calculated simultaneously in the LabVIEW software using point 2s and 4s enthalpies shown in Figure 3.2 and thermodynamics properties of water in the Rankine cycle for every single point with "CoolProp" add-on depending on temperatures and pressures. All equations used in the calculation of thermodynamics properties are given as noted below.

$$\left.\begin{matrix} T_1 \\ P_1 \end{matrix}\right\} \begin{matrix} h_1 \\ v_1 \end{matrix} \tag{11}$$

$$w_{p,in} = v_1 \frac{P_{2a} - P_1}{\eta_{Pump}} \tag{12}$$

$$h_{2a} = h_1 + w_{p,in} \tag{13}$$

$$\left.\begin{matrix} T_3 \\ P_3 \end{matrix}\right\} \begin{matrix} h_3 \\ s_3 \end{matrix} \tag{14}$$

$$\left.\begin{matrix} P_{4s} \\ s_{4s} = s_3 \end{matrix}\right\} x_{4s} = \frac{s_{4s} - s_f}{s_{fg}} \tag{15}$$

$$h_{4s} = h_f + x_{4a} h_{fg} \tag{16}$$

$$\eta_{Turbine} = \frac{h_3 - h_{4a}}{h_3 - h_{4s}} \longrightarrow h_{4a} = h_3 - \eta_{Turbine}(h_3 - h_{4s}) \tag{17}$$

$$\left.\begin{matrix} P_{4a} \\ h_4 \end{matrix}\right\} x_{4a} = \frac{h_{4a} - h_f}{h_{fg}} \tag{18}$$

$$q_{in} = h_3 - h_{2a} \tag{19}$$

$$q_{out} = h_{4a} - h_1 \tag{20}$$

$$w_{net} = q_{in} - q_{out} \tag{21}$$

$$\eta_{Total} = \frac{w_{net}}{q_{in}} \tag{22}$$

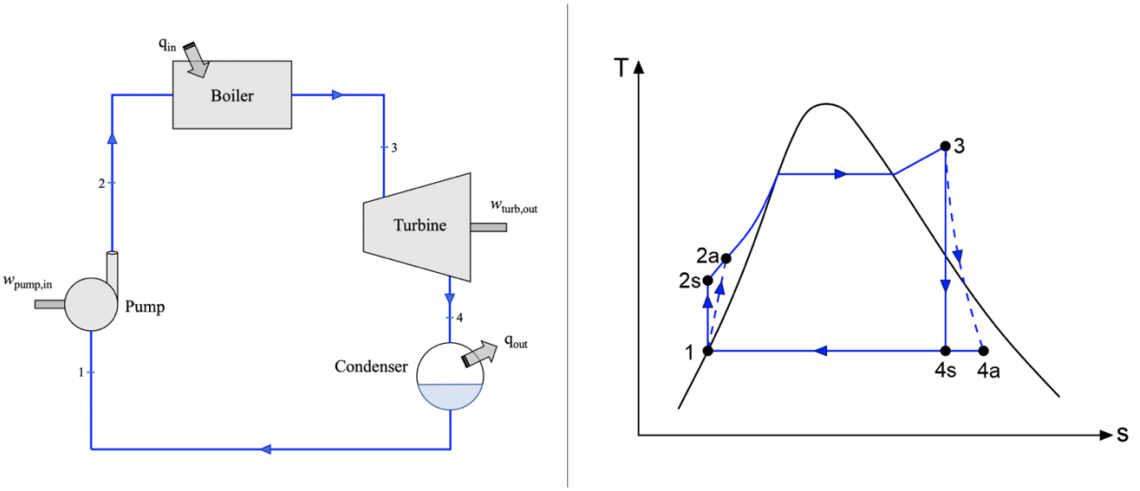


Figure 3.2: Rankine cycle schematic and T-s diagram, respectively.

When it comes to the Rankine cycle modeled on LabVIEW, all equations mentioned above are coded and "CoolProp" is wrapped to LabVIEW. Afterwards, the interface depicted in Figure 3.3 is obtained. Some inputs and outputs given in Figure 3.3 can be seen in the given power cycle interface of LabVIEW.

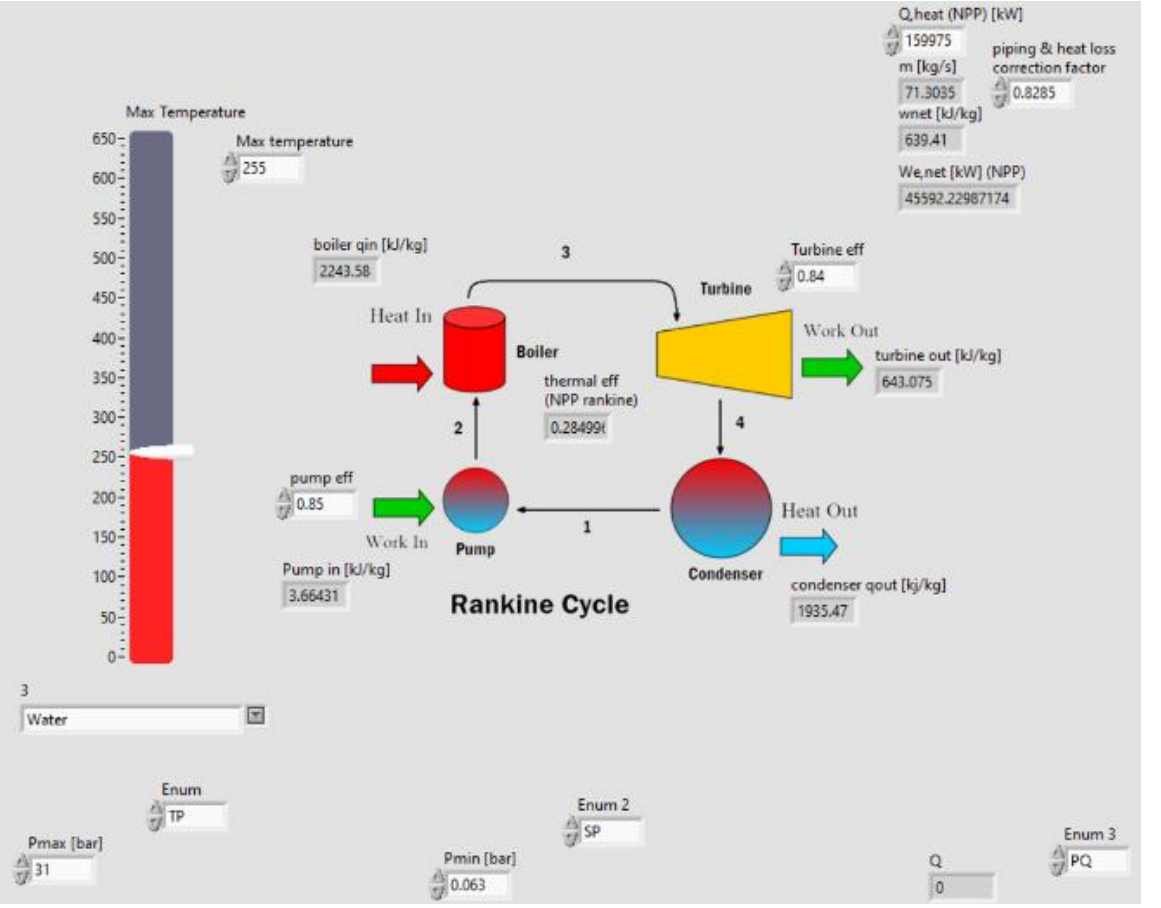


Figure 3.3: System level model of an iPWR type SMR with prototypic Rankine energy conversion cycle, as modeled using LabVIEW [2].

### 3.5.1 Validation of Rankine Cycle

Rankine cycle of integral PWR-type SMR simulation is coded on LabVIEW with the data taken from a reference paper [106] shown in Table 3.1. For validation, outputs shown in Table 3.1 are compared to the outputs of the simulation. According to this comparison, it is observed that the simulation gives the same results with a tolerance of 1% or less. In this way, the simulation-based Rankine cycle on LabVIEW is validated.

This research includes multi-objective optimization. As MATLAB is more sophisticated in multi-objective optimization, the same Rankine cycle is simulated on

MATLAB as well. Rankine cycle simulation on MATLAB is validated with the same reference paper [106] by getting the same results.

SAs a second validation of prototypic iPWR-type SMR / Thermodynamic Side, the Rankine cycle simulation on LabVIEW requires to be verified. Therefore, a fundamental Rankine cycle question is taken from the reference book ($5^{th}$ edition, chaper10-17 of the book) [181]. It is aimed to compare the results in the book with the results in the simulation.

*The given question ($5^{th}$ edition, chaper10-17 of the book) [181] is;*

"Consider a 210-MW steam power plant that operates on a simple ideal Rankine cycle. Steam enters the turbine at 10 MPa and 500°C and is cooled in the condenser at a pressure of 10 kPa. Show the cycle on a *T-s* diagram with respect to saturation lines, and determine (*a*) the quality of the steam at the turbine exit, (*b*) the thermal efficiency of the cycle, and (*c*) the mass flow rate of the steam.

(*Assuming an isentropic efficiency of 85 percent for both the turbine and the pump. Answers: (a) 0.874, (b) 34.1 percent, (c) 194 kg/s*)"

After modeling the non-isentropic Rankine cycle described in the previous section, the inputs given in the question are transferred to the simulation on LabVIEW and simulation results are obtained as indicated in Figure 3.4. Results in the book and on the simulation are shown in Table 3.3.

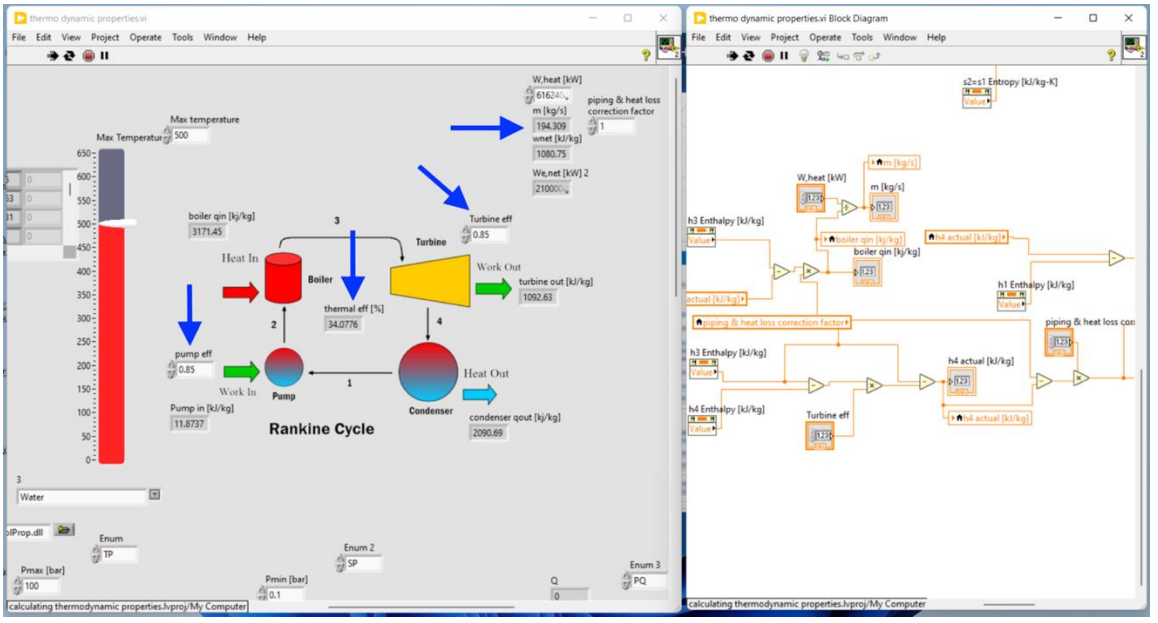


Figure 3.4: Simulation results indication.

Table 3.3: Comparative results for the question taken from a reference book [181].

| **Inputs Given** | |
|---|---|
| Steam power [MW] | 210 |
| Steam inlet temperature [°C] | 500 |
| Steam inlet pressure [MPa] | 10 |
| Condenser pressure [kPa] | 10 |
| Turbine eff. [%] | 85 |
| Pump eff. [%] | 85 |

| **Results** | **In the book** | **In the simulation** |
|---|---|---|
| Steam quality at turbine exit | 0.874 | 0.8746 |
| Thermal eff. of the cycle [%] | 34.1 | 34.0776 |
| Steam mass flow rate [kg/s] | 194 | 194.309 |

When the results given in the question are compared with the answers in the simulation, the results are seen to be the same with a tolerance of less than 1%. In addition to this validation**,** outputs shown in Table 3.1 are compared to the outputs of the simulation for Integral PWR SMR type in the previous section. According to these comparisons, it is obviously seen that the simulation gives the same results with a tolerance of 1%. In this way, this Rankine cycle simulation is validated.

### 3.6 Concentrated Solar Power (CSP)

Hydrogen can be generated using the heat energy from a concentrated solar power (CSP) plant [87, 88]. Sunlight is directed to a receiver via mirrors in concentrated solar power plants. A steam turbine that generates electricity is operated by the thermal energy stored in the receiver [101]. In order to ensure that high-temperature heat energy is given directly to nuclear steam superheating without the need for intermediary conversion, this CSP technology is well suited to supporting nuclear power installations. Three different CSP technology types that can meet high temperatures requirements have been described in the literature. These technologies are categorized using the mirrored CSP technology. Examples of these are the Parabolic Trough (PT), Fresnel Reflectors (FR), and Dish Receiver (DR) [32, 102]. Over 90% of CSP systems included PT technology in 2013 [103], and more recently, over 60% of CSP systems [104]. Similar to the PT collector technology, the FR system concentrates sunlight onto a stationary receiver several meters above the mirror region using a number of ground-based, flat or slightly curved mirrors placed at various angles [105]. Commonly referred to as "central tower" power plants, "heliostat" power plants, or "power towers," solar power towers are a form of solar furnace that focus sunlight through a tower. It directs the sun's beams onto a collection tower using heliostats, a series of flat, adjustable mirrors.

In this research, a hybrid energy system including a solar tower plant and a nuclear SMR are employed to generate hydrogen via a Cu-Cl thermochemical cycle. Since the Solar Tower Plant can run at approximately 530°C when employing molten salt as a fluid, this coupling is advantageous thermodynamically. The solar field, which consists of a considerable number of computer-assisted flat mirrors (heliostats), thermal storage, and power block, are the three main subsystems of this CSP plant as shown in Figure 3.5.

Production can be levelled in this situation by using Thermal Energy Storage (TES). Effectiveness is evaluated based on the amount of thermal energy storage utilised in this CSP system. In Table 3.7, a comparison of thermal energy storages based on hourly volumes is given. 15hour-TES is evaluated as the most effective volume of thermal energy storage. The extremely well-known and benchmarked System Advisor Model (SAM) software is where CSP's data for developing a hybrid system on LabVIEW is obtained from.

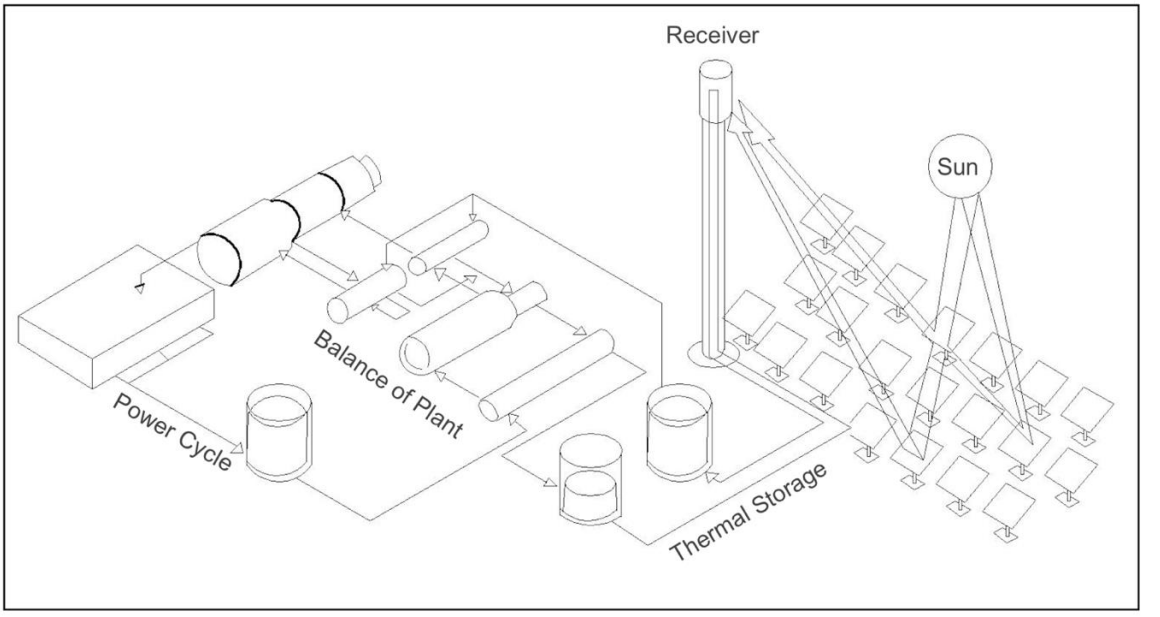


Figure 3.5: A schematic of the CSP Plant [2].

Table 3.4: CSP Plant parameters [2].

| **Power Block Parameters** | |
|---|---|
| Net electric power attributed to solar heat (kW) | 47922 |
| Turbine inlet pressure (MPa) | 10 |
| Condenser pressure (MPa) | 0.0085 |
| Solar heat input required (kW) | 117685 |
| Solar heat to electricity efficiency (%) | 40.72 |
| **Thermal Energy Storage Parameters** | |
| Hours of storage (h) | 15 |
| Nominal storage capacity (MWh) | 1765.3 |
| Nominal storage tank discharge flow rate (kg/s) | 265.1 |
| Nominal hot tank temperature (°C) | 565 |
| Nominal cold tank temperature (°C) | 270 |
| Mass of stored fluid (tonne) | 14177 |
| Storage volume ($m^3$) | 8202 |
| Storage tank height (m) | 9.796 |
| Storage tank diameter (m) | 32.65 |
| **Solar Field Parameters** | |
| Field Configuration | Circular Surround |
| Design point DNI ($kW/m^2$) | 0.915 |
| Solar multiple | 2.5 |
| Solar heat generation required (kW) | 294220 |
| Overall corrected collector efficiency (%) | 56.49 |
| Field Incident thermal power (kW) | 520822.3 |
| Reflective area in solar field ($m^2$) | 569043 |
| Reflective area per heliostat ($m^2$) | 44.59 |
| Number of heliostats | 12760 |
| Tower structure height (m) | 136.1 |
| Tower inner diameter (m) | 11.22 |
| Receiver height (m) | 13.59 |
| Receiver diameter (m) | 10.2 |
| Receiver face area ($m^2$) | 435.5 |
| Distance from tower base to outermost mirror on North side (m) | 1021.1 |
| Distance from tower base to innermost mirrors | 102.1 |
| Heliostat field land area ($m^2$) | 2775818 |

Table 3.5: Design point solar data [2].

| Location: Daggett Barstow, California | |
|---|---|
| Altitude | 586m |
| Latitude | 34.85 °N |
| Longitude | -116.8 °E |
| Time zone | GMT -8 |
| Annual DNI | 7.46 kWh/($m^2$.day) |
| Design point DNI | 0.915 kW/$m^2$ |

System Advisor Model (SAM) software is used to simulate data from [106]. Table 3.4 and Table 3.5 to produce hour-based CSP data. Daggett Barstow in California (230 kms away from the northeast Los Angeles downtown) is selected as a remote, high desert location for which annual, hourly data exists and is well-suited to serve as a generation site. "Electricity to grid", "electricity from grid", "Power Cycle input energy", and "net efficiency" are obtained hourly data from SAM and given to LabVIEW for additional simulations. "Electricity to grid" is divided by "Power Cycle input energy" to calculate "net efficiency". When the electricity amount by CSP is calculated, the “net efficiency” which changes depending on the weather conditions is used. As shown Table 3.6, 8760 data points from SAM are exported to LabVIEW for use in hydrogen and electricity generation in N-RHES, after writing to excel.

Table 3.6: An indication of hourly based data of CSP for one year [2].

| **Total hour** | **Day** | **Month** | **Hour** | **Electricity to grid \| (kW)** | **Electricity from grid \| (kW)** | **PC input energy \| (kW)** | **Net Efficiency** |
|---|---|---|---|---|---|---|---|
| 1 | 1 | 1 | 0 | 9983.5 | 0 | 120593 | 0.083 |
| 2 | 1 | 1 | 1 | 34724.6 | 0 | 123414 | 0.281 |
| 3 | 1 | 1 | 2 | 34659.8 | 0 | 123263 | 0.282 |
| : | : | : | : | : | : | : | : |
| 8758 | 31 | 12 | 21 | 44009.3 | 0 | 121110 | 0.363 |
| 8759 | 31 | 12 | 22 | 43921.1 | 0 | 120896 | 0.363 |
| 8760 | 31 | 12 | 23 | 0 | 0 | 60837.1 | 0 |

In order to examine the effect of different volumes of thermal energy storage, five CSP plants having different thermal energy storage capacities are modelled on SAM. Apart from thermal energy storage capacity based on hour, the other parameters for these five CSP plants are the same with the Table 3.4 and Table 3.5. One year data, accounting for 8760 lines of each hour of the year, of these CSP plants is taken including "electricity from grid" and "electricity to grid" from SAM. By subtracting "electricity to grid" from "electricity from grid", the "total net electricity" amounts are compared according to the thermal energy storage capacities, which are 1hour-TES, 10hour-TES, 100hour-TES, 500hour-TES and 1000hour-TES.

Table 3.7: Net electricity amount in kWh depending on TES capacity for a year [2].

| **TES Capacity** | **Net Electricity** |
|---|---|
| 1 hour-TES | 1.41E+08 |
| 10 hour-TES | 2.47E+08 |
| **15 hour-TES** | **2.75E+08** |
| 100 hour-TES | 2.74E+08 |
| 500 hour-TES | 2.36E+08 |
| 1000 hour-TES | 1.84E+08 |

It is seen that 15 hour-TES is more effective than others in Table 3.7. When looked at the It is seen that 15 hour-TES is more effective than others in Table 3.7. **,** although it increased 10 times from 10 hour-TES to 100 hour-TES, only an approximately 11% increase is seen in the total net electricity amount. Even though the thermal energy storage capacity increases up to 500 hour or 1000 hour from 100 hour, total net electricity amount decreases. By remaining the same the other parameters of CSP for instance, heliostat numbers, even if the TES capacity is increased, it is seen that the total net electricity doesn't increase as much as the capacity. It sometimes even tends to decrease.

### 3.6.1 Validation of CSP

For validation of CSP data, inputs taking part in Table 3.4 and Table 3.5 are transferred to System Advisor Model (SAM) software. After the input parameters are entered in SAM performance model, then total installed costs financial model shown in Figure 3.6 are compared with the reference case's installed cost [106]. When validation is done, the other hourly data provided by SAM is taken such as "electricity to grid".

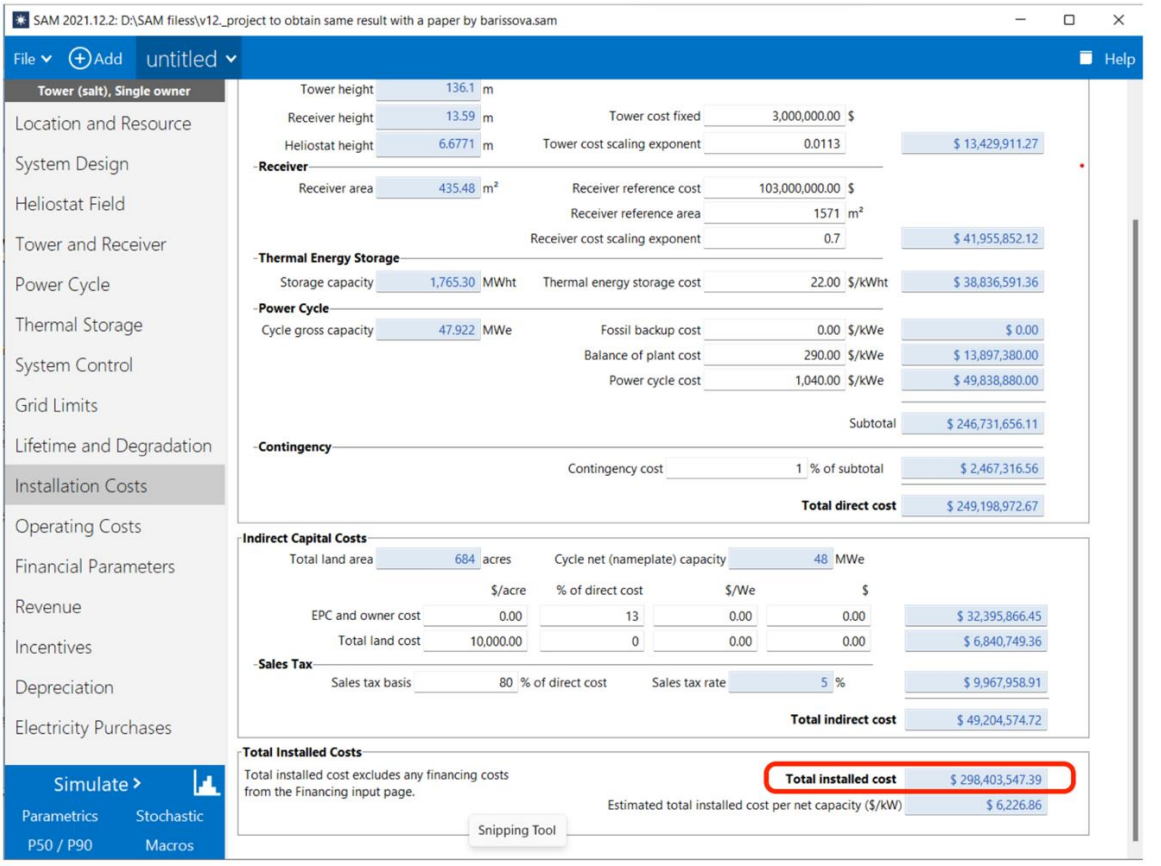


Figure 3.6: CSP simulation on SAM.

- The installed cost in the reference case [106] is US$ 293.5M, rounded (exact from simulations US$ 293,494,800).
- The installed cost on the simulation is calculated as US$ 298.4M, rounded (exactly US$ 298,403,547.39).

To conclude, when comparing the total installed costs, simulation on SAM indicated a difference of 1.67%. Since this difference is acceptable, the simulation on SAM is considered verified in this way.

### 3.7 Cu-Cl Thermochemical Hydrogen Generation Cycle

Cu-Cl thermochemical hydrogen production cycle is a preferable option to produce clean hydrogen as it works with the principle of thermally separating water into oxygen and hydrogen. This cycle requires more heat energy than electrical energy. Therefore, in terms of less energy conversation from heat to electrical energy, this cycle has an advantage. Heat energy can be obtained directly from NPP side and/or CSP side directly. The other advantage of Cu-Cl cycle is that these chemical compounds used in this cycle can be reused.

Cu-Cl cycles come in seven primary categories [65]. The highest energetic and exergetic efficiency, according to the researchers [141], is found in the four-step Cu-Cl cycle, which has a net efficiency of approximately 43% [110]. The heat requirements for Cu-Cl can be satisfied at around 525°C [129, 142] using new-generation nuclear reactors or concentrated solar power (CSP) systems [143, 144]. Utilizing the Cu-CI thermochemical cycle to produce hydrogen is preferable because solar and nuclear energy are both clean sources of energy [142].

Hydrolysis, thermolysis, electrolysis, and drying are the four phases of the Cu-Cl cycle [128, 130, 145]. In the Cu-Cl thermochemical cycle, it requires 200 kJ of heat energy at a temperature of 525°C and 25 kJ of electrical energy to produce 1 mol $H_2$ [179]. To able to start thermochemical reactions, electrical charge difference (25 kJ electrical energy) is necessary. The Cu-Cl hydrogen production chemical equations are as follows;

The copper-chlorine (Cu-Cl) hydrogen production cycle is pointed out here in summary. The first step is hydrolysis:

$$2CuCl_2(s) + H_2O(g) \rightarrow Cu_2OCl_2(s) + 2HCl(g) \rightarrow \text{(at 375-400 °C [145])} \quad (23)$$

The second step consists in the decomposition of copper oxychloride taking place at high temperatures of 500-530°C:

$$Cu_2OCl_2(s) \rightarrow \tfrac{1}{2}\,\mathbf{O_2(g)} + 2CuCl(l) \quad (24)$$

The third step is represented by:

$$2CuCl(aq) + 2HCl(aq) \rightarrow \mathbf{H_2(g)} + 2CuCl_2(aq) \rightarrow \text{(at 25 °C)} \quad (25)$$

The fourth step (drying of aqueous cupric chloride) happens at temperature between 30 to 80°C as:

$$CuCl_2(aq) \rightarrow CuCl_2(s) \quad (26)$$

### 3.8 Thermochemical Heat Pump

In this study, an ideal thermochemical heat pump working with the principle of a reversible chemical reaction is employed to increase the temperature of the fluid coming from NPP side in order to meet the Cu-Cl thermochemical cycle temperature requirement. Heat energy is captured via an endothermic reaction, after then this reaction is reversed by releasing pressure as indicated in Figure 3.7. In this way, it is ensured that the captured heat is transmitted at a higher temperature. This ideal reversible thermochemical heat pump does not require electricity.

The temperature of the fluid leaving the NPP is at 255°C. However, Cu-Cl cycle requires heat energy at a temperature of approximately 525°C. The reference heat pump [179] consumes 0.4235 kJ of heat energy to increase the fluid's temperature by 1°C. The heat energy requirement is met by NPP. In this N-RHES, calculation of heat energy consumed by heat pump ($D_1$) is given with equation (28).

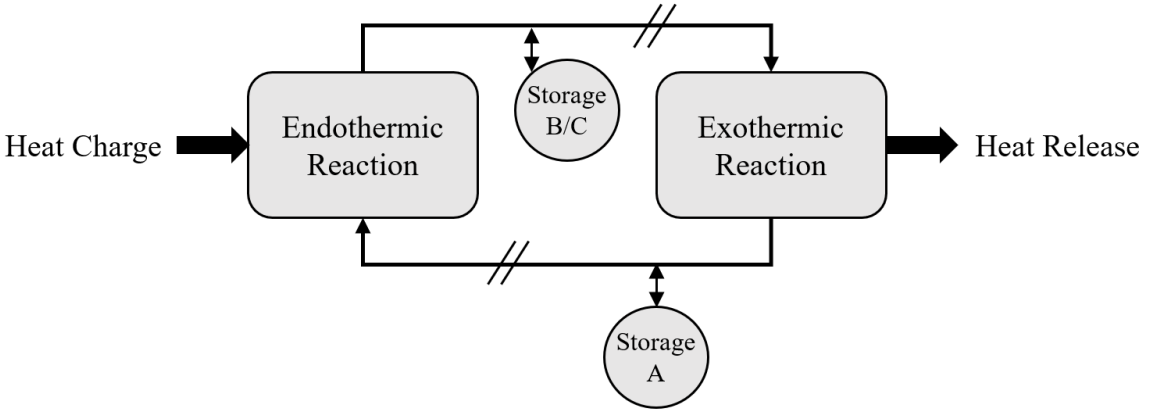


Figure 3.7: Thermochemical heat pump working mechanism.

### 3.9 Nuclear-Renewable Hybrid Energy System (N-RHES)

In this research, productions of hydrogen and electricity by combining nuclear and renewable energies are the final goal. Thus, it is necessary to have a hybrid system as depicted in Figure 3.8. In this section, all subsystems described earlier are assembled together using LabVIEW. Here, nuclear, or renewable power produced by respective plants are expressed in percentage and are adjustable in order to produce hydrogen and/or electricity. Electricity is produced using separate Rankine power cycles by NPP and CSP as their power cycle operating parameters are different. Therefore, these Rankine power cycles perform at different efficiencies. NPP and CSP are not fully integrated since when one of them is shut down, energy production from the other is anticipated. Additionally, NPP must follow to the licence standards established by the regulator; the regulation

restricts them from being completely integrated in terms of safety. As a result, any issues with CSP cannot compromise the safety of NPP. The key point is that they must both be operated while using a hybrid strategy that allows for the possible shutdown of one of them.

The CSP plant depends on the weather, as is widely known. Therefore, when the sun cannot supply enough energy to keep the salt in a liquid form, CSP needs electrical energy to reheat the molten salt. It is necessary to use electrical energy as a result to keep it liquid. Basically, the grid supplies the electrical energy needed to maintain the liquid condition of molten salt. However, here the hybrid energy system is intended to provide the required electricity directly from the NPP instead of the grid.

An ideal reversible thermochemical heat pump is utilized to raise the temperature of the fluid leaving the NPP, which is at 255°C, as the Cu-Cl cycle needs heat energy at a temperature of roughly 525°C. The reference heat pump [179] calls for 0.4235 kJ of heat energy to enhance the fluid's temperature by 1°C. In this N-RHES, the needed heat energy for the pump is provided by the NPP. The reversible thermochemical heat pump does not require any electricity.

The Cu-Cl thermochemical cycle requires 200 kJ of heat energy at a temperature of 525°C and 25 kJ of electrical energy to produce 1 mol-$H_2$ [179]. In this study, a reversible thermochemical heat pump is used to increase the temperature of the fluid, which carries the heat energy coming from the nuclear power plant, in order to meet the temperature requirement of the Cu-Cl thermochemical cycle. On the CSP side, the necessary temperature for Cu-Cl cycle is already provided.

NPP and CSP produce heat energy first. Then, depending on their net electricity production efficiency, they convert their heat energy into electrical energy. By dividing

net electrical efficiencies of NPP and CSP by 25 kJ, it is possible to determine how much heat energy is needed from these two sources to satisfy the electrical energy demand of Cu-Cl required to generate one mole of $H_2$.

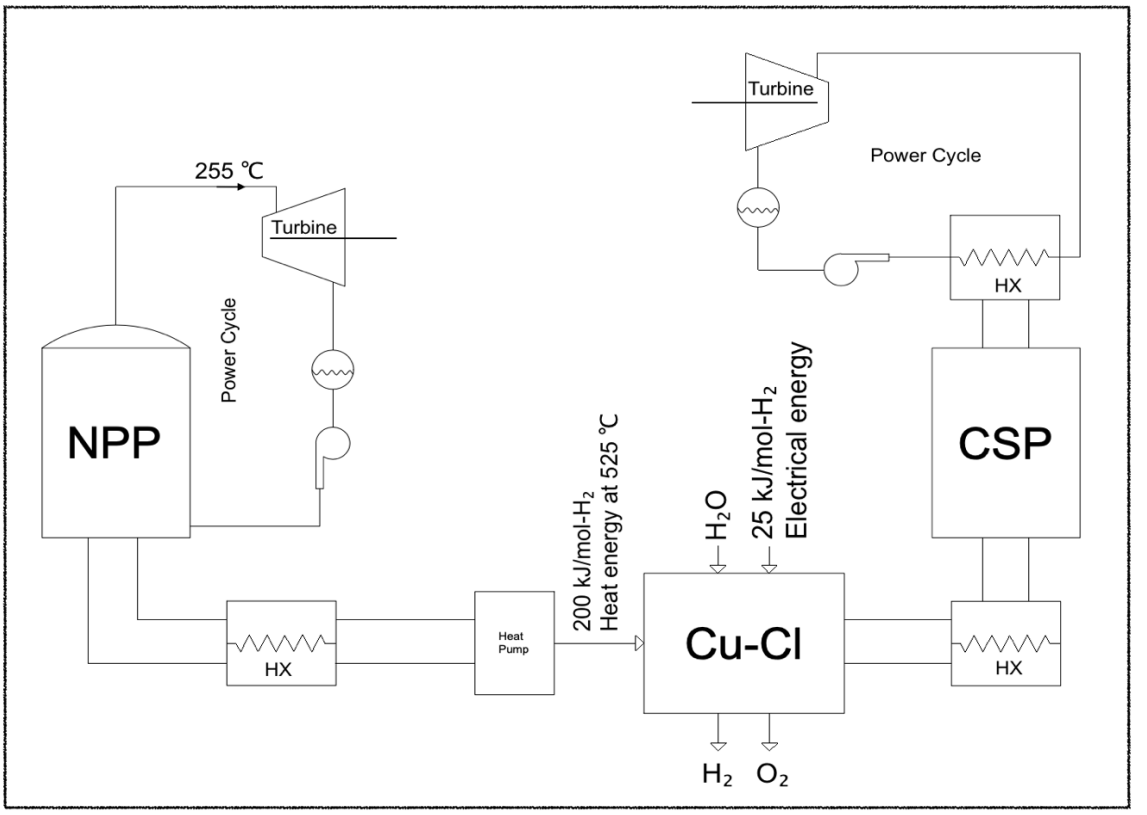


Figure 3.8: A schematic of N-RHES [2].

Utilizing the thermal energy provided by NPP and CSP, hydrogen and/or electricity are produced. The amount of heat power from NPPs and/or CSPs is represented as a percentage for the production of hydrogen, and the leftover heat power is employed to generate electricity as indicated in Figure 3.9, where 24-hour period electricity and hydrogen production amounts are shown. Additionally, the written LabVIEW code allows for the calculation and individual percentages of the amounts of electricity and hydrogen produced based on a date range and is displayed on the graph.

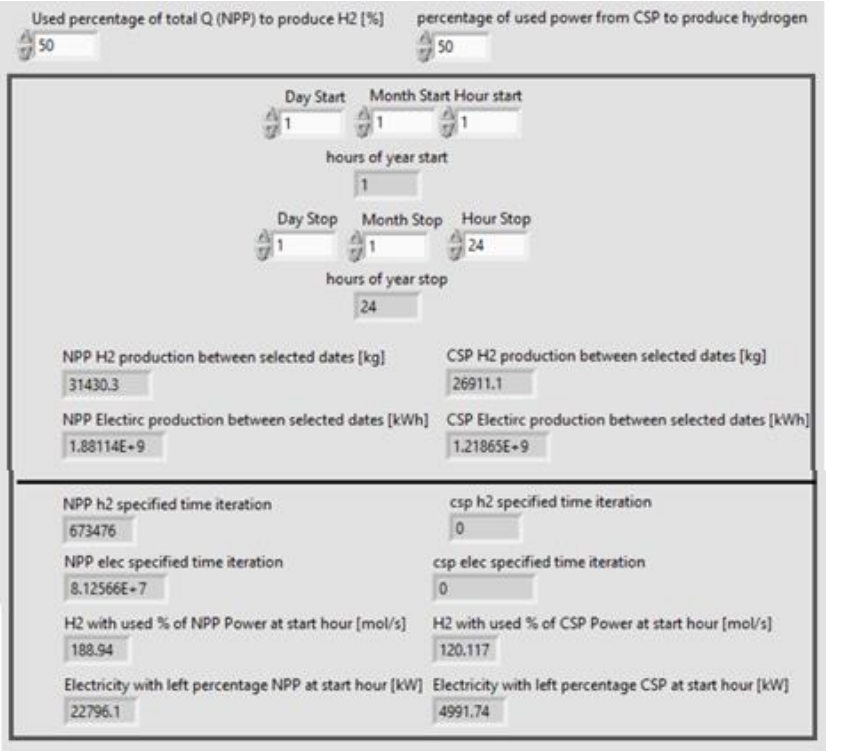


Figure 3.9: Control panel/LabVIEW GUI of NPP and CSP to produce hydrogen and electricity [2].

The total amounts of electricity and hydrogen produced by NPP and CSP are displayed by defining time period similar to Figure 3.10, so that it is possible to see how production amounts fluctuate over time. In this case when the power percentages of the energy sources are 50% to produce hydrogen/electricity, the amounts of hydrogen and electricity starts to increase gradually from the beginning to 02:00. Afterwards, the figures remain the same for two ours between 02:00 and 04:00. Following this, the production trends between 04:00 and 06:00 decreases by decreasing. The trends remaining almost the same for 3 hours (06:00 and 09:00) begin to go up significantly until 10:00am. Although there are minor fluctuations seen especially in the production of electricity, the production amounts stay relatively the same from 10:00 to 21:00. Next, the trend starting to significantly decrease between 21:00 and 22:00 continue by staying almost the same until

00:00. Even if NPP power is the same all time in this N-RHES, CSP power varies with weather-related parameters. Furthermore, the other reason for these fluctuations is that NPP supplies electrical energy to CSP when CSP cannot produce energy to keep its main cycle fluid, which is molten salt, in a liquid form. Graphs superimposed on the same timeline are used to illustrate both electricity and hydrogen because their scales and units are different. In this way, the total hydrogen and electricity amounts are calculated by taking into account the time-dependent changes in the production quantities shown in Figure 3.10.

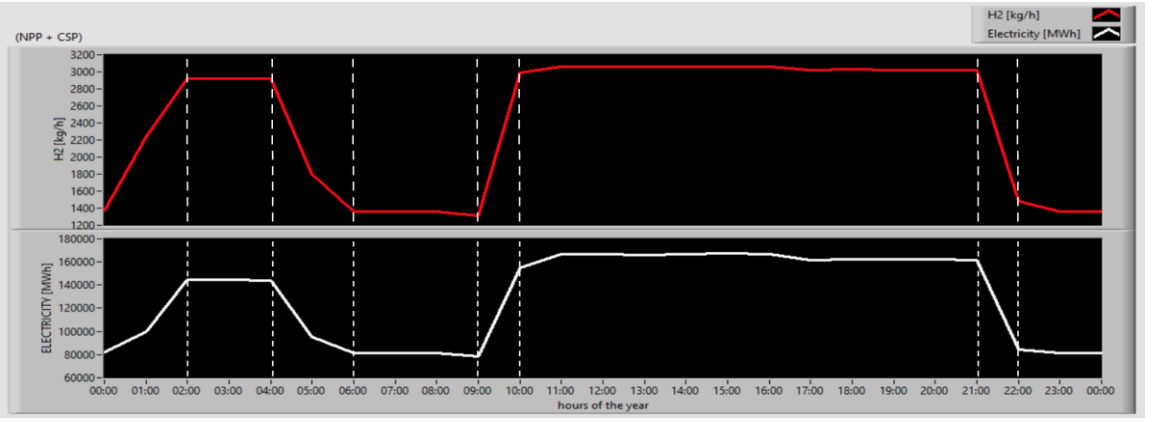


Figure 3.10: Showing the outcomes of a simulation of the 24-hour total electricity generation (MWh) and $H_2$ production (kg) from a combined NPP and CSP source [2].

In this N-RHES, connection losses in places that connect subsystems are neglected. However, as the Cu-Cl thermodynamic cycle requires 200 kJ of heat energy at a temperature of 525°C, a thermochemical heat pump is employed to increase the fluid temperature to 525°C. Here, the temperature of the fluid coming from the NPP side to the heat pump is assumed to be 255°C, which is the same temperature as the fluid in the NPP power cycle.

There are a number of heat-upgrading technologies, such as heat pumps, combustors, and electric heating. In comparison to the other two options, heat pumps are

considered to be a feasible selection with higher energy efficiency [182]. Heat pumps can be powered by renewable energy sources as solar concentrators, geothermal energy, biomass combustion, and waste heat from industry. For integration into a nuclear reactor's secondary loop, thermomechanical and thermochemical heat pumps are two types that work well. In order to boost the source heat from the reactor and deliver it at a higher temperature, a thermomechanical heat pump (also known as a vapor compression heat pump) compresses mechanically. By recovering energy through the expansion of the compressed working fluid, it is more practical and effective than electric heating. The thermochemical heat pump, which relies on a reversible chemical reaction, is the alternative approach. When an endothermic reaction is reversed through a pressure swing, heat is captured and transferred at a higher temperature.

In this study, based on the thermochemical heat pump used in the hydrogen production in article [179], a new thermochemical heat pump suitable for this N-RHES system (taking into account the desired inlet and outlet temperatures) is designed. In reference paper [179], the heat pump increases the temperature from 310°C to 525°C by consuming 108 kJ heat energy per mol-$H_2$. It means that by consuming 108 kJ heat energy, the thermochemical heat pump provides 215°C of temperature increase.

In this N-RHES, it is necessary that the thermochemical heat pump needs to provide 200 kJ heat energy at the temperature of 525°C, which is the requirement of Cu-Cl cycle. Here, the heat pump increases the temperature from 255°C (the temperature of the fluid coming from NPP side) to 525°C by raising 215°C. The thermochemical heat pump for this N-RHES is proportionally designed as calculated in equation (28). The coding of the hydrogen produced in the Cu-Cl cycle with the use of this heat pump on LabVIEW is shown in Figure 3.11.

$T_{Cu\text{-}Cl,\,max}$: Max temperature required for Cu-Cl [°C]

$T_{NPP,\,max}$: Max temperature provided by NPP [°C]

$E_1$: Electricity required for producing per mol $H_2$/s for Cu-Cl, 25 kW

$\eta_{NPP,\,Rankine}$: NPP Rankine cycle efficiency

$A_1$: Heat power amount for electricity required to producing one mol $H_2$ via NPP [kW]

$B_1$: Heat power required for Cu-Cl cycle to produce one mol $H_2$ [kW]

$C_1$: Total heat power required for producing one mol $H_2$ via NPP [kW]

$D_1$: Heat power consumed by heat pump [kW]

$$E_1/\eta_{NPP,\,Rankine} = A_1 \tag{27}$$

$$(T_{Cu\text{-}Cl,\,max} - T_{NPP,\,max}) * (108\text{ kJ} / 215\text{ kJ}) = D_1 \tag{28}$$

$$A_1 + B_1 + D_1 = C_1 \tag{29}$$

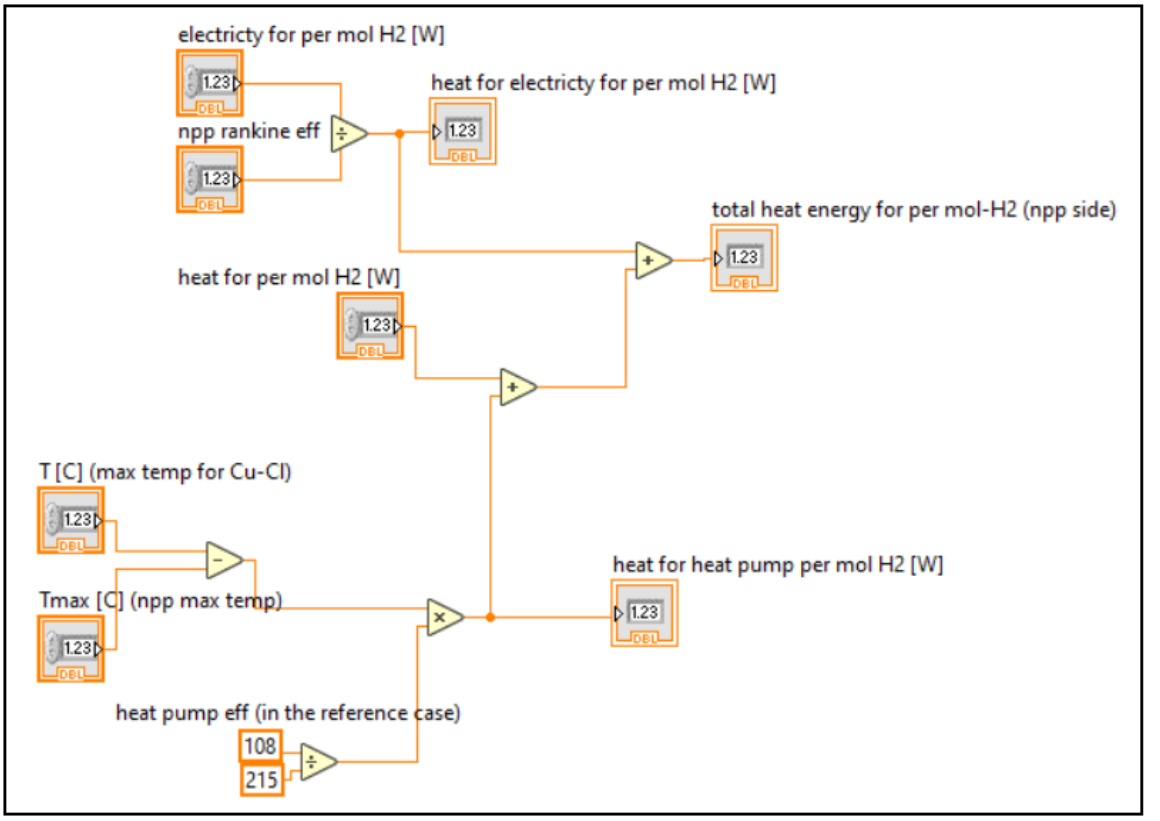


Figure 3.11: The coding of the hydrogen produced in the Cu-Cl cycle with the use of this heat pump on LabVIEW.

Heat is the main energy used to produce hydrogen and electricity in the respective cycles. Also, to produce hydrogen, electricity is necessary for the reasons explained earlier. When hydrogen is generated by NPP, the electrical energy (25kJ) needed to produce 1 mol of hydrogen is provided by the NPP power cycle. The heat power of NPP is converted into electrical energy. To obtain the 25 kJ of electrical energy required to produce 1 mol of hydrogen, the heat energy provided by the NPP is found by dividing the NPP net electrical efficiency by 25 kJ. This heat energy is collected with 200 kJ heat energy which is the basic heat energy requirement to produce 1 mol of hydrogen with Cu-Cl thermochemical cycle. Afterwards, the heat energy required for the heat pump is added to this account.

After knowing how much heat energy is required to produce 1 mol of hydrogen per second by using energy coming from the NPP side ($C_1$), the hydrogen amount at a defined

percentage power of NPP is calculated thanks to the code written on LabVIEW as shown in Figure 3.12. Here, the basic approach is to calculate the hydrogen amount via NPP's heat and electrical power in kW is obtained with the remaining heat power. Defined percentage of nuclear power is multiplied by nuclear heat power, then, divided by $C_1$. By doing so, hydrogen amount per second is found. The amount of hydrogen per second is multiplied by the specified time interval in seconds to obtain the total amount of hydrogen. When it comes to electricity, the remaining percentage of nuclear power is used for electricity generation. Total heat power of NPP is multiplied by the remaining percentage and then, NPP power cycle net thermal efficiency. This calculation gives information about how much electricity per second is produced. The total amount of electricity in kWh is calculated by multiplying the electricity produced per second [kW] by the specified time.

NPP Rankine cycle`s piping and heat loss are taken into account. However, heat transfer efficiencies between subsystems are accepted as 100%. The reason why is that when there is any heat transfer or heat conversion, heat losses occur. Calculation for every single point`s heat loss, other studies need to be done as future works.

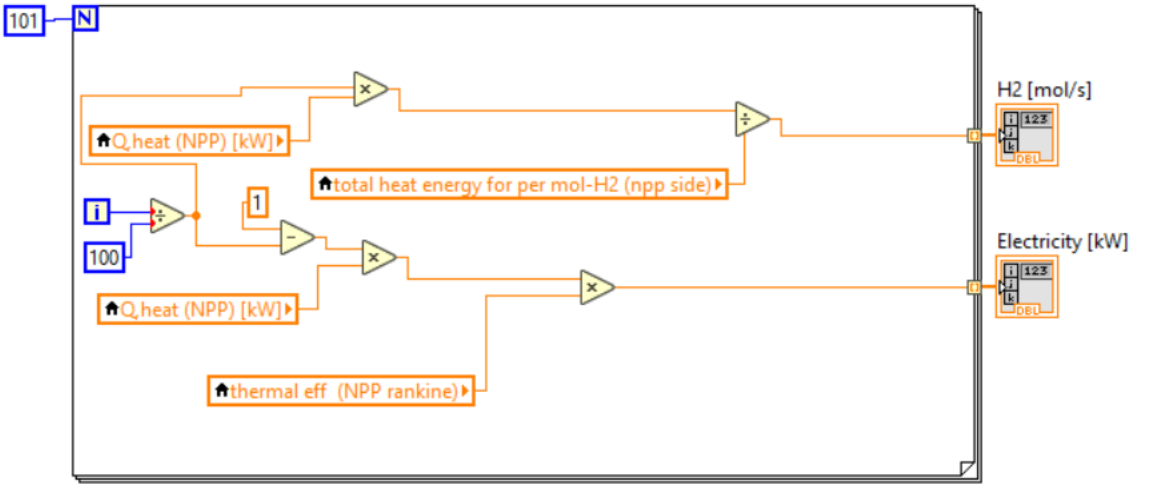


Figure 3.12: Coding of hydrogen and electricity outputs via NPP.

After completing N-RHES simulation on LabVIEW, another coding is carried out on MATLAB to validate these calculation and to be sure that the simulations are valid. In addition to this, as this research include a multi-objective optimization approach at the end; MATLAB is capable of programming routine where multi-objective optimization method can be applied with the principle of Genetic Algorithm. The reason why optimization is necessary is that N-RHES has complexity especially in terms of CSP management strategy. When the objective functions are more than one, multi-objective optimization approach needs be applied to obtain better results. To give a clear example, when the over all benefit coming from selling electricity and hydrogen is aimed to maximize, the total heat equivalent coming from electrical energy and hydrogen produced by this N-RHES is proposed to maximize.

### 3.9.1 Application of MATLAB for N-RHES

To make a model of N-RHES on MATLAB, this N-RHES needs to be a MATLAB function where all critical parameters are considered. By doing so, it can be obtained a system depending on the parameters, which are heat power of NPP, maximum temperature ($T_{max}$), maximum pressure ($P_{max}$), minimum pressure ($P_{min}$), turbine efficiency ($\eta_T$), pump efficiency ($\eta_{pump}$), and piping heat loss correction factor of Rankine Cycle in terms of NPP side. Also, defining a time period and power percentage of NPP to produce hydrogen and electricity (% of NPP power output to produce $H_2$ and MWe), total amount of hydrogen in kg and electricity in kWh are eventually calculated. The Rankine cycle employed here works with the real enthalpy values changing dynamically with parameters explained above. This produces realistic outputs. As used on LabVIEW, to calculate thermodynamic properties of every single point of Rankine Cycle, “CoolProp” is utilized on MATLAB.

After modelling Rankine cycle on MATLAB of NPP, the same results are taken with the Rankine Cycle simulation on LabVIEW.

CSP is first modelled on SAM and the data including "electricity from grid", "electricity to grid", "power cycle input energy" are taken from SAM to calculate "net efficiency" of CSP dynamically changing depending on the weather conditions for every single hour of a year as shown *equation (30).* In this way, it is obtained 8760 data based on hours of a year. All data is exported to excel in ".csv" file. Next, all these information is transferred to MATLAB in a form of matrix.

$$electricity\ to\ grid/power\ cycle\ input = net\ efficiency \qquad (30)$$

By using all data and defining a time period and power percentage of CSP, total amounts of hydrogen and electricity are calculated in kg and kWh, respectively. When there is not enough sun light, CSP is not capable to produce energy. CSP requires to keep its major operating fluid (molten salt) in a liquid form. For this reason, CSP needs electrical energy from the grid whenever not enough heat can be obtained from TES. However, since we have a hybrid energy system and NPP is capable to produce reliable amount of energy, NPP meets the electrical energy needs by CSP in the low insolation conditions: this represents the major advantage of having a hybrid energy system. Instead of getting the required electrical energy, this hybrid energy system compensates the requirement of CSP and is, hence, not dependent on other energy sources if NPP is not shutdown.

When it comes to hydrogen production, in this research, Cu-Cl thermochemical cycle is employed. It is noticed that to generate 1 mol of hydrogen (2.016 g/mol-$H_2$), 200 kJ of heat energy at the temperature of 525 Celsius approximately and 25 kJ of electrical energy are necessary. These requirements can be met by both NPP and CSP even though

in different form. Although CSP is capable to produce heat energy up to 530 Celsius, iPWR-type SMR is not. For this reason, an ideal reversible thermochemical heat pump is utilized to raise the temperature of the fluid leaving the NPP, which is at 255°C, as the Cu-Cl cycle needs heat energy at a temperature of roughly 525°C. The reference heat pump [157] requires for 0.4235 kJ of heat energy to enhance the fluid's temperature by 1°C. In the N-RHES under study, the needed heat energy for the pump is provided by the NPP. The reversible thermochemical heat pump does not require any electricity.

Therefore, there are two energy sources firstly producing heat energy. Then, according to what we need to produce, hydrogen and/or electricity, these sources produce electricity taking into account their instantaneous net electricity production efficiency.

Producing hydrogen by CSP, power cycle input energy is multiplied by a desired percentage of CSP then is divided by total heat energy requirement (200 kJ heat energy + 25 kJ electrical energy./ instantaneous net electricity production efficiency) to produce 1mol of hydrogen of Cu-Cl as shown in equation (*31*). To generate electricity by CSP, power cycle input energy of CSP is multiplied by "100% - desired percentage to produce hydrogen of CSP". Next, the result is multiplied by the instantaneous net electricity production efficiency as shown in equation *(32)*. By doing so, instantaneous full power of CSP is used to produce hydrogen and/or electricity.

$$200\ kJ\ heat + \frac{25\ kJ\ electrical\ energy}{instantaneous\ efficiency\ of\ CSP} = 1\ mol\ of\ H_2 \qquad (31)$$

$$(100\% - desired\ percentage) \times power\ cycle\ input\ energy \times instantaneous\ efficiency\ of\ CSP = electrical\ enegy \qquad (32)$$

As it is mentioned, when CSP requires electrical energy, NPP employed here supplies this electrical energy to CSP when needed. First of all, it is necessary that the required energy is converted into heat energy (the required electrical energy of CSP./instantaneous net electricity production efficiency of NPP) as shown in equation *(33)*. Afterwards, the heat energy amount is deducted from the heat energy produced by the NPP. The leftover heat energy of NPP is utilized to produce hydrogen and/or electricity as indicated in equation *(34)*. Producing hydrogen by NPP, the leftover heat energy of NPP is multiplied by a desired percentage of NPP, then is divided by the total heat energy requirement as shown in equation *(35)*. To generate electricity by NPP, the leftover energy of NPP is multiplied by "100% − desired percentage to produce hydrogen of NPP" as shown in equation *(36)*. Then, it is multiplied by net electric efficiency of NPP. By doing so, instantaneous full power of NPP is used to produce hydrogen and/or electricity.

$$\frac{required\ electrical\ energy\ of\ CSP}{instantaneous\ efficency\ of\ NPP} = required\ heat\ energy\ from\ NPP \quad (33)$$

$$total\ heat\ energy\ of\ NPP - required\ heat\ energy\ from\ NPP = leftover\ heat\ energy\ of\ NPP \quad (34)$$

$$\frac{leftover\ heat\ energy\ of\ NPP \times desired\ \%\ of\ NPP}{total\ heat\ requirement\ to\ produce\ 1\ mol\ H_2\ via\ NPP} = H_2\ amount\ by\ NPP \quad (35)$$

$$leftover\ heat\ energy\ of\ NPP \times (100\% - desired\ percentage) \times net\ efficiency\ of\ NPP = electricity\ amount\ by\ NPP \quad (36)$$

By defining a time period and percentages of NPP and CSP, the total amounts of hydrogen and/or electricity are thus finally calculated. Then, thanks to written code on MATLAB, plots can be obtained. To give a clear example, some calculations are shown in the graphs below. Production amounts of hydrogen and electricity per energy sources that change depending on hours are shown on the example graphs.

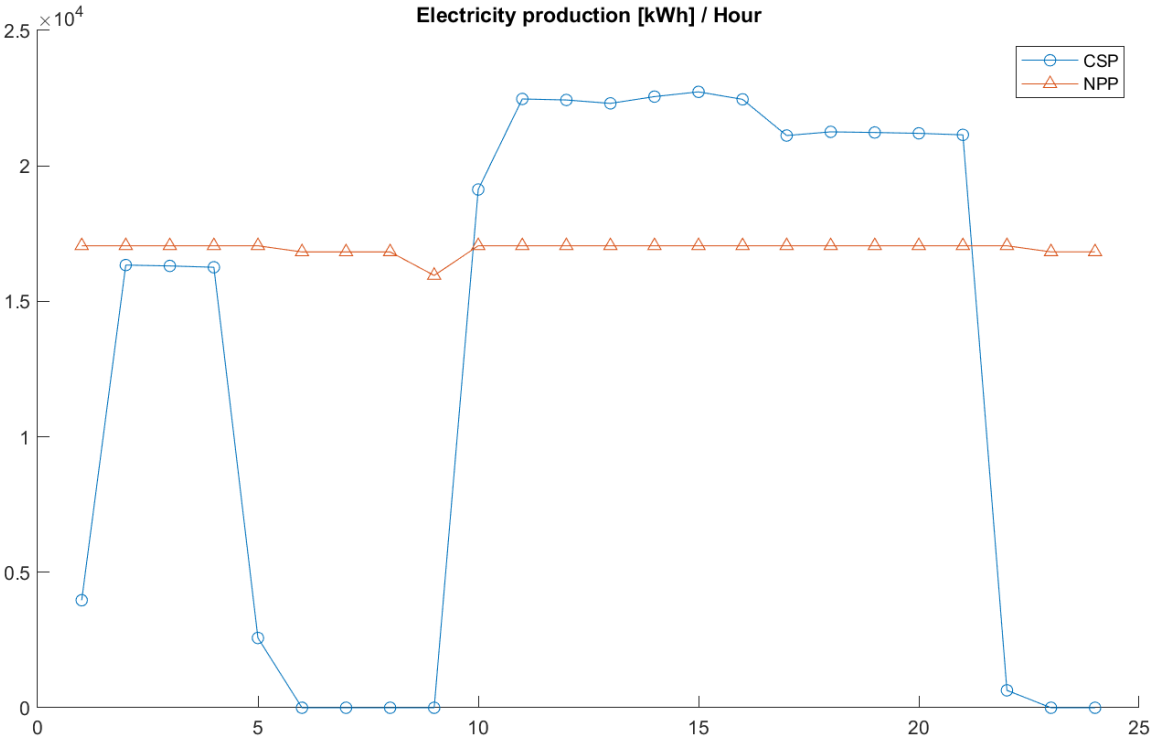


Figure 3.13: An indication of 24-hour period electricity production in kWh by employing 50% of NPP and 50% of CSP, (January 1st).

In Figure 3.13 electricity production amounts are depicted depending on the energy sources and the hours of a day on January 1st. 50% power of the NPP and CSP energy sources are used to produce electricity. It is seen that there is no electricity production via CSP between 6am and 9am. The reason why there is no electricity production is that TES at these times has not enough thermal energy to produce energy.

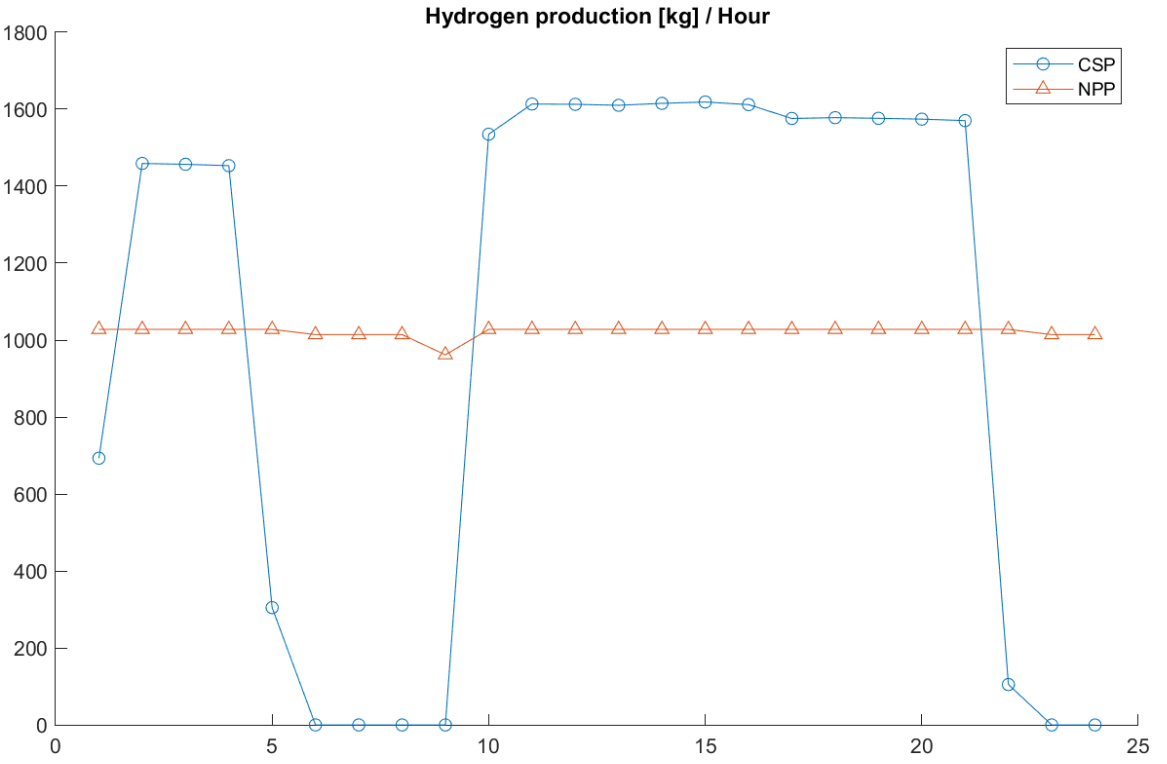


Figure 3.14: An indication of 24-hour period hydrogen production in kg by employing 50% of NPP and 50% of CSP sources, (January 1st).

As there is not enough thermal energy in TES, CSP cannot produce hydrogen between 6:00 am and 9:00 am on January 1$^{st}$ as shown in Figure 3.14.

In Figure 3.13 and Figure 3.14, total hydrogen and total electricity amounts are indicated by sources. In Figure 3.15 and Figure 3.16, total hydrogen and electricity productions of the hybrid system are pointed out.

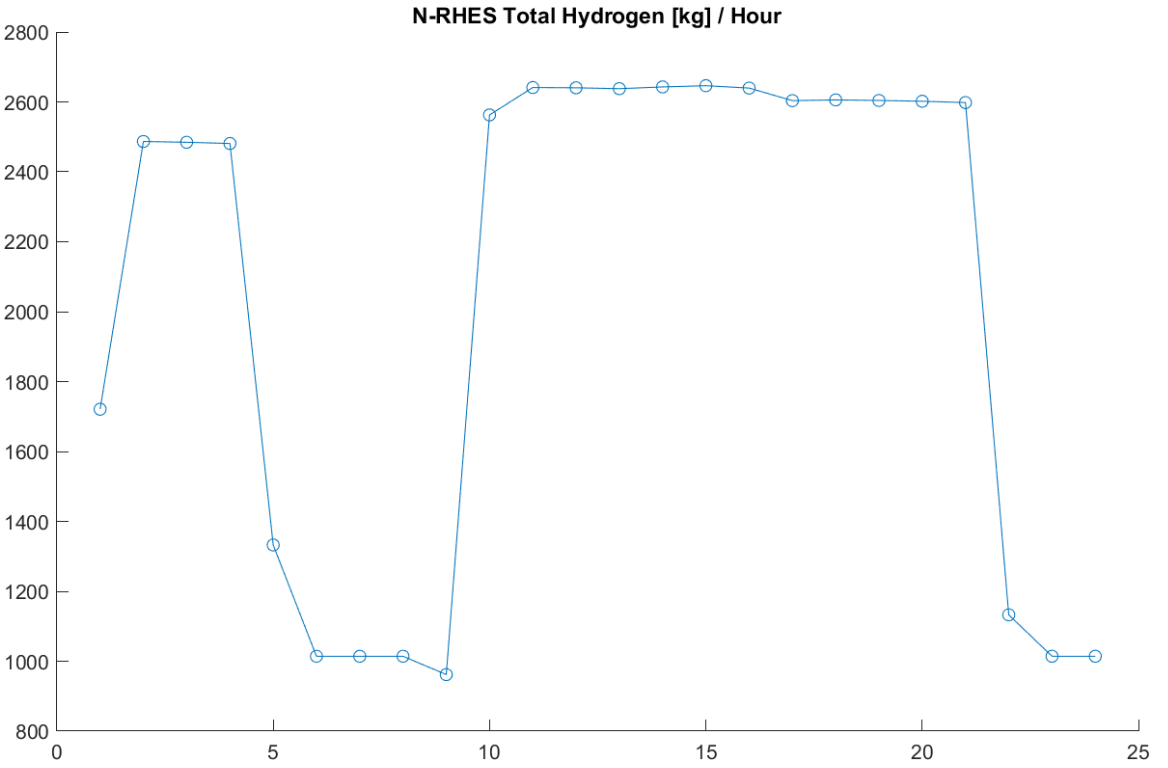


Figure 3.15: An indication of 24-hour period total hydrogen production in kg by employing 50% of NPP and 50% of CSP sources, (January 1st).

In Figure 3.15, total hydrogen amounts produced by N-RHES are indicated. Here, 50% of NPP and CSP powers are used to produce hydrogen for 24-hour period on January 1st. Fluctuations are seen in hydrogen production due to CSP power output varies depending on the weather-related parameters.

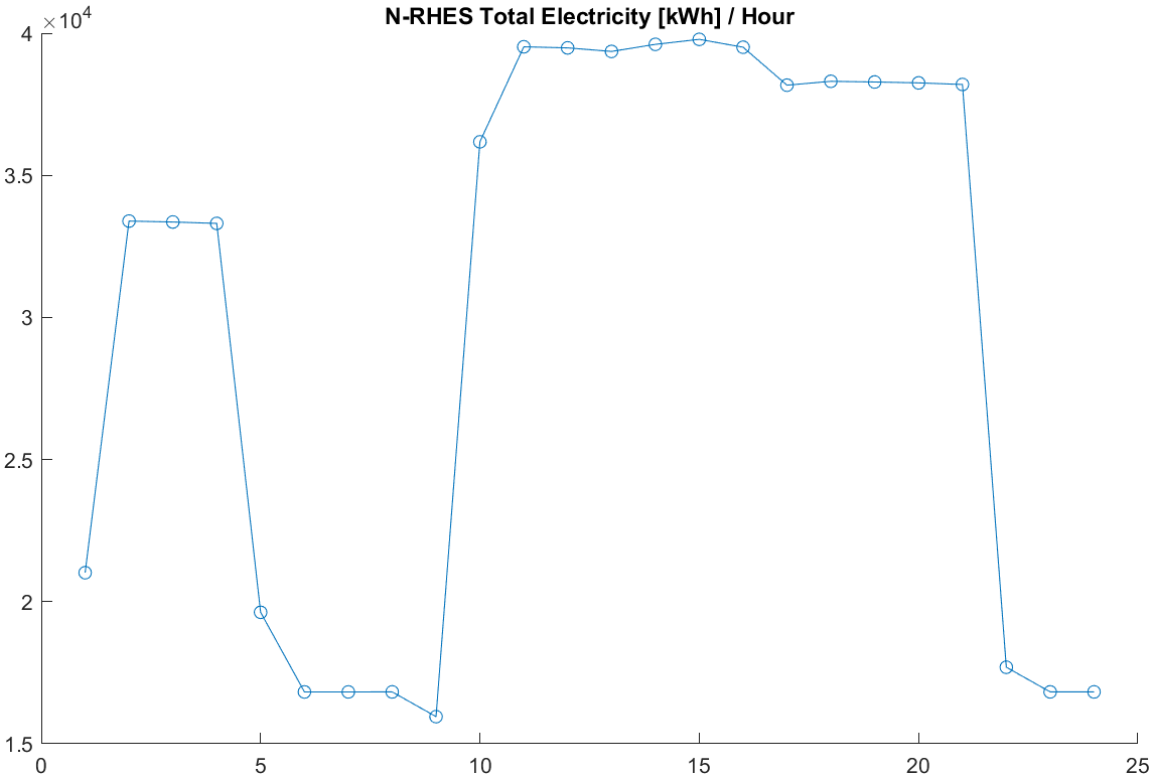


Figure 3.16: An indication of 24-hour period total electricity production in kWh by employing 50% of NPP and 50% of CSP sources, (January 1st is selected as an example to show a trend).

Total electricity amounts produced by N-RHES are shown in Figure 3.16. 50% of NPP power and CSP power are employed in order to produce electricity on January 1st. depending on the CSP power output, electricity production starts to increase. Next, it remains the same and decreases. All these fluctuations are linked to CSP power output.

Profit can be considered as an important concern in any energy production plant. In order to get together electricity and hydrogen in the same unit, their heat equivalents are taken. Therefore, at the end of this research, the first objective is optimizing profit and the second objective is total heat equivalent coming from total electricity and total hydrogen produced. For this reason, total profit needs to be calculated. In terms of electricity price, needed data is taken from "www.ieso.ca" providing Hourly Ontario Electricity Price

(HOEP) of a year (2021). Changing electricity prices on an hourly basis, first to an excel file and then to MATLAB to be processed.

In terms of modelling hydrogen price, hydrogen price is between US$ 1.00 and US$ 1.80 [183]. To have a realistic hydrogen price model, there needs be a relationship between hydrogen price and electricity price. For example, when the electricity price is more than it is average price, hydrogen price needs to be more than US$ 1.80. To compensate these fluctuations, a realistic hydrogen price modelling is done as follows:

First of all, it is accepted that the 1kg of hydrogen is US$ 1 as a base price as hydrogen price is between US$ 1.00 and US$ 1.80 [183]. 1 kg of hydrogen cannot be less than US$ 1 [183]. From a reference paper (Pinsky) [4], it is calculated that producing 1 kg of $H_2$ with electrolysis requires approximately 50 kWh electricity. As the electrolysis is the one of the most common methods to produce hydrogen, it is taken into account. To be able to close to a realistic hydrogen price modeling, the price of 50 kWh electricity (HOEP) is added to the base price (US$ 1).

To calculate a realistic overall $H_2$ price depending on the hours of a day:

- If the hour is between 1:00am to 5:00am, “Hourly Ontario 50 kWh-Electricity Price” is multiplied by the square of “Hourly Ontario 1 kWh Electricity Price”.
- If the hour is not between 1:00am to 5:00am, “Hourly Ontario 50 kWh Electricity Price” is multiplied by “Hourly Ontario 1 kWh Electricity Price”.

In order to calculate heat equivalent of hydrogen, 1 kg of hydrogen is equal to 120.1 MJ heat energy [1]. Moreover, in terms of heat equivalent coming from electrical energy, it is accepted that there is no energy loss when electrical energy is converted into heat energy. It means that 1 kJ electrical energy is equal to 1 kJ heat energy as an assumption.

To conclude, there are two objective functions, being total profit and total heat equivalent, depending on the two variables which are the power percentages of the sources. However, it has to be considered that CSP power fluctuates hourly depending on the weather-related parameters and CSP plays a role in terms of NPP leftover heat energy.

In this research, as hourly based 8760 data is used, it is necessary that there has to be a relationship between the number of hours of the year and date of the year (day/month/hour). When the date is given, it is converted to the hours of the year with the help of the code written on MATLAB.

#### 3.9.1.1 Multi-objective Optimization

Multi-objective optimization approaches that can solve complexity (as contained in systems) is a part of this research as there is more than one objective function. Here, a Genetic Algorithm is used with the principle of Pareto Front is used on MATLAB. The main benefit is that GA assesses the population of solutions concurrently to prevent it from being trapped on local best solutions. The methods that have been so far discussed include multi-objective optimization methods and original formulations that are resolved using conventional optimization Algorithms (single-objective optimization method). However, unlike earlier approaches, technologies like Genetic Algorithms can be modified to proactively solve multi-objective difficulties. This is the rationale behind this thesis's usage of the Genetic Algorithm optimization method. Pareto Front is the idea based on that no single or preference criterion can be improved upon without also impacting upon at least one other person or preference criterion, which is known as Pareto efficiency or Pareto optimality. Vilfredo Pareto (1848–1923), an Italian economist and civil engineer, who employed the idea in his research on income distribution and economic efficiency, is remembered as the concept's namesake [184].

Calculation based on Genetic Algorithm, firstly, it is necessary that constraints are defined, such as lower bounds, upper bounds. Electricity is needed at any time in a day, therefore, in order to produce a reliable amount of electricity produced by N-RHES, it is assumed that NPP and CSP produce electricity by using 15% as a based load of their powers at least in this study. However, by taking into account the location electricity needs, to define the power percentage at least, another study in more details needs to be carried out. After that, number of variables are specified. In this study, the variables are percentages of NPP and CSP to produce electricity and/or hydrogen. The GUI of Genetic Algorithm is shown in Figure 3.17.

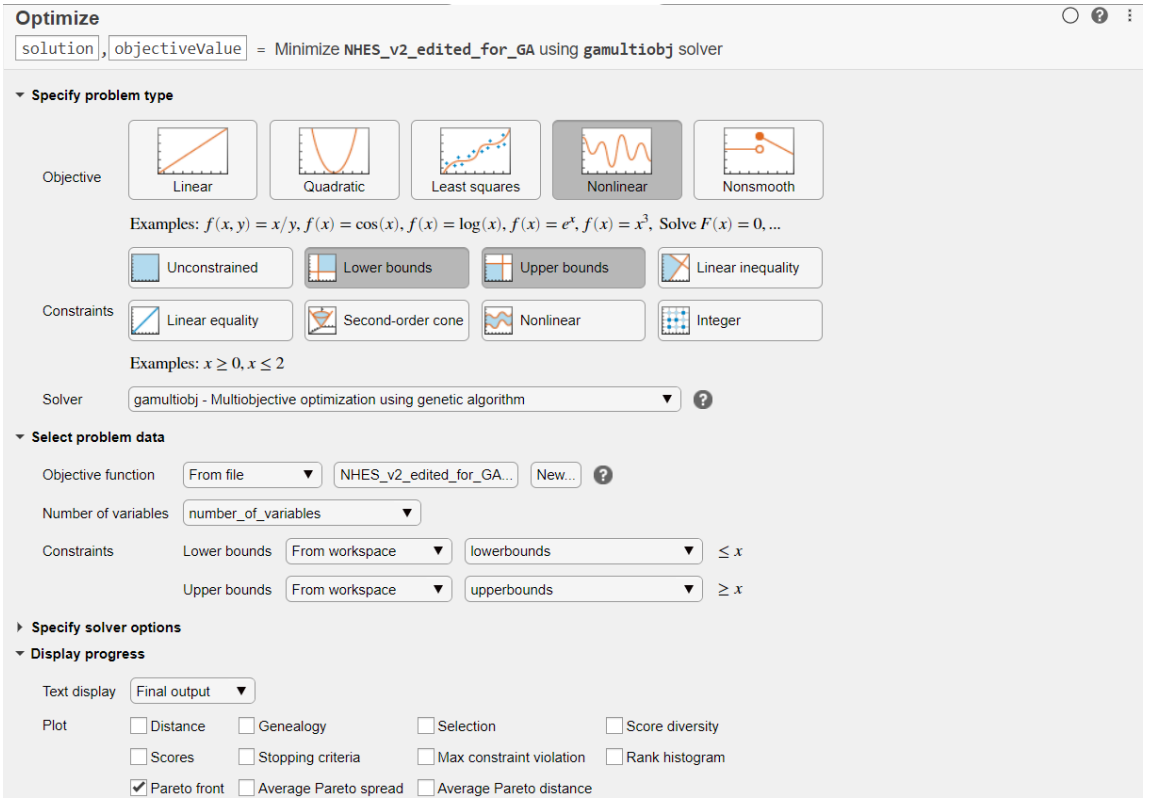


Figure 3.17: GUI of GA on MATLAB

By using GAs, results are depicted on a graph as shown in Figure 3.18**.** Here, objective-1 and objective-2 refer to total profit and total heat equivalent, respectively.

When the time period given includes more than one hour, optimization is carried out for every single hour thanks to a written MATLAB code shown in the appendix.

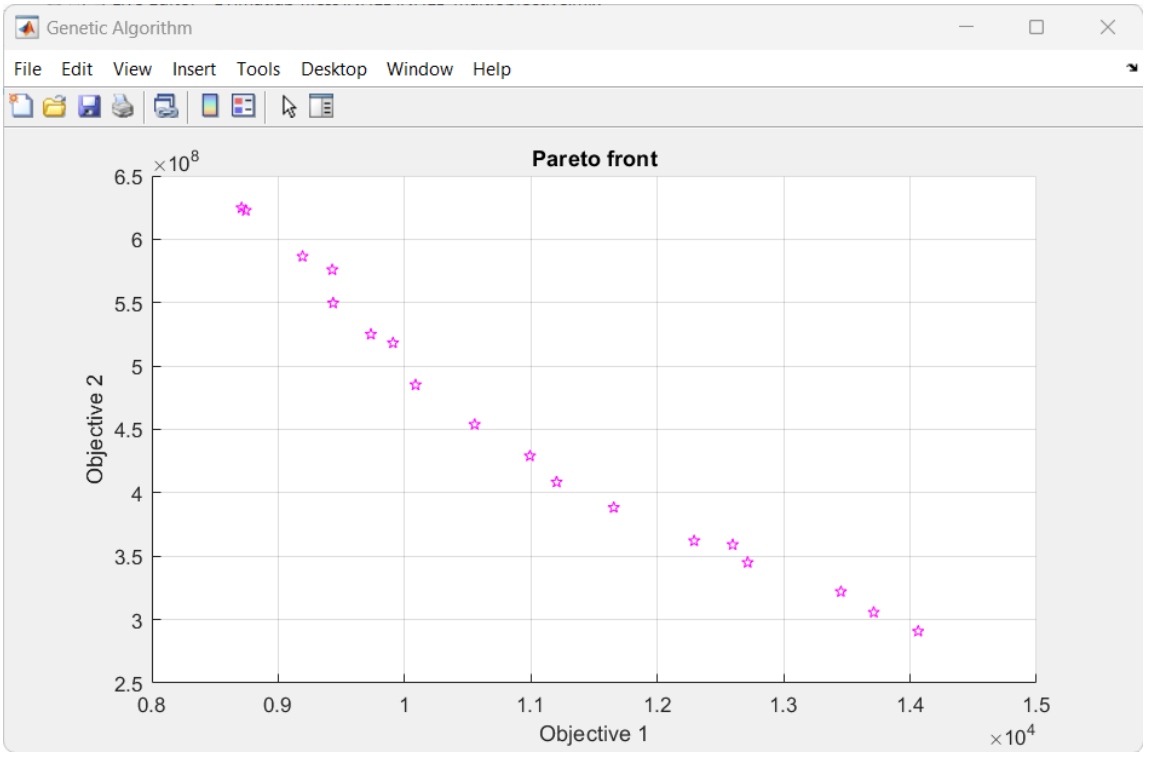


Figure 3.18: An indication of multi-objective Genetic Algorithm Pareto Front (objective-1: total profit in USD and objective-2: total heat equivalent in kJ).

While the result improves for one of the objectives, it is seen that the result worsens for the other. Sometimes these changes do not change linearly. It can be seen that one of the objectives increases more than the other objective decreases. Such changes are important for the Pareto Front principle. Multi-objective optimization gives us results based on objectives. In the Pareto Front graph as shown in Figure 3.18**,** there are points regarding to the objectives**.** Every single point refers to the percentages of NPP and CSP used to produce hydrogen and/or electricity. In this way, instead of defining percentages of the energy sources, optimized percentages are obtained in terms of optimized results. *Please check the Appendices for extra information.*

## Chapter 4. Results

In this chapter, various scenarios are considered, and their results are examined in terms of hydrogen and electricity amounts in kg and kWh, respectively.

In Table 4.1 and Table 4.2, four key scenarios are considered for each season and two different days are selected in terms of temperature. Here, the days with the highest and lowest temperatures in each season are selected. The aim here is to examine the production amounts that change depending on the seasons and temperatures. According to the power percentages of energy resources, four different key scenarios are examined. The power percentages shown in Table 4.1 represent the power of the energy sources used for hydrogen production. The power percentages shown in Table 4.2 represent the power of the energy sources to generate electricity.

In Table 4.1;

a) each of the two power plants contributes for 25% of the energy needed to produce hydrogen,

b) it is 50% - 50% contribution to produce hydrogen,

c) it is a 75% - 75% contribution to produce hydrogen,

d) it is a 100% - 100% contribution to produce hydrogen.

In Table 4.2;

a) each of the two power plants contributes for 25% of the energy needed to generate electricity,

b) it is 50% - 50% contribution to generate electricity,

c) it is a 75% - 75% contribution to generate electricity,

d) it is a 100% - 100% contribution to generate electricity.

These percentages, which are increased by 25%, are given in order to see the differences in trends and production amounts.

The statistical variation of recorded climatic variables is taken into consideration and acknowledged as a limiting factor. The tables comprise two different days from each season, serving as prototypical instances for the complete seasons. The examples given here serve to illustrate how much electricity and hydrogen are generated, for instance, on the coldest and warmest days of each season. The tables also indicate how the amount of output varies according to the season.

The results can be acquired by specifying the date range (per respective yearly season) and power percentage of the sources using the LabVIEW code that has been written. Although the NPP's power is unchanged, there are some variances in the amount of hydrogen and electricity produced via the NPP. In fact, the NPP provides all of the electricity necessary by the CSP to keep the molten salt in a liquid state and all auxiliary components at all times. When it comes to renewable energy, CSP power is reliant on weather factors like temperature, cloudiness, daylight hours, and so on. As a result, the N-RHES experiences power fluctuations. The production amounts of electricity and hydrogen are displayed in Table 4.1 and  for particular days. Despite the fact that the average outside temperature in summer2 is higher than in summer1, it can be seen from the tables that there is a decline in the production of hydrogen using CSP in summer2. The reduction in daylight hours in the summer2 can be cited as the cause of this predicament, despite the fact that there are numerous unknown variables that characterize the weather. Even though fall2's temperature is higher than fall1's, there has been a drop in the amount of hydrogen produced by CSP. This shows that other weather-related factors, in addition to temperature, play a significant impact in the power of the CSP with high level of

complexity, resulting in unpredictable. There are still some unanswered questions, but these need to be considered in greater detail in a subsequent investigation. CSP simulation does not supply these kinds of information.

Table 4.1: Hydrogen production in kg per given seasonal day (as shown), for four alternative NPP and CSP percentage contributions (scenarios) [2].

| | | **$H_2$ in tonne** | | | | | | | |
|---|---|---|---|---|---|---|---|---|---|
| | | **Winter1** | **Winter2** | **Spring1** | **Spring2** | **Summer1** | **Summer2** | **Fall1** | **Fall2** |
| | | DEC-15 *9.4°C* | FEB-11 *26.7°C* | MAR-11 *13.3°C* | MAY-31 *38.9°C* | JUN-10 *30°C* | JUL-10 *47.8°C* | SEP-7 *43.3°C* | OCT-27 *18.3°C* |
| **CSP1** | **25%** | 10.3 | 14.7 | 16.9 | 19.7 | 17.4 | 16.4 | 4.3 | 15.1 |
| **NPP1** | **25%** | 16.4 | 16.4 | 16.4 | 16.5 | 16.4 | 16.4 | 16.3 | 16.4 |
| **CSP2** | **50%** | 20.7 | 29.5 | 33.8 | 39.5 | 34.8 | 32.8 | 8.7 | 30.2 |
| **NPP2** | **50%** | 32.8 | 32.8 | 32.9 | 32.9 | 32.8 | 32.8 | 32.6 | 32.8 |
| **CSP3** | **75%** | 31 | 44.2 | 50.7 | 59.2 | 52.2 | 49.2 | 13.1 | 45.3 |
| **NPP3** | **75%** | 49.2 | 49.3 | 49.3 | 49.4 | 49.3 | 49.2 | 48.9 | 49.3 |
| **CSP4** | **100%** | 41.3 | 58.9 | 67.6 | 78.9 | 69.6 | 65.6 | 17.4 | 60.5 |
| **NPP4** | **100%** | 65.5 | 65.7 | 65.8 | 65.8 | 65.7 | 65.6 | 65.3 | 65.7 |

Table 4.2: Production of electricity in kWh for four distinct NPP and CSP percentage contributions on a specific seasonal day (scenarios) [2].

| | | **Electricity in kWh** | | | | | | | |
|---|---|---|---|---|---|---|---|---|---|
| | | **Winter1** | **Winter2** | **Spring1** | **Spring2** | **Summer1** | **Summer2** | **Fall1** | **Fall2** |
| | | *DEC-15 9.4°C* | *FEB-11 26.7°C* | *MAR-11 13.3°C* | *MAY-31 38.9°C* | *JUN-10 30°C* | *JULY-10 47.8°C* | *SEP-7 43.3°C* | *OCT-26 18.3°C* |
| **CSP1** | **25%** | 1.38E+05 | 1.96E+05 | 2.26E+05 | 2.59E+05 | 2.21E+05 | 2.04E+05 | 5.14E+04 | 2.02E+05 |
| **NPP1** | **25%** | 2.72E+05 | 2.73E+05 | 2.73E+05 | 2.74E+05 | 2.73E+05 | 2.73E+05 | 2.71E+05 | 2.73E+05 |
| **CSP2** | **50%** | 2.76E+05 | 3.92E+05 | 4.52E+05 | 5.18E+05 | 4.43E+05 | 4.08E+05 | 1.03E+05 | 4.04E+05 |
| **NPP2** | **50%** | 5.45E+05 | 5.46E+05 | 5.47E+05 | 5.47E+05 | 5.46E+05 | 5.46E+05 | 5.42E+05 | 5.46E+05 |
| **CSP3** | **75%** | 4.14E+05 | 5.88E+05 | 6.79E+05 | 7.77E+05 | 6.64E+05 | 6.12E+05 | 1.54E+05 | 6.06E+05 |
| **NPP3** | **75%** | 8.17E+05 | 8.19E+05 | 8.20E+05 | 8.21E+05 | 8.19E+05 | 8.19E+05 | 8.14E+05 | 8.19E+05 |
| **CSP4** | **100%** | 5.52E+05 | 7.84E+05 | 9.05E+05 | 1.04E+06 | 8.86E+05 | 8.17E+05 | 2.06E+05 | 8.08E+05 |
| **NPP4** | **100%** | 1.09E+06 | 1.09E+06 | 1.09E+06 | 1.09E+06 | 1.09E+06 | 1.09E+06 | 1.08E+06 | 1.09E+06 |

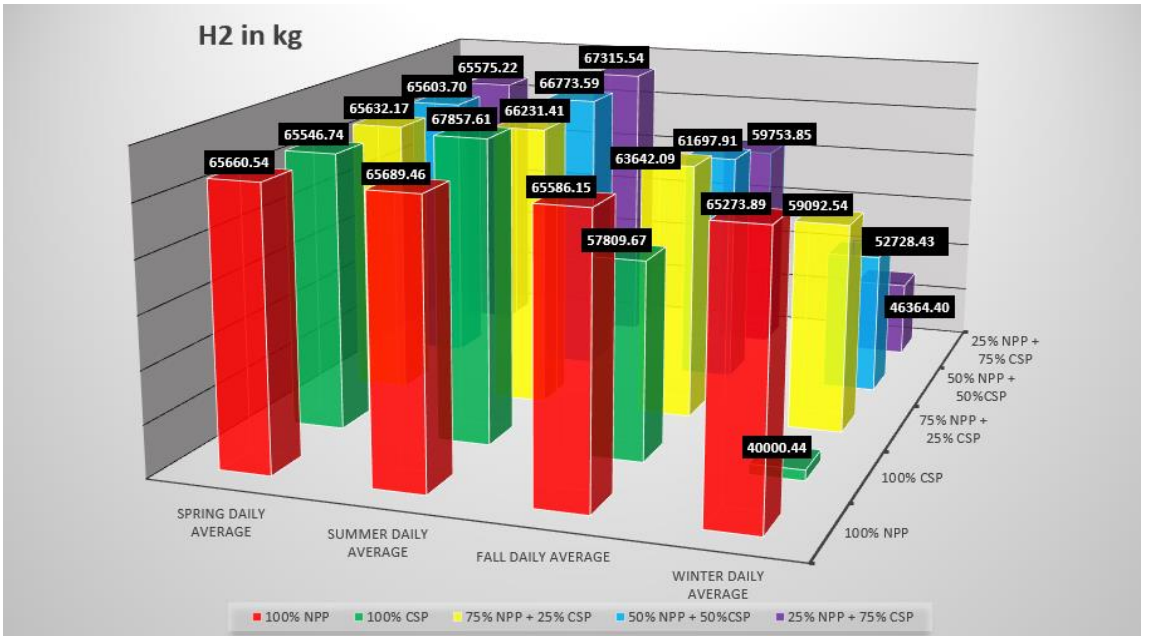


Figure 4.1: A seasonal comparison of hydrogen generation based on a certain percentage of NPP, CSP, or both reliance [2].

Although the percentage rates of the sources are different, it can be observed in Figure 4.1 that the average daily hydrogen production levels for the spring are approximately similar. However, during the summer, more hydrogen is produced as a result of CSP's higher energy output. The amount of hydrogen produced in the winter with 100 percent NPP power is less than the other daily average amounts 100 percent NPP

power. The NPP supplies the electrical energy required to keep the CSP operating throughout the winter, when the CSP's power output drops.

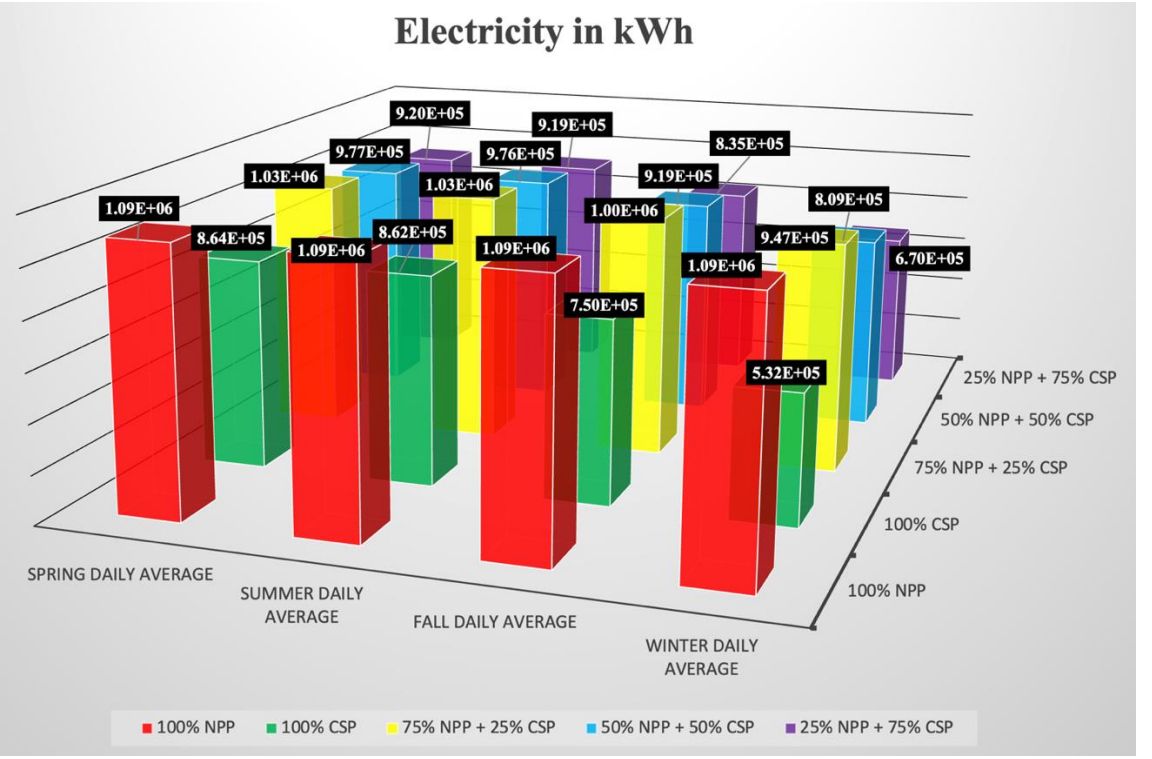


Figure 4.2: A comparison of seasonal and source-based variations in power production (NPP, CPS or combination) [2].

The amount of electricity produced decreases in the fall and winter, as shown in Figure 4.2. Since the molten salt must be in liquid form for CSP to perform, electrical energy is required to keep the liquid molten salt in the liquid form as well as to run the auxiliary equipment.

To conclude, since CSP power fluctuates due to weather related parameters, and sometime CSP requires electrical energy supplied by NPP, overall N-RHES power outputs vary. In addition to this, the price of electricity and hydrogen also fluctuate depending on the supply and demand. Therefore, for instance, when the electricity price and/or demand decreases, better idea is to produce more hydrogen. To give another example, when the

CSP's net electricity production efficiency decreases, better idea to utilize more heat energy, which is produced by CSP, to produce hydrogen instead of converting heat energy into electricity. By taking into account all these scenarios mentioned above, in order to maximize all profit or total heat equivalent coming from N-RHES, it is necessary to apply multi-objective optimization approach here. Thanks to optimization, all complexity taking part in this N-RHES is processed and better outputs are obtained. Next section accounts for comparative results, which are non-optimized and optimized results, to show the benefits of the optimization in this research.

### 4.1 Results of NRHES based on Multi-objective Optimization

After applying optimization, according to the objectives, the hydrogen and/or electricity production percentages of NPP and CSP are defined. By using these defined percentages of the sources, better outputs are selected based on the objectives which are maximizing the total profit and maximizing total heat equivalent.

First of all, a non-optimized result is considered and then compared to its optimized form to show how optimization gives us better results. Every single point on the graphs explains two percentages values. The values on the upper and the bottom sides indicate CSP percentage and NPP percentages used to produce hydrogen, respectively. The remaining powers as percentages are used to generate electricity.

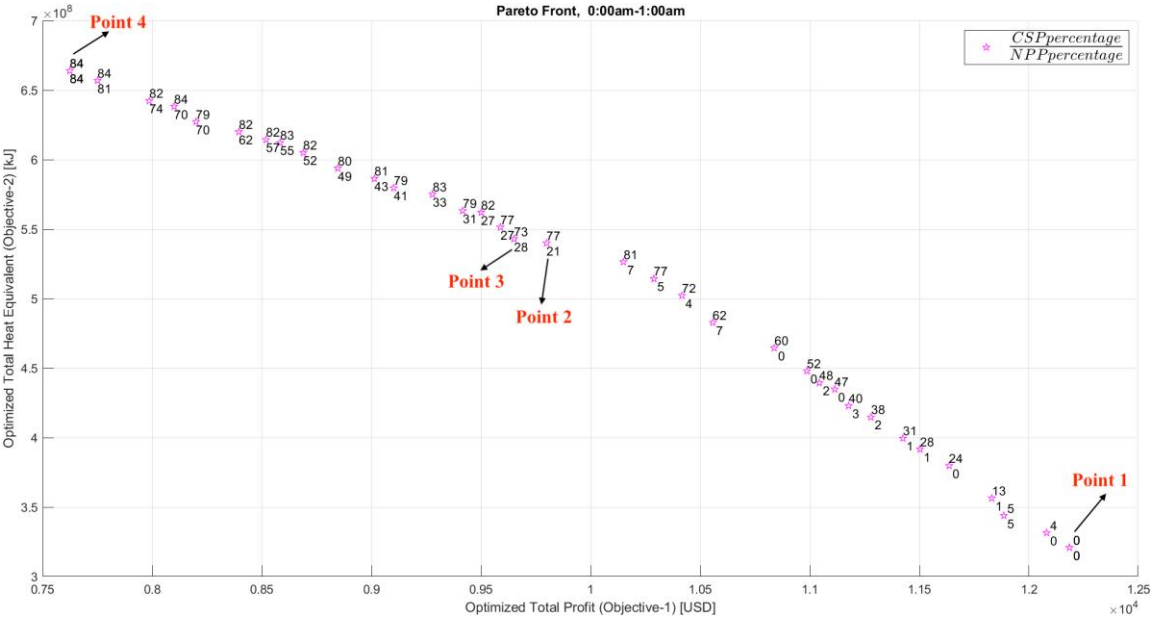


Figure 4.3: Applying MOGA for N-RHES (JUN-15, between 00:00am and 1:00am).

Table 4.3: Comparative results.

| | **Results** / JUN-15, between 00:00am and 1:00am | | | | | |
|---|---|---|---|---|---|---|
| | **Non-Optimized** | **Non-Optimized** | **Optimized Point 1** | **Optimized Point 2** | **Optimized Point 3** | **Optimized Point 4** |
| NPP percentage to produce $H_2$ | 50% | 25% | 0.47% | 21.30% | 28.91% | 84.94% |
| CSP percentage to produce $H_2$ | 50% | 25% | 0.00% | 77.20% | 73.17% | 84.98% |
| Total profit (**Obj.1**) | 9.51E+03 | 1.09E+04 | **1.22E+04** | 9.80E+03 | 9.65E+03 | 7.62E+03 |
| Total heat equivalent (**Obj.2**) | 5.22E+08 | 4.21E+08 | 3.21E+08 | 5.40E+08 | 5.43E+08 | **6.64E+08** |
| Total $H_2$ amount [kg] | 3.02E+03 | 1.51E+03 | 1.28E+01 | 3.13E+03 | 3.20E+03 | 5.13E+03 |
| Total electricity amount [kWh] | 4.45E+04 | 6.67E+04 | 8.87E+04 | 4.57E+04 | 4.40E+04 | 1.34E+04 |

In Figure 4.3, in terms of total profit (objective-1) and total heat equivalent (objective-2), points with percentages of the sources used to produce hydrogen are depicted. While point 1 refers to maximum profit, point 4 indicates maximum total heat equivalent. The purpose of selection point 2 and point 3 is to point out that the total heat equivalent (obj.2) does not change as much as the total profit (obj.1) between point 2 and point 3. This situation is important that although the selections of point 2 or point 3 does

not change the result of total heat equivalent as much as they change the total profit, the point 2 is more effective than point 3 to obtain more benefit in terms of total profit (objective-1). As mentioned, when the total heat equivalent amount changes only 0.5%, the total profit amount changes by 1.5%. Thus, it is obviously seen that point 2 is preferable than point 3 as it does not change linearly.

Comparative results are indicated in Table 4.3. When the focus is on the total profit, non-optimized result when 25% powers of NPP and CSP are employed to produce hydrogen makes profit of US$ 1.09E+04, after optimization, the total profit is US$ 1.22E+04. When it comes to total heat equivalent, it is 5.22E+08 kJ in the scenario of 50% power of NPP and CSP used, it is 6.64E+08 kJ in the optimized result with percentages of 84.94 NPP and 84.98 CSP. When the maximum profit is obtained in Point 1, the maximum heat equivalent amount is attained in Point 4.

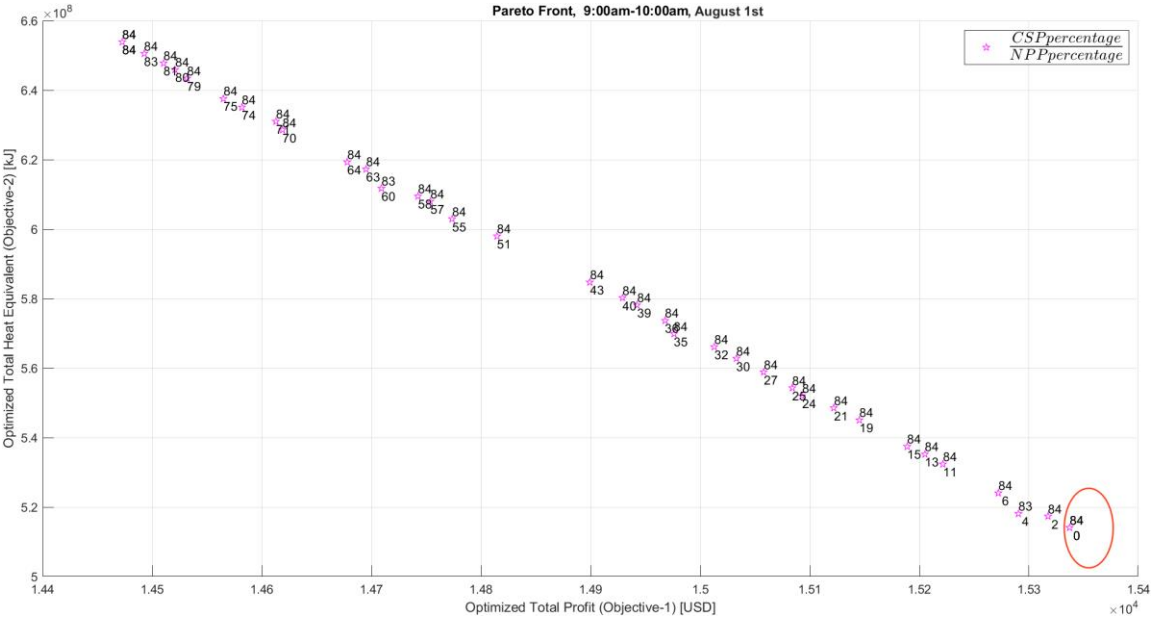


Figure 4.4: An optimized result for August 1st between 9:00am and 10:00am.

When looking at Figure 4.4, it is seen that the maximum profit (US$ 1.53E+4) is obtained when the CSP and NPP percentages to produce hydrogen is 84% and 0%,

respectively. While the total maximum profit is obtained by using the energy sources completely for electricity generation in Jun-15 between 00:00am and 1:00am in Figure 4.3, the total maximum profit on August 1st between 9:00am and 10:00am is obtained by using the entire NPP power and 84% of the CSP power for hydrogen generation. These results are obtained thanks to multi-objective Genetic Algorithm (MOGA).

In this research, multi-objective optimization performs on one-hour timeframes, since hourly based data is used. Therefore, MOGA defines the optimized percentages of NPP and CSP to produce hydrogen and/or electricity for each one-hour time period according to objectives. This optimization of N-RHES is carried out on a computer with Intel i7, 9th Gen, 9750H CPU. An optimization carried out on this computer for one hour-time period is completed in 17 minutes, approximately. An optimization of N-RHES;

- For one day (24 hours) takes 24*17=6.8 hours,
- For one month takes 30*24*17=8.5 days,
- For a season including four months takes 4*30*24*17=34 days.

As this multi-objective optimization requires too much CPU power, at most one-day optimization is carried out with the computer in this research. To point out one-day multi-objective optimization, one day of a year is selected, August 1st. This multi-objective optimization covers 24-hour period starting on August 1st, 12:00am and ending on August 1st, 11:59pm.

Table 4.4: Comparison of the results.

| **All day, August 1st** | | | |
|---|---|---|---|
| **CSP** | **NPP** | **Total Profit** | **Total Heat Equivalent** |
| 50% | 50% | 2.49E+05 | 1.05E+10 |
| 25% | 25% | 2.54E+05 | 8.47E+09 |
| **Optimized** | | 2.72E+05 | 1.33E+10 |

In Table 4.4, scenarios based on different percentages to produce hydrogen of CSP and NPP are compared with optimized results for all day on August 1st. Remaining percentages of the energy sources are used to produce electricity. In the first scenario, CSP and NPP produce hydrogen with 50% of their power during all day. In the second scenario, CSP and NPP produce hydrogen with 25% of their power and they produce electricity with 75% of their power during all day. Results are given Table 4.4. When MOGA is applied to each hour of the day in terms of selected objective (total profit or total heat equivalent), it is obviously seen that better results can be obtained. Optimized scenario accounts for 24-time hour period optimized. Therefore, every single 1-hour time period has their own optimized energy sources power percentages.

Additionally, in order to observe hydrogen and electricity generations, the production trends can be seen on graphs. For instance, according to a scenario of hydrogen production via 50% power of CSP and NPP on August 1$^{st}$, some graphs are depicted as follow:

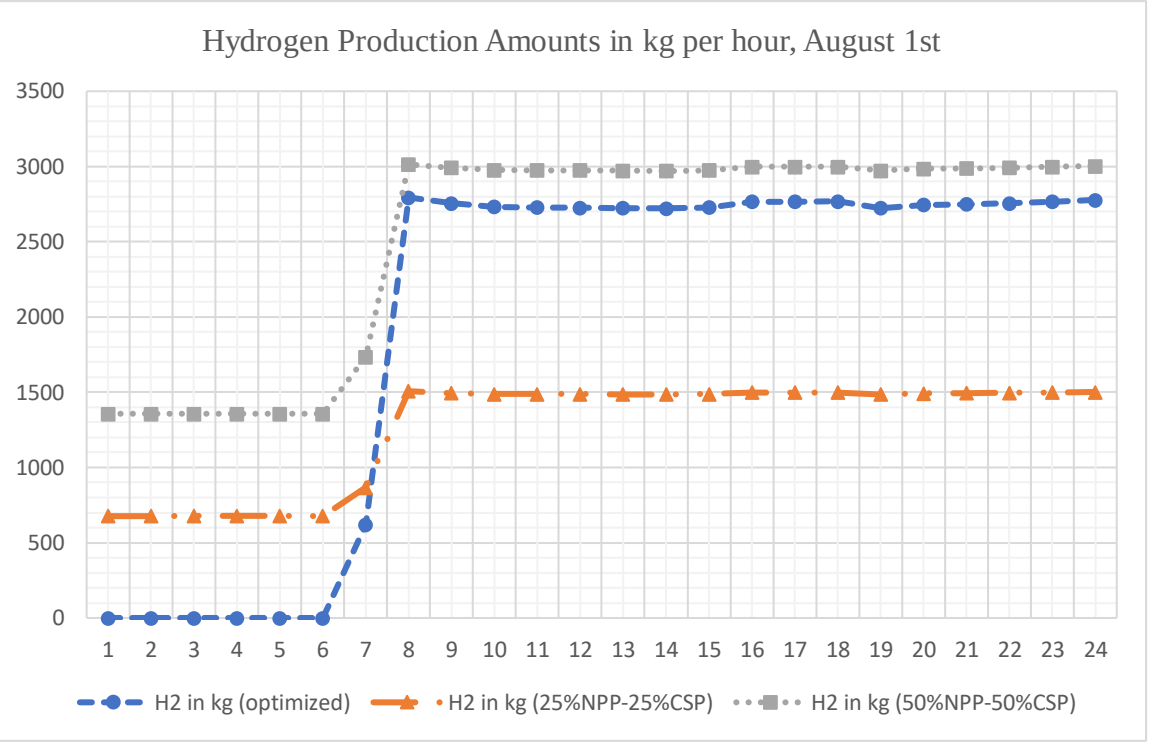


Figure 4.5: Hydrogen production amounts depending on three scenarios (optimized N-RHES for max. profit, 25%NPP-25%CSP and 50%NPP-50%CSP) on August 1st.

Figure 4.5 and Figure 4.6 show the differences in the production amounts of hydrogen and electricity per hour by comparing 3 different scenarios.

Figure 4.5 (where x-axis: hours of the day, y-axis: hydrogen production amount in kg) depicts hydrogen production amounts according to three different scenarios, which are optimized N-RHES for maximum profit, 25%NPP-25%CSP, 50%NPP-50%CSP. Percentages refer to the amount of power from the energy sources used to produce hydrogen. The remaining percentages are the power of the energy sources for electricity generation. In order to achieve maximum profit with N-RHES, it is more profitable to produce only electricity with the power of the energy sources and therefore, hydrogen is not produced during the first six hours.

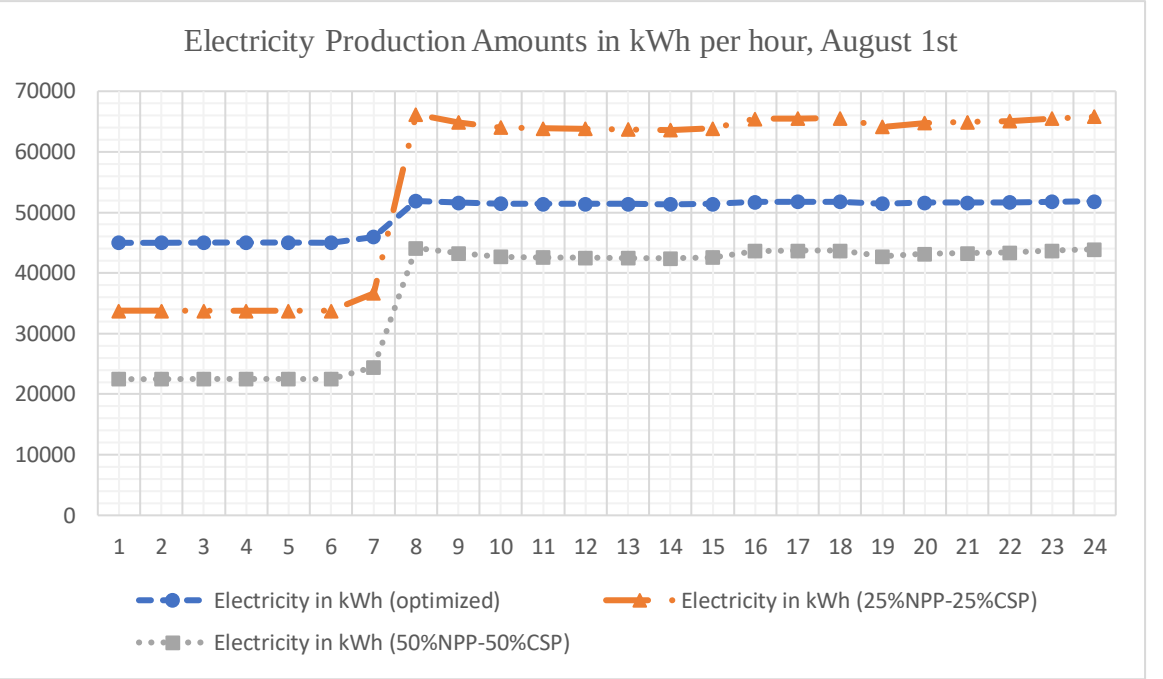


Figure 4.6: Electricity production amounts depending on three scenarios (optimized N-RHES for max. profit, 25%NPP-25%CSP and 50%NPP-50%CSP) on August 1st.

Figure 4.6 (where x-axis: hours of the day, y-axis: electricity production amount in kWh) depicts electricity production amounts according to three different scenarios, which are optimized N-RHES for maximum profit, 25%NPP-25%CSP and 50%NPP-50%CSP. Percentages refer to the amount of power from the energy sources used to produce hydrogen. The remaining percentages are the power of the energy sources for electricity generation. In order to achieve maximum profit with N-RHES, it is observed that electricity and hydrogen are produced via N-RHES at the same time after the first six hours.

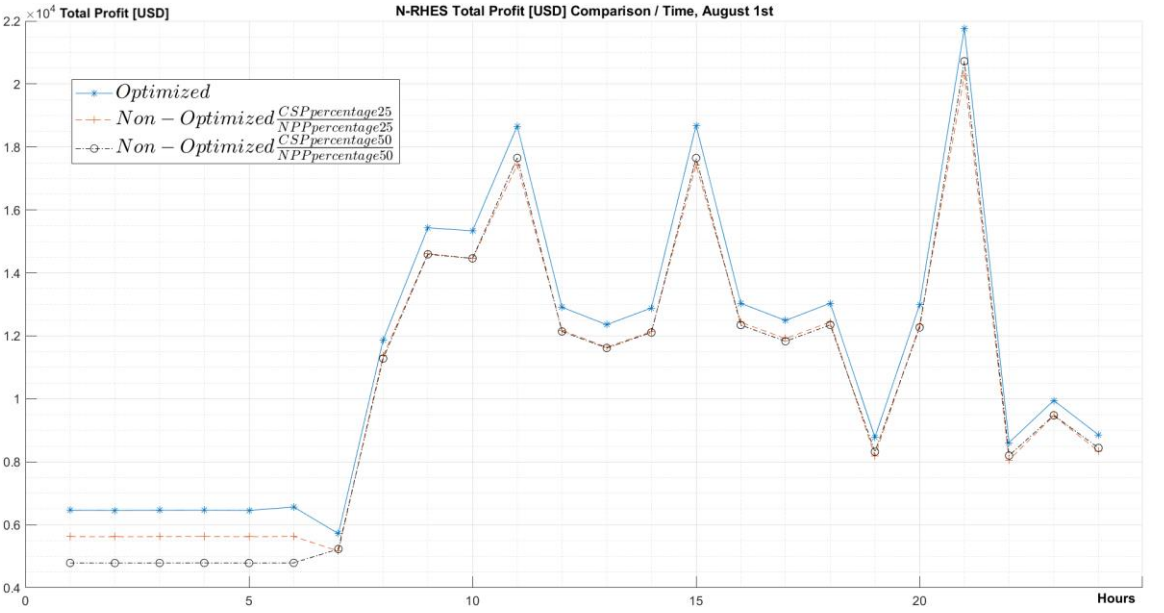


Figure 4.7: Total Profit (objective-1) comparison based on scenarios, optimized N-RHES for maximum profit, 25%NPP-25%CSP and 50%NPP-50%CSP on August 1st.

In Figure 4.7 showing the benefit of this research, total profits for one day are pointed out based on scenarios, optimized N-RHES for maximum profit, 25%NPP-25%CSP and 50%NPP-50%CSP on August 1st. The percentages of the energy sources refer to power percentages of NPP and CSP to produce hydrogen. The remaining percentages are used to generate electricity. Thanks to optimization, the most profit is obtained from the N-RHES. As can be seen in the line graph, the profit for each hour in the optimized scenario is higher than the other two scenarios.

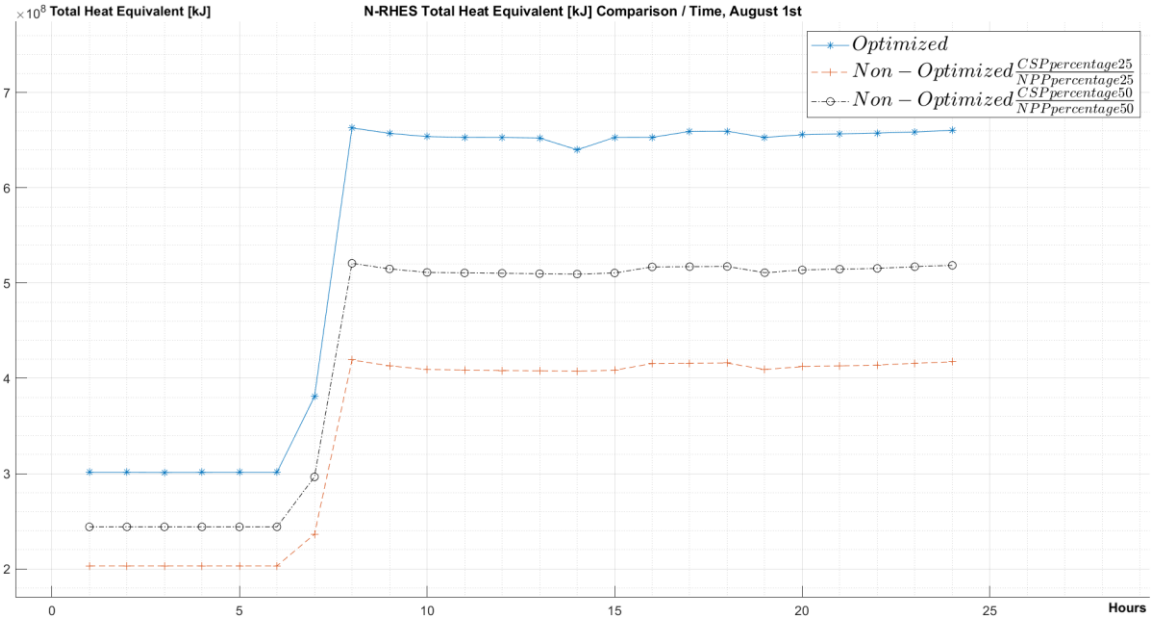


Figure 4.8: Total Heat Equivalent (objective-2) comparison based on scenarios, optimized N-RHES for maximum total heat equivalent, 25%NPP-25%CSP and 50%NPP-50%CSP on August 1st.

Figure 4.8, the simulation result for total Heat Equivalent for one day is depicted out based on scenarios, per optimized N-RHES for maximum heat equivalent: two percentages, 25%NPP-25%CSP and 50%NPP-50%CSP on August 1st. The percentages of the energy sources refer to power percentages of NPP and CSP to produce hydrogen. The remaining percentages are used to generate electricity. Per optimization, the most total most heat (thermal) equivalent is obtained from the N-RHES. As can be seen in the line graph, the total heat equivalent for each hour when optimized is higher than the other two scenarios.

### 4.2 Consideration of NPP Electricity Requirement

Although nuclear power plants produce electricity and supply electricity to the grid, they require electricity from the grid. These electricity requirements depending on the situations as following [185]:

- For 100% full power operation, the electricity requirement (the unit service load) from the grid is around **6%** of the reactor full power capacity (total MWe).
- For decay heat removal per one reactor, required standby power supply is around **2%** of reactor full power capacity (total MWe).
- Required emergency power supply per one reactor is around **0.2%** of reactor full power capacity (total MWe).

Considering this information above, it is assumed that the NPP requires electrical energy up to 6% of its own electrical power from the grid. Here, in this research, as a hybrid energy system is employed, the NPP electricity requirement is aimed to meet from CSP instead of meeting from the grid. However, since CSP output varies due to weather-related parameters, CSP does not meet the electricity requirement of NPP when CSP cannot produce electricity. In order to compensate this situation, electricity generators powered by hydrogen are used. These hydrogen power generators performs with a ~ 60% energy conversion from hydrogen heat energy (120.1 $MW_{th}$ /1kg-$H_2$) to electrical energy (72.06 $MJ_e$ /1kg-$H_2$) [186]. Therefore, 1kg-$H_2$ is equal to 20.01 $kWh_e$.

After calculation of that 1kg-$H_2$ is equal to 20.01 $kWh_e$, the written MATLAB code is updated to calculate how much hydrogen needs to be stored to produce electrical energy via hydrogen-powered electricity generators to meet the NPP electrical energy requirement depending on the time period.

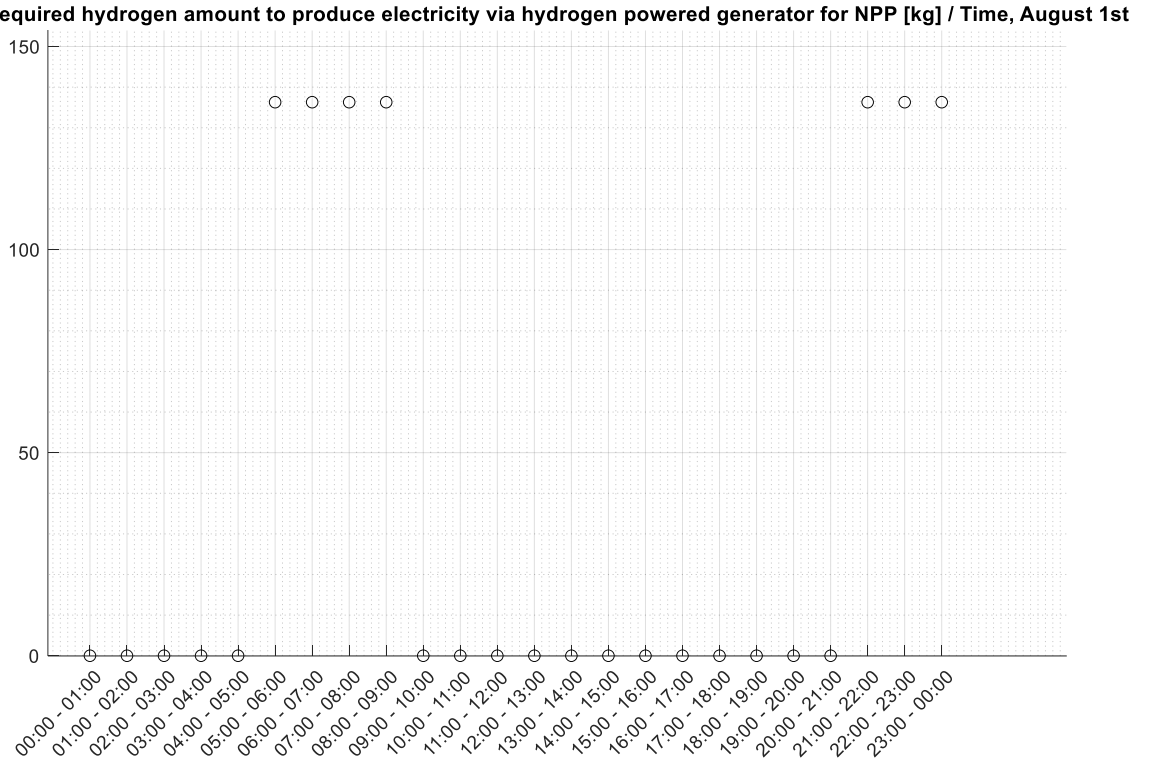


Figure 4.9: Indication of hourly required $H_2$ amount to meet NPP electricity demand on August 1st.

In Figure 4.9, required $H_2$ amounts are shown for every 1 hour-time period in order to meet the electrical energy demand of NPP when CSP does not produce electrical energy on August 1st. Since CSP does not have any power output between 05:00am and 09:00am and between 21:00 and 00:00, NPP electricity demand is met by hydrogen-powered generators. In this case, the total required hydrogen amount is 9.54E+02 in kg for 24 hours on August 1st. Moreover, hourly needed hydrogen amount to be able to supply electrical energy to NPP is 136.29 kg.

In the case of where CSP does not produce any electrical energy for 24 hours, and the total NPP electricity demand is met by hydrogen-powered generators, the total hydrogen amount which is needed to store is 3271 kg when iPWR-type SMR is operated at full power.

### 4.3 Consideration of SMR Safety-in-design

Passive safety system (PSS) R&D and technology advancement have drawn attention in relation to safety-in-design. The most recent ideas on PSS for integral PWR (iPWR) type SMRs are as follows:

- the application of dynamic PRA/PSA techniques.
- the time evolution of any unforeseen event or unforeseen initiating event that has a low-to-low likelihood but a considerable impact on the SMR safety-in-design.

At the system level, there is a substantial correlation between the PSS system's time reaction and many other types of SMR safety-in-design events, especially at the 1-hour, 2-hour, 4-hour, 8-hour, 16-hour, and 24-hour marks after the accident started. These time "slots" are therefore related to safety-in-design and must be taken into account as a design variable and parameter. For demarcation we assume that anything lasting more than 4 (hidden and unanticipated event) hours will need reactor shutdown, and thus the time categories is divided into two categories: under 4 hours and over 4 hours.

The graphs below depict electricity/hydrogen generation and NPP`s electricity demand in the scenario where NPP power drops from 100% to 0% in 4 hours. Here, 50% of the total powers of NPP and CSP is used for hydrogen production. As mentioned in the previous section, NPPs require electricity from grid when NPP is under operation. The required electrical energy is defined as 6% of NPP`s power. In Figure 4.10, while NPP power is decreasing from 100% to 0%, the required electricity of NPP is pointed out. Here, the NPP required energy is supplied from CSP instead of from the grid. CSP can meet NPP electricity requirement as CSP produces energy at these time periods.

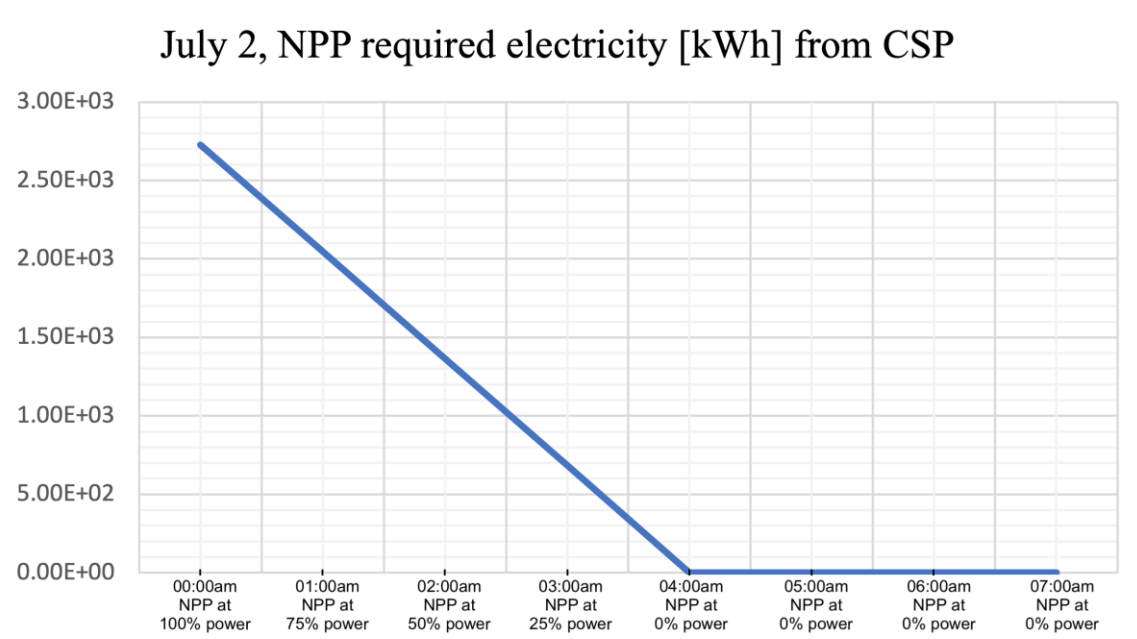


Figure 4.10: NPP electricity requirement while NPP power decreases from 100% to 0% in 4 hours.

In Figure 4.11, hydrogen amount produced by N-RHES is decreasing as the power of NPP also decreases. After 04:00am, the hydrogen production figure continues almost the same as only CSP produces hydrogen.

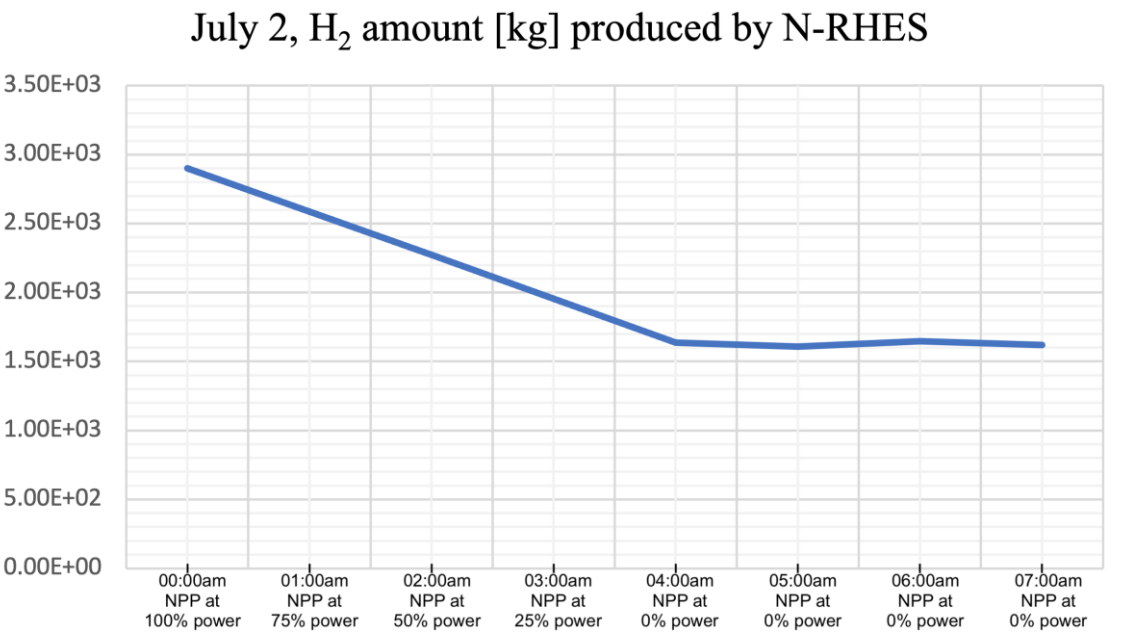


Figure 4.11: Hydrogen production amount via N-RHES while NPP power decreases from 100% to 0% in 4 hours.

In Figure 4.12, electricity amount generated by N-RHES starts to decrease as the power of NPP decreases. After 04:00am, the electricity production continues almost the same as only CSP produces electricity with a 50% of its power.

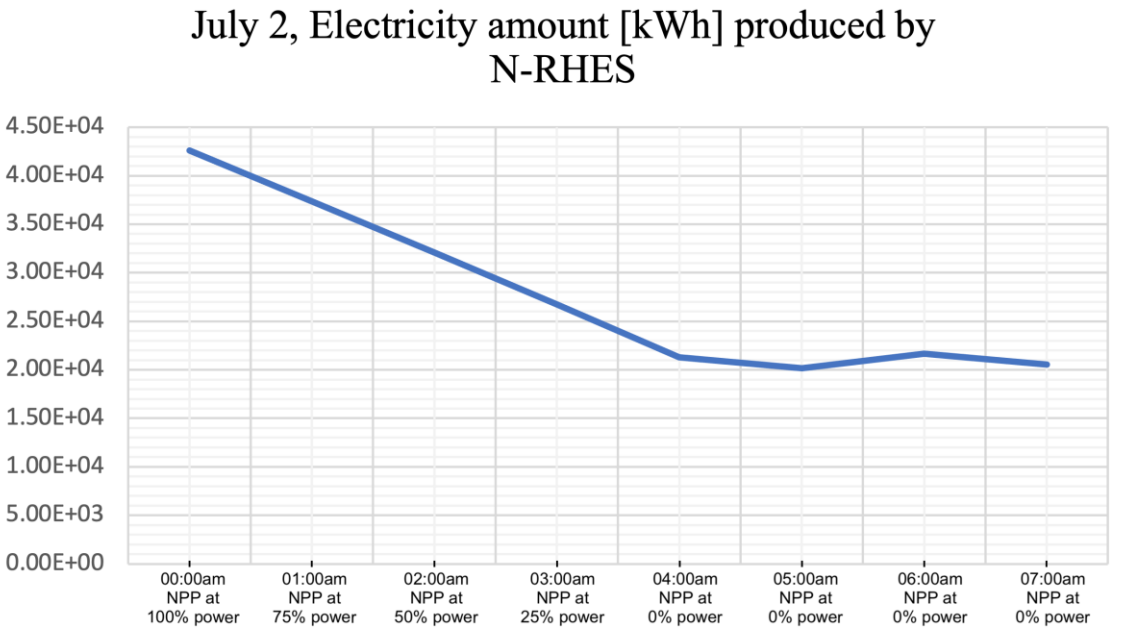


Figure 4.12: Electricity production amount while NPP power decreases from 100% to 0% in 4 hours.

On July 2nd at the time periods shown on the figures above, CSP is capable to meet NPP electricity demand. In order to see that how the NPP electricity requirement is met by electricity generator powered by hydrogen, another time period which is on January 21 between 06:00am and 13:00 is selected. In Figure 4.13, hydrogen amount in kg is pointed out for hydrogen-powered generators to produce electricity. Since NPP power decreases, the electricity demand also decreases. Therefore, hydrogen amount used in the hydrogen-powered generators decreases as well.

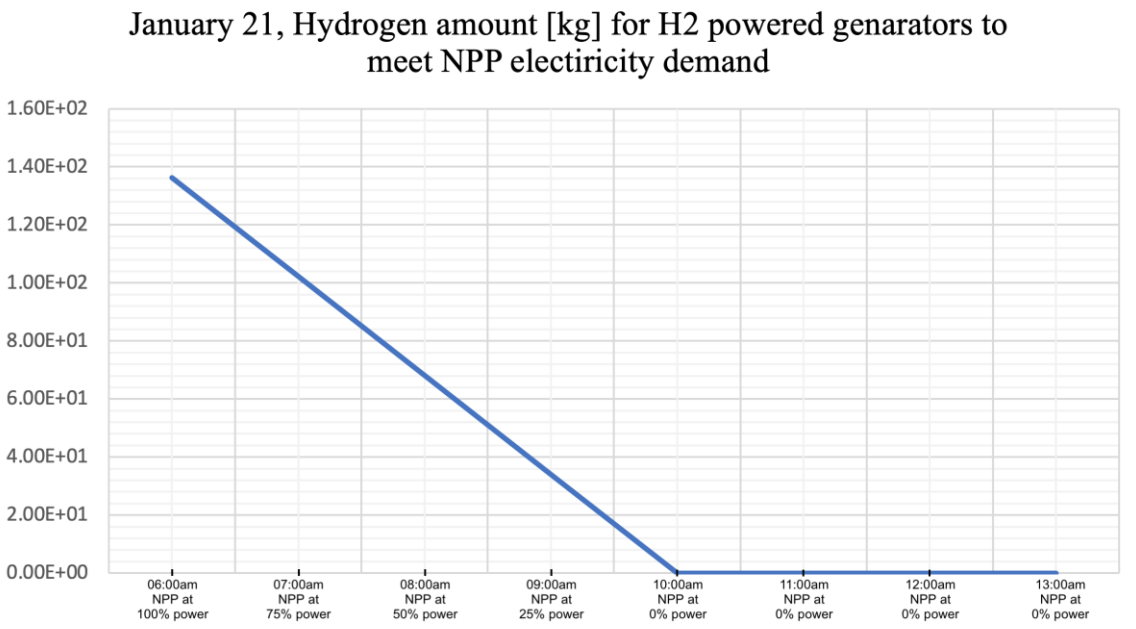


Figure 4.13: NPP electricity requirement is met by hydrogen-powered electricity generators while NPP power decreases from 100% to 0% in 4 hours.

# Chapter 5. Conclusion

## 5.1 Conclusion

As the world's population and economy grow and more people relocate from rural to urban regions, the need for energy is rising. It has been shown that the primary cause of global warming is the persistent use of hydrocarbon-based energy, which significantly increased the atmospheric quantities of $CO_2$ and greenhouse gases. Renewable energy sources are necessary to combat global warming and to preserve the environment. By reducing GHG emissions, renewable energy sources play a significant part in preserving our planet. On the other hand, there are some disadvantages to generating energy from renewable sources. It is difficult to find electric energy from renewable energy sources at a competitive price. In fact, one of these energy sources' most observable qualities is how varied and irregular they are. Thus, it is necessary to use comprehensive and effective technical solutions to resolve these problems. In order to address the volatility and discontinuity of renewable energy sources, large-scale storage devices have been proposed and constructed to meet market demand.

Hydrogen is a useful energy carrier when it comes to energy storage. Hydrogen, for instance, can be utilised to generate energy. Furthermore, hydrogen is already a resource that is used as a feedstock in a variety of industrial operations, such as refineries and the creation of methanol and ammonia. Hydrogen-based energy storage devices are essential for large-scale energy storage because they are portable. This research focus on production of clean hydrogen and electricity. Since utilizing clean energy sources have an important role in the production of clean hydrogen, nuclear and renewable energies are located in an important place, which can help to reduce the greenhouse gases emission of

the world. Coupling renewable energy, which has fluctuations in the energy production, with nuclear energy, which produces reliable amount of energy, is seen as a promising solution to compensate these fluctuations. Another advantage of this N-RHES is that if the electricity demand decreases, N-RHES can produce hydrogen instead of decreasing NPP power output.

Although this research gives information about various hydrogen production technologies and sources including based on fossil-fuels as well, it continues with thermochemical hydrogen production cycles, which are shown as exciting clean hydrogen production technologies when employed with small modular nuclear reactor and/or CSP as a renewable energy source. Therefore, in this study, iPWR-type SMR is preferred combining with CSP to produce clean hydrogen via Cu-Cl thermochemical cycle which requires more heat energy than electrical energy. It makes Cu-Cl cycle more effective as there is less energy conversion from heat to electrical energy.

N-RHES can be enhanced to be more efficient despite its complexity. Multi-objective optimization in the N-RHES is a particularly challenging aspect of optimization processes since almost all real-world optimization problems are structured using several competing objectives. The most common approach to such problems is to combine many objectives into a single target, however the optimal approach tries to solve the multi-objective optimization problem in the real world. Therefore, Genetic Algorithms is used to optimize to achieve preferred objective in this study.

To model CSP in this research SAM software is used by defining inputs. SAM gives 8760-hourly based data depending on the weather-related parameters for one year. Basically, when there is not enough sun light, CSP requires electrical energy from the grid to keep its fluid, molten salt, in a liquid form and to maintain its auxiliary equipment.

However, here, thanks to coupling with NPP, this hybrid energy system is capable to meet the energy requirement of CSP. It can be pointed out another benefit of having a hybrid energy system. Mentioned 8760 hourly based data including for example, “electricity to grid from CSP” or “net electricity production efficiency of CSP” is taken from SAM to written to an excel file. Then, these are transferred to LabVIEW and MATLAB software to process.

After modeling N-RHES accounting for three major subsystems, which are iPWR-type SMR, CSP and Cu-Cl thermochemical hydrogen production cycle, total production amounts of electricity in kWh and hydrogen in kg are calculated in LabVIEW and MATLAB software. After completing validations of these software with each other, it is continued with MATLAB to optimize the hybrid energy system in terms of total profit as an objective-1 and total heat equivalent as an objective-2.

Before applying multi-objective optimization approach, some scenarios results based on power percentages of NPP and CSP to produce hydrogen and/or electricity are shown, afterwards, these results are compared with optimized results in order to show the importance of the optimization on this N-RHES.

At the end of this research, in terms of comparative results which are non-optimized and optimized, are shown. It is seen that, by applying multi-objective optimization approach, better results can be obtained in terms of the objectives defined as shown in Table 4.4. According to aimed functions, maximizing total profit or maximizing total heat equivalent, NPP and CSP percentages can be defined. By doing so, the complexity of N-RHES is taken into account to achieve better outputs.

In a bullet form:

- N-RHES produces hydrogen via reference Cu-Cl thermochemical cycle which requires more heat energy than electrical energy, which means it is more efficient compared to traditional electrolysis, requiring more electrical energy than heat energy, due to the less energy conversion from heat to electrical energy.
- As the temperature requirement of Cu-Cl thermochemical cycle (525°C) that can be met by CSP is less than that of S-I thermochemical cycle (850°C), Cu-Cl is employed to produce hydrogen.
- By using multi-objective optimization approach, two objectives, maximizing total profit and maximizing total heat equivalent, are optimized simultaneously. According to these objectives, preferred results are obtained and explained in this research.
- For the molten salt based CSP that has to be maintained in liquid phase, the electrical and/or thermal energy needed to do so, the required energy of CSP can be provided by the nuclear plant – the SMR.
- The minor result is to show hydrogen and electricity production amounts.
- The major result of this thesis is to show better results obtained in terms of the objectives when GAs based multi-objective optimization with the principle of Pareto Front on MATLAB is applied.
- A variety of weather-related parameters, including cloud coverage, humidity, fog density, and the amount of airborne dust, are uncertain and fuzzy in terms of CSP power production. The aforementioned weather-related data cannot be served by SAM for processing by scientists.

- 8760 hourly based data is taken from SAM to written to an excel file. Then, these are transferred to LabVIEW and MATLAB software to process to calculate hourly based results of hydrogen and electricity productions and optimization as well.
- With Genetic Algorithm method on MATLAB, the hybrid energy system is optimized in terms of total profit as an "objective-1" and total heat equivalent as an "objective-2". GAs is selected for this study because GAs simultaneously assess a population of solutions, which prevents them from being limited to just the best local solutions.
- Results based on power percentages of NPP and CSP to produce hydrogen and/or electricity are pointed out to be able see hydrogen and electricity production amounts in different weather conditions.
- Comparative results, non-optimized versus optimized, are shown. By applying multi-objective optimization, achieving maximized total profit or total heat equivalent are pointed out in this study.

  What makes this research new is that N-RHES is optimized by using GAs with Pareto Front principle. This research provides information about which percentages of NPP and CSP energy sources need to be selected, to obtain preferred results.
- Hydrogen and electricity production amounts are explained after an event where NPP power decreases from 100% to 0% in four hours. Here, it is considered that the external electrical energy needed by the NPP is provided by CSP, if the CSP is capable of providing electricity. If CSP cannot produce energy for NPP electricity demand, then this NPP electricity demand is met by hydrogen-powered generators.

To be able to produce electricity for NPP via hydrogen-powered electricity generators, needed hydrogen amounts in kg are calculated.

## 5.2 Future Works

In terms of CSP output, there are a number of weather-related parameters such as cloud coverage, humidity, fog density, the amount of dust in the air, which are unknown and fuzzy with uncertainties. SAM is not capable to serve those weather-related parameters mentioned above for SAM-users to process. However, the simulation can be still improved if weather-related information can be clarified. Also, multi-objective optimization approach requires so much CPU power due to the iterative calculations of GA to process more data to give better results as the multi-objective optimization approach in this research uses hourly based data. Here, in this study, to apply multi-objective optimization via MATLAB;

- for one day takes 6.8 hours,
- for a month takes 8.5 days,
- for a season takes 34 days approximately.

For this reason, applying optimization for a wider time-period needs computers that can do more calculation in less time. By using more powerful computers, in the future, more comprehensive optimization results can be obtained.

Also, hydrogen storage and distribution systems need to be studied.

Moreover, it should be studied that where there are SMR, solar and wind power plant to produce electricity and hydrogen. New optimization methods can be necessary in these hybrid energy systems including more complexity as they have very high complexity with a number of variables and parameters.

## References


1. M. Ciftcioglu, F. Genco, A. Tokuhiro, “Optimized Clean Hydrogen Production using Nuclear Small Modular Reactors and Renewable Energy Sources: a Review,” Serial | Major Trends in Energy Policy and Nuclear Power, atw, Vol. 67, pp 16-30, 2022.

2. M. Ciftcioglu, F. Genco, A. Tokuhiro, "Considerations and Optimization of Hydrogen Production using Small Modular Reactors and Renewable energy sources", Fourth International Conference on Generation IV & Small Reactors (G4SR-4) Toronto, ON, Canada, 2022.

3. United Nations, Department of Economic and Social Affairs, Population Division (2017). World Population Prospects: The 2017 Revision, Key Findings and Advance Tables. Working Paper No. ESA/P/WP/248.

4. R. Pinsky, P. Sabharwall, J. Hartvigsen, and J. O’Brien, “Comparative review of hydrogen production technologies for nuclear hybrid energy systems,” Prog. Nucl. Energy, vol. 123, p. 103317, 2020, doi: 10.1016/j.pnucene.2020.103317.

5. I. Dincer, “Green methods for hydrogen production,” Int. J. Hydrog. Energy, vol. 37, no. 2, pp. 1954–1971, 2012, doi: 10.1016/j.ijhydene.2011.03.173.

6. A. Miltner, W. Wukovits, T. Pröll, and A. Friedl, “Renewable hydrogen production: a technical evaluation based on process simulation,” J. Clean. Prod., vol. 18, pp. S51–S62, 2010, doi: 10.1016/j.jclepro.2010.05.024.

7. D. Gielen, F. Boshell, D. Saygin, M. D. Bazilian, N. Wagner, and R. Gorini, “The role of renewable energy in the global energy transformation,” Energy Strategy Rev., vol. 24, pp. 38–50, 2019, doi: 10.1016/j.esr.2019.01.006.

8. S. Toghyani, E. Baniasadi, and E. Afshari, “Thermodynamic analysis and optimization of an integrated Rankine power cycle and nano-fluid based parabolic trough solar collector,” Energy Convers. Manag., vol. 121, pp. 93–104, 2016, doi: 10.1016/j.enconman.2016.05.029.

9. F. Zhang, P. Zhao, M. Niu, and J. Maddy, “The survey of key technologies in hydrogen energy storage,” Int. J. Hydrog. Energy, vol. 41, no. 33, pp. 14535–14552, 2016, doi: 10.1016/j.ijhydene.2016.05.293.

10. P. Denholm, J. C. King, C. F. Kutcher, and P. P. H. Wilson, “Decarbonizing the electric sector: Combining renewable and nuclear energy using thermal storage,” Energy Policy, vol. 44, pp. 301–311, 2012, doi: 10.1016/j.enpol.2012.01.055.

11. Y. Tian, “GRID-CONNECTED ENERGY STORAGE SYSTEMS — BENEFITS, PLANNING AND OPERATION,” Michigan State University, 2018. doi: 10.25335/M5SQ8QN4M.

12. H. Blanco and A. Faaij, “A review at the role of storage in energy systems with a focus on Power to Gas and long-term storage,” Renew. Sustain. Energy Rev., vol. 81, pp. 1049–1086, 2018, doi: 10.1016/j.rser.2017.07.062.

13. M. Noussan, P. P. Raimondi, R. Scita, and M. Hafner, “The Role of Green and Blue Hydrogen in the Energy Transition—A Technological and Geopolitical Perspective,” Sustainability, vol. 13, no. 1, p. 298, 2020, doi: 10.3390/su13010298.

14. I. Dincer and C. Zamfirescu, “Sustainable hydrogen production options and the role of IAHE,” Int. J. Hydrog. Energy, vol. 37, no. 21, pp. 16266–16286, 2012, doi: 10.1016/j.ijhydene.2012.02.133.

15. A. Ajanovic and R. Haas, “Economic prospects and policy framework for hydrogen as fuel in the transport sector,” Energy Policy, vol. 123, pp. 280–288, 2018, doi: 10.1016/j.enpol.2018.08.063.

16. R. Sadhankar, “New Reactor Concepts Deployment Challenges and Opportunities,” in Encyclopedia of Nuclear Energy, E. Greenspan, Ed. Oxford: Elsevier, 2021, pp. 864–876. doi: 10.1016/B978-0-12-819725-7.00003-9.

17. Z. L. Wang, G. F. Naterer, K. S. Gabriel, R. Gravelsins, and V. N. Daggupati, “Comparison of sulfur–iodine and copper–chlorine thermochemical hydrogen production cycles,” Int. J. Hydrog. Energy, vol. 35, no. 10, pp. 4820–4830, 2010, doi: 10.1016/j.ijhydene.2009.09.006.

18. P. Moriarty and D. Honnery, “Hydrogen’s role in an uncertain energy future,” Int. J. Hydrog. Energy, vol. 34, no. 1, pp. 31–39, 2009, doi: 10.1016/j.ijhydene.2008.10.060.

19. N. V. Gnanapragasam, B. V. Reddy, and M. A. Rosen, “Hydrogen production from coal gasification for effective downstream CO2 capture,” Int. J. Hydrog. Energy, vol. 35, no. 10, pp. 4933–4943, 2010, doi: 10.1016/j.ijhydene.2009.07.114.

20. IEA, “The Future of Hydrogen,” 2019. Accessed: Nov. 21, 2021. [Online]. Available: https://www.iea.org/reports/the-future-of-hydrogen.

21. C. Acar and I. Dincer, “Comparative assessment of hydrogen production methods from renewable and non-renewable sources,” Int. J. Hydrog. Energy, vol. 39, no. 1, pp. 1–12, 2014, doi: 10.1016/j.ijhydene.2013.10.060.

22. M. Eypasch et al., “Model-based techno-economic evaluation of an electricity storage system based on Liquid Organic Hydrogen Carriers,” Appl. Energy, vol. 185, pp. 320–330, 2017, doi: 10.1016/j.apenergy.2016.10.068.

23. R. Boudries, “Hydrogen as a fuel in the transport sector in Algeria,” Int. J. Hydrog. Energy, vol. 39, no. 27, pp. 15215–15223, 2014, doi: 10.1016/j.ijhydene.2014.06.014.

24. A. Ozbilen, M. Aydin, I. Dincer, and M. A. Rosen, “Life cycle assessment of nuclear-based hydrogen production via a copper–chlorine cycle: A neural network approach,” Int. J. Hydrog. Energy, vol. 38, no. 15, pp. 6314–6322, 2013, doi: 10.1016/j.ijhydene.2013.03.071.

25. T. A. H. Ratlamwala and I. Dincer, “Performance assessment of solar-based integrated Cu–Cl systems for hydrogen production,” Sol. Energy, vol. 95, pp. 345–356, 2013, doi: 10.1016/j.solener.2013.06.018.

26. G. Locatelli, A. Fiordaliso, S. Boarin, and M. E. Ricotti, “Cogeneration: An option to facilitate load following in Small Modular Reactors,” Prog. Nucl. Energy, vol. 97, pp. 153–161, 2017, doi: 10.1016/j.pnucene.2016.12.012.

27. M. Balat, “Potential importance of hydrogen as a future solution to environmental and transportation problems,” Int. J. Hydrog. Energy, vol. 33, no. 15, pp. 4013–4029, 2008, doi: 10.1016/j.ijhydene.2008.05.047.

28. C. E. Finke, H. F. Leandri, E. T. Karumb, D. Zheng, M. R. Hoffmann, and N. A. Fromer, “Economically advantageous pathways for reducing greenhouse gas emissions from industrial hydrogen under common, current economic conditions,” Energy Environ. Sci., vol. 14, no. 3, pp. 1517–1529, 2021, doi: 10.1039/D0EE03768K.

29. M. Al-Zareer, I. Dincer, and M. A. Rosen, “Development and assessment of a novel integrated nuclear plant for electricity and hydrogen production,” Energy Convers. Manag., vol. 134, pp. 221–234, 2017, doi: 10.1016/j.enconman.2016.12.004.

30. S. S. Seyitoglu, I. Dincer, and A. Kilicarslan, “Energy and exergy analyses of hydrogen production by coal gasification,” Int. J. Hydrog. Energy, vol. 42, no. 4, pp. 2592–2600, 2017, doi: 10.1016/j.ijhydene.2016.08.228.

31. M. Newborough and G. Cooley, “Developments in the global hydrogen market: The spectrum of hydrogen colours,” Fuel Cells Bull., vol. 2020, no. 11, pp. 16–22, 2020, doi: 10.1016/S1464-2859(20)30546-0.

32. D. Popov and A. Borissova, “Innovative configuration of a hybrid nuclear-parabolic trough solar power plant,” Int. J. Sustain. Energy, vol. 37, no. 7, pp. 616–639, 2018, doi: 10.1080/14786451.2017.1333509.

33. J. Chen, H. E. Garcia, J. S. Kim, and S. M. Bragg-Sitton, “Operations Optimization of Nuclear Hybrid Energy Systems,” Nucl. Technol., vol. 195, no. 2, pp. 143–156, 2016, doi: 10.13182/NT15-130.

34. Environmental Registry of Ontario, “Ontario Low-Carbon Hydrogen Strategy - discussion paper” 2022. Accessed: Dec. 04, 2022. [Online]. Available: https://ero.ontario.ca/notice/019-2709.

35. D. Wijayasekara, M. Manic, P. Sabharwall, and V. Utgikar, “Optimal artificial neural network architecture selection for performance prediction of compact heat exchanger with the EBaLM-OTR technique,” Nucl. Eng. Des., vol. 241, no. 7, pp. 2549–2557, 2011, doi: 10.1016/j.nucengdes.2011.04.045.

36. M. Gomez-Fernandez, K. Higley, A. Tokuhiro, K. Welter, W.-K. Wong, and H. Yang, “Status of research and development of learning-based approaches in nuclear science and engineering: A review,” Nucl. Eng. Des., vol. 359, p. 110479, 2020, doi: 10.1016/j.nucengdes.2019.110479.

37. A. Zamaniyan, F. Joda, A. Behroozsarand, and H. Ebrahimi, “Application of artificial neural networks (ANN) for modeling of industrial hydrogen plant,” Int. J. Hydrog. Energy, vol. 38, no. 15, pp. 6289–6297, 2013, doi: 10.1016/j.ijhydene.2013.02.136.

38. C. P. Elia, Z. Yang, L. Anders, L. Hailong, and Y. Jinyue, “An Open-source Platform for Simulation and Optimization of Clean Energy Technologies,” Energy Procedia, vol. 105, pp. 946–952, 2017, doi: 10.1016/j.egypro.2017.03.423.

39. M. R. Quitoras, P. E. Campana, and C. Crawford, “Exploring electricity generation alternatives for Canadian Arctic communities using a multi-objective genetic algorithm approach,” Energy Convers. Manag., vol. 210, p. 112471, 2020, doi: 10.1016/j.enconman.2020.112471.

40. V. F. Navarro Torres, J. Ayres, P. L. A. Carmo, and C. G. L. Silveira, “Haul Productivity Optimization: An Assessment of the Optimal Road Grade,” in Proceedings of the 27th International Symposium on Mine Planning and Equipment Selection - MPES 2018, E. Widzyk-Capehart, A. Hekmat, and R. Singhal, Eds. Cham: Springer International Publishing, 2019, pp. 345–353. doi: 10.1007/978-3-319-99220-4_28.

41. LINDO Systems, Inc., “What’sBest!, User’s Manual Version 17.0.” https://www.lindo.com/downloads/PDF/WB.pdf (accessed Nov. 20, 2021).

42. S. Fujiwara et al., “Hydrogen production by high temperature electrolysis with nuclear reactor,” Prog. Nucl. Energy, vol. 50, no. 2–6, pp. 422–426, 2008, doi: 10.1016/j.pnucene.2007.11.025.

43. M. Orhan, I. Dincer, and G. Naterer, “Cost analysis of a thermochemical Cu–Cl pilot plant for nuclear-based hydrogen production,” Int. J. Hydrog. Energy, vol. 33, no. 21, pp. 6006–6020, 2008, doi: 10.1016/j.ijhydene.2008.05.038.

44. H. Hidayatullah, S. Susyadi, and M. H. Subki, “Design and technology development for small modular reactors – Safety expectations, prospects and impediments of their deployment,” Prog. Nucl. Energy, vol. 79, pp. 127–135, 2015, doi: 10.1016/j.pnucene.2014.11.010.

45. W. R. Stewart and K. Shirvan, "Capital Cost Estimation for Advanced Nuclear Power Plants." OSF Preprints, 2021. doi: 10.31219/osf.io/erm3g.

46. G. Locatelli and M. Mancini, "Competitiveness of Small-Medium, New Generation Reactors: A Comparative Study on Decommissioning," J. Eng. Gas Turbines Power, vol. 132, no. 10, p. 102906, 2010, doi: 10.1115/1.4000613.

47. V. Kuznetsov, "Options for small and medium sized reactors (SMRs) to overcome loss of economies of scale and incorporate increased proliferation resistance and energy security," Prog. Nucl. Energy, vol. 50, no. 2–6, pp. 242–250, 2008, doi: 10.1016/j.pnucene.2007.11.006.

48. Nuclear Energy Agency (NEA), "Small Modular Reactors: Nuclear Energy Market Potential for Near-term Deployment," NEA No. 7213 2016. https://www.oecd-nea.org/jcms/pl_14924/small-modular-reactors-nuclear-energy-market-potential-for-near-term-deployment?details=true (accessed Nov. 20, 2021).

49. B. Mignacca and G. Locatelli, "Economics and finance of Small Modular Reactors: A systematic review and research agenda," Renew. Sustain. Energy Rev., vol. 118, p. 109519, 2020, doi: 10.1016/j.rser.2019.109519.

50. R. S. El-Emam and M. H. Subki, "Small modular reactors for nuclear-renewable synergies: Prospects and impediments," Int. J. Energy Res., vol. 45, no. 11, pp. 16995–17004, 2021, doi: 10.1002/er.6838.

51. A. Borissova and D. Popov, "An option for the integration of solar photovoltaics into small nuclear power plant with thermal energy storage," Sustain. Energy Technol. Assess., vol. 18, pp. 119–126, 2016, doi: 10.1016/j.seta.2016.10.002.

52. J. Liman, "Small modular reactors: Methodology of economic assessment focused on incremental construction and gradual shutdown options," Prog. Nucl. Energy, vol. 108, pp. 253–259, 2018, doi: 10.1016/j.pnucene.2018.06.002.

53. T. S. Carless, W. M. Griffin, and P. S. Fischbeck, "The environmental competitiveness of small modular reactors: A life cycle study," Energy, vol. 114, pp. 84–99, 2016, doi: 10.1016/j.energy.2016.07.111.

54. K. Verfondern and W. Von Lensa, "Past and present research in europe on the production of nuclear hydrogen with HTGR," Prog. Nucl. Energy, vol. 47, no. 1–4, pp. 472–483, 2005, doi: 10.1016/j.pnucene.2005.05.048.

55. C. W. Lapp and M. W. Golay, "Modular design and construction techniques for nuclear power plants," Nucl. Eng. Des., vol. 172, no. 3, pp. 327–349, 1997, doi: 10.1016/S0029-5493(97)00031-9.

56. M. Felgenhauer and T. Hamacher, "State-of-the-art of commercial electrolyzers and on-site hydrogen generation for logistic vehicles in South Carolina," Int. J.

Hydrog. Energy, vol. 40, no. 5, pp. 2084–2090, 2015, doi: 10.1016/j.ijhydene.2014.12.043.

57. M. Dejong, A. Reinders, J. Kok, and G. Westendorp, "Optimizing a steam-methane reformer for hydrogen production," Int. J. Hydrog. Energy, vol. 34, no. 1, pp. 285–292, 2009, doi: 10.1016/j.ijhydene.2008.09.084.

58. M. Yu, K. Wang, and H. Vredenburg, "Insights into low-carbon hydrogen production methods: Green, blue and aqua hydrogen," Int. J. Hydrog. Energy, vol. 46, no. 41, pp. 21261–21273, 2021, doi: 10.1016/j.ijhydene.2021.04.016.

59. F. Ustolin, A. Campari, R. Taccani. An Extensive Review of Liquid Hydrogen in Transportation with Focus on the Maritime Sector. Journal of Marine Science and Engineering. 2022; 10(9):1222. https://doi.org/10.3390/jmse10091222.

60. IAEA, "Releases 2019 Data on Nuclear Power Plants Operating Experience," Jun. 25, 2020. https://www.iaea.org/newscenter/news/iaea-releases-2019-data-on-nuclear-power-plants-operating-experience (accessed Nov. 20, 2021).

61. S. Şahin and Y. Wu, "3.14 Fission Energy Production," in Comprehensive Energy Systems, Elsevier, 2018, pp. 590–637. doi: 10.1016/B978-0-12-809597-3.00331-X.

62. I. Pioro, R. Duffey (2015). Nuclear Power as a Basis for Future Electricity Generation. Journal of Nuclear Engineering and Radiation Science, 1(1), 011001. doi:10.1115/1.4029420

63. IEA, "Nuclear Power in a Clean Energy System – Analysis,". https://www.iea.org/reports/nuclear-power-in-a-clean-energy-system (accessed Nov. 20, 2021).

64. M. Al-Zareer, I. Dincer, and M. A. Rosen, "Performance analysis of a supercritical water-cooled nuclear reactor integrated with a combined cycle, a Cu-Cl thermochemical cycle and a hydrogen compression system," Appl. Energy, vol. 195, pp. 646–658, 2017, doi: 10.1016/j.apenergy.2017.03.046.

65. G. F. Naterer, I. Dincer, and C. Zamfirescu, Hydrogen Production from Nuclear Energy. London: Springer London, 2013. doi: 10.1007/978-1-4471-4938-5.

66. S. J. Bae, J. Lee, Y. Ahn, and J. I. Lee, "Preliminary studies of compact Brayton cycle performance for Small Modular High Temperature Gas-cooled Reactor system," Ann. Nucl. Energy, vol. 75, pp. 11–19, 2015, doi: 10.1016/j.anucene.2014.07.041.

67. M. W. Patterson, "Cogeneration of electricity and liquid fuels using a high temperature gas-cooled reactor as the heat source," Nucl. Eng. Des., vol. 329, pp. 204–212, 2018, doi: 10.1016/j.nucengdes.2018.01.029.

68. X. L. Yan and R. Hino, “Nuclear Hydrogen Production Handbook (Green Chemistry and Chemical Engineering),” pp. 898, 2018, ISBN 9781138074682.

69. K. Kunitomi, X. Yan, T. Nishihara, N. Sakaba, and T. Mouri, “JAEA’S VHTR FOR HYDROGEN AND ELECTRICITY COGENERATION : GTHTR300C,” Nucl. Eng. Technol., vol. 39, no. 1, pp. 9–20, 2007, doi: 10.5516/NET.2007.39.1.009.

70. D. Hittner, E. Bogusch, M. Fütterer, S. de Groot, and J. Ruer, “High and very high temperature reactor research for multipurpose energy applications,” Nucl. Eng. Des., vol. 241, no. 9, pp. 3490–3504, 2011, doi: 10.1016/j.nucengdes.2011.08.004.

71. M. Al-Zareer, I. Dincer, and M. A. Rosen, “Analysis and assessment of the integrated generation IV gas-cooled fast nuclear reactor and copper-chlorine cycle for hydrogen and electricity production,” Energy Convers. Manag., vol. 205, p. 112387, 2020, doi: 10.1016/j.enconman.2019.112387.

72. A. Peakman and B. Merk, “The Role of Nuclear Power in Meeting Current and Future Industrial Process Heat Demands,” Energies, vol. 12, no. 19, p. 3664, 2019, doi: 10.3390/en12193664.

73. A. Contreras, “Solar–hydrogen: an energy system for sustainable development in Spain,” Int. J. Hydrog. Energy, vol. 24, no. 11, pp. 1041–1052, 1999, doi: 10.1016/S0360-3199(98)00134-7.

74. C. Acar and I. Dincer, “Review and evaluation of hydrogen production options for better environment,” J. Clean. Prod., vol. 218, pp. 835–849, 2019, doi: 10.1016/j.jclepro.2019.02.046.

75. F. Khalid and Y. Bicer, “Energy and exergy analyses of a hybrid small modular reactor and wind turbine system for trigeneration,” Energy Sci. Eng., vol. 7, no. 6, pp. 2336–2350, 2019, doi: 10.1002/ese3.327.

76. M. Kayfeci, A. Keçebaş, and M. Bayat, “Hydrogen production,” in Solar Hydrogen Production, Elsevier, 2019, pp. 45–83. doi: 10.1016/B978-0-12-814853-2.00003-5.

77. G. Locatelli, S. Boarin, A. Fiordaliso, and M. E. Ricotti, “Load following of Small Modular Reactors (SMR) by cogeneration of hydrogen: A techno-economic analysis,” Energy, vol. 148, pp. 494–505, 2018, doi: 10.1016/j.energy.2018.01.041.

78. IAEA, “Status of Innovative Small and Medium Sized Reactor Designs 2005,” Feb. 28, 2019. https://www.iaea.org/publications/7450/status-of-innovative-small-and-medium-sized-reactor-designs-2005 (accessed Nov. 20, 2021).

79. Idaho National Laboratory report, “NGNP Project 2011 Status and Path Forward,” Idaho National Lab. (INL), Idaho Falls, ID (United States), INL/EXT-11-23907, 2011. doi: 10.2172/1035900.

80. H. Song, J. Van Meter, S. Lomperski, D. Cho, H. Y. Kim, and A. Tokuhiro, “Experimental Investigations of a Printed circuit heat exchanger for Supercritical CO2 and Water Heat Exchange,” no. NTHAS5-N002, 2006.

81. A. Tokuhiro, M. Manic, V. Utgikar, D. Grauer, M. McKellar, “Demonstrating Hybrid Heat Transport and Energy Conversion System Performance Characterization Using Intelligent Control Systems,” 2012. Accessed: Nov. 24, 2021. [Online]. Available: https://neup.inl.gov/SiteAssets/2012%20R_D%20Abstracts/35-%202012_CFP_Abstract_3510.pdf.

82. S. Şahin and H. M. Şahin, “Generation-IV reactors and nuclear hydrogen production,” Int. J. Hydrog. Energy, vol. 46, no. 57, pp. 28936–28948, 2021, doi: 10.1016/j.ijhydene.2020.12.182.

83. M. M. Valujerdi and S. Talebi, “Entropy generation study for a supercritical water reactor (SCWR),” Prog. Nucl. Energy, vol. 118, p. 103129, 2020, doi: 10.1016/j.pnucene.2019.103129.

84. M. A. Rosen, G. F. Naterer, C. C. Chukwu, R. Sadhankar, and S. Suppiah, “Nuclear-based hydrogen production with a thermochemical copper-chlorine cycle and supercritical water reactor: equipment scale-up and process simulation,” Int. J. Energy Res., vol. 36, no. 4, pp. 456–465, 2012, doi: 10.1002/er.1702.

85. G. Locatelli, M. Mancini, and N. Todeschini, “Generation IV nuclear reactors: Current status and future prospects,” Energy Policy, vol. 61, pp. 1503–1520, 2013, doi: 10.1016/j.enpol.2013.06.101.

86. The Economic Modeling Working Group, “Cost Estimating Guidelines for Generation IV Nuclear Energy Systems,” The OECD Nuclear Energy Agency for the Generation IV International Forum, GIF/EMWG/2007/004, 2007.

87. S. Dieckmann and J. Dersch, “Simulation of hybrid solar power plants,” Abu Dhabi, United Arab Emirates, 2017, p. 160005. doi: 10.1063/1.4984539.

88. R. Boudries, “Techno-economic study of hydrogen production using CSP technology,” Int. J. Hydrog. Energy, vol. 43, no. 6, pp. 3406–3417, 2018, doi: 10.1016/j.ijhydene.2017.05.157.

89. D. T. Ingersoll, Z. J. Houghton, R. Bromm, and C. Desportes, “NuScale small modular reactor for Co-generation of electricity and water,” Desalination, vol. 340, pp. 84–93, 2014, doi: 10.1016/j.desal.2014.02.023.

90. G. Alonso, S. Bilbao, and E. del Valle, “Economic competitiveness of small modular reactors versus coal and combined cycle plants,” Energy, vol. 116, pp. 867–879, 2016, doi: 10.1016/j.energy.2016.10.030.

91. G. Locatelli, A. Fiordaliso, S. Boarin, and M. Ricotti, “Load Following by Cogeneration: Options for Small Modular Reactors, GEN IV Reactor and Traditional Large Plants,” in Volume 3: Nuclear Fuel and Material, Reactor Physics and Transport Theory; Innovative Nuclear Power Plant Design and New Technology Application, Shanghai, China, 2017, p. V003T13A013. doi: 10.1115/ICONE25-67180.

92. J.-M. Berniolles, “De-mystifying small modular reactors,” Sustainability Times, Nov. 29, 2019. https://www.sustainability-times.com/low-carbon-energy/de-mystifying-small-modular-reactors/ (accessed Nov. 20, 2021).

93. X. C. Schmidt Rivera, E. Topriska, M. Kolokotroni, and A. Azapagic, “Environmental sustainability of renewable hydrogen in comparison with conventional cooking fuels,” J. Clean. Prod., vol. 196, pp. 863–879, 2018, doi: 10.1016/j.jclepro.2018.06.033.

94. O. Ellabban, H. Abu-Rub, and F. Blaabjerg, “Renewable energy resources: Current status, future prospects and their enabling technology,” Renew. Sustain. Energy Rev., vol. 39, pp. 748–764, 2014, doi: 10.1016/j.rser.2014.07.113.

95. S. R. Bull, “Renewable energy today and tomorrow,” Proc. IEEE, vol. 89, no. 8, pp. 1216–1226, 2001, doi: 10.1109/5.940290.

96. E. Bilgen, “Domestic hydrogen production using renewable energy,” Sol. Energy, vol. 77, no. 1, pp. 47–55, 2004, doi: 10.1016/j.solener.2004.03.012.

97. H. Sato, H. Ohashi, S. Nakagawa, Y. Tachibana, and K. Kunitomi, “Safety design consideration for HTGR coupling with hydrogen production plant,” Prog. Nucl. Energy, vol. 82, pp. 46–52, 2015, doi: 10.1016/j.pnucene.2014.07.032.

98. R. R. Sadhankar, J. Li, H. Li, D. K. Ryland, and S. Suppiah, “Future Hydrogen Production Using Nuclear Reactors,” in 2006 IEEE EIC Climate Change Conference, Ottawa, ON, 2006, pp. 1–9. doi: 10.1109/EICCCC.2006.277205.

99. R. S. El-Emam, H. Ozcan, and I. Dincer, “Comparative cost evaluation of nuclear hydrogen production methods with the Hydrogen Economy Evaluation Program (HEEP),” Int. J. Hydrog. Energy, vol. 40, no. 34, pp. 11168–11177, 2015, doi: 10.1016/j.ijhydene.2014.12.098.

100. D. A. J. Rand and R. M. Dell, “FUELS – HYDROGEN PRODUCTION | Coal Gasification,” in Encyclopedia of Electrochemical Power Sources, Elsevier, 2009, pp. 276–292. doi: 10.1016/B978-044452745-5.00300-2.

101. O. Badran, R. Mamlook, and E. Abdulhadi, “Toward clean environment: evaluation of solar electric power technologies using fuzzy logic,” Clean Technol. Environ. Policy, vol. 14, no. 2, pp. 357–367, 2012, doi: 10.1007/s10098-011-0407-8.

102. A. W. Dowling, T. Zheng, and V. M. Zavala, “Economic assessment of concentrated solar power technologies: A review,” Renew. Sustain. Energy Rev., vol. 72, pp. 1019–1032, 2017, doi: 10.1016/j.rser.2017.01.006.

103. IRENA, “Concentrated Solar Power: Technology brief,” Technical Report, Jan. 2013. Accessed: Nov. 20, 2021. [Online]. Available: http://dspace.khazar.org/handle/20.500.12323/4304.

104. A. Palacios, C. Barreneche, M. E. Navarro, and Y. Ding, “Thermal energy storage technologies for concentrated solar power – A review from a materials perspective,” Renew. Energy, vol. 156, pp. 1244–1265, 2020, doi: 10.1016/j.renene.2019.10.127.

105. E. Bellos, “Progress in the design and the applications of linear Fresnel reflectors – A critical review,” Therm. Sci. Eng. Prog., vol. 10, pp. 112–137, 2019, doi: 10.1016/j.tsep.2019.01.014.

106. D. Popov, A. Borissova, "Innovative configuration of a hybrid nuclear-solar tower power plant", Energy, 2017, doi: 10.1016/j.energy.2017.02.147.

107. R. Loisel, L. Baranger, N. Chemouri, S. Spinu, and S. Pardo, “Economic evaluation of hybrid off-shore wind power and hydrogen storage system,” Int. J. Hydrog. Energy, vol. 40, no. 21, pp. 6727–6739, 2015, doi: 10.1016/j.ijhydene.2015.03.117.

108. C. Rivkin, R. Burgess, and W. Buttner, “Hydrogen Technologies Safety Guide,” NREL/TP--5400-60948, 1169773, 2015. doi: 10.2172/1169773.

109. B. Zohuri, “Hydrogen-Powered Fuel Cell and Hybrid Automobiles of the Near Future,” in Hydrogen Energy, Cham: Springer International Publishing, 2019, pp. 37–59. doi: 10.1007/978-3-319-93461-7_2.

110. G. F. Naterer et al., “Clean hydrogen production with the Cu–Cl cycle – Progress of international consortium, I: Experimental unit operations,” Int. J. Hydrog. Energy, vol. 36, no. 24, pp. 15472–15485, 2011, doi: 10.1016/j.ijhydene.2011.08.012.

111. J. Rostrupnielsen, “Sulfur-passivated nickel catalysts for carbon-free steam reforming of methane,” J. Catal., vol. 85, no. 1, pp. 31–43, 1984, doi: 10.1016/0021-9517(84)90107-6.

112. S. Schröders, K. Verfondern, and H.-J. Allelein, “Energy economic evaluation of solar and nuclear driven steam methane reforming processes,” Nucl. Eng. Des., vol. 329, pp. 234–246, 2018, doi: 10.1016/j.nucengdes.2017.08.007.

113. P. Corbo and F. Migliardini, “Natural gas and biofuel as feedstock for hydrogen production on Ni catalysts,” J. Nat. Gas Chem., vol. 18, no. 1, pp. 9–14, 2009, doi: 10.1016/S1003-9953(08)60083-3.

114. N. Muradov and T. Vezirolu, “From hydrocarbon to hydrogen-carbon to hydrogen economy,” Int. J. Hydrog. Energy, vol. 30, no. 3, pp. 225–237, 2005, doi: 10.1016/j.ijhydene.2004.03.033.

115. P. L. Spath and M. K. Mann, “Life Cycle Assessment of Hydrogen Production via Natural Gas Steam Reforming,” NREL/TP-570-27637, 764485, 2000. doi: 10.2172/764485.

116. F. Syed, M. Fowler, D. Wan, and Y. Maniyali, “An energy demand model for a fleet of plug-in fuel cell vehicles and commercial building interfaced with a clean energy hub,” Int. J. Hydrog. Energy, vol. 35, no. 10, pp. 5154–5163, 2010, doi: 10.1016/j.ijhydene.2009.08.089.

117. A. Ridluan, M. Manic, and A. Tokuhiro, “EBaLM-THP – A neural network thermohydraulic prediction model of advanced nuclear system components,” Nucl. Eng. Des., vol. 239, no. 2, pp. 308–319, 2009, doi: 10.1016/j.nucengdes.2008.10.027.

118. R. S. El-Emam, H. Ozcan, and C. Zamfirescu, “Updates on promising thermochemical cycles for clean hydrogen production using nuclear energy,” J. Clean. Prod., vol. 262, p. 121424, 2020, doi: 10.1016/j.jclepro.2020.121424.

119. I. Dincer, C. O. Colpan, O. Kizilkan, and M. A. Ezan, Eds., Progress in Clean Energy, Volume 2. Cham: Springer International Publishing, 2015. doi: 10.1007/978-3-319-17031-2.

120. A. Z. Weber and T. E. Lipman, “Fuel Cells and Hydrogen Production,” in Fuel Cells and Hydrogen Production: A Volume in the Encyclopedia of Sustainability Science and Technology, Second Edition, T. E. Lipman and A. Z. Weber, Eds. New York, NY: Springer, 2019, pp. 1–8. doi: 10.1007/978-1-4939-7789-5_1051.

121. B. Olateju and A. Kumar, “Techno-economic assessment of hydrogen production from underground coal gasification (UCG) in Western Canada with carbon capture and sequestration (CCS) for upgrading bitumen from oil sands,” Appl. Energy, vol. 111, pp. 428–440, 2013, doi: 10.1016/j.apenergy.2013.05.014.

122. F. Dawood, M. Anda, and G. M. Shafiullah, “Hydrogen production for energy: An overview,” Int. J. Hydrog. Energy, vol. 45, no. 7, pp. 3847–3869, 2020, doi: 10.1016/j.ijhydene.2019.12.059.

123. B. Olateju and A. Kumar, “Hydrogen production from wind energy in Western Canada for upgrading bitumen from oil sands,” Energy, vol. 36, no. 11, pp. 6326–6339, 2011, doi: 10.1016/j.energy.2011.09.045.

124. B. Olateju, A. Kumar, and M. Secanell, “A techno-economic assessment of large scale wind-hydrogen production with energy storage in Western Canada,” Int. J. Hydrog. Energy, vol. 41, no. 21, pp. 8755–8776, 2016, doi: 10.1016/j.ijhydene.2016.03.177.

125. H. Blanco, W. Nijs, J. Ruf, and A. Faaij, “Potential for hydrogen and Power-to-Liquid in a low-carbon EU energy system using cost optimization,” Appl. Energy, vol. 232, pp. 617–639, 2018, doi: 10.1016/j.apenergy.2018.09.216.

126. P. Sabharwall, M. Patterson, and F. Gunnerson, “Theoretical Design of Thermosyphon for Process Heat Transfer From NGNP to Hydrogen Plant,” in Fourth International Topical Meeting on High Temperature Reactor Technology, Volume 1, Washington, DC, USA, 2008, pp. 733–738. doi: 10.1115/HTR2008-58199.

127. A. Allouhi, “Management of photovoltaic excess electricity generation via the power to hydrogen concept: A year-round dynamic assessment using Artificial Neural Networks,” Int. J. Hydrog. Energy, vol. 45, no. 41, pp. 21024–21039, 2020, doi: 10.1016/j.ijhydene.2020.05.262.

128. S. Sadeghi and S. Ghandehariun, “Thermodynamic analysis and optimization of an integrated solar thermochemical hydrogen production system,” Int. J. Hydrog. Energy, vol. 45, no. 53, pp. 28426–28436, 2020, doi: 10.1016/j.ijhydene.2020.07.203.

129. M. F. Orhan, İ. Dinçer, and M. A. Rosen, “Efficiency comparison of various design schemes for copper–chlorine (Cu–Cl) hydrogen production processes using Aspen Plus software,” Energy Convers. Manag., vol. 63, pp. 70–86, 2012, doi: 10.1016/j.enconman.2012.01.029.

130. Z. L. Wang, G. F. Naterer, K. S. Gabriel, R. Gravelsins, and V. N. Daggupati, “Comparison of different copper–chlorine thermochemical cycles for hydrogen production,” Int. J. Hydrog. Energy, vol. 34, no. 8, pp. 3267–3276, 2009, doi: 10.1016/j.ijhydene.2009.02.023.

131. Y. H. Jeong and M. S. Kazimi, “Optimization of the Hybrid Sulfur Cycle for Nuclear Hydrogen Generation,” Nucl. Technol., vol. 159, no. 2, pp. 147–157, 2007, doi: 10.13182/NT07-A3861.

132. A. S. Joshi, I. Dincer, and B. V. Reddy, “Solar hydrogen production: A comparative performance assessment,” Int. J. Hydrog. Energy, vol. 36, no. 17, pp. 11246–11257, 2011, doi: 10.1016/j.ijhydene.2010.11.122.

133. X. Yan, H. Noguchi, H. Sato, Y. Tachibana, K. Kunitomi, and R. Hino, “A hybrid HTGR system producing electricity, hydrogen and such other products as water demanded in the Middle East,” Nucl. Eng. Des., vol. 271, pp. 20–29, 2014, doi: 10.1016/j.nucengdes.2013.11.003.

134. K. Verfondern, X. Yan, T. Nishihara, and H.-J. Allelein, “Safety concept of nuclear cogeneration of hydrogen and electricity,” Int. J. Hydrog. Energy, vol. 42, no. 11, pp. 7551–7559, 2017, doi: 10.1016/j.ijhydene.2016.04.239.

135. IAEA, Technology Roadmap for Small Modular Reactor Deployment, IAEA Nuclear Energy Series No. NR-T-1.18, IAEA, 2021 Vienna.

136. A. Tokuhiro, private communication with me, November 2022.

137. Nuscale, "NuScale’s Emergency Planning Zone boundary methodology validated by the U.S. Nuclear Regulatory Commission Advisory Committee on Reactor Safeguards" (2022). Accessed: Nov. 25 2022. [Online]. Available: https://newsroom.nuscalepower.com/press-releases/news-details/2022/NuScales-Emergency-Planning-Zone-boundary-methodology-validated-by-the-U.S.-Nuclear-Regulatory-Commission-Advisory-Committee-on-Reactor-Safeguards/default.aspx.

138. C. Zeliang, Y. Mi, A. Tokuhiro, L. Lu, A. Rezvoi (2020). Integral PWR-Type Small Modular Reactor Developmental Status, Design Characteristics and Passive Features: A Review. Energies (Basel), 13(11), 2898.

139. D. Çelik and M. Yıldız, “Investigation of hydrogen production methods in accordance with green chemistry principles,” Int. J. Hydrog. Energy, vol. 42, no. 36, pp. 23395–23401, 2017, doi: 10.1016/j.ijhydene.2017.03.104.

140. M. Jaszczur, M. A. Rosen, T. Śliwa, M. Dudek, and L. Pieńkowski, “Hydrogen production using high temperature nuclear reactors: Efficiency analysis of a combined cycle,” Int. J. Hydrog. Energy, vol. 41, no. 19, pp. 7861–7871, 2016, doi: 10.1016/j.ijhydene.2015.11.190.

141. H. Ishaq and I. Dincer, “A comparative evaluation of three Cu Cl cycles for hydrogen production,” Int. J. Hydrog. Energy, vol. 44, no. 16, pp. 7958–7968, 2019, doi: 10.1016/j.ijhydene.2019.01.249.

142. Q. Wang, C. Liu, R. Luo, D. Li, and R. Macián-Juan, “Thermodynamic analysis and optimization of the combined supercritical carbon dioxide Brayton cycle and organic Rankine cycle-based nuclear hydrogen production system,” Int. J. Energy Res., vol. n/a, no. n/a, doi: 10.1002/er.7208.

143. M. F. Orhan, I. Dincer, and M. A. Rosen, “Efficiency analysis of a hybrid copper–chlorine (Cu–Cl) cycle for nuclear-based hydrogen production,” Chem. Eng. J., vol. 155, no. 1–2, pp. 132–137, 2009, doi: 10.1016/j.cej.2009.07.007.

144. S. Ghandehariun, G. F. Naterer, I. Dincer, and M. A. Rosen, “Solar thermochemical plant analysis for hydrogen production with the copper–chlorine cycle,” Int. J. Hydrog. Energy, vol. 35, no. 16, pp. 8511–8520, 2010, doi: 10.1016/j.ijhydene.2010.05.028.

145. S. Ghandehariun, M. A. Rosen, G. F. Naterer, and Z. Wang, “Comparison of molten salt heat recovery options in the Cu–Cl cycle of hydrogen production,” Int. J. Hydrog. Energy, vol. 36, no. 17, pp. 11328–11337, 2011, doi: 10.1016/j.ijhydene.2010.11.093.

146. J. Zhou et al., “Thermal efficiency evaluation of open-loop SI thermochemical cycle for the production of hydrogen, sulfuric acid and electric power,” Int. J. Hydrog. Energy, vol. 32, no. 5, pp. 567–575, 2007, doi: 10.1016/j.ijhydene.2006.06.043.

147. K. Scott, “Chapter 1 Introduction to Electrolysis, Electrolysers and Hydrogen Production,” pp. 1–27, 2019, doi: 10.1039/9781788016049-00001.

148. J. Chi and H. Yu, “Water electrolysis based on renewable energy for hydrogen production,” Chin. J. Catal., vol. 39, no. 3, pp. 390–394, 2018, doi: 10.1016/S1872-2067(17)62949-8.

149. K.-M. Mangold, “Introduction to Hydrogen Technology</b> .By Roman J. Press, K. S. V. Santhanam, Massoud J. Miri, Alla V. Bailey, and Gerald A. Takacs,” ChemSusChem, vol. 2, no. 8, pp. 781–781, 2009, doi: 10.1002/cssc.200900109.

150. Y. Yürüm, Ed., Hydrogen Energy System. Dordrecht: Springer Netherlands, 1995. doi: 10.1007/978-94-011-0111-0.

151. R. D. Boardman, “Figures of Merit for Technical and Economic Assessment of Nuclear Hydrogen Hybrid Energy Systems,” Idaho National Lab. (INL), Idaho Falls, ID (United States), INL/EXT-17-41484, 2017. doi: 10.2172/1374504.

152. S. M. Bragg-Sitton et al., “Nuclear-Renewable Hybrid Energy Systems: 2016 Technology Development Program Plan,” Idaho National Lab. (INL), Idaho Falls, ID (United States); Oak Ridge National Lab. (ORNL), Oak Ridge, TN (United States), INL/EXT-16-38165, 2016. doi: 10.2172/1333006.

153. D. Yurman, “U.S. nuclear plants to produce carbon-free hydrogen,” Energy Post, Sep. 17, 2019. https://energypost.eu/u-s-nuclear-plants-to-produce-carbon-free-hydrogen/ (accessed Nov. 21, 2021).

154. R. T. Marler, J. S. Arora, (2004). Survey of multi-objective optimization methods for engineering. Structural and Multidisciplinary Optimization, 26(6), 369–395. doi:10.1007/s00158-003-0368-6.

155. S. S. Rao, Engineering Optimization: Theory and Practice. John Wiley & Sons, 2019, ISBN: 978-1-119-45471-7.

156. T. Goel, R. Vaidyanathan, R. T. Haftka, W. Shyy, N. V. Queipo, and K. Tucker, "Response surface approximation of Pareto optimal front in multi-objective optimization," Comput. Methods Appl. Mech. Eng., vol. 196, no. 4–6, pp. 879–893, 2007, doi: 10.1016/j.cma.2006.07.010.

157. S. Upadhyay and M. P. Sharma, "Selection of a suitable energy management strategy for a hybrid energy system in a remote rural area of India," Energy, vol. 94, pp. 352–366, 2016, doi: 10.1016/j.energy.2015.10.134.

158. J. R. Geschwindt, L. J. Lommers, F. H. Southworth, and F. Shahrokhi, "Performance and optimization of an HTR cogeneration system," Nucl. Eng. Des., vol. 251, pp. 297–300, 2012, doi: 10.1016/j.nucengdes.2011.10.029.

159. T. Aittokoski and K. Miettinen, "Efficient evolutionary approach to approximate the Pareto-optimal set in multiobjective optimization, UPS-EMOA," Optim. Methods Softw., vol. 25, no. 6, pp. 841–858, 2010, doi: 10.1080/10556780903548265.

160. Y. Censor, "Pareto optimality in multiobjective problems," Appl. Math. Optim., vol. 4, no. 1, pp. 41–59, 1977, doi: 10.1007/BF01442131.

161. H. A. Gabbar, M. R. Abdussami, and Md. I. Adham, "Optimal Planning of Nuclear-Renewable Micro-Hybrid Energy System by Particle Swarm Optimization," IEEE Access, vol. 8, pp. 181049–181073, 2020, doi: 10.1109/ACCESS.2020.3027524.

162. J. A. C. Hekman, "LINDO en What's Best: evaluatie van optimalisatiesoftware (summary)," 2000, Accessed: Dec. 11, 2021. [Online]. Available: https://repository.tudelft.nl/islandora/object/uuid%3A92490109-c5da-4f83-8fec-d39da9300230.

163. Nash, C. John, Optimizing Add-Ins: The Educated Guess, What'sBest! New York, N.Y.: PC Magazine, 1991. Accessed: Nov. 21, 2021. [Online]. Available: Vol. 10 no. 7. Ziff Davis. pp. 130, 132. ISSN 0888-8507.

164. Spreadsheet Optimizer Ported to Macintosh. San Mateo, Calif.: InfoWorld Pub., 1988. [Online]. Available: Vol. 10 no. 35. IDG. p. 24. ISSN 0199-6649.

165. A. Messac, Mattson, C.A. 2002: Generating well-distributed sets of Pareto points for engineering design using physical programming. Optim. Eng. 3 431–450.

166. S. N. Sivanandam and S. N. Deepa. "Genetic algorithms." Introduction to genetic algorithms. Springer, Berlin, Heidelberg, 2008. 15-37.

167. D. E. Goldberg, "Genetic Algorithms in Search", Optimization and Machine Learning, Addison-Wesley, USA, 1989.

168. Srinivas, Mandavilli, and M. P. Lalit "Adaptive probabilities of crossover and mutation in genetic algorithms." IEEE Transactions on Systems, Man, and Cybernetics 24.4, 1994: 656-667.

169. J. S. R. Jang , Neuro-Fuzzy and Soft Computing: A Computational Approach To Learning and Machine Intelligence, Chapter 7: Derivative-Free Optimization, Prentice-Hall, 1997, USA, s. 173-196.

170. Smith, P. George. "Evolution of Repeated DNA Sequences by Unequal Crossover: DNA whose sequence is not maintained by selection will develop periodicities as a result of random crossover." Science 191.4227, 1976: 528-535.

171. M. F. Yeo and E. O. Agyel, "Optimising Engineering Problems Using Genetic Algorithms", Engineering Computations, Volume: 15, Number: 2, 1996, s. 268-280.

172. Gen, Mitsuo, and Runwei Cheng. Genetic algorithms and engineering optimization. Vol. 7. John Wiley & Sons, 1999.

173. Beasley, David, R. Bull David and R. R. Martin. "An overview of genetic algorithms: Part 1, fundamentals." University computing 15.2, 1993: 56-69.

174. O. Braysy, "Local Search and Variable Neighborhood Search Algorithms for The Vehicle Routing Problem With Time Windows", 2001, PH D Thesis.

175. C. L. Karr and M. L. Freeman, "Industrial Applications of Genetic Algorithms", 1999, CRC Press, USA.

176. L. Zhang, L. Wang, G. Hinds, C. Lyu, J. Zheng, J. Li (2014). Multi-objective optimization of lithium-ion battery model using genetic algorithm approach. Journal of Power Sources, 270, 367–378. doi:10.1016/j.jpowsour.2014.07.110.

177. A. R Starke, J. M. Cardemil, R. Escobar, S. Colle (2018). Multi-objective optimization of hybrid CSP+PV system using genetic algorithm. Energy, 147, 490–503. doi:10.1016/j.energy.2017.12.116.

178. The MathWorks Inc, . The Mathworks. 2015. URL: http://www.mathworks.com.

179. R. S. El-Emam, I. Dincer, C. Zamfirescu (2019). Enhanced CANDU reactor with heat-upgrading hybrid chemical-mechanical heat pump for combined power and hydrogen production. International Journal of Hydrogen Energy. doi:10.1016/j.ijhydene.2019.06.181.

180. I. H. Bell, J. Wronski, S. Quoilin, V. Lemort (2014). Pure and Pseudo-pure Fluid Thermophysical Property Evaluation and the Open-Source Thermophysical Property Library CoolProp. Industrial & Engineering Chemistry Research, 53(6), 2498–2508. doi:10.1021/ie4033999 ,www.coolprop.org.

181. Y. A. Cengel, A. B. Michael. "Thermodynamics: An Engineering Approach Seventh Edition." (2011).

182. PJ Luickx, LM Helse, WD D'haeseleer "Influence of massive heat-pump introduction on the electricity-generation mix and the GHG effect: comparison between Belgium, France, Germany and The Netherlands". Renew Sustain Energy Rev 2008;12(8):2140e58.

183. Hydrogen Energy Systems, LLC [Internet]. 2022 Nov 1. Available from: https://heshydrogen.com/hydrogen-fuel-cost-vs-gasoline/.

184. Hochman, M. Harold, D. R. James "Pareto Optimal Redistribution." The American Economic Review, vol. 59, no. 4, 1969, pp. 542–57. JSTOR, http://www.jstor.org/stable/1813216. Accessed 4 Nov. 2022.

185. S. Ali, "Regarding approximate electricity requirements in a nuclear generating station itself", private communication, November 2022.

186. A. G. Stern (2018). A new sustainable hydrogen clean energy paradigm. International Journal of Hydrogen Energy, 43(9), 4244–4255. doi:10.1016/j.ijhydene.2017.12.180.

## Appendices

## Appendix A. Matlab Code

Introduction. What is this Appendix A. Write a short description of what it is and how it was used in your thesis research.

### A1. Main function of N-RHES

```
function [output] = NHES_v2_edited_for_GA(x)
%% given values NPP
Q_heat_input_kW = 159975;
T_max_Celsius = 255 ;
T_max_Kelvin = T_max_Celsius + 273 ;
P_max_Pascal = 3100000;
P_min_Pascal = 6500;
turbine_efficiency = 0.84;
pump_efficiency = 0.85;
piping_heat_loss_correction_factor = 0.8292;
npp_percentage= x(1); %percentage of used power from NPP to produce hydrogen


Q_heat_input_kW = Q_heat_input_kW * 1000;
P_max_Pascal = P_max_Pascal * 1000000;
P_min_Pascal = P_min_Pascal * 1000000;
if Q_heat_input_kW > 200000
    Q_heat_input_kW = Q_heat_input_kW / 1000;
end
```

```
if P_max_Pascal > 4000000
    P_max_Pascal = P_max_Pascal / 1000000;
end
if P_min_Pascal > 7000
    P_min_Pascal = P_min_Pascal / 1000000;
end
%% given values Cu-Cl cycle to produce 1mol-hydrogen
T_cu_cl_requirement_celsius_for_per_molH2 = 525;
Heat_energy_requirement_kJ_kg_cu_cl_for_per_molH2 = 200;
Electrical_energy_requirement_kJ_kg_cu_cl_for_per_molH2 = 25;
%% given values CSP
csp_percentage = x(2); %percentage of used power from CSP to produce hydrogen
%% point3
H3_kJ_kg = py.CoolProp.CoolProp.PropsSI('H', 'T', T_max_Kelvin, 'P', P_max_Pascal,
'Water')/1000;
S3_kJ_kgK = py.CoolProp.CoolProp.PropsSI('S', 'T', T_max_Kelvin, 'P', P_max_Pascal,
'Water')/1000;
%% point4s
S4s_kJ_kgK = S3_kJ_kgK;
H4s_kJ_kg = py.CoolProp.CoolProp.PropsSI('H', 'S', S4s_kJ_kgK*1000, 'P',
P_min_Pascal, 'Water')/1000;
%% point4a
H4a_kJ_kg = H3_kJ_kg - turbine_efficiency*(H3_kJ_kg - H4s_kJ_kg);
%% point1
```

```
H1_kJ_kg = py.CoolProp.CoolProp.PropsSI('H', 'P', P_min_Pascal, 'Q', 0, 'Water')/1000;
Density1_kg_m3 = py.CoolProp.CoolProp.PropsSI('D', 'P', P_min_Pascal, 'Q', 0, 'Water');
Specific_volume1_m3_kg = 1/ Density1_kg_m3;
w_pump_in_kj_kg = Specific_volume1_m3_kg * ((P_max_Pascal -
P_min_Pascal)/(pump_efficiency*1000));
%% point2a
H2a_kJ_kg = H1_kJ_kg + w_pump_in_kj_kg ;
%% npp energy in and energy out
boiler_q_in_kj_kg = (H3_kJ_kg - H2a_kJ_kg) * piping_heat_loss_correction_factor;
turbine_out_kj_kg = (H3_kJ_kg - H4a_kJ_kg) * piping_heat_loss_correction_factor;
pump_in_kj_kg = (H2a_kJ_kg - H1_kJ_kg);
w_net_kj_kg = turbine_out_kj_kg - pump_in_kj_kg;
npp_total_efficiency = w_net_kj_kg / boiler_q_in_kj_kg ;
%% producing 1 mol H2 with npp
npp_heat_kJ_required_for_heat_pump_per_molH2 =
(T_cu_cl_requirement_celsius_for_per_molH2 - T_max_Celsius)*(108/215);
npp_heat_kJ_required_electric_per_molH2 =
Electrical_energy_requirement_kJ_kg_cu_cl_for_per_molH2 / npp_total_efficiency;
npp_TOTAL_kJ_heat_energy_required_per_molH2 =
Heat_energy_requirement_kJ_kg_cu_cl_for_per_molH2 +
npp_heat_kJ_required_for_heat_pump_per_molH2 +
npp_heat_kJ_required_electric_per_molH2;
%% SYSTEM ADVISOR MODEL (SAM) and HOEP
```

```
% SAM_Table = readtable('results_csp (elect to grid, elect from grid, pc input energy, hoep, h2 price).csv');
% %day_SAM_Table= table2array (SAM_Table(:,1));
% %month_SAM_Table= table2array (SAM_Table(:,2));
% %hour_SAM_Table= table2array (SAM_Table(:,3));
% %Electricity_to_grid_kW_SAM_Table= table2array (SAM_Table(:,4));
% electricity_from_grid_kW_SAM_Table= table2array (SAM_Table(:,5));
% PC_input_energy_kWthermal_SAM_Table= table2array (SAM_Table(:,6));
% Net_efficiency_SAM_Table= table2array (SAM_Table(:,7));
% %Net_electricty_to_grid_minus_from_grid= table2array (SAM_Table(:,8));
% HOEP_cad = table2array (SAM_Table(:,9))./100;
% H2_hourly_kg_cad = table2array (SAM_Table(:,10));

%% producing 1 mol H2 with csp
csp_heat_kJ_required_electric_per_molH2 =
Electrical_energy_requirement_kJ_kg_cu_cl_for_per_molH2 ./
Net_efficiency_SAM_Table;
csp_TOTAL_kJ_heat_energy_required_per_molH2 =
csp_heat_kJ_required_electric_per_molH2 +
Heat_energy_requirement_kJ_kg_cu_cl_for_per_molH2;
%% CSP production
CSP_H2_mol_s = (PC_input_energy_kWthermal_SAM_Table .* (csp_percentage/100))
./ csp_TOTAL_kJ_heat_energy_required_per_molH2;
```

```
CSP_electricity_kW = (PC_input_energy_kWthermal_SAM_Table .* (1-
csp_percentage/100)) .* Net_efficiency_SAM_Table;
%% NPP production
npp_leftover_heat_kW = (electricity_from_grid_kW_SAM_Table ./
npp_total_efficiency) + Q_heat_input_kW;
NPP_H2_mol_s = (npp_leftover_heat_kW * npp_percentage/100) ./
npp_TOTAL_kJ_heat_energy_required_per_molH2;
NPP_electricity_kW = npp_leftover_heat_kW * (1-npp_percentage/100) *
npp_total_efficiency;
%%selecting hours of year
hours_of_year_start=x(3);
hours_of_year_stop=x(4)-1;
%% indexing values electricity&H2
selected_dates_NPP_electricity_kW=NPP_electricity_kW(hours_of_year_start:hours_of
_year_stop);
selected_dates_NPP_H2_mol_s=NPP_H2_mol_s(hours_of_year_start:hours_of_year_st
op);
selected_dates_CSP_electricity_kW=CSP_electricity_kW(hours_of_year_start:hours_of
_year_stop);
selected_dates_CSP_H2_mol_s=CSP_H2_mol_s(hours_of_year_start:hours_of_year_sto
p);
%% total production amounts
total_electricity_kWh_selected_dates_NPP=sum(selected_dates_NPP_electricity_kW);
```

```
total_H2_kg_selected_dates_NPP=sum(selected_dates_NPP_H2_mol_s)*3600*2.01588/
1000;
total_electricity_kWh_selected_dates_CSP=sum(selected_dates_CSP_electricity_kW);
total_H2_kg_selected_dates_CSP=sum(selected_dates_CSP_H2_mol_s)*3600*2.01588/
1000;
%% energy comparison
grand_total_electricity_kWh = total_electricity_kWh_selected_dates_NPP +
total_electricity_kWh_selected_dates_CSP;
grand_total_H2_kg = total_H2_kg_selected_dates_NPP +
total_H2_kg_selected_dates_CSP;
H2_kg_to_kJthermal = 120100;
grand_total_H2_kg_to_kJthermal=H2_kg_to_kJthermal*grand_total_H2_kg;
Thermal_power = grand_total_H2_kg_to_kJthermal +
grand_total_electricity_kWh*3600;
%% profit electricity
Profit_from_csp_electricity_USD = HOEP_USD .* CSP_electricity_kW;
Profit_from_npp_electricity_USD = HOEP_USD .* NPP_electricity_kW;
%indexing profits electricity
selected_dates_Profit_from_csp_electricity_USD=Profit_from_csp_electricity_USD(hou
rs_of_year_start:hours_of_year_stop);
selected_dates_Profit_from_npp_electricity_USD=Profit_from_npp_electricity_USD(ho
urs_of_year_start:hours_of_year_stop);
%total amounts electricity
```

```
total_Profit_from_npp_electricity_USD_selected_dates=sum(selected_dates_Profit_from
_npp_electricity_USD);
total_Profit_from_csp_electricity_USD_selected_dates=sum(selected_dates_Profit_from
_csp_electricity_USD);
%% profit hydrogen
Profit_from_csp_hydrogen_USD = H2_hourly_kg_USD .*
(CSP_H2_mol_s*3600*2.01588/1000);
Profit_from_npp_hydrogen_USD = H2_hourly_kg_USD .*
(NPP_H2_mol_s*3600*2.01588/1000);
%indexing profits hydrogen
selected_dates_Profit_from_csp_hydrogen_USD=Profit_from_csp_hydrogen_USD(hour
s_of_year_start:hours_of_year_stop);
selected_dates_Profit_from_npp_hydrogen_USD=Profit_from_npp_hydrogen_USD(hou
rs_of_year_start:hours_of_year_stop);
%total amounts hydrogen
total_Profit_from_npp_hydrogen_USD_selected_dates=sum(selected_dates_Profit_from
_npp_hydrogen_USD);
total_Profit_from_csp_hydrogen_USD_selected_dates=sum(selected_dates_Profit_from
_csp_hydrogen_USD);
%% profit maximization
Profit = (total_Profit_from_npp_hydrogen_USD_selected_dates +
total_Profit_from_csp_hydrogen_USD_selected_dates +
total_Profit_from_npp_electricity_USD_selected_dates +
total_Profit_from_csp_electricity_USD_selected_dates);
```

```
output = [-Profit , -Thermal_power];
end
```

## A2. Multi-objective optimization and date range selection code

```
% clear; clc;



% month_start= input('month_start = ');
% day_start=input('day_start = ');
% hour_start=input('hour_start = ');
% month_stop=input('month_stop = ');
% day_stop=input('day_stop = ');
% hour_stop=input('hour_stop = ');



month_start=2;
day_start=1;
hour_start=1;
month_stop=3;
day_stop=1;
hour_stop=1;



if month_start == 1
   hours_of_year_start = hour_start + 24 * (day_start-1);
```

```
elseif month_start == 2
    hours_of_year_start = hour_start + 24 * (day_start-1) + 744;
elseif month_start == 3
    hours_of_year_start = hour_start + 24 * (day_start-1) + 1416;
elseif month_start == 4
    hours_of_year_start = hour_start + 24 * (day_start-1) + 2160;
elseif month_start == 5
    hours_of_year_start = hour_start + 24 * (day_start-1) + 2880;
elseif month_start == 6
    hours_of_year_start = hour_start + 24 * (day_start-1) + 3624;
elseif month_start == 7
    hours_of_year_start = hour_start + 24 * (day_start-1) + 4344;
elseif month_start == 8
    hours_of_year_start = hour_start + 24 * (day_start-1) + 5088;
elseif month_start == 9
    hours_of_year_start = hour_start + 24 * (day_start-1) + 5832;
elseif month_start == 10
    hours_of_year_start = hour_start + 24 * (day_start-1) + 6552;
elseif month_start == 11
    hours_of_year_start = hour_start + 24 * (day_start-1) + 7296;
elseif month_start == 12
    hours_of_year_start = hour_start + 24 * (day_start-1) + 8016;
else
    disp('incorrect start date');
```

```
end



if month_stop == 1
   hours_of_year_stop = (hour_stop) + 24 * (day_stop-1);
elseif month_stop == 2
   hours_of_year_stop = (hour_stop) + 24 * (day_stop-1) + 744;
elseif month_stop == 3
   hours_of_year_stop = (hour_stop) + 24 * (day_stop-1) + 1416;
elseif month_stop == 4
   hours_of_year_stop = (hour_stop) + 24 * (day_stop-1) + 2160;
elseif month_stop == 5
   hours_of_year_stop = (hour_stop) + 24 * (day_stop-1) + 2880;
elseif month_stop == 6
   hours_of_year_stop = (hour_stop) + 24 * (day_stop-1) + 3624;
elseif month_stop == 7
   hours_of_year_stop = (hour_stop) + 24 * (day_stop-1) + 4344;
elseif month_stop == 8
   hours_of_year_stop = (hour_stop) + 24 * (day_stop-1) + 5088;
elseif month_stop == 9
   hours_of_year_stop = (hour_stop) + 24 * (day_stop-1) + 5832;
elseif month_stop == 10
   hours_of_year_stop = (hour_stop) + 24 * (day_stop-1) + 6552;
elseif month_stop == 11
```

```
    hours_of_year_stop = (hour_stop) + 24 * (day_stop-1) + 7296;
elseif month_stop == 12
    hours_of_year_stop = (hour_stop) + 24 * (day_stop-1) + 8016;
else
    disp('incorrect stop date');
end
```

```
hours_between_selected_dates = hours_of_year_stop - hours_of_year_start
% solutions = zeros(1,hours_between_selected_dates);
% objectiveValues = zeros(1,hours_between_selected_dates);
```

```
number_of_variables=4;
npp_percentage_lb=0;
csp_percentage_lb=0;
npp_percentage_ub=85;
csp_percentage_ub=85;


hours_of_year_start_boundary=hours_of_year_start;
hours_of_year_stop_boundary=hours_of_year_start+1;
```

for iteration = 1:hours_between_selected_dates

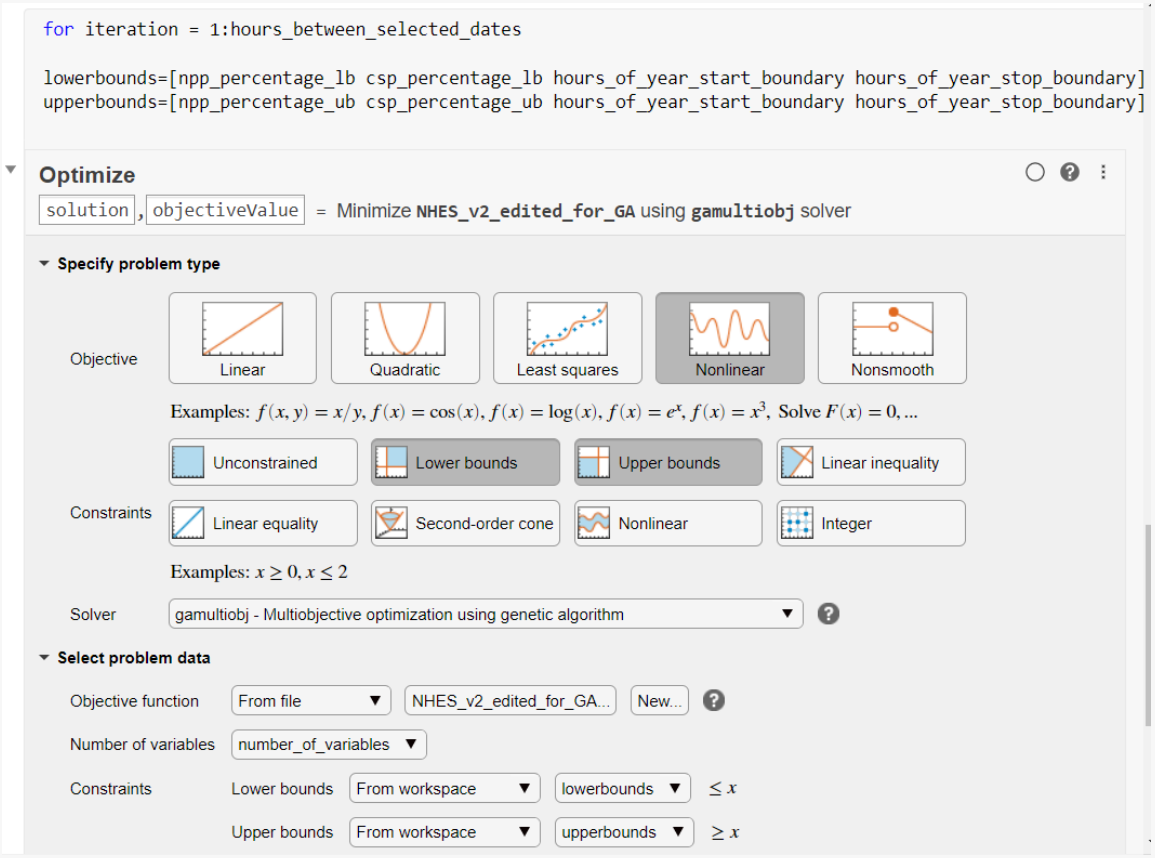


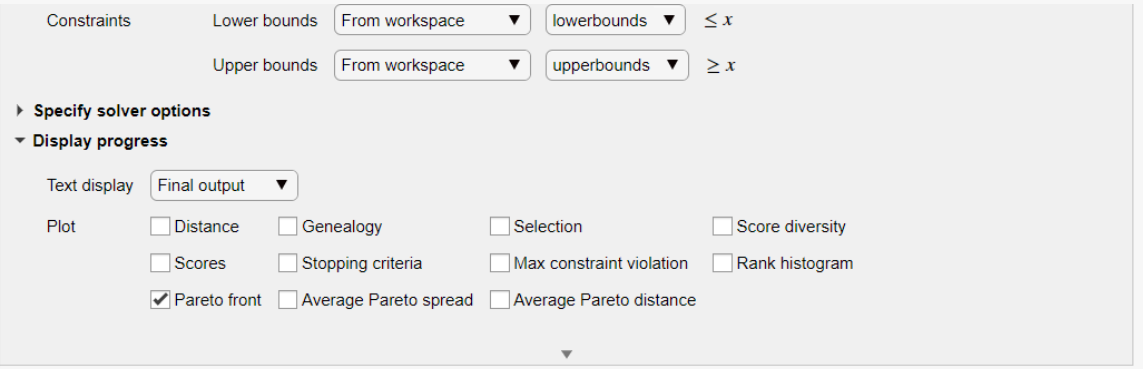


lowerbounds=[npp_percentage_lb csp_percentage_lb hours_of_year_start_boundary hours_of_year_stop_boundary];

upperbounds=[npp_percentage_ub csp_percentage_ub hours_of_year_start_boundary hours_of_year_stop_boundary];

```
solutions{iteration}=solution;
objectiveValues{iteration}=objectiveValue;


hours_of_year_start_boundary=hours_of_year_start_boundary+1
hours_of_year_stop_boundary=hours_of_year_stop_boundary+1
end
```

### A3. Pareto graphs code

```
close all; clc
hour_to_check=1;

optimized_objective_1hour=cell2mat(objectiveValues(1,hour_to_check));
optimized_total_profit=optimized_objective_1hour(:,1).*(-1);
optimized_total_heat_equivalent=optimized_objective_1hour(:,2).*(-1);

optimization_corresponding_percentages=cell2mat(solutions(1,hour_to_check));
optimized_npp_percentage=optimization_corresponding_percentages(:,1);
optimized_csp_percentage=optimization_corresponding_percentages(:,2);
floor_optimized_npp_percentage=floor(optimized_npp_percentage);
floor_optimized_csp_percentage=floor(optimized_csp_percentage);
```

```
%
percentages_for_graph_text={num2str(floor_optimized_npp_percentage),num2str(floor_
optimized_csp_percentage)};

figure (1)
hold on
title(strcat('Pareto Front',{', '},num2str(hour_to_check-1),':00am-
',num2str(hour_to_check),':00am'))
plot(optimized_total_profit,optimized_total_heat_equivalent,'m p');
% plot(one_to_hours_between_selected_dates,selected_dates_NPP_H2_kg_h,'-o');
% set(gca, 'XTick', xtickat, 'XTickLabel', cellstr( num2str( mod(round(xtickat .' ./ 1),24) )
) )
legend('$\frac{CSP percentage}{NPP percentage}$','Interpreter','latex','FontSize',18)
xlabel('Optimized Total Profit (Objective-1) [USD]')
ylabel('Optimized Total Heat Equivalent (Objective-2) [kJ]')
text(optimized_total_profit,optimized_total_heat_equivalent,strcat(num2str(floor_optimi
zed_npp_percentage),''),'VerticalAlignment','top','HorizontalAlignment','left','FontSize',1
0);
text(optimized_total_profit,optimized_total_heat_equivalent,strcat(num2str(floor_optimi
zed_csp_percentage),''),'VerticalAlignment','bottom','HorizontalAlignment','left','FontSiz
e',10);
grid on
hold off
```

## Appendix B. What's Best validation with MATLAB on a HX problem

What'sBest is a software that can minimize or maximize an objective function by defining adjustables and constraints. This section includes information about validation of What'sBest. To validate What'sBest software, the other software which is MATLAB is selected and a sample heat exchanger problem is optimized by using What'sBest and MATLAB.

As a first step, a heat exchanger question from "Book_7th Edition_Fundamentals of Heat and Mass Transfer-Incropera" is selected as an example.

**The sample heat exchanger question 11.22** is; "A shell-and-tube heat exchanger must be designed to heat 2.5 kg/s of water from 15 to 85 °C. The heating is to be accomplished by passing hot engine oil, which is available at 160 °C, through the shell side of the exchanger. The oil is known to provide an average convection coefficient of $h_o$ = 400 W/m2.K on the outside of the tubes. Ten tubes pass the water through the shell. Each tube is thin walled, of diameter $D$ = 25 mm, and makes eight passes through the shell. If the oil leaves the exchanger at 100 °C, what is its flow rate? How long must the tubes be to accomplish the desired heating?"

First, engine oil and water's respective thermodynamic values are added to another excel sheet as shown in Figure B1 in order to determine Reynolds and Nusselt numbers or other necessary thermodynamic properties by linear interpolation. By doing this, the SRS1 Splines tool in excel is able to extract the necessary thermodynamic data at an exact temperature.

| | engine oil | | | water | | | |
|---|---|---|---|---|---|---|---|
| | T (K) | cp (j/kg.K) | T (K) | cp (j/kg.K) | $\mu$ (N.s/m^2) | k (W/m.K) | Pr |
| 9 | 380 | 2250 | 300 | 4180.9 | 0.00085375 | 0.60944 | 5.8569 |
| 10 | 390 | 2294 | 305 | 4179.8 | 0.00076679 | 0.61711 | 5.1936 |
| 11 | 400 | 2337 | 310 | 4179.5 | 0.00069332 | 0.62422 | 4.6422 |
| 12 | 410 | 2381 | 315 | 4179.8 | 0.00063064 | 0.63082 | 4.1787 |
| 13 | 420 | 2427 | 320 | 4180.7 | 0.00057671 | 0.63695 | 3.7854 |
| 14 | | | 325 | 4182.1 | 0.00052995 | 0.64262 | 3.4488 |
| 15 | | | 330 | 4183.8 | 0.00048913 | 0.64787 | 3.1587 |
| 16 | | | 335 | 4186 | 0.00045328 | 0.6527 | 2.907 |
| 17 | | | 340 | 4188.5 | 0.00042161 | 0.65713 | 2.6873 |
| 18 | | | 345 | 4191.3 | 0.00039351 | 0.66117 | 2.4946 |
| 19 | | | 350 | 4194.6 | 0.00036845 | 0.66484 | 2.3246 |
| 20 | | | 355 | 4198.3 | 0.00034602 | 0.66815 | 2.1742 |
| 21 | | | 360 | 4202.4 | 0.00032585 | 0.67109 | 2.0405 |
| 22 | | | | | | | |

... | Objectives | interpolation_tables | correction_factor | moody_calculator

Figure B1: An indication of thermodynamic properties of engine oil and water depending on temperature.

The given data is then entered into Microsoft excel, where the necessary formulas are defined to produce the results. According to Figure B2, the excel sheet can resolve the issue depending on the specified criteria. As evidence, the question's "the length of the tube" is found on excel to **match the answer**, **which is 37.8m.**

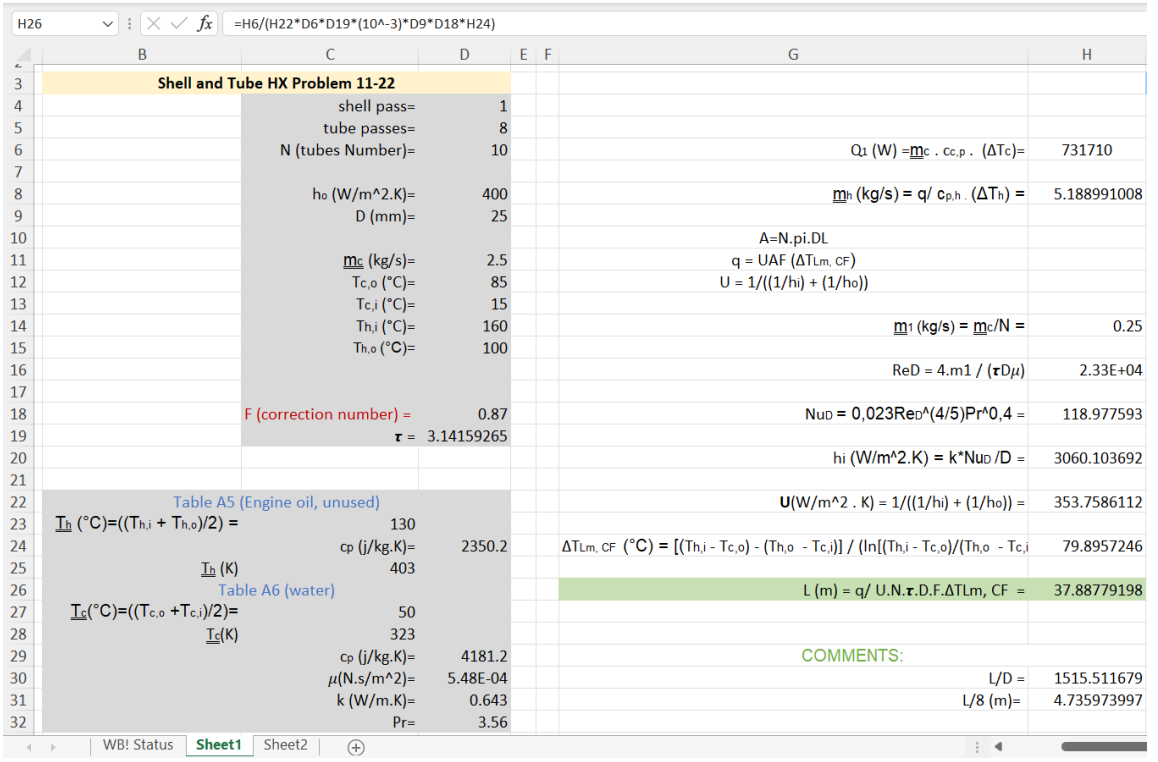

| | B | C | D | E | F | G | H |
|---|---|---|---|---|---|---|---|
| 3 | **Shell and Tube HX Problem 11-22** | | | | | | |
| 4 | | shell pass= | 1 | | | | |
| 5 | | tube passes= | 8 | | | | |
| 6 | | N (tubes Number)= | 10 | | | $Q_1$ (W) =$\underline{m}_c$ . $c_{c,p}$ . ($\Delta T_c$)= | 731710 |
| 7 | | | | | | | |
| 8 | | $h_o$ (W/m^2.K)= | 400 | | | $\underline{m}_h$ (kg/s) = q/ $c_{p,h}$ . ($\Delta T_h$) = | 5.188991008 |
| 9 | | D (mm)= | 25 | | | | |
| 10 | | | | | | A=N.pi.DL | |
| 11 | | $\underline{m}_c$ (kg/s)= | 2.5 | | | q = UAF ($\Delta T_{Lm,\ CF}$) | |
| 12 | | $T_{c,o}$ (°C)= | 85 | | | U = 1/((1/hi) + (1/$h_o$)) | |
| 13 | | $T_{c,i}$ (°C)= | 15 | | | | |
| 14 | | $T_{h,i}$ (°C)= | 160 | | | $\underline{m}_1$ (kg/s) = $\underline{m}_c$/N = | 0.25 |
| 15 | | $T_{h,o}$ (°C)= | 100 | | | | |
| 16 | | | | | | ReD = 4.m1 / ($\tau$D$\mu$) | 2.33E+04 |
| 17 | | | | | | | |
| 18 | | F (correction number) = | 0.87 | | | $Nu_D$ = 0,023$Re_D$^(4/5)Pr^0,4 = | 118.977593 |
| 19 | | $\tau$ = | 3.14159265 | | | | |
| 20 | | | | | | hi (W/m^2.K) = k*$Nu_D$ /D = | 3060.103692 |
| 21 | | | | | | | |
| 22 | Table A5 (Engine oil, unused) | | | | | **U**(W/m^2 . K) = 1/((1/hi) + (1/$h_o$)) = | 353.7586112 |
| 23 | $\underline{T}_h$ (°C)=(($T_{h,i}$ + $T_{h,o}$)/2) = | 130 | | | | | |
| 24 | | cp (j/kg.K)= | 2350.2 | | | $\Delta T_{Lm,\ CF}$ (°C) = [($T_{h,i}$ - $T_{c,o}$) - ($T_{h,o}$ - $T_{c,i}$)] / (ln[($T_{h,i}$ - $T_{c,o}$)/($T_{h,o}$ - $T_{c,i}$ | 79.8957246 |
| 25 | $\underline{T}_h$ (K) | 403 | | | | | |
| 26 | Table A6 (water) | | | | | L (m) = q/ U.N.$\tau$.D.F.$\Delta$TLm, CF = | 37.88779198 |
| 27 | $\underline{T}_c$(°C)=(($T_{c,o}$ +$T_{c,i}$)/2)= | 50 | | | | | |
| 28 | $\underline{T}_c$(K) | 323 | | | | | |
| 29 | | cp (j/kg.K)= | 4181.2 | | | COMMENTS: | |
| 30 | | $\mu$(N.s/m^2)= | 5.48E-04 | | | L/D = | 1515.511679 |
| 31 | | k (W/m.K)= | 0.643 | | | L/8 (m)= | 4.735973997 |
| 32 | | Pr= | 3.56 | | | | |

Figure B2: Solution of “Shell and Tube Heat Exchanger Problem 11-22” on Microsoft excel.

When it comes to "optimization", for instance, What'sBest!, which is an optimization tool in excel, can compute the minimal tube length. Adjustable parameters and constraints are described here. The objective function to minimize or maximize is then defined. In this example, the length of the tube is preferred to minimize as an objective function to demonstrate how What'sBest works. Afterwards, the same optimization problem will be carried out on MATLAB to compare the results.

As seen in **Figure B3**, a correction factor calculator based on a heat exchanger's parameters is imported into excel. This calculator, which is important in the computation of the heat exchanger problem, allows for the simultaneous acquisition and consideration of the necessary correction factor.

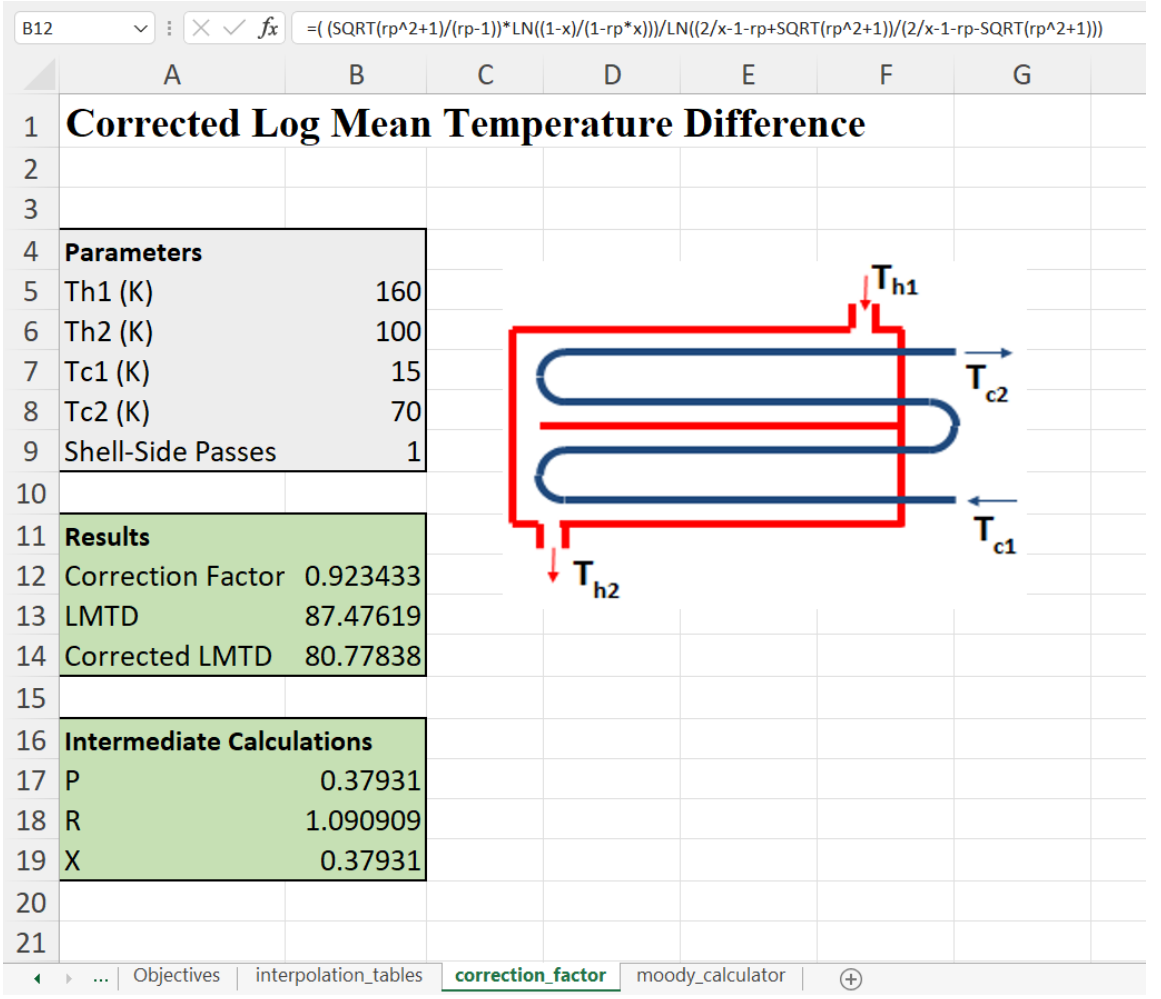


**Figure B3**: An indication of calculation of correction factor.

After adding correction factor calculation and thermodynamic properties of engine oil and water depending on temperature to excel, adjustable parameters and their constraints (upper and lower bounds) are defined as shown in the **Figure B4**. Next, the objective function that is the tube length is minimized. In this way, the new tube length (L) optimized by minimizing taking into account the bounds is found as **15.72m** as indicated in the **Figure B4**.

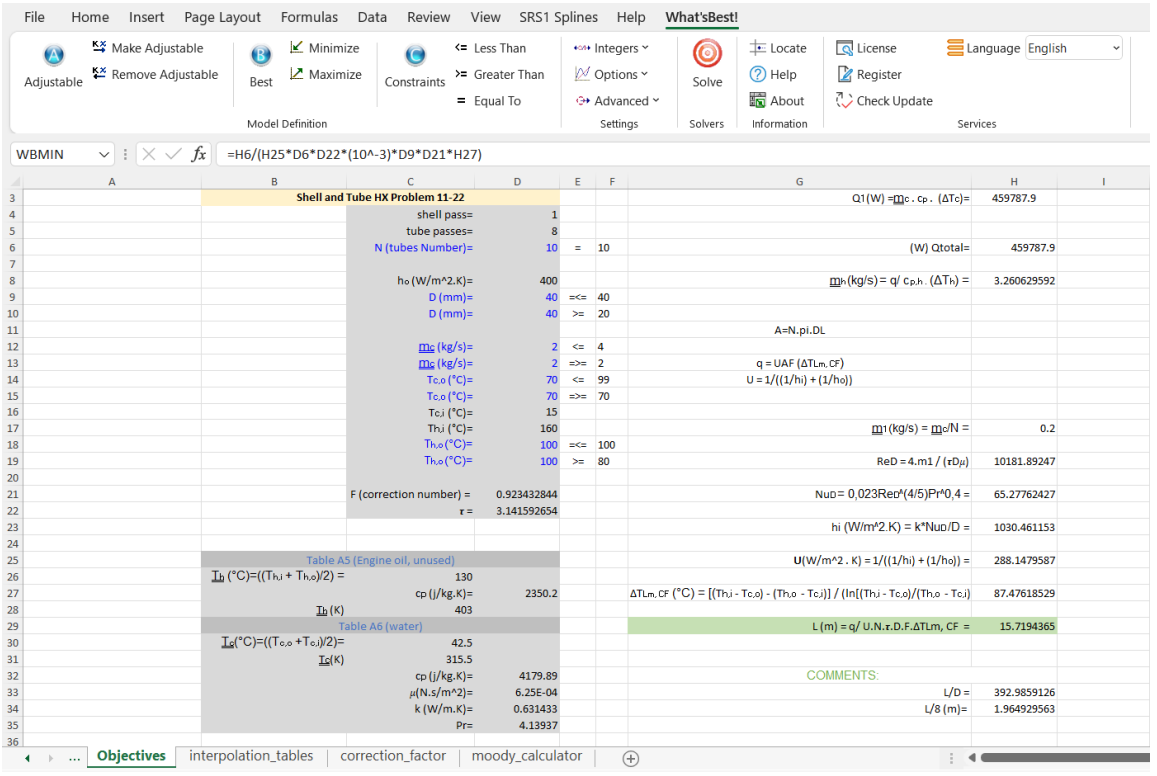


**Figure B4**: Showing adjustable parameters and their constraints (upper and lower bounds).

Next step is to considered the same question to optimize with the same adjustable parameters and constraints on MATLAB. In order to calculate thermodynamic properties at precise temperatures by interpolating, values shown in **Figure B1** are written to MATLAB. Also, MATLAB code is written to calculate the correction factor that changes depending on the variables. To minimize the objective function on MATLAB, an optimization program is written as indicated in **Figure B5**.

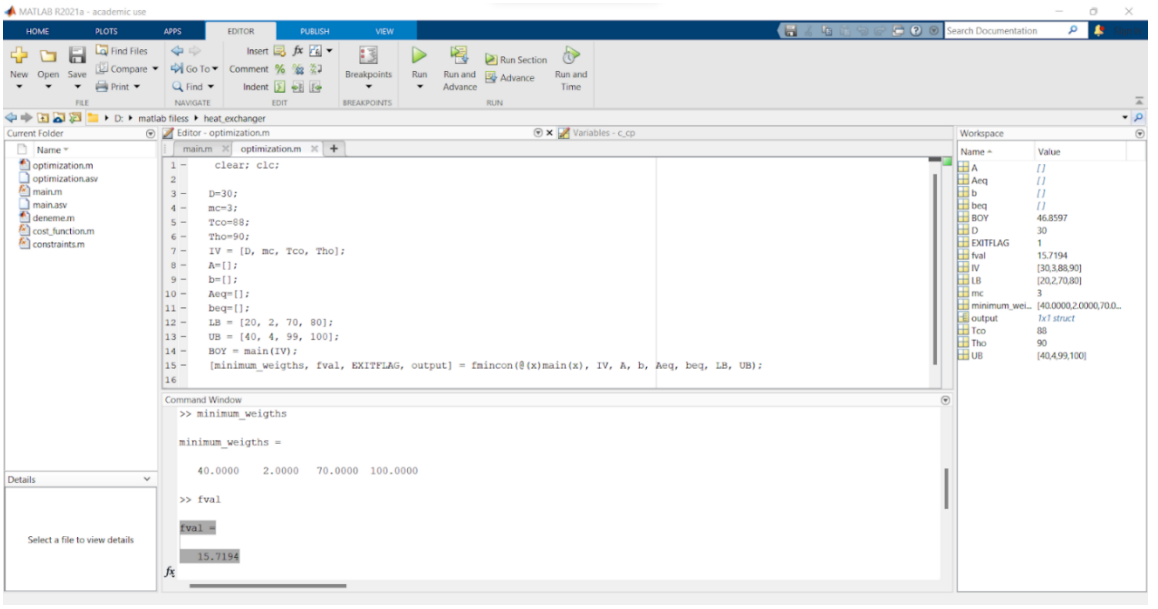


**Figure B5:** MATLAB optimization for a heat exchanger problem.

On MATLAB, the tube length that is the objective function ("fval" on MATLAB) is found as **15.7194 meters.** It is seen that when comparing the optimization results on excel and MATLAB, these are the same.

In summary, first of all, a heat exchanger problem is selected. This problem is coded to excel and MATLAB. By using What'sBest optimization tool on excel, the tube length, which is the objective function, is optimized to minimize. The same optimization objective function is solved with the code written in MATLAB. According to these optimizations, the same results are obtained on excel and MATLAB. In this way, What'sBest Optimization tool is validated with MATLAB.

**Encodings for a)the main heat exchanger question and b)optimization in Matlab are given below.**

**a)The main heat exchanger question coding;**

```
function [L]= main (x)
 D = x(1);
```

```
 mc = x(2);
 Tco = x(3);
 Tho = x(4);
 shell_pass = 1;
%  tube_passes = 8; nonused
 N_tube_amount = 10;
 ho = 400; %[W/m^.K]
%  D = 30; %[mm]
%  mc = 4.03917098753466; %[kg/s]
%  Tco = 105; %[Celcius]
 Tci = 15; %[Celcius]
 Thi = 160; %[Celcius]
%  Tho = 100; %[Celcius]
% le = 2257; %[j/g]

 %%%%%%%interpolation table
 table_T=[300,305,310,315,320,325,330,335,340,345,350,355,360];
 table_cp=[4180.9,4179.8,4179.5,4179.8,4180.7,4182.1,4183.8,4186,4188.5,4191.3,4194
.6,4198.3,4202.4];
 table_mu=[0.00085375,0.00076679,0.00069332,0.00063064,0.00057671,0.00052995,0.
00048913,0.00045328,0.00042161,0.00039351,0.00036845,0.00034602,0.00032585];
 table_k=[0.60944,0.61711,0.62422,0.63082,0.63695,0.64262,0.64787,0.6527,0.65713,0.
66117,0.66484,0.66815,0.67109];
```

```
table_pr=[5.8569,5.1936,4.6422,4.1787,3.7854,3.4488,3.1587,2.907,2.6873,2.4946,2.32
46,2.1742,2.0405];
%%%%%%%interpolations
Tca=(Tco+Tci)/2+273; %average temperature
c_cp = interp1(table_T,table_cp,Tca);
mu = interp1(table_T,table_mu,Tca);
Pr = interp1(table_T,table_pr,Tca);
k = interp1(table_T,table_k,Tca);
%%%%%%%

%  h_cp = 2350.2; %[j/kg.K] used for mh nonused
%c_cp = 4188.2
%mu = 0.00004167; %[N.s/m^2]
%Pr = 2.638; %prandtl
%k = 0.6604; %[w/m.K]

Q1 = mc * c_cp * (Tco-Tci); %[W]
% Q2 = mc * le;
% Q3 = mc * c_cp * (Tco-100);
% Q= Q1+Q2+Q3;
Q= Q1;

%  mh = Q / (h_cp * (Thi-Tho)); %[kg/s] non used
```

```
m1 = mc / N_tube_amount;
ReD = 4 * m1 /(D*(10^-3) *pi* mu);
NuD = 0.023*ReD^(4/5) * Pr^0.4;
hi = k*NuD/(D*(10^-3)); %[W/m^2.K]
U = 1/((1/hi)+(1/ho));
deltaT_Lm = (((Thi-Tco)-(Tho-Tci))/(log((Thi-Tco)/(Tho-Tci))));

%%%%%%%% correction factor
t_h1 = Thi;
t_h2 = Tho;
t_c1 = Tci;
t_c2 = Tco;
N = shell_pass;

rp = (t_h1-t_h2)/(t_c2-t_c1);
P = (t_c2-t_c1)/(t_h1-t_c1);
x = (1 - ((rp*P-1)/(P-1))^(1/N))/(rp - ((rp*P-1)/(P-1))^(1/N));
F = ( (sqrt(rp^2+1)/(rp-1))*log((1-x)/(1-rp*x)))/log((2/x-1-rp+sqrt(rp^2+1))/(2/x-1-rp-
sqrt(rp^2+1)));
%%%%%%%% correction factor

L = Q / (U*N_tube_amount*pi*D*(10^-3)*F*deltaT_Lm);

end
```

## B1. Optimization coding

```
clear; clc;


D=30;

mc=3;

Tco=88;

Tho=90;

IV = [D, mc, Tco, Tho];

A=[];

b=[];

Aeq=[];

beq=[];

LB = [20, 2, 70, 80];

UB = [40, 4, 99, 100];

BOY = main(IV);

[minimum_weigths, fval, EXITFLAG, output] = fmincon(@(x)main(x), IV, A, b, Aeq,

beq, LB, UB);
```

Appendix C. HX Optimization on Microsoft excel via What'sBest! Software

To give a clear example of a heat exchanger optimization problem, a question from "th Edition, Fundamentals of Heat and Mass Transfer, F. Incropera and D. DeWitt" is taken as an example.

**The sample question '11.22** is; "*A shell-and-tube heat exchanger must be designed to heat 2.5 kg/s of water from 15 to 85C. The heating is to be accomplished by passing hot engine oil, which is available at 160C, through the shell side of the exchanger. The oil is known to provide an average convection coefficient of ho = 400 W/m2.K on the outside of the tubes. Ten tubes pass the water through the shell. Each tube is thin walled, of diameter D = 25 mm, and makes eight passes through the shell. If the oil leaves the exchanger at 100C, what is its flow rate? How long must the tubes be to accomplish the desired heating?*

Firstly, to calculate Reynolds and Nusselt numbers or required thermodynamic properties by linear interpolation, thermodynamic properties of engine oil and water are added to another excel sheet as indicated Figure B1. By doing so, at a precise temperature, required thermodynamic numbers are obtained by SRS1 Splines tool on excel.

| 21 | engine oil | | | water | | | | |
|---|---|---|---|---|---|---|---|---|
| 22 | T (K) | cp (j/kg.K) | | T (K) | cp (j/kg.K) | μ (N.s/m^2) | k (W/m.K) | Pr |
| 23 | 380 | 2250 | | 320 | 4180 | 5.77E-04 | 0.64 | 3.77 |
| 24 | 390 | 2294 | | 325 | 4182 | 5.28E-04 | 0.645 | 3.42 |
| 25 | 400 | 2337 | | 330 | 4184 | 4.89E-04 | 0.65 | 3.15 |
| 26 | 410 | 2381 | | 335 | 4186 | 4.53E-04 | 0.656 | 2.88 |
| 27 | 420 | 2427 | | 340 | 4188 | 4.20E-04 | 0.66 | 2.66 |

WB! Status | Sheet1 | Sheet2

Figure B1: An indication of thermodynamic properties of engine oil and water depending on temperature.

Afterwards, the given data is written to Microsoft excel and needed formulas are defined on excel to obtain the answers. As indicated **Figure B2**, depending on the given parameters, the excel sheet can solve the problem. As a proof, “the length of the tube” asked is found on excel the same as the answer of the question, which is 37.8 m.

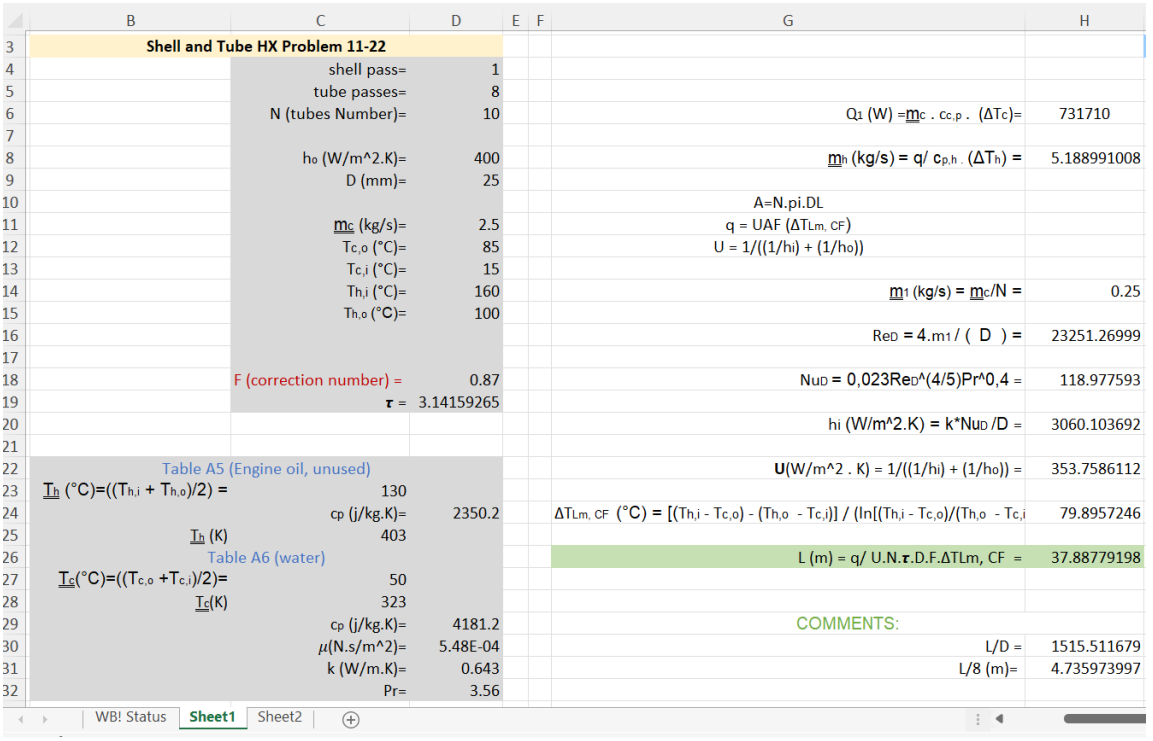

| | B | C | D | E | F | G | H |
|---|---|---|---|---|---|---|---|
| 3 | **Shell and Tube HX Problem 11-22** | | | | | | |
| 4 | | shell pass= | 1 | | | | |
| 5 | | tube passes= | 8 | | | | |
| 6 | | N (tubes Number)= | 10 | | | $Q_1$ (W) =$\underline{m}_c$ . $c_{c,p}$ . ($\Delta T_c$)= | 731710 |
| 7 | | | | | | | |
| 8 | | $h_o$ (W/m^2.K)= | 400 | | | $\underline{m}_h$ (kg/s) = q/ $c_{p,h}$ . ($\Delta T_h$) = | 5.188991008 |
| 9 | | D (mm)= | 25 | | | | |
| 10 | | | | | | A=N.pi.DL | |
| 11 | | $\underline{m}_c$ (kg/s)= | 2.5 | | | q = UAF ($\Delta T_{Lm, CF}$) | |
| 12 | | $T_{c,o}$ (°C)= | 85 | | | U = 1/((1/hi) + (1/ho)) | |
| 13 | | $T_{c,i}$ (°C)= | 15 | | | | |
| 14 | | $T_{h,i}$ (°C)= | 160 | | | $\underline{m}_1$ (kg/s) = $\underline{m}_c$/N = | 0.25 |
| 15 | | $T_{h,o}$ (°C)= | 100 | | | | |
| 16 | | | | | | $Re_D$ = 4.$m_1$ / ( D ) = | 23251.26999 |
| 17 | | | | | | | |
| 18 | | F (correction number) = | 0.87 | | | $Nu_D$ = 0,023$Re_D$^(4/5)Pr^0,4 = | 118.977593 |
| 19 | | τ = | 3.14159265 | | | | |
| 20 | | | | | | hi (W/m^2.K) = k*$Nu_D$ /D = | 3060.103692 |
| 21 | | | | | | | |
| 22 | | Table A5 (Engine oil, unused) | | | | U(W/m^2 . K) = 1/((1/hi) + (1/ho)) = | 353.7586112 |
| 23 | $\underline{T}_h$ (°C)=(($T_{h,i}$ + $T_{h,o}$)/2) = | 130 | | | | | |
| 24 | | $c_p$ (j/kg.K)= | 2350.2 | | | $\Delta T_{Lm, CF}$ (°C) = [($T_{h,i}$ - $T_{c,o}$) - ($T_{h,o}$ - $T_{c,i}$)] / (ln[($T_{h,i}$ - $T_{c,o}$)/($T_{h,o}$ - $T_{c,i}$ | 79.8957246 |
| 25 | $\underline{T}_h$ (K) | 403 | | | | | |
| 26 | | Table A6 (water) | | | | L (m) = q/ U.N.τ.D.F.$\Delta$TLm, CF = | 37.88779198 |
| 27 | $\underline{T}_c$(°C)=(($T_{c,o}$ +$T_{c,i}$)/2)= | 50 | | | | | |
| 28 | $\underline{T}_c$(K) | 323 | | | | | |
| 29 | | $c_p$ (j/kg.K)= | 4181.2 | | | COMMENTS: | |
| 30 | | $\mu$(N.s/m^2)= | 5.48E-04 | | | L/D = | 1515.511679 |
| 31 | | k (W/m.K)= | 0.643 | | | L/8 (m)= | 4.735973997 |
| 32 | | Pr= | 3.56 | | | | |

WB! Status | Sheet1 | Sheet2

**Figure B2**: Solution of "Shell and Tube Heat Exchanger Problem 11-22" on Microsoft excel.

When it comes to "optimization", for example, obtaining minimum tube length can be calculated by What'sBest! Optimization tool on excel. Here, adjustable parameters and restrictions are defined. Next, it is necessary to define objective function to minimize or maximize. In this example, to show how What'sBest works, minimizing the length of the tube is preferred to minimize as an objective function.

Before applying optimization, to increase the complexity and parameters, the cold fluid, which is water in the sample problem 11-22, is intended to undergo a phase change from liquid form to vapor and, new parameters to have finned pipes are added to the sample problem. Added new parameters are "thickness of fin", "distance between two fins" and "the number of fins per 1 meter". Moreover, although the tube on the sample problem does

not have different internal and external diameters, internal and external diameters information are added in this optimization problem.

A calculator of correction factor depending on the parameters of a heat exchanger is imported to excel as shown in **Figure B3**. Thanks to this calculator that has an important role in calculation of heat exchanger problem, needed correction factor is simultaneously obtained and taken into account.

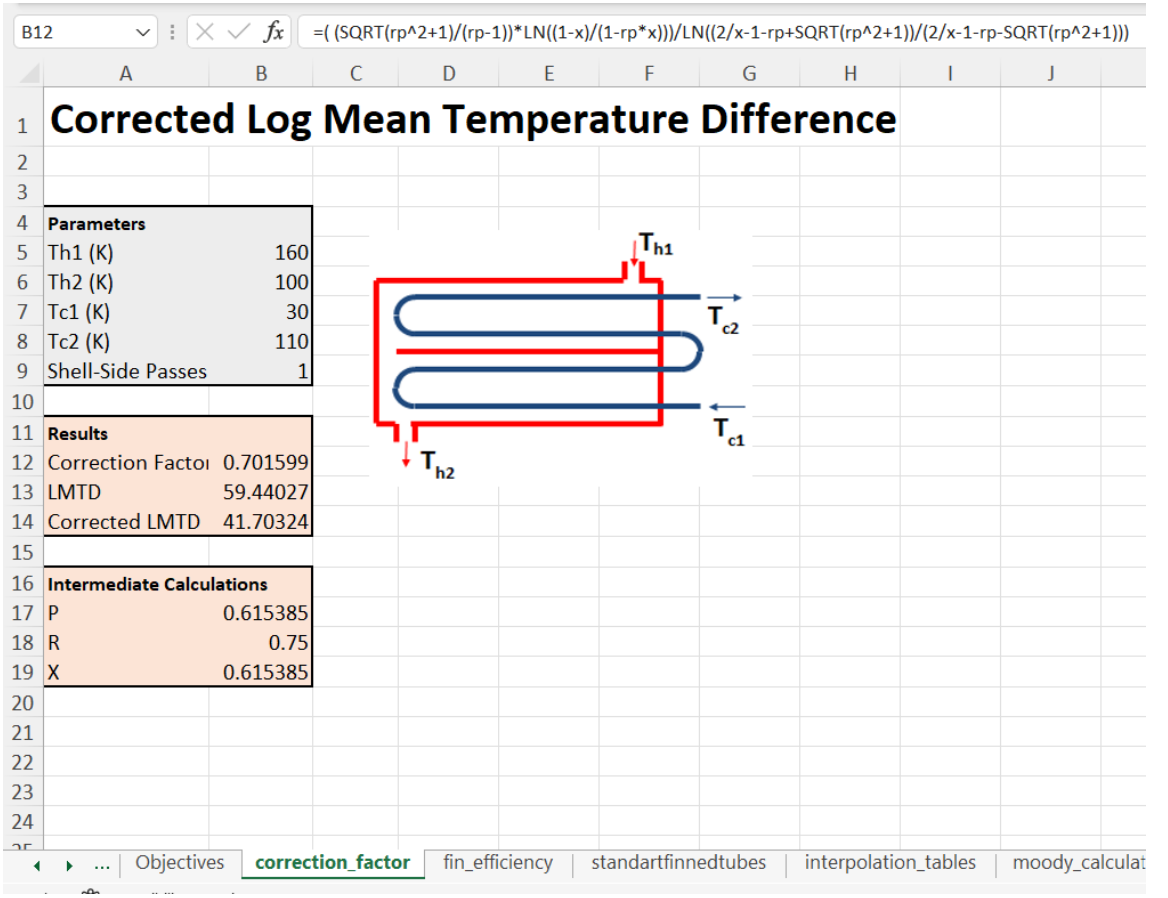


**Figure B3**: An indication of calculation of correction factor.

When it comes to fins, it is necessary to calculate fin efficiency. This helps to attain more realistic results in terms of heat exchanger calculations. Fin efficiency calculator indicated in **Figure B4** is added to another sheet of the excel file. Fin efficiency obtained is transferred to the main excel sheet and simultaneous calculations are made.

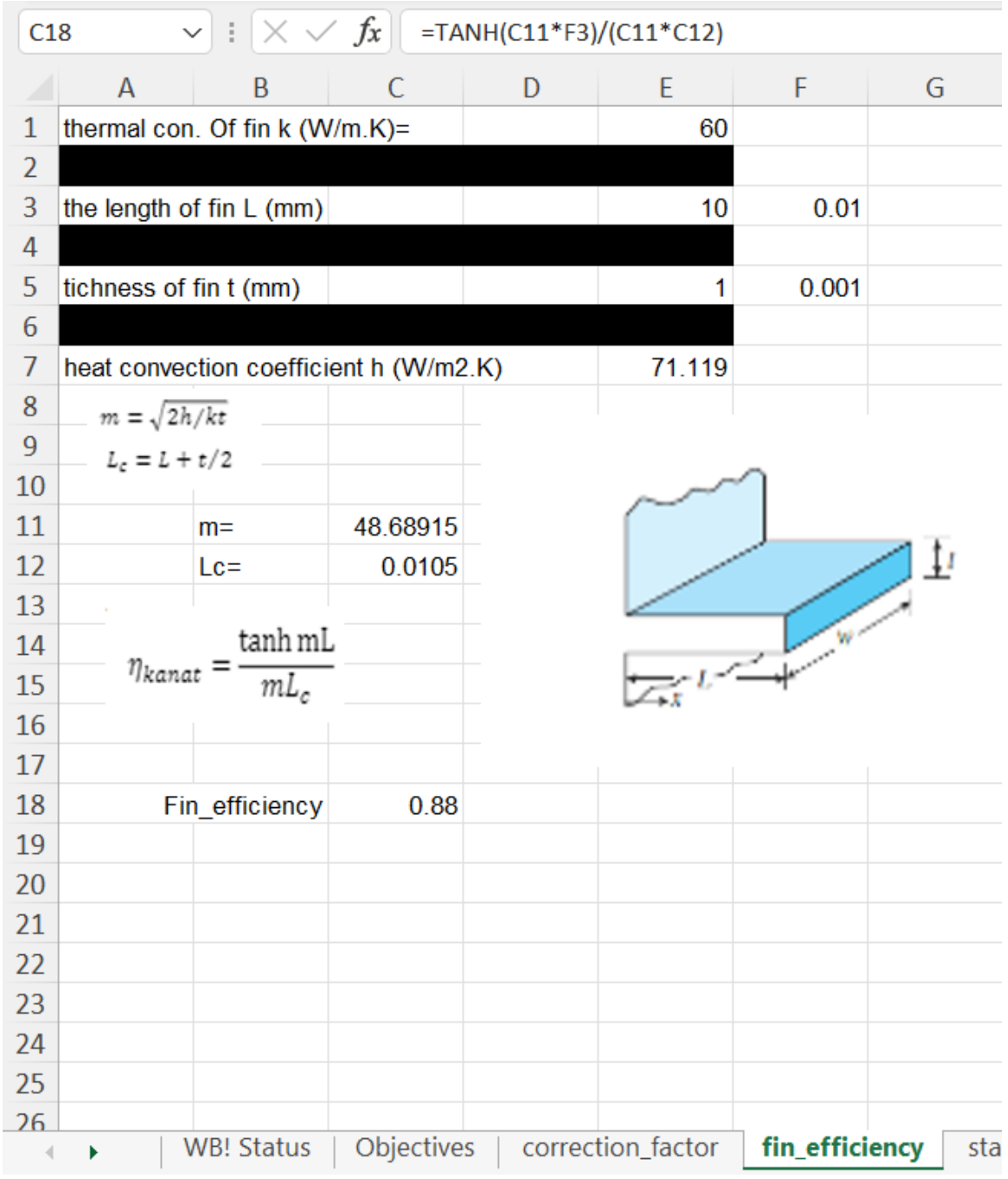


**Figure B4:** Fin efficiency calculation on excel.

After taking into account these improvements on the heat exchanger problem, new tube length is calculated with the same inputs given in the problem 11-22. As the heat amount transferred increases thanks to these improvements, the new tube length is calculated as **54.78 meters** as pointed out in **Figure B5**.

| | |
|---|---|
| $\dot{m}_1$ (kg/s) = $\dot{m}_c$/N = | 0.25 |
| | |
| $Re_D$ = 4.$m_1$ / ( D ) = | 29064.08749 |
| | |
| $Nu_D$ = 0,023$Re_D$^(4/5)Pr^0,4 = | 142.2306481 |
| | |
| $h_i$ (W/m^2.K) = k*$Nu_D$ /D = | 4572.715336 |
| | |
| **U**(W/m^2 . K) = 1/((1/$h_i$) + (1/$h_o$)) = | 367.82442 |
| | |
| $\Delta T_{Lm, CF}$ (°C) = [($T_{h,i}$ - $T_{c,o}$) - ($T_{h,o}$ - $T_{c,i}$)] / (ln[($T_{h,i}$ - $T_{c,o}$)/($T_{h,o}$ - $T_{c,i}$)]) | 79.8957246 |
| | |
| L (m) = q/ U.N.**τ**.D.F.ΔTLm, CF = | 54.77531116 |

**Figure B5**: The tube length after adding improvements to the sample problem.

As for optimization, to reduce the tube length, which is the objective function, with constraints desired, adjustable parameters are defined and as shown in **Figure B6.**

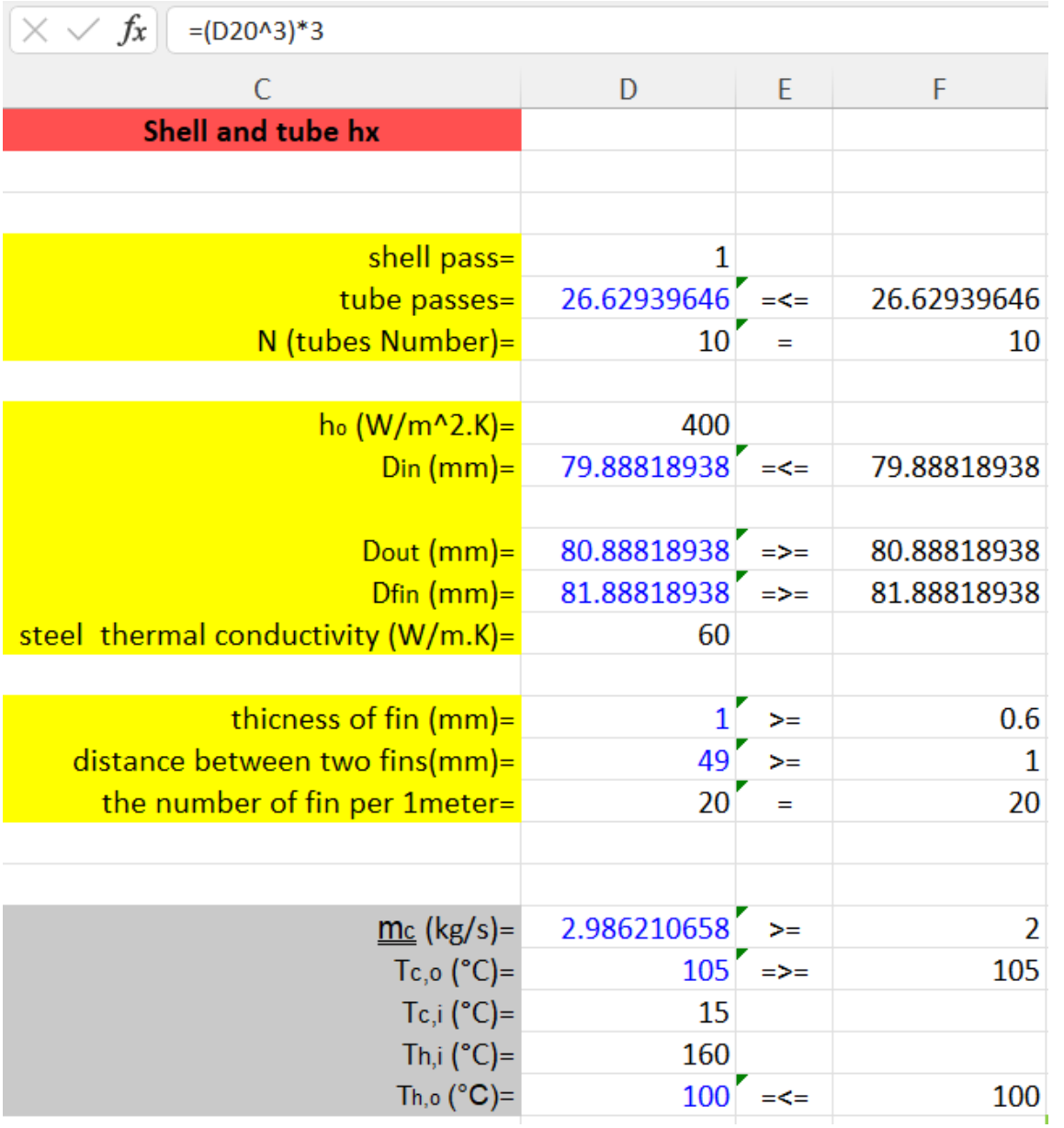

=(D20^3)*3

| C | D | E | F |
|---|---|---|---|
| **Shell and tube hx** | | | |
| | | | |
| | | | |
| shell pass= | 1 | | |
| tube passes= | 26.62939646 | =<= | 26.62939646 |
| N (tubes Number)= | 10 | = | 10 |
| | | | |
| $h_o$ (W/m^2.K)= | 400 | | |
| Din (mm)= | 79.88818938 | =<= | 79.88818938 |
| | | | |
| Dout (mm)= | 80.88818938 | =>= | 80.88818938 |
| Dfin (mm)= | 81.88818938 | =>= | 81.88818938 |
| steel thermal conductivity (W/m.K)= | 60 | | |
| | | | |
| thicness of fin (mm)= | 1 | >= | 0.6 |
| distance between two fins(mm)= | 49 | >= | 1 |
| the number of fin per 1meter= | 20 | = | 20 |
| | | | |
| | | | |
| $\underline{m_c}$ (kg/s)= | 2.986210658 | >= | 2 |
| $T_{c,o}$ (°C)= | 105 | =>= | 105 |
| $T_{c,i}$ (°C)= | 15 | | |
| $T_{h,i}$ (°C)= | 160 | | |
| $T_{h,o}$ (°C)= | 100 | =<= | 100 |

**Figure B6:** Showing adjustable parameters and constraints determined.

After applying optimization to minimize the tube length by using What'sBest! and considering these constraints with adjustable parameters, the new tube length is found as **44,96** meters as pointed in **Figure B7**. It is seen that optimized tube length is 18% less that it was.

| | |
|---|---|
| $\underline{\underline{m}}_1$ (kg/s) = $\underline{\underline{m}}_c/N$ = | 0.298621066 |
| $Re_D = 4.m_1 / ( D )$ = | 10182.61383 |
| $Nu_D = 0{,}023Re_D^{(4/5)}Pr^{0,4}$ = | 57.30169809 |
| $h_i$ (W/m^2.K) = $k*Nu_D/D$ = | 468.8100977 |
| **U**(W/m^2 . K) = $1/((1/h_i) + (1/h_o))$ = | 215.8400778 |
| $\Delta T_{Lm, CF}$ (°C) = $[(T_{h,i} - T_{c,o}) - (T_{h,o} - T_{c,i})] / (\ln[(T_{h,i} - T_{c,o})/(T_{h,o} - T_{c,i})])$ | 68.91512662 |
| L (m) = q/ U.N.$\tau$.D.F.$\Delta$TLm, CF = | 44.95525734 |

**Figure B7:** The tube length after applying optimization.

To conclude, objective functions can be increased or decreased by adhering to constraints and iterating through variable parameters.

## Appendix C. Published Papers and Presentation.

# Optimized Clean Hydrogen Production using Nuclear Small Modular Reactors and Renewable Energy Sources: a Review

Mustafa Ciftcioglu, Filippo Genco, Akira Tokuhiro

**1 Introduction** As the world's population and economy grow while people migrate from rural areas to urban areas, the demand for energy rises [1]. Most of the modern electric energy comes globally from fossil fuels (hydrocarbons) [2], which are depleted and constrained by geographical distribution and extraction ease [3,4]. The constant use of hydrocarbon-based energy resulted in significant increases of $CO_2$ and Greenhouse Gases in the atmosphere and has been indicated as the primary cause of global warming [5]. Sustainable and renewable energy resources play a critical role in the world's future in order to mitigate global warming and maintain a clean environment [6–9]. Electric energy can be challenging to obtain from renewable energy sources at a very competitive price. In fact, one of the most striking features of these types of energy sources is its variability and irregularity [10]. It is then necessary to implement efficient and large-scale technical solutions to address these problems. To cope with the volatility and discontinuity of renewable energy sources, large-scale storage systems have been proposed and designed to meet the market demand [11]. By transferring generated energy on multiple time scales, storage devices are able to decouple supply and demand (hourly, daily, and seasonally) [12].

Hydrogen is a good energy transporter when it comes to storing energy [13–16]. Furthermore, Hydrogen is already a commodity that is utilized as a feedstock in a variety of industrial applications, from refineries to the manufacturing of ammonia and methanol [17]. Hydrogen-based energy storage systems are rising in importance for large-scale energy storage due to their ability to be stored and transported, as well as for cost effectiveness [3,13,18]. From less than 20 Mt in 1975 to more than 70 Mt in 2018, the global demand for pure hydrogen has surged dramatically [19]. While several researchers support the use of hydrogen as an energy carrier for the reasons just described [20], most of the latest studies, have however concluded that a fully hydrogen-dependent economy is still disputed and unattainable [13,21], despite the fact that it has just begun to show promise [22]. Whatever the difficulties, the trend is toward clean hydrogen generation to reduce $CO_2$ emissions and meet global energy demand [5,14,23–25].

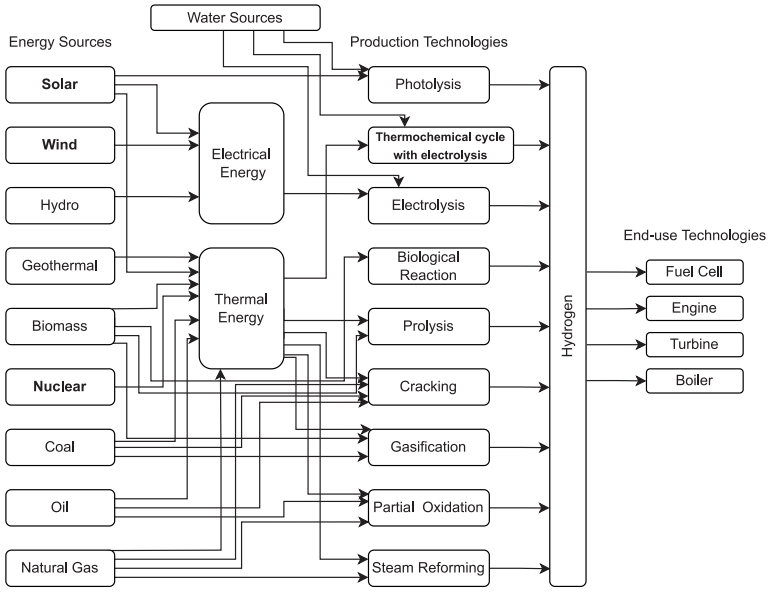


**Fig. 1**
The most common alternate ways for producing hydrogen from energy sources as described by [26].

According to the type of energy sources, hydrogen can be named. The use of a color-coded approach to describe hydrogen generating technology is becoming more common. Hydrogen production methods according to colors are indicated in Fig. 2. The following are the key colors that are being considered [30]:

- Grey (or brown/black) hydrogen, which is produced by fossil fuels (mostly natural gas and coal) and emits carbon dioxide;
- Blue hydrogen, which is produced by combining grey hydrogen with carbon capture and storage (CCS) to avoid the majority of the process' GHG emissions;

- Turquoise hydrogen, which is produced by pyrolysis of a fossil fuel and produces solid carbon as a by-product;
- Green hydrogen, when produced by electrolyzers powered by renewable energy (and in some situations, other bioenergy-based processes like biomethane reforming or solid biomass gasification);
- Yellow (or purple) hydrogen, when produced by electrolyzers powered by nuclear power.

Traditional water electrolysis, steam reforming, steam electrolysis at high temperatures, hybrid and thermochemical cycles are only a few of the approaches documented in the literature that can produce heat and electricity while also creating hydrogen from water in the same nuclear power reactor [26,30]. One of the most attractive technologies is the nuclear hybrid energy system (NHES). The NHES can generate hydrogen as well as low-cost power [31,32].

Due to the complexity of NHES, when optimized, NHES can be more efficient [32]. Multi-objective optimization in the NHES is a very complex aspect of optimization processes because almost all real-world optimization problems are formulated using multiple conflicting objectives. The usual way to solve such problems is to combine multiple objectives into one, but the right approach tries to solve the multi-objective optimization problem in the real world. Artificial intelligence and algorithms can be used to optimize a variety of processes in complicated systems [8,23,33–37]. Moreover, for linear, integer, and nonlinear optimization, the Lindo® What's Best (or similar) tool can be used [38,39]. The tool provides the best answer with defined constructions and parameters [38]. Thus, the purpose of this paper is to explore and report the most recent technologies proposed to generate hydrogen based on nuclear and renewable energy using optimization techniques.

Briefly, this study provides an overview of nuclear-renewable clean hydrogen generation processes, with a focus on basically water-based approaches. In addition to this, it contains an overview of small modular reactors with its temperature ranges and potential usage areas. It continues by giving information about hydrogen such as potential uses in different sectors. In the next sections, there is a comparison of hydrogen production technologies, namely, thermochemical cycles and electrolysis in terms of cost, efficiencies, global warming potential (GWP) etc. and followed by, this research indicates technology readiness level of the hydrogen production technologies. Finally, the goal of this research is to optimize each stage of the hybrid system in order to achieve better outputs while taking into account complexity and multi-objectivity.

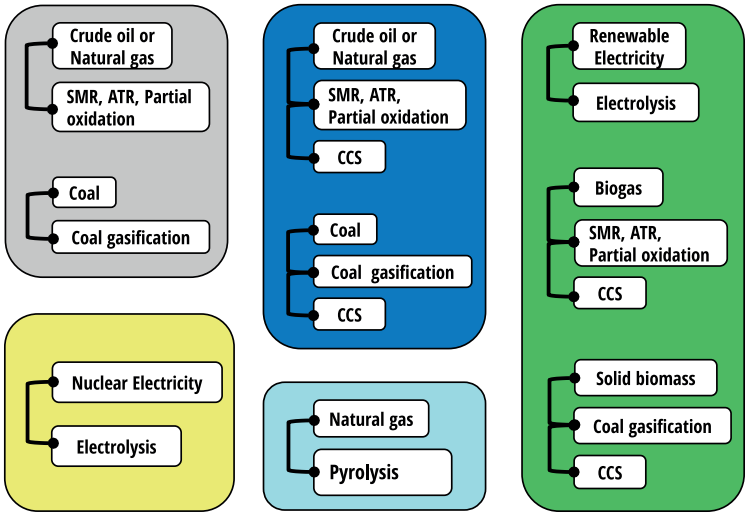


**Fig. 2**
Hydrogen production methods according to most commonly used color schemes.

## 2. Nuclear Power Plant

Nuclear power plants produce heat energy without emitting carbon dioxide due to nuclear (fission) processes. Heat is utilized to generate steam, which drives a steam turbine attached to an electricity generator, as characteristic of thermal power plants. There are approximately 440 nuclear power reactors operating globally providing approximately 11.5 % of the world's electricity demand [40,41]. Nuclear power plants have reduced $CO_2$ emissions by 60 gigatons during the previous 50 years [42]. Table 1 shows a summary of information of six different nuclear reactors in terms of coolant type, neutron spectrum, capacity (MWe), fuel cycle and outlet temperature (°C).

It is feasible to produce hydrogen using a nuclear reactor due to its great thermal energy capabilities [50,51]. There are numerous technologies and techniques for producing hydrogen from a variety of sources, including fossil fuels, renewable sources and nuclear energy [22,52,53]. The nuclear hybrid energy system is one of the most appealing technologies (NHES) [2]. The NHES can produce both hydrogen and low-cost electricity [31,54]. The same nuclear power reactor can deliver heat and electricity while also producing hydrogen from water with different methods [54]: water electrolysis, steam reforming, steam electrolysis at high temperatures, hybrid and thermochemical cycles are just a few of the techniques covered in the literature [6,55,56].

According to the capacity, nuclear power reactors are divided into three, which are small, medium

| | Supercritical-Water-Cooled Reactor | Gas-Cooled Fast Reactor | Lead-Cooled Fast Reactor | Molten Salt-Cooled Reactor | Sodium-Cooled Fast Reactor | Very-High Temperature Reactor |
|---|---|---|---|---|---|---|
| Coolant | Water | Helium | Lead/Lead-Bismuth | Fluoride Salts | Sodium | Helium |
| Neutron Spectrum | Thermal/Fast | Fast | Fast | Thermal/Fast | Fast | Thermal |
| Capacity (MWe) | 300-1500 | 1-200 | 20-1000 | 800-700 | 50-1600 | 250-300 |
| Fuel Cycle | Open/Closed | Closed | Closed | Closed | Closed | Open |
| Outlet temperature (°C) | 510-625 | 850 | 480-570 | 700-800 | 500-550 | 900-100 |
| Reference | [43,44] | [44–46] | [44,47] | [44,47] | [44,47] | [48,49] |

**Tab. 1**
The data of six distinct nuclear reactors.

and large reactors [57]. Currently, as small modular reactors (SMRs) are promising technology, this study continues with SMRs in the section 4.

## 3. Generation-IV Nuclear Reactors

Generation IV's six reactor concepts were first proposed by the US DOE and under the Generation IV International Forum (GIF): select nations proposed advancing the development of one or more of GEN IV concepts. Originally, two to three concepts were slated to be (down) selected and constructed for operation by 2030. As part of the Generation IV initiatives, the US proposed interest in the Next Generation Nuclear Plant (NGNP) as a type of VHTR with accompanying interest in a hydrogen production plant (INL) [58] and according to Patterson [46], performed studies of (State of) Hawaii to produce liquid fuel from biomass by hosting a VHTR plant. The use of $CO_2$ gas in the VHTR also peaked interest in supercritical phenomena ($CO_2$, light water) and higher overall plant efficiencies, due to potential downsizing of turbine components and the availability of printed circuit heat exchangers (PCHE). Song et al. reported on testing a PCHE in a supercritical $CO_2$ Brayton cycle in partnership with ANL [59]. Finally, a US Nuclear Energy University Program by Tokuhiro et al. used a high-temperature gas circulator (to simulate a VHTR) and an intelligent control system (applied neural networks) needed to extract energy from approximately 950 °C to 50 °C [60].

When looking at traditional nuclear reactors, it is well known that they are not thermally very efficient due mostly to limitations imposed on moderator temperatures. As a result, over two-thirds of thermal energy produced in conventional nuclear reactors is wasted and lost into the environment. To make nuclear reactors more efficient, the temperature difference (ΔT between highest and lowest Rankine cycle points) must be increased: for example, by increasing coolant temperature. By doing so, thermodynamic efficiency can be increased [61].

As part of Generation-IV nuclear reactors, six different types of nuclear reactors have been developed, including the Gas-Cooled Fast Reactor (GFR), Very-High-Temperature Reactor (VHTR), Lead-Cooled Fast Reactor (LFR), Molten Salt-Cooled Fast Reactor (MSFR), Supercritical-Water-Cooled Reactor (SCWR), and Sodium-Cooled Fast Reactor (SFR). Gen-IV reactors are being developed all around the world aiming for higher cycle efficiency, high temperature steam electrolysis, high temperature thermo-chemical cycling, or hybrid water separation for hydrogen production. The SCWR, for example (Canada's Gen-IV concept) has a higher net thermal efficiency of 45 % [62], and it can be configured to produce hydrogen employing Cu-Cl thermo-chemical cycle. This cycle demands higher temperatures provided by the projected SCWR design. The reason for its higher efficiency is that SCWR can function at temperatures and pressures up to 500 °C and 28 MPa, due to the supercritical thermophysical properties gains. According to Atomic Energy of Canada Limited, the SCWR concept can generate hydrogen via Cu-Cl is shown as the most promising technology based on nuclear systems [63]. In addition to improved efficiency, Generation-IV nuclear reactors have enhanced safety and reliability, sustainability, proliferation resistance, and physical protection [64].

Generation-IV nuclear reactors are important because temperature differences (ΔT) or heat

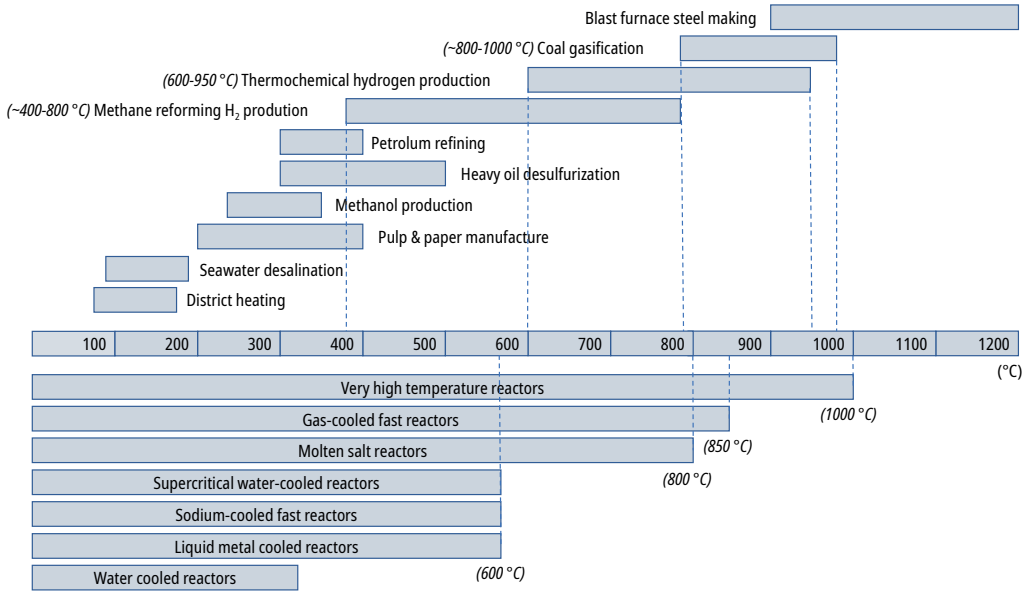


**Fig. 3**
SMRs for non-electric applications. Data taken from [78].

energy at high temperatures play a key role in hydrogen production [61,65]. In terms of temperature difference, concentrated solar power (CSP) technologies can be suggested for usage with Generation-IV nuclear reactors, such as SCWR, to contribute to the hydrogen economy by raising the temperature difference: CSPs in fact can meet the high-temperature requirement as reported in the literature [31,66,67].

## 4. Small Modular Reactors (SMRs)

SMRs are nuclear fission reactors that are a fraction of the size, power and cost of conventional large reactors. They can be built in a factory and transported to a location ready to be installed in prefabricated modules. Modular reactors thus minimize building time on-site, improve containment efficiency, reduce fabrication costs and are considered to be safer than existing conventional designs (PWR, BWR and CANDU) [68–70] . The implementation of completely passive safety elements that can operate without human involvement results in increased safety [71,72]. In comparison to conventional nuclear reactors, SMRs require less personnel [73]. SMRs are being actively designed and proposed for their capacity to overcome most of the financial and safety constraints that prevent large conventional reactors from being built globally on a large scale [74].

According to the International Atomic Energy Agency (IAEA), small reactors are those that produce an equivalent electric power of less than 300 megawatts electric (MWe) [75], while the reactors that are between 300 MWe and 700 MWe are named as “medium modular reactors” [57,76]. SMR designs cover the spectrum of possible reactors from scaled-down plants of previous designs to full Generation-IV innovative designs. Thermal-neutron reactors and fast-neutron reactors, as well as molten salt and gas-cooled reactor concepts, have all been proposed in the last years [77]. When compared to typical large nuclear power plants (NPPs of 1 GWe), Small Modular Reactors (SMRs) have significant and clear advantages. In part to these advantages, sophisticated SMRs can be used for more than just power generation. They can also be used to produce hydrogen, desalinated water, liquid transportation fuels, and some chemicals needed in the petroleum industry as depicted in Fig. 3 (when co-located) [78] .

Small Modular Reactors (SMR) with advanced features are projected to have a simpler design [79], lower cost due to their mass production, and a smaller physical footprint [80,81]. SMRs also have higher levels of safety, security, and resistance to proliferation [80–82]. Modularizing construction technique is not new in the manufacturing industry, and it has been used in the construction of major reactors in the past [83]. However, modularizations provide reduced initial capital investment, scalability, and siting flexibility in regions where traditional big reactors are not feasible nor needed [81]. Since this review focuses on nuclear-renewable hybrid systems to produce hydrogen, in the next section, renewable energy is reviewed.

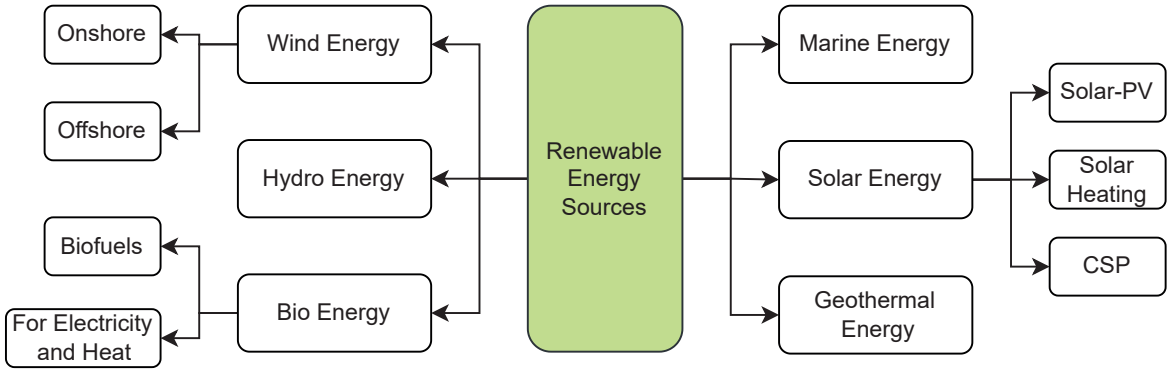


**Fig. 4**
An indication of renewable energy sources.

## 5. Renewable Energy

Traditional energy generation from fossil resources (coal, oil, and natural gas), has been very effective in providing economic development on a global scale and it plays still a key role in satisfying the world's energy needs [7,22]. However, global primary energy consumption is increasing due to increasing population and rising energy demand due to improved living standards [1]. Renewable energy contributes to the majority of the greenhouse gas emissions reductions required between now and with 2050 in mind to keep global average surface temperature rise below two degrees Celsius [7]. Thus, renewable energy sources have begun to gain significance in order to meet the rising energy demand of the world and to reduce carbon dioxide emissions in terms of environmental issues [14]. We can prevent future extreme weather and climate consequences by using renewable energy sources, which reduce greenhouse gas emissions ensuring reliable, timely, and cost-effective energy delivery [84]. Deployment is key.

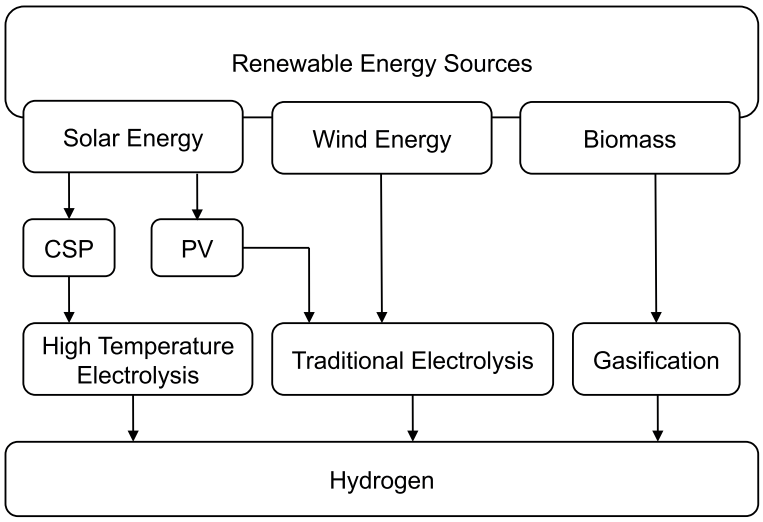


**Fig. 5**
Hydrogen production methods with renewable energy.

Renewable energy is derived from renewable resources that are regenerated naturally on a human timescale, such as carbon-neutral sources as sunshine, wind, rain, tides, waves, and geothermal heat [85]. Despite the fact that the majority of renewable energy sources are sustainable, others, such as biomass are not and are finite (eroding possibly other feedstocks) [6]. Fig. 4 depicts a breakdown of renewable energy sources [86]. Renewable energy sources are transformed into useful energy forms such as electricity, fuels, hydrogen, and heat thanks to renewable energy technology [87].

Finding more dependable, sustainable, and diversified energy sources might be a realistic option for reducing and eliminating greenhouse gas emissions while fulfilling global energy demands. As a consequence, hydrogen has several benefits over other choices and may be utilized to reduce pollution and dependency on imported oil [5,88,89]. Although hydrogen is not a primary energy source, it becomes an attractive energy carrier when separated from other elements utilizing an energy source [20,67,90]. Hydrogen production methods with renewable energy are shown in Fig. 5 [6,22,67]. Hydrogen is a clean energy carrier in fuel cells since it reacts with oxygen without producing $CO_2$ and producing water as the only by-product [90].

Some direct or indirect advantages of hydrogen can be listed as follows [22];

- Help reducing oil imports for an oil-lacking nation.
- Help achieving relative long-term sustainability compared to current energy sources.
- Change the current environment outlook by enabling emission reduction.

### 5.1. Solar Photovoltaic (PV)

The cost of hydrogen generated by solar electrolysis is roughly 25 times greater than fossil fuel alternatives with this technology, which is one of the

highest-cost hydrogen generation methods. The cost of solar PV, on the other hand, is projected to fall even further, as it has already dropped from 25 to 6 times [22,91]. More efforts are then needed in order for this hybrid system to be effectively competitive on the market both for cost and coupling efficiency.

### 5.2. Concentrated Solar Power (CSP)

It is possible to produce hydrogen by using heat energy coming from a concentrated solar power (CSP) plant [66,67]. Mirrors direct sunlight to a receiver in concentrated solar power installations. The thermal energy gathered in the receiver is utilized to power a steam turbine, which then generates electricity [92]. This CSP technology very suitable to assist nuclear power plants ensuring that heat energy at high-temperature is provided directly and without intermediate conversion for the nuclear steam superheating. Three kinds of CSP technologies meeting the high-temperature requirements, are commonly reported in the literature. These technologies are categorized according to the mirrors devices used in CSP. These are the Parabolic Trough (PT), Fresnel Reflectors (FR), Dish Receiver (DR) [31, 93]. PT technology made over 90 % in operation in 2013 [94], and recently more than 60 % of CSP systems [95]. The FR system is similar to PT collector technology, but it employs a number of ground-based, flat or slightly curved mirrors positioned at various angles to focus sunlight onto a stationary receiver several meters above the mirror region [96]. Solar power towers, also known as "central tower" power plants, "heliostat" power plants, or "power towers," are a form of solar furnace that receives concentrated sunlight through a tower. It focuses the sun's beams onto a collection tower using a system of flat, moveable mirrors known as heliostats. One possible alternative for sustainable, pollution-free energy is concentrated solar thermal power [31].

### 5.3. Wind Energy

This approach, which uses energy generated by wind turbines for electrolysis, has one of the most potential among renewable sources for producing pollution-free hydrogen, especially for dispersed systems [97]. The drawbacks of using wind energy to create hydrogen include not only the expensive cost of wind turbines and electrolyzers, but also the optimization of the turbine electrolyser-storage system. The cost of generating hydrogen with wind turbines is about 6-10 times as much to produce hydrogen as fossil fuel alternatives and so not yet competitive. In the future, this rate is projected to be reduced by half [22,91].

## 6. Hydrogen

Hydrogen is a chemical element having a H symbol and its atom number is “1”. Hydrogen ($H_2$) is one of the most prevalent elements in the universe, and it is found mostly in water and organic compounds on our planet [7]. It's a combustible gas that's colorless and odorless [98]. Because hydrogen's atomic weight number is 1.008 amu, it was decided that October 8th (10/08) should be designated as National Hydrogen and Fuel Cell Day in the United States [99].

Hydrogen is extensively employed in industrial areas such as petrochemicals, agriculture (such as ammonia for fertilizers), food processing, plastics, manufacturing, and, increasingly, transportation [100].

One of the most important components in the petroleum and petrochemical sectors is hydrogen. Because of novel fuel cell applications, hydrogen has recently become more important [35,101]. Hydrogen can be produced utilizing a variety of methods, including various feedstocks, routes, and technologies, as well as various energy sources such as fossil fuels and renewable energy sources [31,35,102–104].

Steam reforming of natural gas (methane) has become the most cost-effective and widely used process for hydrogen production, accounting for around half of all hydrogen produced worldwide [6,105,106]. According to [100], currently, over 97 % of the world's hydrogen is produced by steam-methane reforming of fossil fuels like coal or methane (SMR), which emits significant amounts of $CO_2$ into the atmosphere [107]. The global warming potential of hydrogen generation via the steam methane reforming method has been estimated to be 13.7 kg $CO_2$ per kilogram of net hydrogen generated ($CO_2$ consists of 77.6 % of the system's global warming potential) [107,108]. A typical steam methane reforming hydrogen plant that produces one million cubic meters of hydrogen per day emits 0.3-0.4 million standard cubic meters of $CO_2$, which is generally dumped into the atmosphere [107]. In the next section, potential nuclear based hydrogen generation methods are explained.

Hydrogen can be part of an integrated system that offers dispersed renewable energy while also being connected to a base-loaded nuclear power grid, where it can be stored and utilized to create electricity for a facility or in mobility applications [109].

### 6.1. Prediction of Hydrogen's Future against Gasoline

Efficiency can be substantially reduced to an economics issue to be handled at the entire value chain level provided that $CO_2$ emissions are taken into account. This is significant because hydrogen can be used far more efficiently in some applications and can be produced without emitting almost no greenhouse gases. A hydrogen fuel cell in a vehicle, for instance, has about 60 % efficiency, while an internal combustion gasoline engine has approximately 20 % efficiency [19]. In terms of energy per unit of mass, hydrogen has three times higher energy (120.1 MJ/kg) than gasoline and contains more energy than natural gas as well. Thus, hydrogen is seen as a very promising fuel for transportation.

After taking into account the efficiency of converting hydrogen into power, the price of gasoline paid by automobile owners is roughly 10 USD/kg$H_2$ for hydrogen provided in most regions by 2030. It means that the hydrogen costs delivered by 2030 will be affordable when compared to expected hydrogen price (USD 7.5-9.0 per kg-hydrogen) in 2030 [19]. For these reasons, it is possible that hydrogen will be replaced by gasoline in the future years.

## 7. Nuclear Hydrogen Production

Nuclear Power Plants have a significant role in meeting the increasing energy demand of the world [110]. In terms of clean hydrogen generation, renewable and nuclear energy are the only carbon-free (or low-carbon) options [111]. Electrolysis utilizing electricity from intermittent renewable or dependable nuclear sources and direct utilization of heat from nuclear energy, may enable thermochemical process using high-temperature reactors, and can increase hydrogen production plans [45].

Green hydrogen is an expensive strategy compared to fossil-based hydrogen production [112]. Green hydrogen produced from renewable energy costs between US$2.56-7.39/kg-$H_2$, which is more expensive than black, blue, and grey hydrogen, as indicated in Table 2. As an example, calculation of green hydrogen cost employing traditional electrolysis (alkaline) is pointed in Table 3 [2]. To obtain 1 kg of hydrogen, 180 MJ electricity, 26.2 MJ heat energy and 11.5 kg of water are used via low-temperature electrolysis at 60 °C and 0.1 MPa. According to the prices of heat and electrical energies per unit, the product cost of 1 kg-hydrogen is equal to $US 5.92 [2] .The cost of aqua hydrogen that does not emit $CO_2$ is US$ 0.23 per kg-hydrogen as reported in [112]. In Table 2, the information of the costs of producing hydrogen using various technologies is given.

Moreover, using renewable energy sources is an excellent choice for clean hydrogen production, since the cost of producing hydrogen via traditional electrolysis (low temperature electrolysis) plays such a significant role in the clean hydrogen economy. For this reason, to calculate electrolytic hydrogen cost, photovoltaic (PV) panels as a clean energy source were used in a study including all major techno-economic parameters [113];

- Electricity consumption: 57.85 kWh/kg-$H_2$
- Investment cost: 368 $/kWe
- Operation life of the electrolyzer: 7 years
- Project lifetime: 30 years
- Discount rate: 6 %
- Hydrogen capacity production: 250 t/year

According to the study, the cost of green hydrogen produced through electrolysis is around $7/kg-$H_2$, which is more than the cost of other types of hydrogen such as black, blue, and grey hydrogen. It is also demonstrated that electricity expenses account for more than 70 % of the cost of production hydrogen using a PV energy source.

| | Methods | | | | | | | | |
|---|---|---|---|---|---|---|---|---|---|
| | Black Hydrogen without CCUS | Grey Hydrogen without CCUS | | Blue Hydrogen with CCUS | | Green Hydrogen | | | |
| Energy Source | Coal | Natural Gas | | Coal | Natural Gas | Renewable Electricity | | | |
| Location | Canada | Canada | | Canada | | Canada | | | Europe |
| Hydrogen Cost (US$/kgH₂) | 1.35 | 1.31 | 0.67-1.05 | 1.60-2.05 | 1.61-1.83 | 7.39 | 2.56-6.84 | 2.28-3.69 | 2.36-8.26 |
| Reference | [112,115] | [112,115] | [112,116] | [112,115] | | [112,117] | [112,118] | [112,116] | [112,119] |
| Note: Hydrogen prices in €/kg are converted into US$/kgH₂. | | | | | | | | | |

**Tab. 2**
A summary of the costs reported in the literature for producing hydrogen using various technologies. (CCUS: carbon capture use and storage)

According to another study done [114], the cost of production hydrogen employing low temperature electrolysis, which has parameters of production capacity 1500 kg/day, capital cost $0.96, feedstock $5.06, operation and maintenance cost (O&M) $0.73, is shown as $6.75 per kg-$H_2$.

Hydrogen derived from fossil fuels produces a considerable quantity of emissions, which is not good for the environment and the issue of climate change [84]. On the other hand, hydrogen can be obtained by using energy coming from nuclear power plants almost without any carbon emission. Nuclear as clean energy source can be used to separate hydrogen from the ocean water [16]. When looked from this perspective, nuclear power plants will be critical in producing hydrogen on a large scale in the future [61]. Hydrogen generation with nuclear energy is shown in Fig. 6. In this model, heat and electrical energy are transferred from nuclear power plant to hydrogen generation plant to obtain hydrogen by separating water [120].

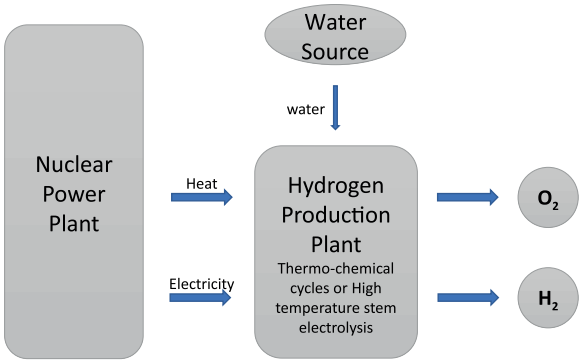


**Fig. 6**
A schematic of nuclear hydrogen production.

reported for generating hydrogen in such way [124]. In terms of some criteria, such as efficiency, cost analysis, complexity, industry adaptability, two thermochemical cycles have an important role in producing hydrogen: copper-chlorine and sulfur-iodine indicated as very promising in [130]. Both of them have different requirements and also different efficiency. Heat, rather than electricity, is the primary source of energy for splitting water to generate hydrogen by using sulfur-iodine (S-I) or copper-chlorine (Cu-Cl) thermo-chemical cycles [17]. In these cycles, chemicals are recovered and reused [17,124]. Sulfur-iodine thermochemical cycle requires about 850 °C which is higher than copper-chlorine's temperature requirements (around 530 °C): therefore, it can be used coupled with a Very High Temperature Nuclear Reactor (VHTR) - gas cooled [16,43,131]. Cu-Cl thermochemical cycle, on the other hand, can be preferred with other available energy sources because it requires a lower temperature than S-I [17].

| Parameters | | Inputs (kg $H_2$) | | Outputs (kg $H_2$) | |
|---|---|---|---|---|---|
| $T_{max}$ (°C) | 60 | Electricity (MJ) | 180 | $H_2$ | 1 |
| Pressure (MPa) | 0.1 | Heat (MJ) | 26.2 | $O_2$ | 8 |
| TRL | 9 | Water (kg) | 11.5 | $CO_2$ | 0 |
| $H_2$ Yield eff. (HHV)** | 29.8 | | | Production cost* | $US 5.92 |

*Production cost (est. $US 2019).
**Assuming a power cycle conversion efficiency of 40%. (HHV: Higher heating value)

**Tab. 3**
Calculation of per kg of hydrogen employing alkaline electrolysis [2].

Hydrogen may be produced in a variety of ways, including steam reforming, steam reforming at high temperatures, coal gasification, conventional water electrolysis, thermo-chemical cycles, hybrid, and high temperature electrolysis, according to the literature [22,29,56,67,89,90, and 121–128].

Nuclear power plants are more effective in terms of heat generation than that of electricity. In addition to this, since thermo-chemical cycles and high temperature electrolysis require electricity and especially high temperatures which are 500-830 °C, which means requiring more heat energy than electrical energy, nuclear energy can be used to generate hydrogen [17,56,103,129].

### 7.1. Thermochemical Hydrogen Production Cycles

Many thermochemical hydrogen generation cycles operate on the idea of thermally separating water into oxygen and hydrogen using clean energy sources that do not emit greenhouse gases, owing to chemical compounds and reactions. In the literature, there are about 200 thermochemical cycles

#### 7.1.1. Copper-Chlorine (Cu-Cl) Cycle

Cu-Cl cycles come in seven different varieties [44]. The four-step Cu-Cl cycle having about 43 % net efficiency [100] offers the highest energetic and exergetic efficiency, according to the researchers [132]. The heat requirements at about 530 °C for

Cu-Cl [123,133] can be met with new generation nuclear reactors or concentrated solar power (CSP) systems [134,135]. Because solar and nuclear energy are both clean sources of energy, using the Cu-CI thermochemical cycle to produce hydrogen may be preferable [133].
The four-step Cu-Cl cycle involves hydrolysis, thermolysis, electrolysis, and drying steps [122,124,136].

The first step which is hydrolysis:
$2CuCl_2(s) + H_2O(g) \rightarrow Cu_2OCl_2(s) + 2HCl(g)$
(at 375-400 °C [136]) *(1)*

The second step which is thermolysis consists in the decomposition of copper oxychloride taking place at high temperatures of about 500-530 °C;
$Cu_2OCl_2(s) \rightarrow ½\ O_2(g) + 2CuCl(l)$ *(2)*

The third step which is electrolysis;
$2CuCl(aq) + 2HCl(aq) \rightarrow H_2(g) + 2CuCl_2(aq)$
(at 25 °C) *(3)*

The fourth step (drying of aqueous cupric chloride) happens at temperature between 30 to 80 °C;
$CuCl_2(aq) \rightarrow CuCl_2(s)$ *(4)*

As the heat requirement is at a temperature below 550 °C, Super-critical water reactor (SCWR) can be used to meet the heat requirements for Cu-Cl cycle [63,89]. The Generation IV reactor (SCWR) generates electricity at a 42 percent efficiency, which translates to a net efficiency of roughly 30 percent for hydrogen production via electrolysis [100].

### 7.1.2. Sulfur-Iodine (S-I) Cycle

In the literature, even though there are various types of S-I cycles, the most prevalent is the three-step S-I cycle [131,137]. S-I cycle has a similar efficiency with Cu-CI [17].

The first step (exothermic) is hydrolysis:
$I_2\ (l+g) + SO_2(g) + H_2O(g) \rightarrow 2HI(g) + H_2SO_4(l)$
at 120 °C *(5)*

The second step (endothermic) is oxygen generation:
$H_2SO_4(g) \rightarrow SO_2(g) + H_2O(g) + ½O^2(g)$,
endothermic at 850 °C *(6)*

In the third step (endothermic) hydrogen production if finally obtained;
$2HI(g) \rightarrow I2(g) + H2(g)$ at 450 °C. *(7)*
This procedure needs the use of water and heat, as well as three chemical interactions. The water in this cycle is split into oxygen and hydrogen, and the other materials are recycled to be used again. Heat of at least 850 °C is necessary in the first process, known as "catalytic decomposition of sulfuric acid" [17,137]. Low pressure also contributes to safety by minimizing the risks of pressurization in chemical plants and reducing high temperature stresses. A lot of work has gone into matching this cycle to high-temperature nuclear reactors, as well as estimating total process efficiency and hydrogen cost. Early estimates suggested that the S-I processes might create hydrogen at 45 to 55 percent efficiency and co-produce hydrogen and power at a rate of above 60 percent [89].

### 7.2. High Temperature Electrolysis (HTE)

Electrolysis may also be used to produce hydrogen from water [20,67,100,102,103]. There are two types of electrolysis described in the literature: conventional and high temperature electrolysis [67,90]. Temperature differences are the cause of the discrepancies [90]. While typicaly electrolysis is carried out at temperatures below 100 °C [138], high temperature electrolysis needs heat at temperatures above 100 °C [56]. Due to the fact that water is in the form of steam at working temperature, high temperature electrolysis is also known as "high temperature steam electrolysis". In this section, "high temperature" refers to above 600 degrees Celsius [56].
The technique of conventional electrolysis is well-established: hydrogen is generated on the cathode by transferring energy via electrochemical cells inside the water electrolysis unit while pure oxygen is obtained on the anode [56,139]. Conventional electrolysis contributes to the production of 4 % of the world's hydrogen [140]. It means that traditional electrolysis does not meet the world's demand for hydrogen. Thus, high temperature electrolysis (HTE) is necessary for large scale hydrogen production.
High temperature electrolysis differs from regular electrolysis in that the majority of the energy required for HTE comes from heat rather than electricity. Water is decomposed into hydrogen and oxygen via thermolysis at 2500 °C; electricity then is not required [141]. Therefore, it is more efficient than traditional electrolysis because it eliminates the somewhat wasteful process of converting heat to electricity, but it requires a much higher temperature source. The HTE can use energy coming from nuclear reactors generating electricity and heat which is necessary for steam needed for electrolysis [103]. The HTE is powered by nuclear reactors, which provide electricity and heat, both of which are required to produce steam for electrolysis [89,103]. Such HTE plants might play a significant

role in grid balancing by delivering extra energy to the grid when demand is high and taking electricity from the grid when demand is low to generate hydrogen. The energy input is a mix of electricity and heat over the whole temperature range of 0 °C to 2500°C [56]. At a temperature of 850°C (a common temperature), the high temperature steam electrolysis (HTSE) requires 2.5 [$kWh_e/Nm^3$] and 0.92 [$kWh_t/Nm^3$] of electrical and thermal energy, respectively [47,56]. Because high-temperature electrolysis needs a high-temperature environment, typically more than 600 °C, nuclear reactors with Generation-IV Small Modular Reactors are ideal to ensure the heat energy needed [16,103].

An electrolysis cell in the HTE mechanism consists of a cathode (hydrogen electrode), anode (oxygen electrode) and an electrolyte. One side of the electrolyte is connected to the cathode, while the other is connected to the anode. Water is heated by external heat before entering the electrolysis cell as steam in the HTE process. As can be seen in equation (8) applying steam to the cathode of an electrolysis cell decomposes steam into hydrogen and oxygen ions. The hydrogen is then extracted as a hydrogen product, and the oxygen ion is delivered to the anode through the oxygen ion conductivity of the electrolyte. As can be observed in equation (9),

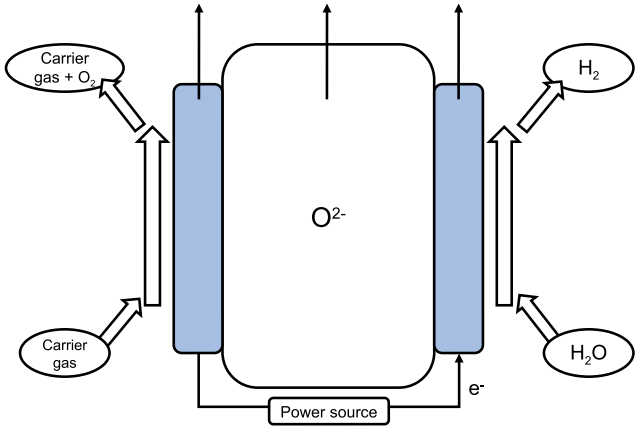


**Fig. 7**
A schematic of HTE mechanism.

the oxygen ion is obtained as the oxygen product at the anode. Eq. (8) and eq. (9) describe the high-temperature electrolysis processes, and eq. (10) is the sum of eq. (8) and eq. (9). Equation (10) depicts the process that splits water into hydrogen and oxygen. The HTE working mechanism is shown in Fig. 7.

$$H_2O + 2e^- \rightarrow H_2 + O^-_2 \quad (8)$$

$$O^-_2 \rightarrow ½\, O_2 + 2e^- \quad (9)$$

$$H_2O \rightarrow H_2 + ½\, O_2 \quad (10)$$

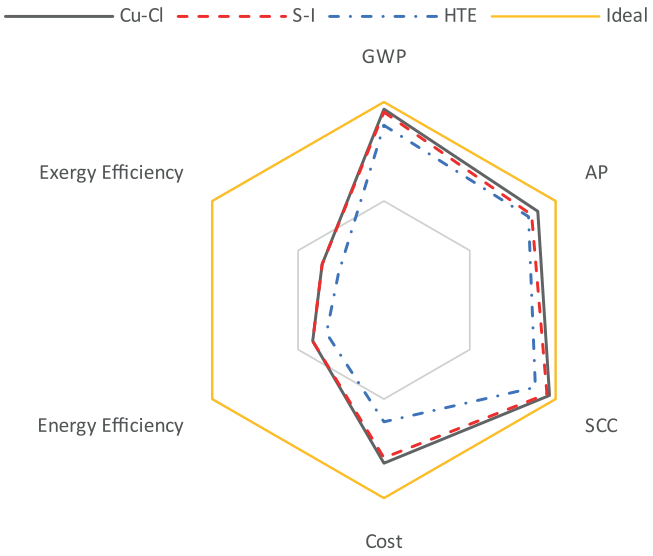


**Fig. 8**
Comparison of nuclear methods, namely, Cu-Cl and S-I cycles, HTE.

Despite the fact that the HTE efficiency of conversion from electricity to hydrogen may reach up to 80 %, the overall efficiency of the hybrid system (nuclear and HTE) is significantly lower due to nuclear power plant efficiencies of approximately 33 % [91].

### 7.3. Comparison of The Potential Methods

The performance comparison of global warming potential (GWP), acidification potential (AP), social cost of carbon (SCC), hydrogen production cost, energy and exergy efficiencies of the HTE, Cu-Cl, and S-I cycles to produce hydrogen (most common cycles used to produce hydrogen and explained in the following paragraph) using nuclear energy is shown in Fig. 8 [14,22].

### 7.4. Technology Readiness Level

The level of vulnerabilities for each of the proposed technologies that must be reviewed before to deployment, and this is referred to as "development risk". The technology development strategy should specify a technology development and demonstration program allowing NHES to be distributed in time. As a result, development risk has been transformed into a qualitative composite score based sub-systems readiness. The focus is on generic technology-specific components instead of industry-standard procedures like water treatment or waste management [142].

For the main components of the Nuclear-Renewable Hybrid Energy System (N-R HES) Technology Development Program Plan, each technology has defined its current Technology Readiness Level (TRL) [2,143]. In Fig. 10, the TRLs of the potential hydrogen production methods with its costs and maximum temperature requirements are depicted.

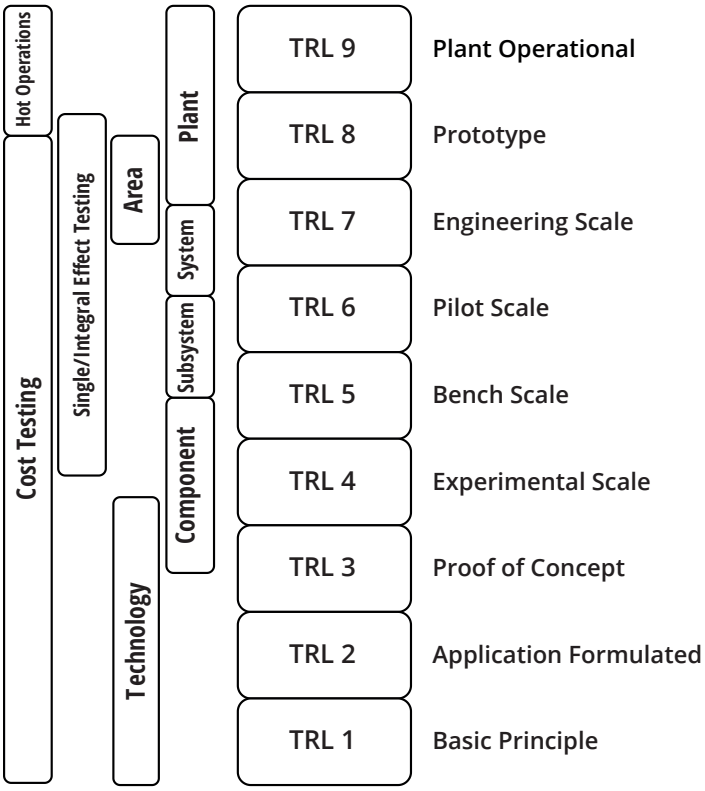


**Fig. 9**
An indication of TRLs [142].

When a hybrid system is evaluated in terms of TRL, the lowest component TRL score defines the system TRL score. Fig. 9 indicates a simplified overview of TRLs for N-R HES.

Three commercial electric utilities and Idaho National Laboratory have been selected to modify facilities to produce carbon-free hydrogen via electrolysis. Hydrogen will be utilized as a main energy source, as well as for transportation and storage. In the project, light water nuclear reactors are to produce 100 % carbon free hydrogen via alkaline electrolysis (low temperature electrolysis) which a TRL rating of nine. The ultimate goal of this research project is to improve the long-term economic competitiveness [144] showing the competitiveness offered by nuclear power when compared with renewable energy.

To achieve the highest efficiency outputs from the primary energy sources mentioned and the hydrogen production method compared previously, it is sensible to look at the most compatible subsystems when optimized. As a result, optimization is discussed in the following section.

## 8. Optimization

The term "optimization" refers to the process of obtaining the best results (outputs) possible in a particular situation [8,32,36,37,145]. An optimization problem, in its most basic form, involves selecting input values from a set of acceptable options and computing the value of a real function to maximize or minimize it. The generalization of optimization theory and techniques to new formulations is an important field of practical mathematics. Optimization, in general, entails determining the "best available" values of some objective function given a certain input, and it can apply to a wide range of objective functions and domains [145].

### 8.1. Complexity and Multi-objective Optimization

Engineering systems including design and analysis can have complexity, meaning multi-tasks with multiple parameters. In simple terms, complexity can be characterized by the number of variables, parameters, and multiple objectives in dynamic system behavior. For instance, while it is desirable to decrease cost, the amount of yield (hydrogen) depending on more than one parameter, is expected to increase. This exemplifies the difference between single and multiple objective optimizations.

In the literature, it can be seen that different optimization methods are applied for various areas [104,110,119,125,146–148]. One of them is Pareto Optimality (Pareto Efficiency) describing a scenario in which no choice criterion may be better off without causing at least one other preference criterion to be worse off or lose its optimal ”value” [149,150]. Pareto optimality that can be applied from economy to nuclear systems plays a role in multi-objective optimization problems having complexity [134] where trade-off choices become critical in teaching the “most suitable” system for the underlying conditions and not necessarily the “best” in mathematical terms. Thanks to flexibility of the complexity, objective functions can be redefined according to the output needed at the moment. To give a clear example, in a hybrid nuclear-renewable hydrogen production plants, when the price or demand of electricity decreases, more hydrogen can be produced instead of generating electricity. By doing so, more efficiency can be obtained.

In the nuclear technology industry, data-driven approaches have been used to improve the outputs [34]. There are a number of processes that can be optimized in complex systems by using artificial intelligence with algorithms [32,110,125,151]. The Lindo® What’s Best tool can be used for example linear, integer and nonlinear optimization [38,39]. Firstly, it was initially published for Lotus thereafter then for Microsoft Excel [152–154]. The tool gives the optimal solution with defined configurations and parameters [37].

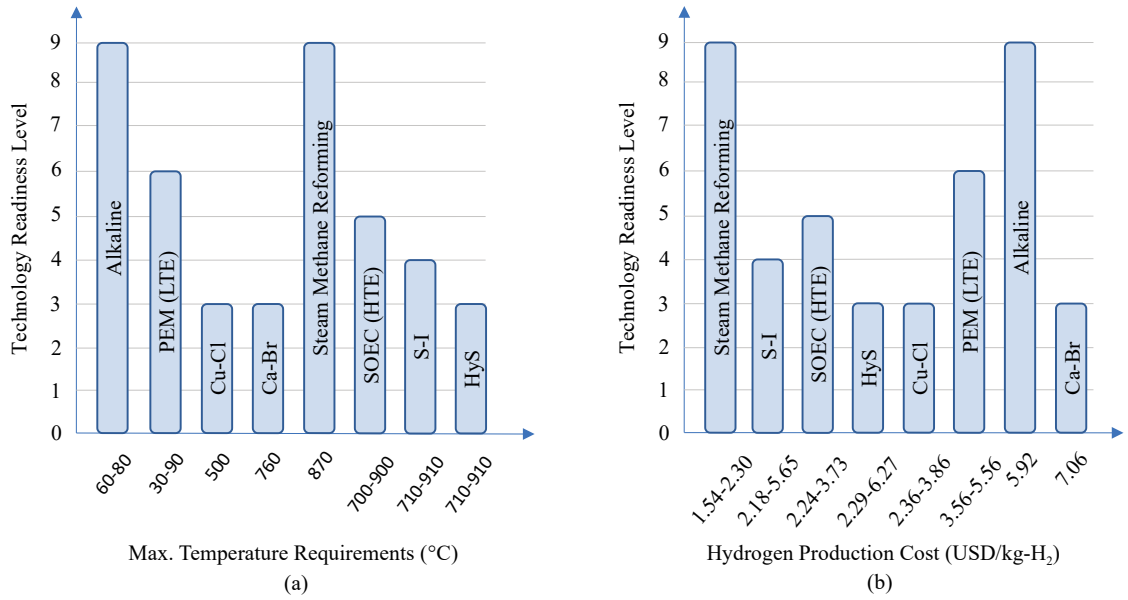


**Fig. 10**
TRL of different NHES hydrogen production technologies according to maximum temperature requirements (a) and hydrogen production cost (b) [2].

## 9. Conclusion

Hydrogen has now been widely used in a variety of industries, including fertilizer production and oil refineries. In the near future, this is likely to develop significantly to serve new sectors and larger markets in energy storage, particularly transportation, and power generation. Clean hydrogen generation via a number of thermochemical cycles and high-temperature electrolysis techniques has been shown to have a promising future. When comparing water-based hydrogen generation technologies, it is clear that HTE is not cost competitive with Cu-Cl and S-I thermochemical cycles in terms of hydrogen cost, as HTE's electricity need reduces HTE's benefits. Even though the maximum temperature requirements of the S-I cycle are higher than those of the Cu-Cl cycle, their overall efficiency and cost are remarkably similar. As a result, the Cu-Cl cycle has an advantage in terms of temperature needs. The readiness level of the S-I cycle (TRL-4), on the other hand, is higher than that of the Cu-Cl cycle (TRL-3). Furthermore, provided that Cu-Cl or S-I cycles are used to produce hydrogen with a nuclear reactor, there may be a waste of heat energy. In Fig. 3, it is seen that the waste of heat energy can be used in some industries, such as petroleum refining, heavy oil desulfurization or seawater desalination, or even data storage.

Hydrogen is a developing energy carrier that can help to significantly decarbonize the global energy and industrial sectors. As a result, creating hydrogen from renewable energy sources, as well as nuclear energy, is one of today's most important engineering challenges. In the long-term one of the key issues for reducing greenhouse gas emissions and transitioning to a low-carbon future will be represented by the innovation in the hybridization of nuclear and renewable industries as they play a crucial role for thermal and electrical energy demand. Nuclear and renewable technologies will be critical for the production of clean energy needed for complete electrification in a variety of areas, including automobiles, public transportation, construction-related vehicles, home heating, and various thermal processes in the fight against climate change. As a result, nuclear and renewable energy as primary energy sources for large-scale hydrogen generation are required to accomplish a full sustainable energy future.

In the case of nuclear energy, commercial SMR technologies, which offer compact designs, better safety, increased reliability, and lower capital investment, are advantageous and appealing for a variety of industry sectors. In comparison to traditional design, SMRs offer technological advantages ranging from safer and passively actioned system design to more robust capabilities with respect to design basis accidents, ultimately resulting in lower core damage frequency. Because each of the energy sources (renewable and nuclear) has advantages and disadvantages, hybrid energy systems are considered more successful. Because NHES are multi-objective and complex systems, improving them to create power and hydrogen can provide better outcomes. More comprehensive optimizations need to be carried out in the future, as well as the development of generic optimization methods specifically designed for the NHES. Particularly important is the implementation of specific

optimization algorithms for predicting accurately prices for hydrogen generation.

## References


[1] United Nations, Department of Economic and Social Affairs, Population Division, "World Population Prospects: The 2017 Revision, Key Findings and Advance Tables," 2017. Working Paper No. ESA/P/WP/248

[2] R. Pinsky, P. Sabharwall, J. Hartvigsen, and J. O'Brien, "Comparative review of hydrogen production technologies for nuclear hybrid energy systems," Prog. Nucl. Energy, vol. 123, p. 103317, 2020, doi: 10.1016/j.pnucene.2020.103317.

[3] P. Moriarty and D. Honnery, "Hydrogen's role in an uncertain energy future," Int. J. Hydrog. Energy, vol. 34, no. 1, pp. 31–39, 2009, doi: 10.1016/j.ijhydene.2008.10.060.

[4] V. T. Le, E.-N. Dragoi, F. Almomani, and Y. Vasseghian, "Artificial Neural Networks for Predicting Hydrogen Production in Catalytic Dry Reforming: A Systematic Review," Energies, vol. 14, no. 10, p. 2894, 2021, doi: 10.3390/en14102894.

[5] I. Dincer, "Green methods for hydrogen production," Int. J. Hydrog. Energy, vol. 37, no. 2, pp. 1954–1971, 2012, doi: 10.1016/j.ijhydene.2011.03.173.

[6] A. Miltner, W. Wukovits, T. Pröll, and A. Friedl, "Renewable hydrogen production: a technical evaluation based on process simulation," J. Clean. Prod., vol. 18, pp. S51–S62, 2010, doi: 10.1016/j.jclepro.2010.05.024.

[7] D. Gielen, F. Boshell, D. Saygin, M. D. Bazilian, N. Wagner, and R. Gorini, "The role of renewable energy in the global energy transformation," Energy Strategy Rev., vol. 24, pp. 38–50, 2019, doi: 10.1016/j.esr.2019.01.006.

[8] S. Toghyani, E. Baniasadi, and E. Afshari, "Thermodynamic analysis and optimization of an integrated Rankine power cycle and nano-fluid based parabolic trough solar collector," Energy Convers. Manag., vol. 121, pp. 93–104, 2016, doi: 10.1016/j.enconman.2016.05.029.

[9] F. Zhang, P. Zhao, M. Niu, and J. Maddy, "The survey of key technologies in hydrogen energy storage," Int. J. Hydrog. Energy, vol. 41, no. 33, pp. 14535–14552, 2016, doi: 10.1016/j.ijhydene.2016.05.293.

[10] P. Denholm, J. C. King, C. F. Kutcher, and P. P. H. Wilson, "Decarbonizing the electric sector: Combining renewable and nuclear energy using thermal storage," Energy Policy, vol. 44, pp. 301–311, 2012, doi: 10.1016/j.enpol.2012.01.055.

[11] Y. Tian, "GRID-CONNECTED ENERGY STORAGE SYSTEMS — BENEFITS, PLANNING AND OPERATION," Michigan State University, 2018. doi: 10.25335/M5SQ8QN4M.

[12] H. Blanco and A. Faaij, "A review at the role of storage in energy systems with a focus on Power to Gas and long-term storage," Renew. Sustain. Energy Rev., vol. 81, pp. 1049–1086, 2018, doi: 10.1016/j.rser.2017.07.062.

[13] M. Noussan, P. P. Raimondi, R. Scita, and M. Hafner, "The Role of Green and Blue Hydrogen in the Energy Transition—A Technological and Geopolitical Perspective," Sustainability, vol. 13, no. 1, p. 298, 2020, doi: 10.3390/su13010298.

[14] I. Dincer and C. Zamfirescu, "Sustainable hydrogen production options and the role of IAHE," Int. J. Hydrog. Energy, vol. 37, no. 21, pp. 16266–16286, 2012, doi: 10.1016/j.ijhydene.2012.02.133.

[15] A. Ajanovic and R. Haas, "Economic prospects and policy framework for hydrogen as fuel in the transport sector," Energy Policy, vol. 123, pp. 280–288, 2018, doi: 10.1016/j.enpol.2018.08.063.

[16] R. Sadhankar, "New Reactor Concepts Deployment Challenges and Opportunities," in Encyclopedia of Nuclear Energy, E. Greenspan, Ed. Oxford: Elsevier, 2021, pp. 864–876. doi: 10.1016/B978-0-12-819725-7.00003-9.

[17] Z. L. Wang, G. F. Naterer, K. S. Gabriel, R. Gravelsins, and V. N. Daggupati, "Comparison of sulfur–iodine and copper–chlorine thermochemical hydrogen production cycles," Int. J. Hydrog. Energy, vol. 35, no. 10, pp. 4820–4830, 2010, doi: 10.1016/j.ijhydene.2009.09.006.

[18] N. V. Gnanapragasam, B. V. Reddy, and M. A. Rosen, "Hydrogen production from coal gasification for effective downstream $CO_2$ capture," Int. J. Hydrog. Energy, vol. 35, no. 10, pp. 4933–4943, 2010, doi: 10.1016/j.ijhydene.2009.07.114.

[19] IEA, "The Future of Hydrogen," 2019. Accessed: Nov. 21, 2021. [Online]. Available: https://www.iea.org/reports/the-future-of-hydrogen

[20] R. Boudries, "Hydrogen as a fuel in the transport sector in Algeria," Int. J. Hydrog. Energy, vol. 39, no. 27, pp. 15215–15223, 2014, doi: 10.1016/j.ijhydene.2014.06.014.

[21] M. Eypasch et al., "Model-based techno-economic evaluation of an electricity storage system based on Liquid Organic Hydrogen Carriers," Appl. Energy, vol. 185, pp. 320–330, 2017, doi: 10.1016/j.apenergy.2016.10.068.

[22] C. Acar and I. Dincer, "Comparative assessment of hydrogen production methods from renewable and non-renewable sources," Int. J. Hydrog. Energy, vol. 39, no. 1, pp. 1–12, 2014, doi: 10.1016/j.ijhydene.2013.10.060.

[23] A. Ozbilen, M. Aydin, I. Dincer, and M. A. Rosen, "Life cycle assessment of nuclear-based hydrogen production via a copper–chlorine cycle: A neural network approach," Int. J. Hydrog. Energy, vol. 38, no. 15, pp. 6314–6322, 2013, doi: 10.1016/j.ijhydene.2013.03.071.

[24] T. A. H. Ratlamwala and I. Dincer, "Performance assessment of solar-based integrated Cu–Cl systems for hydrogen production," Sol. Energy, vol. 95, pp. 345–356, 2013, doi: 10.1016/j.solener.2013.06.018.

[25] G. Locatelli, A. Fiordaliso, S. Boarin, and M. E. Ricotti, "Cogeneration: An option to facilitate load following in Small Modular Reactors," Prog. Nucl. Energy, vol. 97, pp. 153–161, 2017, doi: 10.1016/j.pnucene.2016.12.012.

[26] M. Balat, "Potential importance of hydrogen as a future solution to environmental and transportation problems," Int. J. Hydrog. Energy, vol. 33, no. 15, pp. 4013–4029, 2008, doi: 10.1016/j.ijhydene.2008.05.047.

[27] C. E. Finke, H. F. Leandri, E. T. Karumb, D. Zheng, M. R. Hoffmann, and N. A. Fromer, "Economically advantageous pathways for reducing greenhouse gas emissions from industrial hydrogen under common, current economic conditions," Energy Environ. Sci., vol. 14, no. 3, pp. 1517–1529, 2021, doi: 10.1039/D0EE03768K.

[28] M. Al-Zareer, I. Dincer, and M. A. Rosen, "Development and assessment of a novel integrated nuclear plant for electricity and hydrogen production," Energy Convers. Manag., vol. 134, pp. 221–234, 2017, doi: 10.1016/j.enconman.2016.12.004.

[29] S. S. Seyitoglu, I. Dincer, and A. Kilicarslan, "Energy and exergy analyses of hydrogen production by coal gasification," Int. J. Hydrog. Energy, vol. 42, no. 4, pp. 2592–2600, 2017, doi: 10.1016/j.ijhydene.2016.08.228.

[30] M. Newborough and G. Cooley, "Developments in the global hydrogen market: The spectrum of hydrogen colours," Fuel Cells Bull., vol. 2020, no. 11, pp. 16–22, 2020, doi: 10.1016/S1464-2859(20)30546-0.

[31] D. Popov and A. Borissova, "Innovative configuration of a hybrid nuclear-parabolic trough solar power plant," Int. J. Sustain. Energy, vol. 37, no. 7, pp. 616–639, 2018, doi: 10.1080/14786451.2017.1333509.

[32] J. Chen, H. E. Garcia, J. S. Kim, and S. M. Bragg-Sitton, "Operations Optimization of Nuclear Hybrid Energy Systems," Nucl. Technol., vol. 195, no. 2, pp. 143–156, 2016, doi: 10.13182/NT15-130.

[33] D. Wijayasekara, M. Manic, P. Sabharwall, and V. Utgikar, "Optimal artificial neural network architecture selection for performance prediction of compact heat exchanger with the EBaLM-OTR technique," Nucl. Eng. Des., vol. 241, no. 7, pp. 2549–2557, 2011, doi: 10.1016/j.nucengdes.2011.04.045.

[34] M. Gomez-Fernandez, K. Higley, A. Tokuhiro, K. Welter, W.-K. Wong, and H. Yang, "Status of research and development of learning-based approaches in nuclear science and engineering: A review," Nucl. Eng. Des., vol. 359, p. 110479, 2020, doi: 10.1016/j.nucengdes.2019.110479.

[35] A. Zamaniyan, F. Joda, A. Behroozsarand, and H. Ebrahimi, "Application of artificial neural networks (ANN) for modeling of industrial hydrogen plant," Int. J. Hydrog. Energy, vol. 38, no. 15, pp. 6289–6297, 2013, doi: 10.1016/j.ijhydene.2013.02.136.

[36] C. P. Elia, Z. Yang, L. Anders, L. Hailong, and Y. Jinyue, "An Open-source Platform for Simulation and Optimization of Clean Energy Technologies," Energy Procedia, vol. 105, pp. 946–952, 2017, doi: 10.1016/j.egypro.2017.03.423.

[37] M. R. Quitoras, P. E. Campana, and C. Crawford, "Exploring electricity generation alternatives for Canadian Arctic communities using a multi-objective genetic algorithm approach," Energy Convers. Manag., vol. 210, p. 112471, 2020, doi: 10.1016/j.enconman.2020.112471.

[38] V. F. Navarro Torres, J. Ayres, P. L. A. Carmo, and C. G. L. Silveira, "Haul Productivity Optimization: An Assessment of the Optimal Road Grade," in Proceedings of the 27th International Symposium on Mine Planning and Equipment Selection - MPES 2018, E. Widzyk-Capehart, A. Hekmat, and R. Singhal, Eds. Cham: Springer International Publishing, 2019, pp. 345–353. doi: 10.1007/978-3-319-99220-4_28.

[39] LINDO Systems, Inc., "What'sBest!, User's Manual Version 17.0." https://www.lindo.com/downloads/PDF/WB.pdf (accessed Nov. 20, 2021).

[40] "IAEA Releases 2019 Data on Nuclear Power Plants Operating Experience," Jun. 25, 2020. https://www.iaea.org/newscenter/news/iaea-releases-2019-data-on-nuclear-power-plants-operating-experience (accessed Nov. 20, 2021).

[41] S. Şahin and Y. Wu, "3.14 Fission Energy Production," in Comprehensive Energy Systems, Elsevier, 2018, pp. 590–637. doi: 10.1016/B978-0-12-809597-3.00331-X.

[42] "Nuclear Power in a Clean Energy System – Analysis," IEA. https://www.iea.org/reports/nuclear-power-in-a-clean-energy-system (accessed Nov. 20, 2021).

[43] M. Al-Zareer, I. Dincer, and M. A. Rosen, "Performance analysis of a supercritical water-cooled nuclear reactor integrated with a combined cycle, a Cu-Cl thermochemical cycle and a hydrogen compression system," Appl. Energy, vol. 195, pp. 646–658, 2017, doi: 10.1016/j.apenergy.2017.03.046.

[44] G. F. Naterer, I. Dincer, and C. Zamfirescu, Hydrogen Production from Nuclear Energy. London: Springer London, 2013. doi: 10.1007/978-1-4471-4938-5.

[45] S. J. Bae, J. Lee, Y. Ahn, and J. I. Lee, "Preliminary studies of compact Brayton cycle performance for Small Modular High Temperature Gas-cooled Reactor system," Ann. Nucl. Energy, vol. 75, pp. 11–19, 2015, doi: 10.1016/j.anucene.2014.07.041.

[46] M. W. Patterson, "Cogeneration of electricity and liquid fuels using a high temperature gas-cooled reactor as the heat source," Nucl. Eng. Des., vol. 329, pp. 204–212, 2018, doi: 10.1016/j.nucengdes.2018.01.029.

[47] X. L. Yan and R. Hino, "Nuclear Hydrogen Production Handbook (Green Chemistry and Chemical Engineering)," pp. 898, 2018, ISBN 9781138074682.

[48] K. Kunitomi, X. Yan, T. Nishihara, N. Sakaba, and T. Mouri, "JAEA'S VHTR FOR HYDROGEN AND ELECTRICITY COGENERATION : GTHTR300C," Nucl. Eng. Technol., vol. 39, no. 1, pp. 9–20, 2007, doi: 10.5516/NET.2007.39.1.009.

[49] D. Hittner, E. Bogusch, M. Fütterer, S. de Groot, and J. Ruer, "High and very high temperature reactor research for multipurpose energy applications," Nucl. Eng. Des., vol. 241, no. 9, pp. 3490–3504, 2011, doi: 10.1016/j.nucengdes.2011.08.004.

[50] M. Al-Zareer, I. Dincer, and M. A. Rosen, "Analysis and assessment of the integrated generation IV gas-cooled fast nuclear reactor and copper-chlorine cycle for hydrogen and electricity production," Energy Convers. Manag., vol. 205, p. 112387, 2020, doi: 10.1016/j.enconman.2019.112387.

[51] A. Peakman and B. Merk, "The Role of Nuclear Power in Meeting Current and Future Industrial Process Heat Demands," Energies, vol. 12, no. 19, p. 3664, 2019, doi: 10.3390/en12193664.

[52] A. Contreras, "Solar–hydrogen: an energy system for sustainable development in Spain," Int. J. Hydrog. Energy, vol. 24, no. 11, pp. 1041–1052, 1999, doi: 10.1016/S0360-3199(98)00134-7.

[53] C. Acar and I. Dincer, "Review and evaluation of hydrogen production options for better environment," J. Clean. Prod., vol. 218, pp. 835–849, 2019, doi: 10.1016/j.jclepro.2019.02.046.

[54] F. Khalid and Y. Bicer, "Energy and exergy analyses of a hybrid small modular reactor and wind turbine system for trigeneration," Energy Sci. Eng., vol. 7, no. 6, pp. 2336–2350, 2019, doi: 10.1002/ese3.327.

[55] M. Kayfeci, A. Keçebaş, and M. Bayat, "Hydrogen production," in Solar Hydrogen Production, Elsevier, 2019, pp. 45–83. doi: 10.1016/B978-0-12-814853-2.00003-5.

[56] G. Locatelli, S. Boarin, A. Fiordaliso, and M. E. Ricotti, "Load following of Small Modular Reactors (SMR) by cogeneration of hydrogen: A techno-economic analysis," Energy, vol. 148, pp. 494–505, 2018, doi: 10.1016/j.energy.2018.01.041.

[57] IAEA, "Status of Innovative Small and Medium Sized Reactor Designs 2005," Feb. 28, 2019. https://www.iaea.org/publications/7450/status-of-innovative-small-and-medium-sized-reactor-designs-2005 (accessed Nov. 20, 2021).

[58] Idaho National Laboratory report, "NGNP Project 2011 Status and Path Forward," Idaho National Lab. (INL), Idaho Falls, ID (United States), INL/EXT-11-23907, 2011. doi: 10.2172/1035900.

[59] H. Song, J. Van Meter, S. Lomperski, D. Cho, H. Y. Kim, and A. Tokuhiro, "Experimental Investigations of a Printed circuit heat exchanger for Supercritical CO2 and Water Heat Exchange," no. NTHAS5-N002, 2006.

[60] A.Tokuhiro, M. Manic, V. Utgikar, D. Grauer, M. McKellar, "Demonstrating Hybrid Heat Transport and Energy Conversion System Performance Characterization Using Intelligent Control Systems," 2012. Accessed: Nov. 24, 2021. [Online]. Available: https://neup.inl.gov/SiteAssets/2012%20R_D%20Abstracts/35-%202012_CFP_Abstract_3510.pdf

[61] S. Şahin and H. M. Şahin, "Generation-IV reactors and nuclear hydrogen production," Int. J. Hydrog. Energy, vol. 46, no. 57, pp. 28936–28948, 2021, doi: 10.1016/j.ijhydene.2020.12.182.

[62] M. M. Valujerdi and S. Talebi, "Entropy generation study for a supercritical water reactor (SCWR)," Prog. Nucl. Energy, vol. 118, p. 103129, 2020, doi: 10.1016/j.pnucene.2019.103129.

[63] M. A. Rosen, G. F. Naterer, C. C. Chukwu, R. Sadhankar, and S. Suppiah, "Nuclear-based hydrogen production with a thermochemical copper-chlorine cycle and supercritical water reactor: equipment scale-up and process simulation," Int. J. Energy Res., vol. 36, no. 4, pp. 456–465, 2012, doi: 10.1002/er.1702.

[64] G. Locatelli, M. Mancini, and N. Todeschini, "Generation IV nuclear reactors: Current status and future prospects," Energy Policy, vol. 61, pp. 1503–1520, 2013, doi: 10.1016/j.enpol.2013.06.101.

[65] The Economic Modeling Working Group, "Cost Estimating Guidelines for Generation IV Nuclear Energy Systems," The OECD Nuclear Energy Agency for the Generation IV International Forum, GIF/EMWG/2007/004, 2007.

[66] S. Dieckmann and J. Dersch, "Simulation of hybrid solar power plants," Abu Dhabi, United Arab Emirates, 2017, p. 160005. doi: 10.1063/1.4984539.

[67] R. Boudries, "Techno-economic study of hydrogen production using CSP technology," Int. J. Hydrog. Energy, vol. 43, no. 6, pp. 3406–3417, 2018, doi: 10.1016/j.ijhydene.2017.05.157.

[68] H. Hidayatullah, S. Susyadi, and M. H. Subki, "Design and technology development for small modular reactors – Safety expectations, prospects and impediments of their deployment," Prog. Nucl. Energy, vol. 79, pp. 127–135, 2015, doi: 10.1016/j.pnucene.2014.11.010.

[69] D. T. Ingersoll, Z. J. Houghton, R. Bromm, and C. Desportes, "NuScale small modular reactor for Co-generation of electricity and water," Desalination, vol. 340, pp. 84–93, 2014, doi: 10.1016/j.desal.2014.02.023.

[70] W. R. Stewart and K. Shirvan, "Capital Cost Estimation for Advanced Nuclear Power Plants." OSF Preprints, 2021. doi: 10.31219/osf.io/erm3g.

[71] G. Locatelli and M. Mancini, "Competitiveness of Small-Medium, New Generation Reactors: A Comparative Study on Decommissioning," J. Eng. Gas Turbines Power, vol. 132, no. 10, p. 102906, 2010, doi: 10.1115/1.4000613.

[72] V. Kuznetsov, "Options for small and medium sized reactors (SMRs) to overcome loss of economies of scale and incorporate increased proliferation resistance and energy security," Prog. Nucl. Energy, vol. 50, no. 2–6, pp. 242–250, 2008, doi: 10.1016/j.pnucene.2007.11.006.

[73] Nuclear Energy Agency (NEA), "Small Modular Reactors: Nuclear Energy Market Potential for Near-term Deployment," NEA No. 7213 2016. https://www.oecd-nea.org/jcms/pl_14924/small-modular-reactors-nuclear-energy-market-potential-for-near-term-deployment?details=true (accessed Nov. 20, 2021).

[74] B. Mignacca and G. Locatelli, "Economics and finance of Small Modular Reactors: A systematic review and research agenda," Renew. Sustain. Energy Rev., vol. 118, p. 109519, 2020, doi: 10.1016/j.rser.2019.109519.

[75] G. Alonso, S. Bilbao, and E. del Valle, "Economic competitiveness of small modular reactors versus coal and combined cycle plants," Energy, vol. 116, pp. 867–879, 2016, doi: 10.1016/j.energy.2016.10.030.

[76] G. Locatelli, A. Fiordaliso, S. Boarin, and M. Ricotti, "Load Following by Cogeneration: Options for Small Modular Reactors, GEN IV Reactor and Traditional Large Plants," in Volume 3: Nuclear Fuel and Material, Reactor Physics and Transport Theory; Innovative Nuclear Power Plant Design and New Technology Application, Shanghai, China, 2017, p. V003T13A013. doi: 10.1115/ICONE25-67180.

[77] J.-M. Bernolles, "De-mystifying small modular reactors," Sustainability Times, Nov. 29, 2019. https://www.sustainability-times.com/low-carbon-energy/de-mystifying-small-modular-reactors/ (accessed Nov. 20, 2021).

[78] R. S. El-Emam and M. H. Subki, "Small modular reactors for nuclear-renewable synergies: Prospects and impediments," Int. J. Energy Res., vol. 45, no. 11, pp. 16995–17004, 2021, doi: 10.1002/er.6838.

[79] A. Borisova and D. Popov, "An option for the integration of solar photovoltaics into small nuclear power plant with thermal energy storage," Sustain. Energy Technol. Assess., vol. 18, pp. 119–126, 2016, doi: 10.1016/j.seta.2016.10.002.

[80] J. Liman, "Small modular reactors: Methodology of economic assessment focused on incremental construction and gradual shutdown options," Prog. Nucl. Energy, vol. 108, pp. 253–259, 2018, doi: 10.1016/j.pnucene.2018.06.002.

[81] T. S. Carless, W. M. Griffin, and P. S. Fischbeck, "The environmental competitiveness of small modular reactors: A life cycle study," Energy, vol. 114, pp. 84–99, 2016, doi: 10.1016/j.energy.2016.07.111.

[82] K. Verfondern and W. Von Lensa, "Past and present research in europe on the production of nuclear hydrogen with HTGR," Prog. Nucl. Energy, vol. 47, no. 1–4, pp. 472–483, 2005, doi: 10.1016/j.pnucene.2005.05.048.

[83] C. W. Lapp and M. W. Golay, "Modular design and construction techniques for nuclear power plants," Nucl. Eng. Des., vol. 172, no. 3, pp. 327–349, 1997, doi: 10.1016/S0029-5493(97)00031-9.

[84] X. C. Schmidt Rivera, E. Topriska, M. Kolokotroni, and A. Azapagic, "Environmental sustainability of renewable hydrogen in comparison with conventional cooking fuels," J. Clean. Prod., vol. 196, pp. 863–879, 2018, doi: 10.1016/j.jclepro.2018.06.033.

[85] O. Ellabban, H. Abu-Rub, and F. Blaabjerg, "Renewable energy resources: Current status, future prospects and their enabling technology," Renew. Sustain. Energy Rev., vol. 39, pp. 748–764, 2014, doi: 10.1016/j.rser.2014.07.113.

[86] S. R. Bull, "Renewable energy today and tomorrow," Proc. IEEE, vol. 89, no. 8, pp. 1216–1226, 2001, doi: 10.1109/5.940290.

[87] E. Bilgen, "Domestic hydrogen production using renewable energy," Sol. Energy, vol. 77, no. 1, pp. 47–55, 2004, doi: 10.1016/j.solener.2004.03.012.

[88] H. Sato, H. Ohashi, S. Nakagawa, Y. Tachibana, and K. Kunitomi, "Safety design consideration for HTGR coupling with hydrogen production plant," Prog. Nucl. Energy, vol. 82, pp. 46–52, 2015, doi: 10.1016/j.pnucene.2014.07.032.

[89] R. R. Sadhankar, J. Li, H. Li, D. K. Ryland, and S. Suppiah, "Future Hydrogen Production Using Nuclear Reactors," in 2006 IEEE EIC Climate Change Conference, Ottawa, ON, 2006, pp. 1–9. doi: 10.1109/EICCCC.2006.277205.

[90] R. S. El-Emam, H. Ozcan, and I. Dincer, "Comparative cost evaluation of nuclear hydrogen production methods with the Hydrogen Economy Evaluation Program (HEEP)," Int. J. Hydrog. Energy, vol. 40, no. 34, pp. 11168–11177, 2015, doi: 10.1016/j.ijhydene.2014.12.098.

[91] D. A. J. Rand and R. M. Dell, "FUELS – HYDROGEN PRODUCTION | Coal Gasification," in Encyclopedia of Electrochemical Power Sources, Elsevier, 2009, pp. 276–292. doi: 10.1016/B978-044452745-5.00300-2.

[92] O. Badran, R. Mamlook, and E. Abdulhadi, "Toward clean environment: evaluation of solar electric power technologies using fuzzy logic," Clean Technol. Environ. Policy, vol. 14, no. 2, pp. 357–367, 2012, doi: 10.1007/s10098-011-0407-8.

[93] A. W. Dowling, T. Zheng, and V. M. Zavala, "Economic assessment of concentrated solar power technologies: A review," Renew. Sustain. Energy Rev., vol. 72, pp. 1019–1032, 2017, doi: 10.1016/j.rser.2017.01.006.

[94] "Concentrated Solar Power: Technology brief," IRENA, Technical Report, Jan. 2013. Accessed: Nov. 20, 2021. [Online]. Available: http://dspace.khazar.org/handle/20.500.12323/4304

[95] A. Palacios, C. Barreneche, M. E. Navarro, and Y. Ding, "Thermal energy storage technologies for concentrated solar power – A review from a materials perspective," Renew. Energy, vol. 156, pp. 1244–1265, 2020, doi: 10.1016/j.renene.2019.10.127.

[96] E. Bellos, "Progress in the design and the applications of linear Fresnel reflectors – A critical review," Therm. Sci. Eng. Prog., vol. 10, pp. 112–137, 2019, doi: 10.1016/j.tsep.2019.01.014.

[97] R. Loisel, L. Baranger, N. Chemouri, S. Spinu, and S. Pardo, "Economic evaluation of hybrid offshore wind power and hydrogen storage system," Int. J. Hydrog. Energy, vol. 40, no. 21, pp. 6727–6739, 2015, doi: 10.1016/j.ijhydene.2015.03.117.

[98] C. Rivkin, R. Burgess, and W. Buttner, "Hydrogen Technologies Safety Guide," NREL/TP--5400-60948, 1169773, 2015. doi: 10.2172/1169773.

[99] B. Zohuri, "Hydrogen-Powered Fuel Cell and Hybrid Automobiles of the Near Future," in Hydrogen Energy, Cham: Springer International Publishing, 2019, pp. 37–59. doi: 10.1007/978-3-319-93461-7_2.

[100] G. F. Naterer et al., "Clean hydrogen production with the Cu–Cl cycle – Progress of international consortium, I: Experimental unit operations," Int. J. Hydrog. Energy, vol. 36, no. 24, pp. 15472–15485, 2011, doi: 10.1016/j.ijhydene.2011.08.012.

[101] J. Rostrupnielsen, "Sulfur-passivated nickel catalysts for carbon-free steam reforming of methane," J. Catal., vol. 85, no. 1, pp. 31–43, 1984, doi: 10.1016/0021-9517(84)90107-6.

[102] M. Felgenhauer and T. Hamacher, "State-of-the-art of commercial electrolyzers and on-site hydrogen generation for logistic vehicles in South Carolina," Int. J. Hydrog. Energy, vol. 40, no. 5, pp. 2084–2090, 2015, doi: 10.1016/j.ijhydene.2014.12.043.

[103] S. Fujiwara et al., "Hydrogen production by high temperature electrolysis with nuclear reactor," Prog. Nucl. Energy, vol. 50, no. 2–6, pp. 422–426, 2008, doi: 10.1016/j.pnucene.2007.11.025.

[104] M. Dejong, A. Reinders, J. Kok, and G. Westendorp, "Optimizing a steam-methane reformer for hydrogen production," Int. J. Hydrog. Energy, vol. 34, no. 1, pp. 285–292, 2009, doi: 10.1016/j.ijhydene.2008.09.084.

[105] S. Schröders, K. Verfondern, and H.-J. Allelein, "Energy economic evaluation of solar and nuclear driven steam methane reforming processes," Nucl. Eng. Des., vol. 329, pp. 234–246, 2018, doi: 10.1016/j.nucengdes.2017.08.007.

[106] P. Corbo and F. Migliardini, "Natural gas and biofuel as feedstock for hydrogen production on Ni catalysts," J. Nat. Gas Chem., vol. 18, no. 1, pp. 9–14, 2009, doi: 10.1016/S1003-9953(08)60083-3.

[107] N. Muradov and T. Vezirolu, "From hydrocarbon to hydrogen-carbon to hydrogen economy," Int. J. Hydrog. Energy, vol. 30, no. 3, pp. 225–237, 2005, doi: 10.1016/j.ijhydene.2004.03.033.

[108] P. L. Spath and M. K. Mann, "Life Cycle Assessment of Hydrogen Production via Natural Gas Steam Reforming," NREL/TP-570-27637, 764485, 2000. doi: 10.2172/764485.

[109] F. Syed, M. Fowler, D. Wan, and Y. Maniyali, "An energy demand model for a fleet of plug-in fuel cell vehicles and commercial building interfaced with a clean energy hub," Int. J. Hydrog. Energy, vol. 35, no. 10, pp. 5154–5163, 2010, doi: 10.1016/j.ijhydene.2009.08.089.

[110] A. Ridluan, M. Manic, and A. Tokuhiro, "EBaLM-THP – A neural network thermohydraulic prediction model of advanced nuclear system components," Nucl. Eng. Des., vol. 239, no. 2, pp. 308–319, 2009, doi: 10.1016/j.nucengdes.2008.10.027.

[111] R. S. El-Emam, H. Ozcan, and C. Zamfirescu, "Updates on promising thermochemical cycles for clean hydrogen production using nuclear energy," J. Clean. Prod., vol. 262, p. 121424, 2020, doi: 10.1016/j.jclepro.2020.121424.

[112] M. Yu, K. Wang, and H. Vredenburg, "Insights into low-carbon hydrogen production methods: Green, blue and aqua hydrogen," Int. J. Hydrog. Energy, vol. 46, no. 41, pp. 21261–21273, 2021, doi: 10.1016/j.ijhydene.2021.04.016.

[113] I. Dincer, C. O. Colpan, O. Kizilkan, and M. A. Ezan, Eds., Progress in Clean Energy, Volume 2. Cham: Springer International Publishing, 2015. doi: 10.1007/978-3-319-17031-2.

[114] A. Z. Weber and T. E. Lipman, "Fuel Cells and Hydrogen Production," in Fuel Cells and Hydrogen Production: A Volume in the Encyclopedia of Sustainability Science and Technology, Second Edition, T. E. Lipman and A. Z. Weber, Eds. New York, NY: Springer, 2019, pp. 1–8. doi: 10.1007/978-1-4939-7789-5_1051.

[115] B. Olateju and A. Kumar, "Techno-economic assessment of hydrogen production from underground coal gasification (UCG) in Western Canada with carbon capture and sequestration (CCS) for upgrading bitumen from oil sands," Appl. Energy, vol. 111, pp. 428–440, 2013, doi: 10.1016/j.apenergy.2013.05.014.

[116] F. Dawood, M. Anda, and G. M. Shafiullah, "Hydrogen production for energy: An overview," Int. J. Hydrog. Energy, vol. 45, no. 7, pp. 3847–3869, 2020, doi: 10.1016/j.ijhydene.2019.12.059.

[117] B. Olateju and A. Kumar, "Hydrogen production from wind energy in Western Canada for upgrading bitumen from oil sands," Energy, vol. 36, no. 11, pp. 6326–6339, 2011, doi: 10.1016/j.energy.2011.09.045.

[118] B. Olateju, A. Kumar, and M. Secanell, "A techno-economic assessment of large scale wind-hydrogen production with energy storage in Western Canada," Int. J. Hydrog. Energy, vol. 41, no. 21, pp. 8755–8776, 2016, doi: 10.1016/j.ijhydene.2016.03.177.

[119] H. Blanco, W. Nijs, J. Ruf, and A. Faaij, "Potential for hydrogen and Power-to-Liquid in a low-carbon EU energy system using cost optimization," Appl. Energy, vol. 232, pp. 617–639, 2018, doi: 10.1016/j.apenergy.2018.09.216.

[120] P. Sabharwall, M. Patterson, and F. Gunnerson, "Theoretical Design of Thermosyphon for Process Heat Transfer From NGNP to Hydrogen Plant," in Fourth International Topical Meeting on High Temperature Reactor Technology, Volume 1, Washington, DC, USA, 2008, pp. 733–738. doi: 10.1115/HTR2008-58199.

[121] A. Allouhi, "Management of photovoltaic excess electricity generation via the power to hydrogen concept: A year-round dynamic assessment using Artificial Neural Networks," Int. J. Hydrog. Energy, vol. 45, no. 41, pp. 21024–21039, 2020, doi: 10.1016/j.ijhydene.2020.05.262.

[122] S. Sadeghi and S. Ghandehariun, "Thermodynamic analysis and optimization of an integrated solar thermochemical hydrogen production system," Int. J. Hydrog. Energy, vol. 45, no. 53, pp. 28426–28436, 2020, doi: 10.1016/j.ijhydene.2020.07.203.

[123] M. F. Orhan, İ. Dinçer, and M. A. Rosen, "Efficiency comparison of various design schemes for copper–chlorine (Cu–Cl) hydrogen production processes using Aspen Plus software," Energy Convers. Manag., vol. 63, pp. 70–86, 2012, doi: 10.1016/j.enconman.2012.01.029.

[124] Z. L. Wang, G. F. Naterer, K. S. Gabriel, R. Gravelsins, and V. N. Daggupati, "Comparison of different copper–chlorine thermochemical cycles for hydrogen production," Int. J. Hydrog. Energy, vol. 34, no. 8, pp. 3267–3276, 2009, doi: 10.1016/j.ijhydene.2009.02.023.

[125]Y. H. Jeong and M. S. Kazimi, "Optimization of the Hybrid Sulfur Cycle for Nuclear Hydrogen Generation," Nucl. Technol., vol. 159, no. 2, pp. 147–157, 2007, doi: 10.13182/NT07-A3861.

[126]A. S. Joshi, I. Dincer, and B. V. Reddy, "Solar hydrogen production: A comparative performance assessment," Int. J. Hydrog. Energy, vol. 36, no. 17, pp. 11246–11257, 2011, doi: 10.1016/j.ijhydene.2010.11.122.

[127]X. Yan, H. Noguchi, H. Sato, Y. Tachibana, K. Kunitomi, and R. Hino, "A hybrid HTGR system producing electricity, hydrogen and such other products as water demanded in the Middle East," Nucl. Eng. Des., vol. 271, pp. 20–29, 2014, doi: 10.1016/j.nucengdes.2013.11.003.

[128]K. Verfondern, X. Yan, T. Nishihara, and H.-J. Allelein, "Safety concept of nuclear cogeneration of hydrogen and electricity," Int. J. Hydrog. Energy, vol. 42, no. 11, pp. 7551–7559, 2017, doi: 10.1016/j.ijhydene.2016.04.239.

[129]M. Orhan, I. Dincer, and G. Naterer, "Cost analysis of a thermochemical Cu–Cl pilot plant for nuclear-based hydrogen production," Int. J. Hydrog. Energy, vol. 33, no. 21, pp. 6006–6020, 2008, doi: 10.1016/j.ijhydene.2008.05.038.

[130]D. Çelik and M. Yıldız, "Investigation of hydrogen production methods in accordance with green chemistry principles," Int. J. Hydrog. Energy, vol. 42, no. 36, pp. 23395–23401, 2017, doi: 10.1016/j.ijhydene.2017.03.104.

[131]M. Jaszczur, M. A. Rosen, T. Śliwa, M. Dudek, and L. Pieńkowski, "Hydrogen production using high temperature nuclear reactors: Efficiency analysis of a combined cycle," Int. J. Hydrog. Energy, vol. 41, no. 19, pp. 7861–7871, 2016, doi: 10.1016/j.ijhydene.2015.11.190.

[132]H. Ishaq and I. Dincer, "A comparative evaluation of three Cu Cl cycles for hydrogen production," Int. J. Hydrog. Energy, vol. 44, no. 16, pp. 7958–7968, 2019, doi: 10.1016/j.ijhydene.2019.01.249.

[133]Q. Wang, C. Liu, R. Luo, D. Li, and R. Macián-Juan, "Thermodynamic analysis and optimization of the combined supercritical carbon dioxide Brayton cycle and organic Rankine cycle-based nuclear hydrogen production system," Int. J. Energy Res., vol. n/a, no. n/a, doi: 10.1002/er.7208.

[134]M. F. Orhan, I. Dincer, and M. A. Rosen, "Efficiency analysis of a hybrid copper–chlorine (Cu–Cl) cycle for nuclear-based hydrogen production," Chem. Eng. J., vol. 155, no. 1–2, pp. 132–137, 2009, doi: 10.1016/j.cej.2009.07.007.

[135]S. Ghandehariun, G. F. Naterer, I. Dincer, and M. A. Rosen, "Solar thermochemical plant analysis for hydrogen production with the copper–chlorine cycle," Int. J. Hydrog. Energy, vol. 35, no. 16, pp. 8511–8520, 2010, doi: 10.1016/j.ijhydene.2010.05.028.

[136]S. Ghandehariun, M. A. Rosen, G. F. Naterer, and Z. Wang, "Comparison of molten salt heat recovery options in the Cu–Cl cycle of hydrogen production," Int. J. Hydrog. Energy, vol. 36, no. 17, pp. 11328–11337, 2011, doi: 10.1016/j.ijhydene.2010.11.093.

[137]J. Zhou et al., "Thermal efficiency evaluation of open-loop SI thermochemical cycle for the production of hydrogen, sulfuric acid and electric power," Int. J. Hydrog. Energy, vol. 32, no. 5, pp. 567–575, 2007, doi: 10.1016/j.ijhydene.2006.06.043.

[138]K. Scott, "Chapter 1 Introduction to Electrolysis, Electrolysers and Hydrogen Production," pp. 1–27, 2019, doi: 10.1039/9781788016049-00001.

[139]J. Chi and H. Yu, "Water electrolysis based on renewable energy for hydrogen production," Chin. J. Catal., vol. 39, no. 3, pp. 390–394, 2018, doi: 10.1016/S1872-2067(17)62949-8.

[140]K.-M. Mangold, "Introduction to Hydrogen Technology</b> .By Roman J. Press, K. S. V. Santhanam, Massoud J. Miri, Alla V. Bailey, and Gerald A. Takacs," ChemSusChem, vol. 2, no. 8, pp. 781–781, 2009, doi: 10.1002/cssc.200900109.

[141]Y. Yürüm, Ed., Hydrogen Energy System. Dordrecht: Springer Netherlands, 1995. doi: 10.1007/978-94-011-0111-0.

[142]R. D. Boardman, "Figures of Merit for Technical and Economic Assessment of Nuclear Hydrogen Hybrid Energy Systems," Idaho National Lab. (INL), Idaho Falls, ID (United States), INL/EXT-17-41484, 2017. doi: 10.2172/1374504.

[143]S. M. Bragg-Sitton et al., "Nuclear-Renewable Hybrid Energy Systems: 2016 Technology Development Program Plan," Idaho National Lab. (INL), Idaho Falls, ID (United States); Oak Ridge National Lab. (ORNL), Oak Ridge, TN (United States), INL/EXT-16-38165, 2016. doi: 10.2172/1333006.

[144]Dan Yurman, "U.S. nuclear plants to produce carbon-free hydrogen," Energy Post, Sep. 17, 2019. https://energypost.eu/u-s-nuclear-plants-to-produce-carbon-free-hydrogen/ (accessed Nov. 21, 2021).

[145]S. S. Rao, Engineering Optimization: Theory and Practice. John Wiley & Sons, ISBN: 978-1-119-45471-7, 2019.

[146]T. Goel, R. Vaidyanathan, R. T. Haftka, W. Shyy, N. V. Queipo, and K. Tucker, "Response surface approximation of Pareto optimal front in multi-objective optimization," Comput. Methods Appl. Mech. Eng., vol. 196, no. 4–6, pp. 879–893, 2007, doi: 10.1016/j.cma.2006.07.010.

[147]S. Upadhyay and M. P. Sharma, "Selection of a suitable energy management strategy for a hybrid energy system in a remote rural area of India," Energy, vol. 94, pp. 352–366, 2016, doi: 10.1016/j.energy.2015.10.134.

[148]J. R. Geschwindt, L. J. Lommers, F. H. Southworth, and F. Shahrokhi, "Performance and optimization of an HTR cogeneration system," Nucl. Eng. Des., vol. 251, pp. 297–300, 2012, doi: 10.1016/j.nucengdes.2011.10.029.

[149]T. Aittokoski and K. Miettinen, "Efficient evolutionary approach to approximate the Pareto-optimal set in multiobjective optimization, UPS-EMOA," Optim. Methods Softw., vol. 25, no. 6, pp. 841–858, 2010, doi: 10.1080/10556780903548265.

[150]Y. Censor, "Pareto optimality in multiobjective problems," Appl. Math. Optim., vol. 4, no. 1, pp. 41–59, 1977, doi: 10.1007/BF01442131.

[151]H. A. Gabbar, M. R. Abdussami, and Md. I. Adham, "Optimal Planning of Nuclear-Renewable Micro-Hybrid Energy System by Particle Swarm Optimization," IEEE Access, vol. 8, pp. 181049–181073, 2020, doi: 10.1109/ACCESS.2020.3027524.

[152]J. a. C. Hekman, "LINDO en What's Best: evaluatie van optimalisatiesoftware (summary)," 2000, Accessed: Dec. 11, 2021. [Online]. Available: https://repository.tudelft.nl/islandora/object/uuid%3A92490109-c5da-4f83-8fec-d39da9300230

[153]Nash, John C, Optimizing Add-Ins: The Educated Guess, What'sBest! New York, N.Y.: PC Magazine, 1991. Accessed: Nov. 21, 2021. [Online]. Available: Vol. 10 no. 7. Ziff Davis. pp. 130, 132. ISSN 0888-8507

[154]Spreadsheet Optimizer Ported to Macintosh. San Mateo, Calif.: InfoWorld Pub., 1988. [Online]. Available: Vol. 10 no. 35. IDG. p. 24. ISSN 0199-66

## Authors

**Mustafa Ciftcioglu**
Graduate Student
Ontario Tech University, Ontario, Canada
mustafa.ciftcioglu@ontotechu.net

Mustafa Ciftcioglu is a graduate student in the Faculty of Energy Systems and Nuclear Science at Ontario Tech University in Oshawa, Ontario, Canada. His primary R&D interests are in nuclear hydrogen production including safety of nuclear and optimizing complex systems. He has energy R&D experiences in Turkey and Canada.

**Prof. Filippo Genco**
Professor at the Faculty of Energy Systems and Nuclear Science
Ontario Tech University, Ontario, Canada
Filippo.Genco@ontariotechu.ca

Filippo Genco is Associate Teaching Faculty in the Faculty of Energy Systems and Nuclear Science at Ontario Tech University in Oshawa, Ontario, Canada. His primary R&D interests are in development of advanced energy system, including next generation nuclear and renewable systems. He also holds expertise in computational material science and aeronautical engineering. He has nuclear and energy R&D experiences in Chile, United Arab Emirates, USA and Canada.

**Prof. Akira Tokuhiro**
Professor at the Faculty of Energy Systems and Nuclear Science
Ontario Tech University, Ontario, Canada
Akira.Tokuhiro@ontariotechu.ca

Akira Tokuhiro is Professor in the Faculty of Energy Systems and Nuclear Science at Ontario Tech University in Oshawa, Ontario, Canada. His primary R&D interests are in development of advanced reactor concepts, including small modular reactors. He joined Ontario Tech University from NuScale Power. He has nuclear and energy R&D experiences in Switzerland, Japan, USA and Canada

# Considerations and Optimization of Hydrogen Production using Small Modular Reactors and Renewable energy sources

**Mustafa Ciftcioglu[1], F. Genco[1], and A. Tokuhiro[1]**

[1] Faculty of Energy Systems and Nuclear Science, Ontario Tech University, 2000 Simcoe Street North, Oshawa, Ontario L1K 2K2 Canada

*mustafa.ciftcioglu@ontariotechu.net, filippo.genco@ontariotechu.ca, akira.tokuhiro@ontariotechu.ca*

## Abstract

*Hydrogen is projected today to become the key fuel- and energy-source for the imminent energy transition to a low- to net-zero carbon society. Although a strong debate persists, there is consensus on the urgency to reduce to greenhouse gas (GHG) emissions to massively mitigate the negative impacts of global climate change. The production of hydrogen – as fuel and as stored energy, generated via electrolysis and/or high-temperature thermal-chemical processes, from various energy sources, including existing fossil-fuelled plants, nuclear energy (small modular reactors, SMRs) and renewable sources, is attracting more and more attention. In this work a systems engineering perspective is considered via modeling and simulations, of a nuclear plant linked to a concentrated solar power plant to produce both electricity and hydrogen. For industry practicality, the merits of technology readiness level per production method have been considered. Scenarios, under which optimization will be needed, have been studied and analyzed. Rudiments of complexity are also described; characterized as multi-objectives and consisting of many variables and parameters.*

## 1. Introduction

The demand for energy rises as the world's population and economy grow, and people shift from rural to urban areas [1]. The majority of current electric energy comes from fossil fuels (hydrocarbons) [2], which are depleted and confined by geographical distribution and ease of extraction [3,4]. Constant usage of hydrocarbon-based energy led in huge increases in $CO_2$ and Greenhouse Gases in the atmosphere, which has been linked to global warming [5]. In order to minimize global warming and maintain a clean environment, sustainable and renewable energy resources are crucial to the world's future [6–9]. For instance, for the past three decades, the United Nations Framework Convention on Climate Change (UNFCCC) has presented climate change mitigation as a demand-side concern, avoiding an explicit focus on fossil fuel production [10]. Massive production of electricity from renewable energy sources can be a difficult target to achieve at a very reasonable price. In fact, the variety and irregularity of these types of energy sources is one of its most noticeable characteristics [11]. To address these issues, efficient and large-scale technical solutions must be implemented. Large-scale storage systems have been developed and designed to suit market demand in order to deal with the volatility and discontinuity of renewable energy sources [12]. Storage devices can decouple supply and demand (hourly, daily, and seasonally) by transferring generated energy on several time scales [13].

Hydrogen-based energy storage systems are becoming more popular for large-scale energy storage as a result of their ability to store and transmit energy, as well as their cost effectiveness [3,13,15]. The global demand for pure hydrogen has risen rapidly from less than 20 Mt in 1975 to more than 70 Mt in 2018 [16]. Despite the fact that some researchers endorse hydrogen as an energy carrier for the reasons previously stated [17], most recent studies have determined that a wholly hydrogen-dependent economy is still controversial and unreachable [13,18], even now that it has begun to show promise [19]. Whatever the challenges, clean hydrogen generation is on the rise to reduce $CO_2$ emissions and meet global energy demand [5,20,21–23].

By using some energy sources, such as coal, natural gas, nuclear, biomass, solar, and wind, hydrogen can be produced. However, because fossil fuels such as natural gas, oil, and coal are currently still the most cost-effective method, with costs ranging from 1 to 3 USD per kilogram of hydrogen produced, they are still used to supply primary current hydrogen demand [24–26].

Traditional water electrolysis, steam reforming, high-temperature steam electrolysis, hybrid, and thermochemical cycles are only a few of the ways documented in the literature for producing heat and electricity while also producing hydrogen from water in the same nuclear power reactor [27,28]. The nuclear hybrid energy system is one of the most appealing technologies (NHES) as it can produce both hydrogen and low-cost electricity [29,30] at the same time.

This research primarily looks at hydrogen and electricity generation. The demands of electricity and hydrogen highly depend on the location and vary. To give a clear example, the energy demand of Nunavut, which is a small territory where less people live, is less than that of the city of Toronto. In addition to this, to reduce greenhouse gas emissions and meet the world's current energy needs, fossil-based energy sources must be replaced with clean energy sources.

In summary, this study provides information on nuclear-renewable clean hydrogen hybrid systems, with a focus on the water-based Cu-Cl thermochemical hydrogen production method. To acquire data, LabVIEW is used to model nuclear small modular reactor (SMR) prototypic integral pressurized water reactor-type (iPWR-type) and the Cu-Cl thermochemical cycle, while System Adviser Model (SAM) is utilised to simulate CSP (Concentrated Solar Power) plants. The amount of hydrogen in kg and electricity in kwh are calculated by importing hourly data from SAM into LabVIEW and showing possible scenarios.

## 2. MATHEMATICAL MODELS OF SUBSYSTEMS

### 2.1. Prototypic iPWR-type SMR / Thermodynamic Side

A nuclear power plant using pressurized water reactor (PWR) light water technology was preferred in this study. This is the most common with over 250 PWRs for power generation. PWRs employ water as both a coolant and a moderator. The primary coolant (water) is delivered into the reactor core under high pressure and heated by atomic fission energy. The heated water then goes via a steam generator, transferring its thermal energy to a secondary circuit, where steam is created and transmitted through turbines that rotate an electric generator, resulting in the production of electricity. A reactor pressure vessel (RPV), steam generators, pumps, and pressurizer, as well as connecting pipes, make up the primary circuit in large power plants [31].

An integrated configuration is found in the majority of modern small modular reactor designs. The principal coolant system components, including steam generators, pressurizers, and pumps, are housed within the RPV in integrated reactors. Some external plumbing and components are eliminated, a compact containment is adopted, and nuclear power plant (NPP) dimensions are reduced thanks to the integrated solution.

A prototypic iPWR-type Small Modular Nuclear Reactor type, being a typical small PWR with integral design, is adopted in this study. When it comes to Technology Readiness Level (TRL), prototypic iPWR-type SMR's components and design have been tested and, this type of SMR will be soon commercially available. Moreover, because this reactor contains a pressurizer, it can run under natural circulation primary flow, removing the need for reactor coolant pumps. The prototypic iPWR-type SMR`s steam generator considered is a helical-coil heat exchanger that stands in the annular space between the hot leg riser and the reactor vessel's inside wall. At the bottom, feedwater enters the tubes, and slightly superheated steam escapes at the top. Each reactor is contained in its own high-pressure containment vessel, which is placed underwater in a concrete pool coated with stainless steel. A modest 45 MW conventional steam turbine generator set designed for the prototypic SMR steam generator outlet conditions is installed in the reactor. The moisture separator and, eventually, the re-heater, as in every PWR plant, must be considered to prevent erosion at the final turbine stages. Table 1 shows the major technical data of the SMR type single core plant considered.

**Table 1**: Technical data of the prototypic Integral PWR SMR type used similar to [31].

| **Parameters** | |
|---|---|
| Live steam flow [kg/s] | 71.3 |
| Turbine inlet temperature [ºC] | 255 |
| Turbine inlet pressure [MPa] | 3.1 |
| Condenser pressure [MPa] | 0.0063 |
| Exit steam quality [%] | 80.6 |
| | |
| Nuclear heat input [kW] | 159975 |
| Total heat input [kW] | 159975 |
| Net electric power [kW] | 45005 |
| Net electric efficiency [%] | 28.14 |

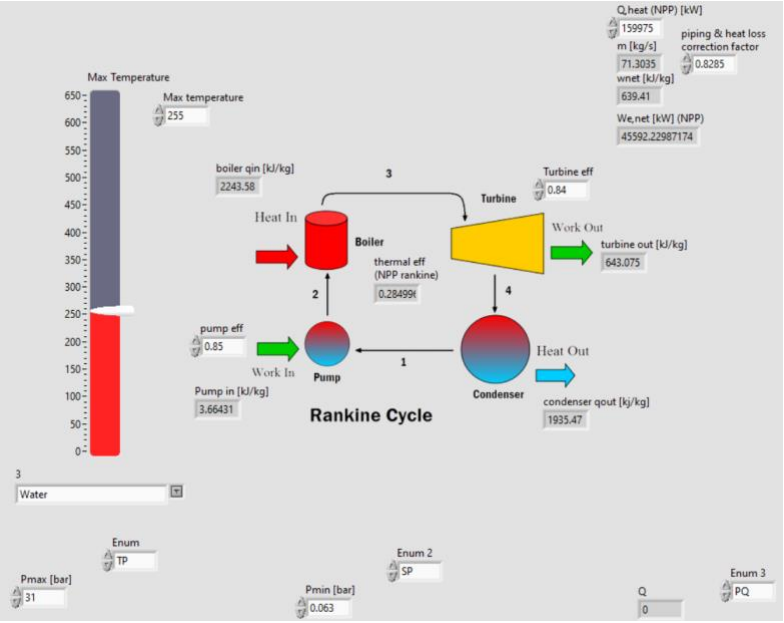


**Figure 1**: System level model of a iPWR type SMR with prototypic Rankine energy conversion cycle, as modeled using LabVIEW.

## 2.2. Concentrated Solar Power (CSP)

The heat energy from a concentrated solar power (CSP) plant can be used to produce hydrogen [32,33]. In concentrated solar power plants, mirrors direct sunlight to a receiver. The thermal energy collected in the receiver powers a steam turbine, which provides electricity [34]. This CSP technology is well suited to assisting nuclear power facilities in ensuring that high-temperature heat energy is delivered directly to nuclear steam superheating without the need for intermediary conversion. In the literature, there are three types of CSP technologies that meet the high-temperature requirements. The mirrored devices utilised in CSP are used to categorise these technologies. The Parabolic Trough (PT), Fresnel Reflectors (FR) and Dish Receiver (DR) are examples of these [29,35]. In 2013, PT technology was used in over 90% of CSP systems [36], and more recently in over 60% of CSP systems [37]. The FR system uses a series of ground-based, flat or slightly curved mirrors positioned at various angles to focus sunlight onto a stationary receiver several meters above the mirror region, similar to the PT collector technology [38]. Solar power towers are a type of solar furnace that gets focused sunlight through a tower, commonly known as "central tower" power plants, "heliostat" power plants, or "power towers". It uses heliostats, a series of flat, adjustable mirrors, to focus the sun's beams onto a collection tower.

In this research, Solar Tower Plant is combined in hybrid form with a nuclear SMR to produce hydrogen via Cu-Cl thermo-chemical cycle. Thermodynamically this coupling is very favourable since the Solar Tower Plant using molten salt as a fluid can operate at around 530 $^{0}$C. This CSP plant accounts for three major subsystems, which are solar field consisting of a huge number of computer-assisted flat mirrors (heliostats), thermal storage, and power block. Here, thermal energy storage can be used to level production. The volume of the thermal energy storage used in this CSP plant is considered in terms of effectiveness. Depending on variables such as location, the

number of heliostats, SAM defines the optimum volume of the energy storage. Thermal energy storages based on hour-based volumes were compared and the volume defined by SAM is seen the most efficient. Data of CSP for obtaining a hybrid system on LabVIEW is taken from the very well known and benchmarked System Advisor Model (SAM).

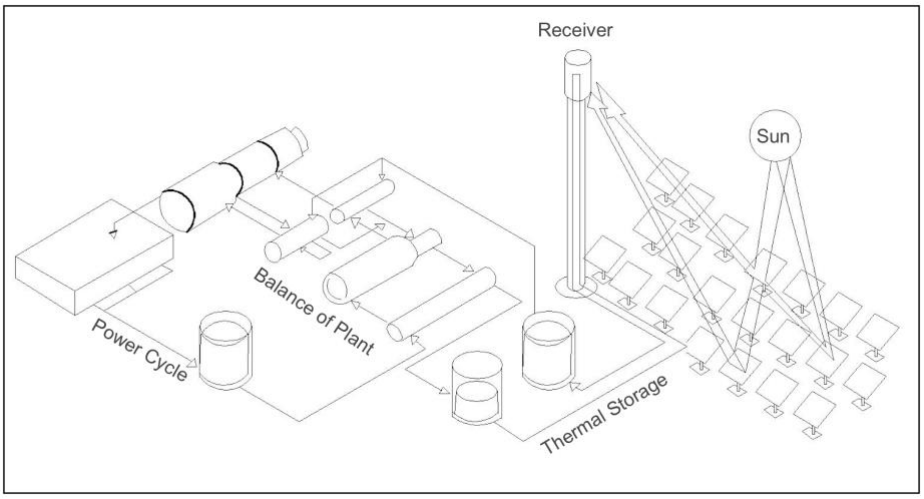


**Figure 2**: A schematic of the CSP Plant.

**Table 2**: Parameters of CSP Plant [31]

| | |
|---|---|
| ***Power Block Parameters*** | |
| Net electric power attributed to solar heat [kW] | 47922 |
| Turbine inlet pressure [Bar] | 100 |
| Condenser pressure [Bar] | 0.085 |
| Solar heat input required [kW] | 117685 |
| Solar heat to electricity efficiency [%] | 40.72 |
| ***Thermal Energy Storage Parameters*** | |
| Hours of storage [h] | 15 |
| Nominal storage capacity [MWh] | 1765.3 |
| Nominal storage tank discharge flow rate [kg/s] | 265.1 |
| Nominal hot tank temperature [°C] | 565 |
| Nominal cold tank temperature [°C] | 270 |
| Mass of stored fluid [ton] | 14177 |
| Storage volume [$m^3$] | 8202 |
| Storage tank height [m] | 9.796 |
| Storage tank diameter [m] | 32.65 |
| ***Solar Field Parameters*** | |
| Field Configuration | Circular Surround |
| Design point DNI [$kW/m^2$] | 0.915 |
| Solar multiple | 2.5 |
| Solar heat generation required [kW] | 294220 |

| | |
|---|---|
| Overall corrected collector efficiency [%] | 56.49 |
| Field Incident thermal power [kW] | 520822.3 |
| Reflective area in solar field [m²] | 569043 |
| Reflective area per heliostat [m²] | 44.59 |
| Number of heliostats | 12760 |
| Tower structure height [m] | 136.1 |
| Tower inner diameter [m] | 11.22 |
| Receiver height [m] | 13.59 |
| Receiver diameter [m] | 10.2 |
| Receiver face area [m²] | 435.5 |
| Distance from tower base to outermost mirror on North side [m] | 1021.1 |
| Distance from tower base to innermost mirrors [m] | 102.1 |
| Heliostat field land area [m²] | 2775818 |

**Table 3**: Design point solar data (DNI: Direct Normal Irradiation) [31]

| Location: Daggett Barstow, California | |
|---|---|
| Altitude | 586m |
| Latitude | 34,85 °N |
| Longitude | 116,8 °E |
| Time zone | GMT -8 |
| Annual DNI | 7,46 kWh/($m^2$.day) |
| Design point DNI | 0.915 kW/m2 |

Hour-based data of CSP is obtained by simulating data presented in Table 2 and Table 3 on System Advisor Model (SAM) software. The location chosen for the simulation of the solar data is Daggett Barstow in California. The acquired hourly data from SAM ("electricity to grid", "electricity from grid", "power cycle input energy" and "net efficiency") are then fed to LabVIEW for further simulations. To calculate "net efficiency", "electricity to grid" is divided by "pc input energy". As shown in Table 4, 8761 data from SAM are written in excel and then exported to LabVIEW.

**Table 4:** An indication of one year of hourly based data of CSP.

| Total hour | Day | Month | Hour | Electricity to grid \| ($kW_e$) | Electricity from grid \| ($kW_e$) | PC input energy \| ($kW_{th}$) | Net efficiency |
|---|---|---|---|---|---|---|---|
| 1 | 1 | 1 | 0 | 9983.48 | 0 | 120593 | 0.08278656 |
| 2 | 1 | 1 | 1 | 34724.6 | 0 | 123414 | 0.28136678 |
| 3 | 1 | 1 | 2 | 34659.8 | 0 | 123263 | 0.28118576 |
| : | : | : | : | : | : | : | : |
| 8759 | 31 | 12 | 21 | 44009.3 | 0 | 121110 | 0.36338288 |
| 8760 | 31 | 12 | 22 | 43921.1 | 0 | 120896 | 0.36329655 |
| 8761 | 31 | 12 | 23 | 0 | 0 | 60837.1 | 0 |

### 2.3. Cu-Cl Hydrogen Production Cycle

There are seven main types of Cu-Cl cycles [39]. According to the researchers [40], the four-step Cu-Cl cycle, which has a net efficiency of roughly 43 percent [41], has the highest energetic and exergetic efficiency. New generation nuclear reactors or concentrated solar power (CSP) systems [42,43] can meet the heat needs for Cu-Cl at around 525 °C [44,45]. Because solar and nuclear energy are both clean sources of energy, it may be preferable to produce hydrogen utilising the Cu-CI thermochemical cycle [45].

The four-step Cu-Cl cycle involves hydrolysis, thermolysis, electrolysis, and drying steps [46,47,48]. The corresponding chemical equations are given in the Appendix A. In the Cu-Cl thermo-chemical cycle, to produce 1 mol $H_2$ it is necessary to spend 200 kJ heat energy at temperature of 525 °C, and 25 kJ electric energy [49].

## 3. Modelling & Integration of Nuclear Hybrid Energy System (NHES)

The NHES shown in Fig. 3 is made up of the subsystems as mentioned above. We generate heat and electricity using NPP and CSP, and then use these energy to produce hydrogen utilizing the Cu-Cl cycle. NPP and CSP each have their own Rankine power cycle for energy generation. The reason why NPP and CSP are not integrated totally is that when one of them is shut down, the other is expected to produce energy. Moreover, NPP has to follow the licence requirements defined by the regulator, the regulation doesn't allow them to be integrated totally in terms of safety. Therefore, if any trouble in CSP, it cannot impact the safety of NPP. The point is that they have to be maintained in a hybrid approach where one of them can be shut down if necessary.

It is well known that the CSP plant is weather dependent. Therefore, CSP requires electrical energy to reheat molten salt when the sun is not providing enough energy to maintain a liquid state. As a result, we have to use electrical energy to keep it liquid. Basically, the grid provides the electrical energy to keep molten salt in a liquid state. However, thanks to this hybrid system, the required electricity is provided directly by the NPP rather than from the grid.

The production of heat energy in CSP is significantly influenced by location. There is no distinction for NPP. It could be argued that CSP might be ineffective in areas that do not receive enough sunlight. Therefore, it is assumed that CSP outputs would change when the location is

changed. Additionally, it should not be overlooked that CSP contains some inputs, such as the quantity of heliostats, which is correlated with results. If more heliostats are employed in an area that receives less sunshine, it is possible to achieve the same resutls with fewer heliostats in an area that receives more sunlight.

Since the Cu-Cl cycle requires heat energy at the temperature around 525 °C, an ideal reversible thermochemical heat pump is employed to increase the temperature of the fluid coming from the NPP, which is at 255 °C. The heat pump used as a reference [49] requires 0.4235 kJ heat energy to increase the temperature of the fluid by 1 °C. In this NHES, the needed heat energy is provided by the NPP. The reversible thermochemical heat pump does not require any electricity.

To produce 1 mol-$H_2$ in the Cu-Cl thermochemical cycle, 200 kJ heat energy and 25 kJ electric energy must be provided at a temperature of 525 °C [49]. Here, a heat pump is utilised to obtain the needed temperature from the nuclear plant in order to supply heat energy at the required temperature. The required temperature is already achieved on the CSP side. Defining how much heat energy is required from NPP and CSP to meet the electrical demand for Cu-Cl required to produce 1 mol of $H_2$ is calculated by dividing the dynamically changing net electrical efficiencies of NPP and CSP by 25 kJ.

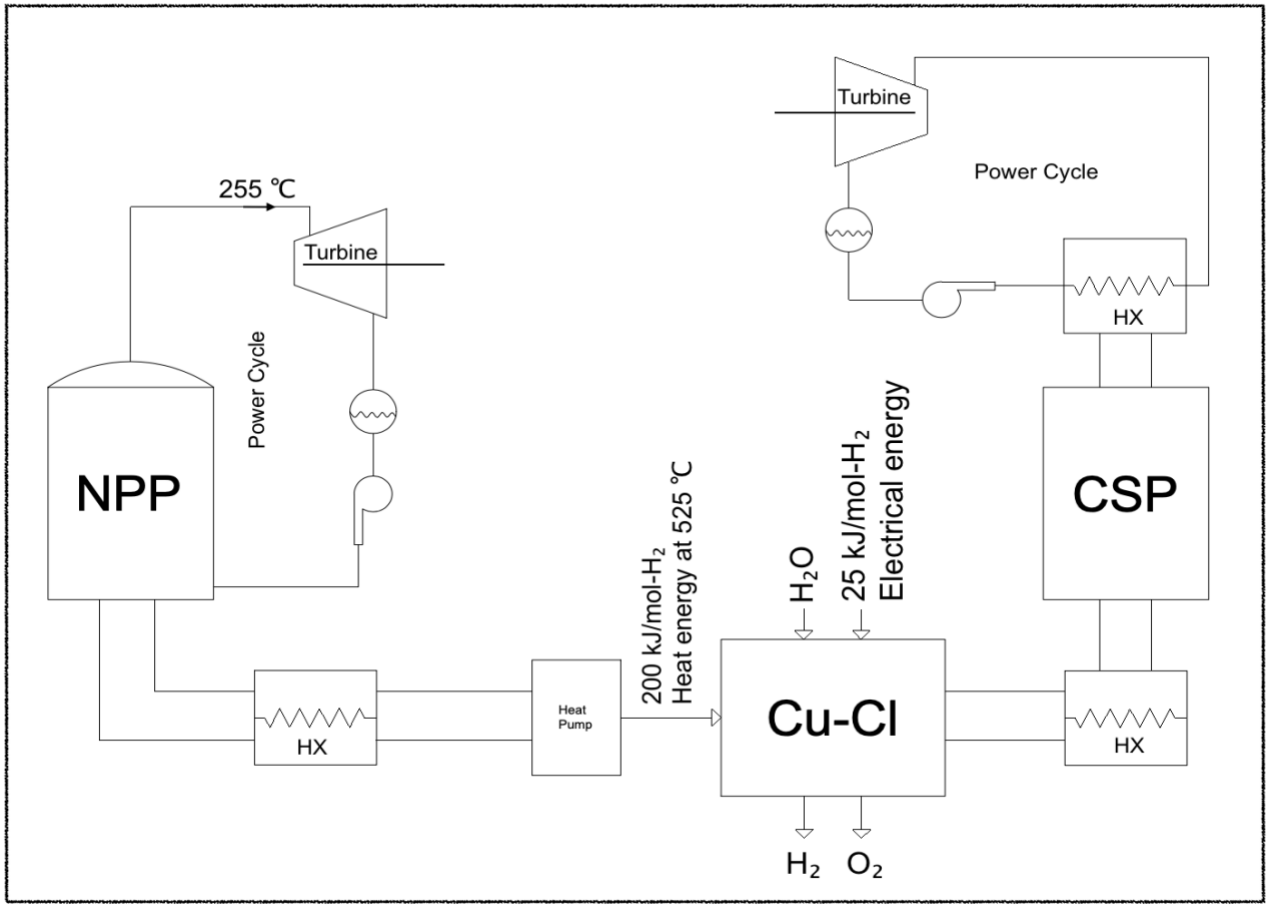


**Figure 3**: A schematic of NHES.

Hydrogen and/or electricity are produced using thermal energy generated by NPP and CSP. The amount of heat power of NPP and/or CSP are defined as a percentage to produce hydrogen and the left heat power of NPP and/or CSP is used to produce electricity as shown in Fig. 4. Furthermore, by specifying a date range, the amount of hydrogen and power produced is calculated and presented individually on the graph, thanks to the code written using LabVIEW.

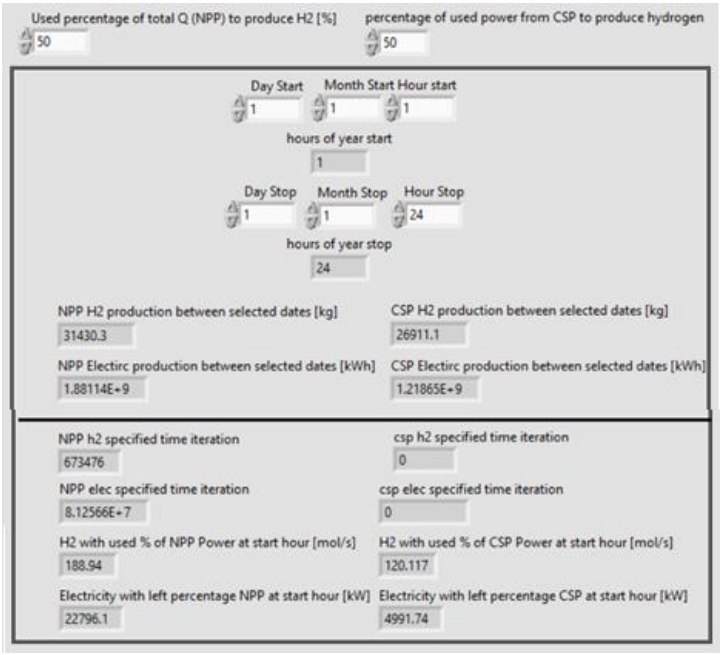


**Figure 4**: Control panel / LabVIEW GUI of NPP and CSP to produce hydrogen and electricity.

As in Fig. 5, the total amounts of hydrogen and electricity generated by NPP and CSP are plotted by indicating hours or dates: it allows to see how production amounts change over time. Because the scale and units of hydrogen and electricity differ, graphs superimposed on the same timeline are used to depict both.

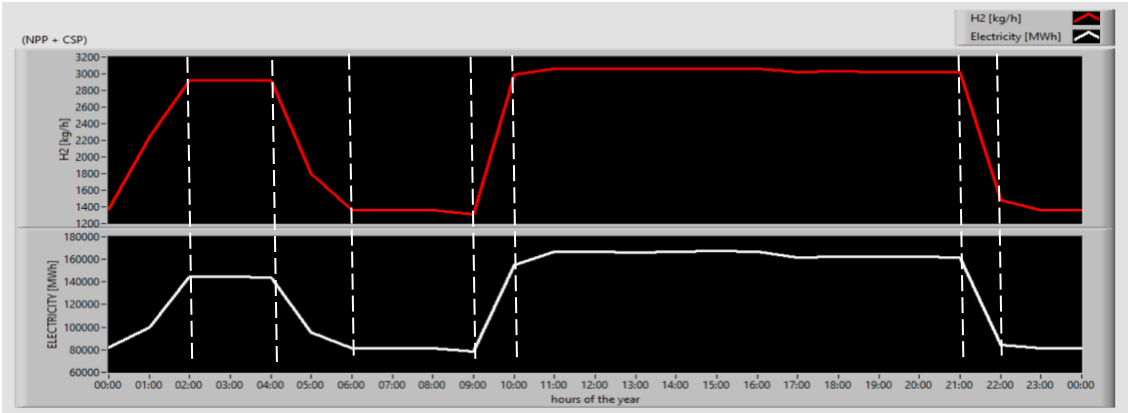


**Figure 5**: Results from simulation of total hydrogen [kg] and electricity production [MWh] for 24 hour period, from a combined NPP and CSP source.

## 4. Results

In Table 5 and Table 6, the percentage values describe how much of the energy resource is used for hydrogen production. The tables contain two different days from each season, as prototypic examples for the all seasons: the statistical variance of measured meteorological variables is accounted for and recognized as a limiting factor. The examples are herein presented to represent the amount of hydrogen and electricity produced, for example on the coldest and warmest days of each season. Furthermore, the tables reveal the differences in the amount of production between the seasons. Four major scenarios are examined in this work per each season: a) each of the two power plants contributes for 25% of the energy needed to produce hydrogen b) it is 50% -50% contribution c) 75% 75 % of the contribution and finally d) both plants contribute to 100% of the energy needed for hydrogen/electricity generation.

Using the written code in LabVIEW, the results can be obtained by defining date range (per respective yearly season) and power percentage of the sources. Although the NPP's power remains the same, some differences are observed in the production amount of hydrogen and electricity via NPP: in fact the NPP meets the CSP required electricity for keeping molten salt in a liquid form and all auxiliary components needed at all times. When it comes to renewable, CSP power is highly dependent on the weather conditions such as daylight time, temperature, cloudy weather and so on. Therefore, this NHES make fluctuations in terms of its power. In Table 5 and Table 6, the production amounts of hydrogen and electricity are shown for specific dates. When looked at the tables in more details, despite that the summer2 average outside temperature is more than that of summer1, it is seen that there is a decrease in the production of hydrogen via CSP in the summer2. Although there are many unknown parameters depending on the weather conditions, the decrease in daylight time in summer2 can be shown as the reason for this situation. When considering fall1 and fall2, the decrease in the amount of hydrogen produced by CSP despite the fact that the temperature in fall2 is higher than that in fAll1 is an indication that not only the temperature but also other weather-related parameters play a very important role in the power of the CSP. For instance, the angle of the sun at a specific time of year and place, the amount of dust in the air, the concentration of various gases in the atmosphere, or the butterfly effect. There are several questions that still need to be answered, but they should be covered in more detail in another study. That kind of information is not provided by CSP simulation.

**Table 5**: Hydrogen production [kg] per given seasonal day (as shown), for four different NPP and CSP percentage contributions (scenarios).

| | | **$H_2$ in kg** | | | | | | | |
|---|---|---|---|---|---|---|---|---|---|
| | | **Winter1** | **Winter2** | **Spring1** | **Spring2** | **Summer1** | **Summer2** | **Fall1** | **Fall2** |
| | | *DEC-15 (9.4 °C)* | *FEB-11 (26.7 °C)* | *MAR-11 (13.3 °C)* | *MAY-31 (38.9 °C)* | *JUN-10 (30 °C)* | *JULY-10 (47.8 °C)* | *OCT-26 (18.3 °C)* | *SEP-7 (43.3 °C)* |
| **CSP1** | **25%** | 10331.9 | 14733.2 | 16909.9 | 19728.3 | 17388.7 | 16409.7 | 15115.1 | 4355.77 |
| **NPP1** | **25%** | 16386.2 | 16420.1 | 16440.6 | 16454 | 16417.1 | 16411.4 | 16420.4 | 16312.5 |
| **CSP2** | **50%** | 20663.8 | 29466.4 | 33819.9 | 39456.6 | 34777.4 | 32819.3 | 30230.2 | 8711.53 |
| **NPP2** | **50%** | 32772.5 | 32840.2 | 32881.2 | 32908.1 | 32834.1 | 32822.9 | 32840.8 | 32625.1 |
| **CSP3** | **75%** | 30995.6 | 44199.6 | 50729.8 | 59184.8 | 52166.1 | 49229 | 45345.3 | 13067.3 |
| **NPP3** | **75%** | 49158.7 | 49260.3 | 49321.7 | 49362.1 | 49251.2 | 49234.3 | 49261.1 | 48937.6 |
| **CSP4** | **100%** | 41327.5 | 58932.8 | 67639.7 | 78913.1 | 69554.9 | 65638.6 | 60460.5 | 17423.1 |
| **NPP4** | **100%** | 65545 | 65680.5 | 65762.3 | 65816.2 | 65668.2 | 65645.8 | 65681.5 | 65250.2 |

**Table 6**: Electricity production [kWh] per given seasonal day (as shown), for fours different NPP and CSP percentage contribution (scenarios).

| | | **Electricity in kWh** | | | | | | | |
|---|---|---|---|---|---|---|---|---|---|
| | | **Winter1** | **Winter2** | **Spring1** | **Spring2** | **Summer1** | **Summer2** | **Fall1** | **Fall2** |
| | | *DEC-15 (9.4 °C)* | *FEB-11 (26.7 °C)* | *MAR-11 (13.3 °C)* | *MAY-31 (38.9 °C)* | *JUN-10 (30 °C)* | *JULY-10 (47.8 °C)* | *OCT-26 (18.3 °C)* | *SEP-7 (43.3 °C)* |
| **CSP1** | **75%** | 4.14E+05 | 5.88E+05 | 6.79E+05 | 7.77E+05 | 6.64E+05 | 6.12E+05 | 6.06E+05 | 1.54E+05 |
| **NPP1** | **75%** | 8.17E+05 | 8.19E+05 | 8.20E+05 | 8.21E+05 | 8.19E+05 | 8.19E+05 | 8.19E+05 | 8.14E+05 |
| **CSP2** | **50%** | 2.76E+05 | 3.92E+05 | 4.52E+05 | 5.18E+05 | 4.43E+05 | 4.08E+05 | 4.04E+05 | 1.03E+05 |
| **NPP2** | **50%** | 5.45E+05 | 5.46E+05 | 5.47E+05 | 5.47E+05 | 5.46E+05 | 5.46E+05 | 5.46E+05 | 5.42E+05 |
| **CSP3** | **25%** | 1.38E+05 | 1.96E+05 | 2.26E+05 | 2.59E+05 | 2.21E+05 | 2.04E+05 | 2.02E+05 | 5.14E+04 |
| **NPP3** | **25%** | 2.72E+05 | 2.73E+05 | 2.73E+05 | 2.74E+05 | 2.73E+05 | 2.73E+05 | 2.73E+05 | 2.71E+05 |
| **CSP4** | **100%** | 5.52E+05 | 7.84E+05 | 9.05E+05 | 1.04E+06 | 8.86E+05 | 8.17E+05 | 8.08E+05 | 2.06E+05 |
| **NPP4** | **100%** | 1.09E+06 | 1.09E+06 | 1.09E+06 | 1.09E+06 | 1.09E+06 | 1.09E+06 | 1.09E+06 | 1.08E+06 |

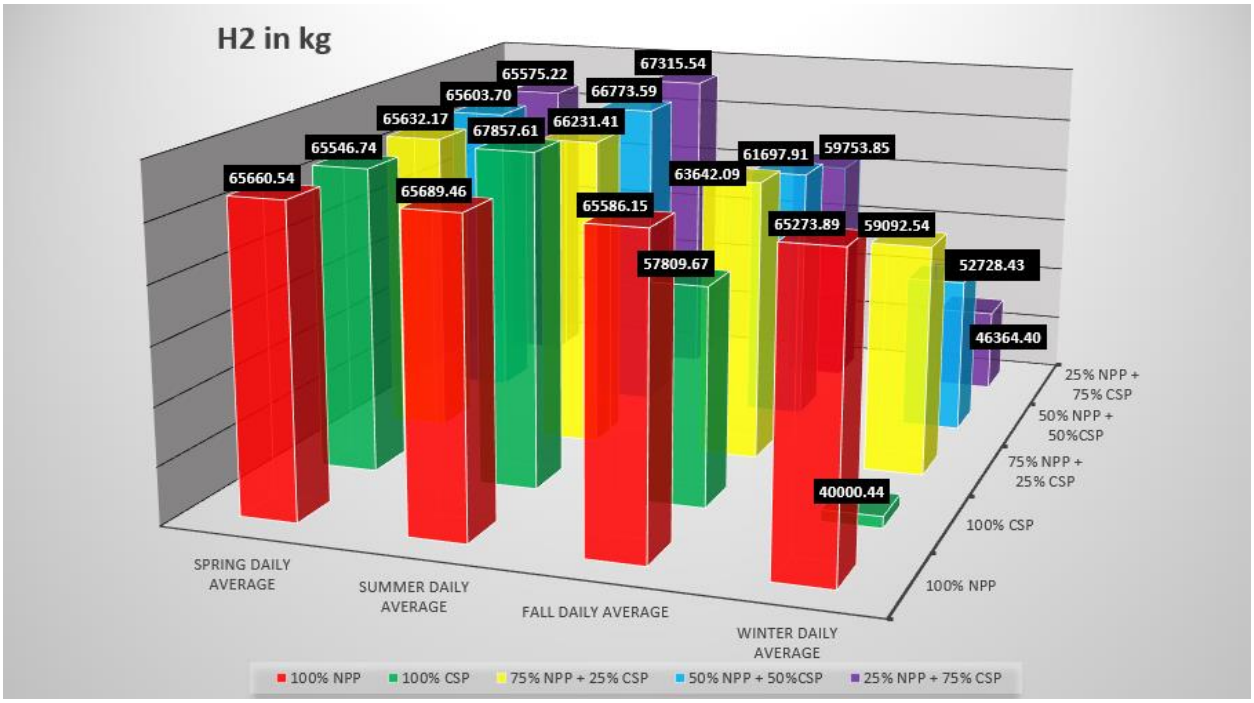


**Figure 6**: Seasonal comparison of hydrogen production depending on reliance on NPP, CSP or jointly in percentage given.

In Fig. 6, when looked at the average daily hydrogen production amounts for the spring, it is seen that almost equal amounts of hydrogen are produced, although the percentage rates of the sources are different. However, when it is summer, there is an increase in hydrogen production due to the increased energy of CSP. When comparing daily average hydrogen production amounts in the winter, the amount of hydrogen produced with 100 percent NPP power is lower. The reason for this is that the CSP's power decreases in the winter, and the NPP provides the electrical energy needed to keep the CSP running.

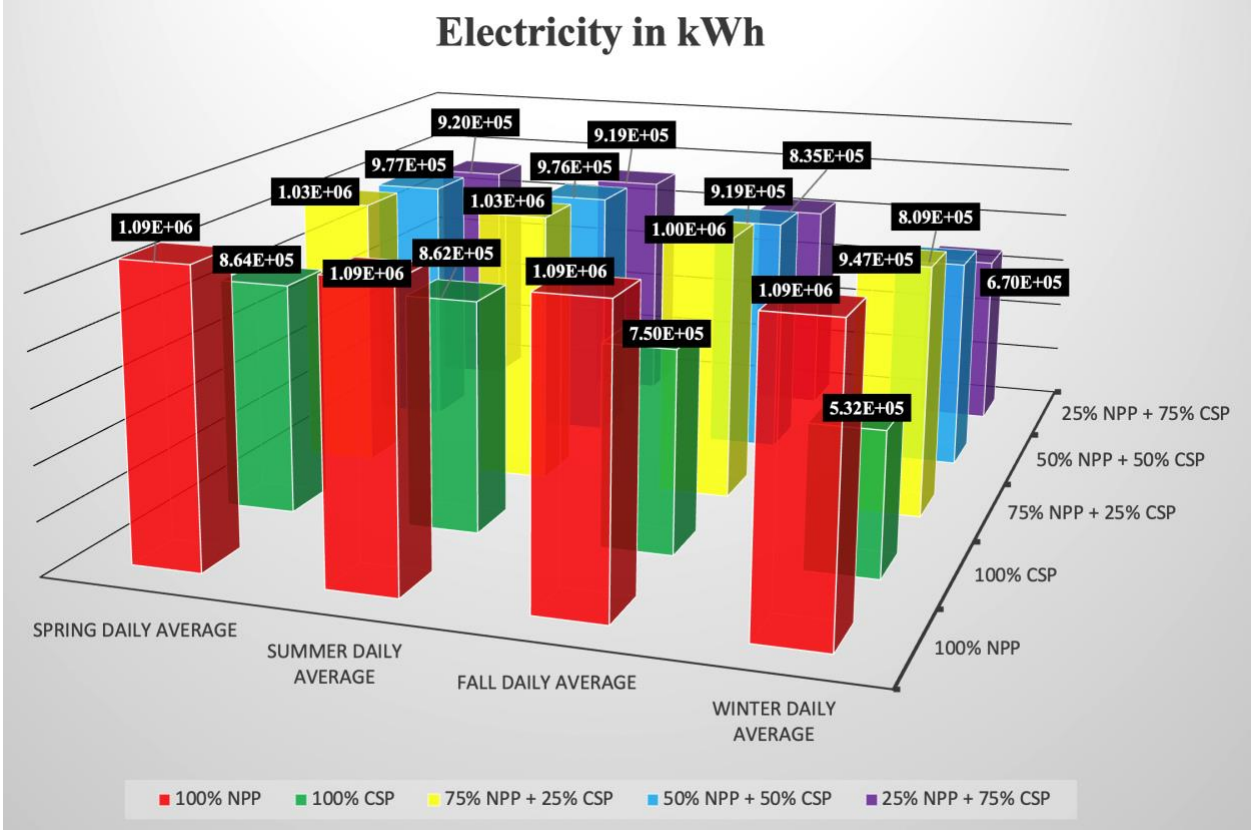


**Figure 7**: Comparison of electricity production depending on seasonal, and generation source (NPP, CPS or combination).

As indicated in Fig. 7, the amount of electricity generated is decreasing in fall and winter. CSP requires the molten salt to be in liquid form, therefore, it needs electrical energy to heat the molten salt liquid and also to operate the auxiliary equipment.

## 5. Conclusions

Nuclear energy and hydrogen produced by nuclear energy can be argued, respectively as sensible known electricity source and energy carrier that has the potential to sustain global energy demand while transitioning to a lower carbon economy of scale. As a result, one of today's most pressing engineering challenges is producing hydrogen from renewable energy sources as well as nuclear energy, in tandem. Long-term, innovation in the hybridization of nuclear and renewable industries will be a key issue for decreasing greenhouse gas emissions and transitioning to a low-carbon future, since they address postulated thermal and electrical energy demands. In order to counter climate change, nuclear and renewable technologies will be important for producing “clean energy” needed for total electrification in a variety of industries, including automobiles, public transport, construction-related vehicles, home heating, and a spectrum of thermally-driven

industries. The amounts of hydrogen and electricity produced via a prototypic i-PWR NPP and CSP are detailed in this research.

Furthermore, the constant volume of hydrogen and electricity may not be significant. However, it is important for the optimization that is necessary because CSP outputs vary throughout the day. The based load is a consistent volume of hydrogen and power. It is made possible by continuous optimization of the weather variations that affect CSP performance.

**References:** For brevity here, additional references are listed in the literature review paper [12].

[1] United Nations, Department of Economic and Social Affairs, Population Division, "World Popula- tion Prospects: The 2017 Revision, Key Findings and Advance Tables," 2017. Working Paper No. ESA/P/WP/248
[2] R. Pinsky, P. Sabharwall, J. Hartvigsen, and J. O'Brien, "Comparative review of hydrogen produc- tion technologies for nuclear hybrid energy systems," Prog. Nucl. Energy, vol. 123, p. 103317, 2020, doi: 10.1016/j.pnucene.2020.103317.
[3] P. Moriarty and D. Honnery, "Hydrogen's role in an uncertain energy future," Int. J. Hydrog. Ener- gy, vol. 34, no. 1, pp. 31–39, 2009, doi: 10.1016/j.ijhydene.2008.10.060.
[4] V. T. Le, E.-N. Dragoi, F. Almomani, and Y. Vasseghian, "Artificial Neural Networks for Predicting Hydrogen Production in Catalytic Dry Reforming: A Systematic Review," Energies, vol. 14, no. 10, p. 2894, 2021, doi: 10.3390/en14102894.
[5] I. Dincer, "Green methods for hydrogen production," Int. J. Hydrog. Energy, vol. 37, no. 2, pp. 1954–1971, 2012, doi: 10.1016/j.ijhydene.2011.03.173.
[6] A. Miltner, W. Wukovits, T. Pröll, and A. Friedl, "Renewable hydrogen production: a technical evaluation based on process simulation," J. Clean. Prod., vol. 18, pp. S51–S62, 2010, doi: 10.1016/j.jclepro.2010.05.024.
[7] D. Gielen, F. Boshell, D. Saygin, M. D. Bazilian, N. Wagner, and R. Gorini, "The role of renewable energy in the global energy transformation," Energy Strategy Rev., vol. 24, pp. 38–50, 2019, doi: 10.1016/j.esr.2019.01.006.
[8] S. Toghyani, E. Baniasadi, and E. Afshari, "Thermodynamic analysis and optimization of an in- tegrated Rankine power cycle and nano-fluid based parabolic trough solar collector," Energy Convers. Manag., vol. 121, pp. 93–104, 2016, doi: 10.1016/j.enconman.2016.05.029.
[9] F. Zhang, P. Zhao, M. Niu, and J. Maddy, "The survey of key technologies in hydrogen energy storage," Int. J. Hydrog. Energy, vol. 41, no. 33, pp. 14535–14552, 2016, doi: 10.1016/j.ijhyde- ne.2016.05.293.
[10] K. Kühne, N. Bartsch, R. D. Tate, J. Higson, and A. Habet, "'Carbon Bombs' - Mapping key fossil fuel projects," *Energy Policy*, vol. 166, p. 112950, Jul. 2022, doi: 10.1016/j.enpol.2022.112950.
[11] P. Denholm, J. C. King, C. F. Kutcher, and P. P. H. Wilson, "Decarbonizing the electric sector: Com- bining renewable and nuclear energy using thermal storage," Energy Policy, vol. 44, pp. 301– 311, 2012, doi: 10.1016/j.enpol.2012.01.055.
[12] M. Ciftcioglu, F. Genco, and A. Tokuhiro, "Optimized Clean Hydrogen Production using Nuclear Small Modular Reactors and Renewable Energy Sources: a Review", ATW, Major Trends in Energy Policy and Nuclear Power, 2022.
https://www.researchgate.net/publication/359013133_ATW_Major_Trends_in_Energy_Policy_a

nd_Nuclear_Power.
[13] H. Blanco and A. Faaij, "A review at the role of storage in energy systems with a focus on Power to Gas and long-term storage," Renew. Sustain. Energy Rev., vol. 81, pp. 1049–1086, 2018, doi: 10.1016/j.rser.2017.07.062.
[14] M. Noussan, P. P. Raimondi, R. Scita, and M. Hafner, "The Role of Green and Blue Hydrogen in the Energy Transition—A Technological and Geopolitical Perspective," Sustainability, vol. 13, no. 1, p. 298, 2020, doi: 10.3390/su13010298.
[15] N. V. Gnanapragasam, B. V. Reddy, and M. A. Rosen, "Hydrogen production from coal gasification for effective downstream CO2 capture," Int. J. Hydrog. Energy, vol. 35, no. 10, pp. 4933–4943, 2010, doi: 10.1016/j.ijhydene.2009.07.114.
[16] IEA, "The Future of Hydrogen," 2019. Accessed: Nov. 21, 2021. [Online]. Available: https://www.iea.org/reports/the-future-of-hydrogen
[17] R. Boudries, "Hydrogen as a fuel in the transport sector in Algeria," Int. J. Hydrog. Energy, vol. 39, no. 27, pp. 15215–15223, 2014, doi: 10.1016/j.ijhydene.2014.06.014.
[18] M. Eypasch et al., "Model-based techno-economic evaluation of an electricity storage system based on Liquid Organic Hydrogen Carriers," Appl. Energy, vol. 185, pp. 320–330, 2017, doi: 10.1016/j.apenergy.2016.10.068.
[19] C. Acar and I. Dincer, "Comparative assessment of hydrogen production methods from renewable and non-renewable sources," Int. J. Hydrog. Energy, vol. 39, no. 1, pp. 1–12, 2014, doi: 10.1016/j.ijhydene.2013.10.060.
[20] I. Dincer and C. Zamfirescu, "Sustainable hydrogen production options and the role of IAHE," *Int. J. Hydrog. Energy*, vol. 37, no. 21, pp. 16266–16286, 2012, doi: 10.1016/j.ijhydene.2012.02.133.
[21] A. Ozbilen, M. Aydin, I. Dincer, and M. A. Rosen, "Life cycle assessment of nuclear-based hydrogen production via a copper–chlorine cycle: A neural network approach," Int. J. Hydrog. Energy, vol. 38, no. 15, pp. 6314–6322, 2013, doi: 10.1016/j.ijhydene.2013.03.071.
[22] T. A. H. Ratlamwala and I. Dincer, "Performance assessment of solar-based integrated Cu–Cl systems for hydrogen production," Sol. Energy, vol. 95, pp. 345–356, 2013, doi: 10.1016/j.solener.2013.06.018.
[23] G. Locatelli, A. Fiordaliso, S. Boarin, and M. E. Ricotti, "Cogeneration: An option to facilitate load following in Small Modular Reactors," Prog. Nucl. Energy, vol. 97, pp. 153–161, 2017, doi: 10.1016/j.pnucene.2016.12.012.
[24] C. E. Finke, H. F. Leandri, E. T. Karumb, D. Zheng, M. R. Hoffmann, and N. A. Fromer, "Economically advantageous pathways for reducing greenhouse gas emissions from industrial hydrogen under common, current economic conditions," *Energy Environ. Sci.*, vol. 14, no. 3, pp. 1517–1529, 2021, doi: 10.1039/D0EE03768K.
[25] M. Al-Zareer, I. Dincer, and M. A. Rosen, "Development and assessment of a novel integrated nuclear plant for electricity and hydrogen production," Energy Convers. Manag., vol. 134, pp. 221–234, 2017, doi: 10.1016/j.enconman.2016.12.004.
[26] S. S. Seyitoglu, I. Dincer, and A. Kilicarslan, "Energy and exergy analyses of hydrogen production by coal gasification," Int. J. Hydrog. Energy, vol. 42, no. 4, pp. 2592–2600, 2017, doi: 10.1016/j.ijhydene.2016.08.228.
[27] M. Balat, "Potential importance of hydrogen as a future solution to environmental and transportation problems," Int. J. Hydrog. Energy, vol. 33, no. 15, pp. 4013–4029, 2008, doi: 10.1016/j.ijhydene.2008.05.047.
[28] M. Newborough and G. Cooley, "Developments in the global hydrogen market: The

spectrum of hydrogen colours," Fuel Cells Bull., vol. 2020, no. 11, pp. 16–22, 2020, doi: 10.1016/S1464-2859(20)30546-0.
[29] D. Popov and A. Borissova, "Innovative configuration of a hybrid nuclear-parabolic trough solar power plant," *Int. J. Sustain. Energy*, vol. 37, no. 7, pp. 616–639, 2018, doi: 10.1080/14786451.2017.1333509.
[30] J. Chen, H. E. Garcia, J. S. Kim, and S. M. Bragg-Sitton, "Operations Optimization of Nuclear Hybrid Energy Systems," *Nucl. Technol.*, vol. 195, no. 2, pp. 143–156, 2016, doi: 10.13182/NT15-130.
[31] D. Popov, A. Borissova, Innovative configuration of a hybrid nuclear-solar tower power plant, Energy, 2017, doi: 10.1016/j.energy.2017.02.147.
[32] S. Dieckmann and J. Dersch, "Simulation of hybrid solar power plants," Abu Dhabi, United Arab Emirates, 2017, p. 160005. doi: 10.1063/1.4984539.
[33] R. Boudries, "Techno-economic study of hydrogen production using CSP technology," *Int. J. Hydrog. Energy*, vol. 43, no. 6, pp. 3406–3417, 2018, doi: 10.1016/j.ijhydene.2017.05.157.
[34] O. Badran, R. Mamlook, and E. Abdulhadi, "Toward clean environment: evaluation of solar electric power technologies using fuzzy logic," *Clean Technol. Environ. Policy*, vol. 14, no. 2, pp. 357–367, 2012, doi: 10.1007/s10098-011-0407-8.
[35] A. W. Dowling, T. Zheng, and V. M. Zavala, "Economic assessment of concentrated solar power technologies: A review," *Renew. Sustain. Energy Rev.*, vol. 72, pp. 1019–1032, 2017, doi: 10.1016/j.rser.2017.01.006.
[36] "Concentrated Solar Power: Technology brief," IRENA, Technical Report, Jan. 2013. Accessed: Nov. 20, 2021. [Online]. Available at: http://dspace.khazar.org/handle/20.500.12323/4304
[37] A. Palacios, C. Barreneche, M. E. Navarro, and Y. Ding, "Thermal energy storage technologies for concentrated solar power – A review from a materials perspective," *Renew. Energy*, vol. 156, pp. 1244–1265, 2020, doi: 10.1016/j.renene.2019.10.127.
[38] E. Bellos, "Progress in the design and the applications of linear Fresnel reflectors – A critical review," *Therm. Sci. Eng. Prog.*, vol. 10, pp. 112–137, 2019, doi: 10.1016/j.tsep.2019.01.014.
[39] G. F. Naterer, I. Dincer, and C. Zamfirescu, *Hydrogen Production from Nuclear Energy*. London: Springer London, 2013. doi: 10.1007/978-1-4471-4938-5.
[40] H. Ishaq and I. Dincer, "A comparative evaluation of three Cu Cl cycles for hydrogen production," *Int. J. Hydrog. Energy*, vol. 44, no. 16, pp. 7958–7968, 2019, doi: 10.1016/j.ijhydene.2019.01.249.
[41] G. F. Naterer *et al.*, "Clean hydrogen production with the Cu–Cl cycle – Progress of international consortium, I: Experimental unit operations," *Int. J. Hydrog. Energy*, vol. 36, no. 24, pp. 15472–15485, 2011, doi: 10.1016/j.ijhydene.2011.08.012.
[42] M. F. Orhan, I. Dincer, and M. A. Rosen, "Efficiency analysis of a hybrid copper–chlorine (Cu–Cl) cycle for nuclear-based hydrogen production," *Chem. Eng. J.*, vol. 155, no. 1–2, pp. 132–137, 2009, doi: 10.1016/j.cej.2009.07.007.
[43] S. Ghandehariun, G. F. Naterer, I. Dincer, and M. A. Rosen, "Solar thermochemical plant analysis for hydrogen production with the copper–chlorine cycle," *Int. J. Hydrog. Energy*, vol. 35, no. 16, pp. 8511–8520, 2010, doi: 10.1016/j.ijhydene.2010.05.028.
[44] M. F. Orhan, İ. Dinçer, and M. A. Rosen, "Efficiency comparison of various design schemes for copper–chlorine (Cu–Cl) hydrogen production processes using Aspen Plus

software," *Energy Convers. Manag.*, vol. 63, pp. 70–86, 2012, doi: 10.1016/j.enconman.2012.01.029.
[45] Q. Wang, C. Liu, R. Luo, D. Li, and R. Macián-Juan, "Thermodynamic analysis and optimization of the combined supercritical carbon dioxide Brayton cycle and organic Rankine cycle-based nuclear hydrogen production system," *Int. J. Energy Res.*, vol. n/a, no. n/a, doi: 10.1002/er.7208.
[46] S. Sadeghi and S. Ghandehariun, "Thermodynamic analysis and optimization of an integrated solar thermochemical hydrogen production system," *Int. J. Hydrog. Energy*, vol. 45, no. 53, pp. 28426–28436, 2020, doi: 10.1016/j.ijhydene.2020.07.203.
[47] Z. L. Wang, G. F. Naterer, K. S. Gabriel, R. Gravelsins, and V. N. Daggupati, "Comparison of different copper–chlorine thermochemical cycles for hydrogen production," *Int. J. Hydrog. Energy*, vol. 34, no. 8, pp. 3267–3276, 2009, doi: 10.1016/j.ijhydene.2009.02.023.
[48] S. Ghandehariun, M. A. Rosen, G. F. Naterer, and Z. Wang, "Comparison of molten salt heat recovery options in the Cu–Cl cycle of hydrogen production," *Int. J. Hydrog. Energy*, vol. 36, no. 17, pp. 11328–11337, 2011, doi: 10.1016/j.ijhydene.2010.11.093.
[49] El-Emam, R. S., Dincer, I., & Zamfirescu, C. (2019). Enhanced CANDU reactor with heat-upgrading hybrid chemical-mechanical heat pump for combined power and hydrogen production. International Journal of Hydrogen Energy. doi:10.1016/j.ijhydene.2019.06.181

## Appendix A. Copper – Chlorine hydrogen production cycle equations.

The copper-chlorine (Cu-Cl) hydrogen production cycle is given here in summary. The first step is hydrolysis:

$$2CuCl_2(s) + H_2O(g) \rightarrow Cu_2OCl_2(s) + 2HCl(g) \quad \text{(at 375-400°C [48])} \quad (1)$$

The second step which is thermolysis consists in the decomposition of copper oxychloride taking place at high temperatures of about 500-530°C;

$$Cu_2OCl_2(s) \rightarrow \tfrac{1}{2}\,\mathbf{O_2(g)} + 2CuCl(l) \quad (2)$$

The third step which is electrolysis;

$$2CuCl(aq) + 2HCl(aq) \rightarrow \mathbf{H_2(g)} + 2CuCl_2(aq) \quad \text{(at 25°C)} \quad (3)$$

The fourth step (drying of aqueous cupric chloride) happens at temperature between 30 to 80°C;

$$CuCl_2(aq) \rightarrow CuCl_2(s) \quad (4)$$

## Appendix B. Equations

Actual enthalpy values of the power cycle of the NPP are generated simultaneously in the LabVIEW software using data in Table 1 and thermodynamics properties of water for every single point of the cycle with COOLPROP add-on depending on temperatures and pressures. All equations for calculation of thermodynamics properties are given as noted below.

$$\left.\begin{matrix} T_1 \\ P_1 \end{matrix}\right\} \begin{matrix} h_1 \\ v_1 \end{matrix} \tag{5}$$

$$w_{p,in} = v_1 \frac{P_2 - P_1}{\eta_P} \tag{6}$$

$$h_2 = h_1 + w_{p,in} \tag{7}$$

$$\left.\begin{matrix} T_3 \\ P_3 \end{matrix}\right\} \begin{matrix} h_3 \\ s_3 \end{matrix} \tag{8}$$

$$\left.\begin{matrix} P_{4s} \\ s_{4s} = s_3 \end{matrix}\right\} x_{4s} = \frac{s_{4s} - s_f}{s_{fg}} \tag{9}$$

$$h_{4s} = h_f + x_4 h_{fg} \tag{10}$$

$$\eta_T = \frac{h_3 - h_4}{h_3 - h_{4s}} \longrightarrow h_4 = h_3 - \eta_T (h_3 - h_{4s}) \tag{11}$$

$$\left.\begin{matrix} P_4 \\ h_4 \end{matrix}\right\} x_4 = \frac{h_4 - h_f}{h_{fg}} \tag{12}$$

$$q_{in} = h_3 - h_2 \tag{13}$$

$$q_{out} = h_4 - h_1 \tag{14}$$

$$w_{net} = q_{in} - q_{out} \tag{15}$$

$$\eta_T = \frac{w_{net}}{q_{in}} \tag{16}$$

# Optimized Clean Hydrogen Production using Nuclear Small Modular Reactor and Concentrated Solar Power as a Renewable

Student: Mustafa Ciftcioglu
Research Supervisor: Akira Tokuhiro
Research Co-supervisor: Filippo Genco
Examining Committee Member: Dan Hoornweg

Faculty of Energy Systems and Nuclear Science, Ontario Tech University,
2000 Simcoe Street North, Oshawa, Ontario L1K 2K2 Canada

OntarioTech Energy Systems & Nuclear Science

A thesis submitted to the
School of Graduate and Postdoctoral Studies in partial fulfillment of the requirements for the degree of

**Master of Applied Science in Nuclear Engineering**

Faculty of Energy Systems and Nuclear Science

Ontario Tech University

Oshawa, Ontario, Canada
December 2022

# Outlines

- Hydrogen
- Subsystems
  - NPP
  - CSP
  - Cu-Cl
- N-RHES
- Results
  - Multi-objective optimization
  - Comparative results
- SMR Safety-in-design
- Conclusion

# Hydrogen

- Energy carrier (120.1 MJ/kg),
- Heating or electricity production,
- Vehicles powered by hydrogen,
- A commodity used as a **feedstock** in many industrial processes, including **refineries** and the **production of methanol and ammonia**,
- The demand for pure hydrogen from less than 20 Mt in 1975 to more than 70 Mt in 2018.
- Hydrogen is a key issue for decreasing GHG emissions and transitioning to a low-carbon future.

*IEA, "The Future of Hydrogen," 2019. Accessed: Nov. 21, 2021. [Online]. Available: https://www.iea.org/reports/the-future-of-hydrogen.*

# Hydrogen

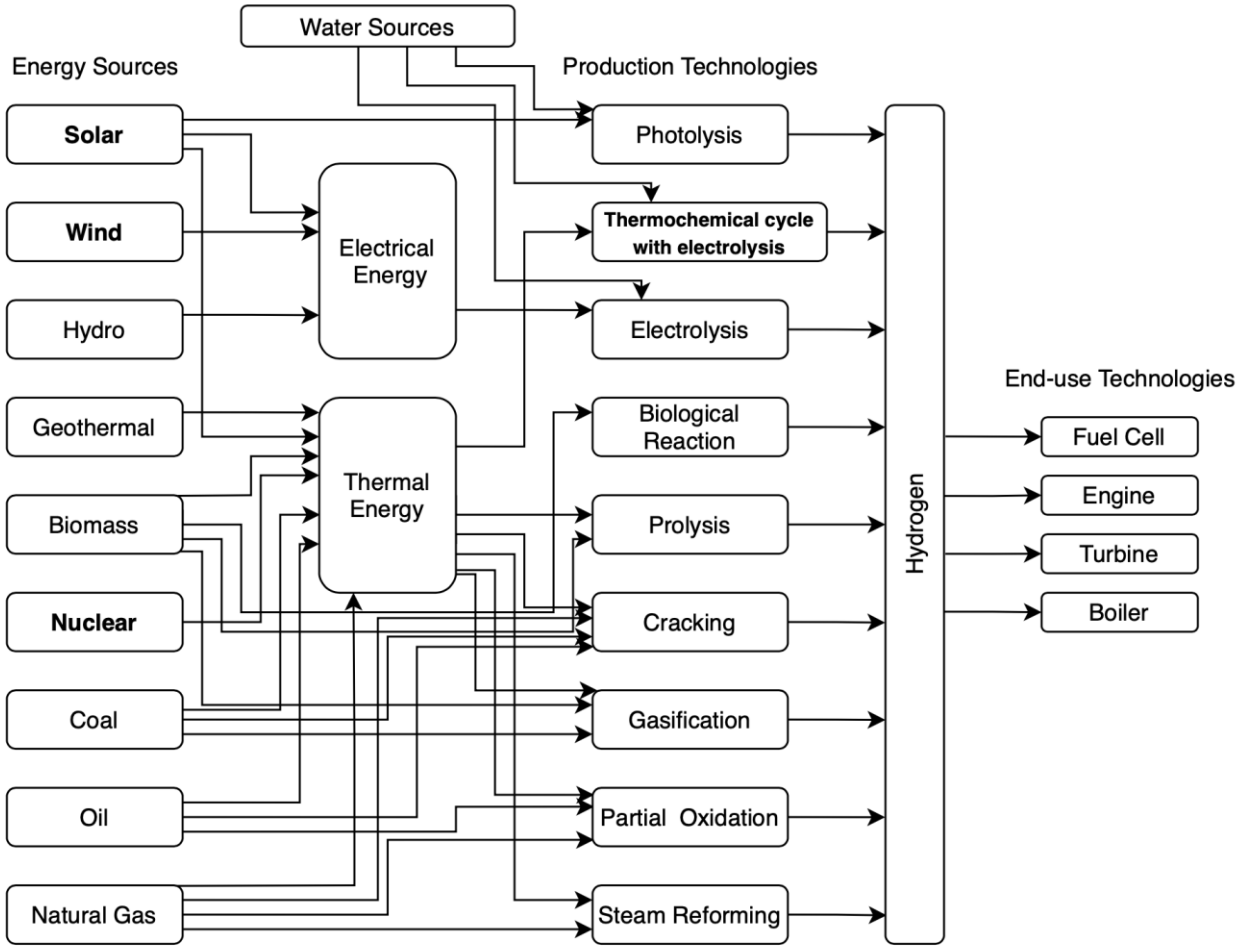


The most preferred methods of generating hydrogen from energy sources.

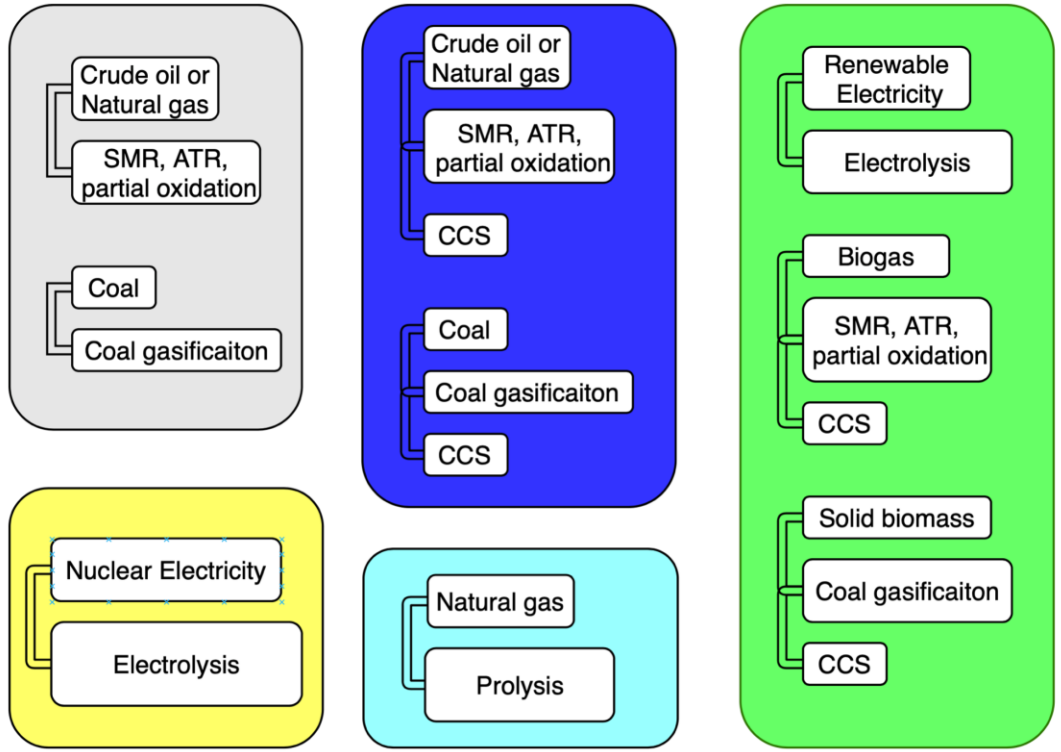


Methods for producing hydrogen using the most popular color schemes.

*M. Ciftcioglu, F. Genco, A. Tokuhiro, "Optimized Clean Hydrogen Production using Nuclear Small Modular Reactors and Renewable Energy Sources: a Review," Serial | Major Trends in Energy Policy and Nuclear Power, atw, Vol. 67, pp 16-30, 2022.*

# Nuclear Hydrogen Production

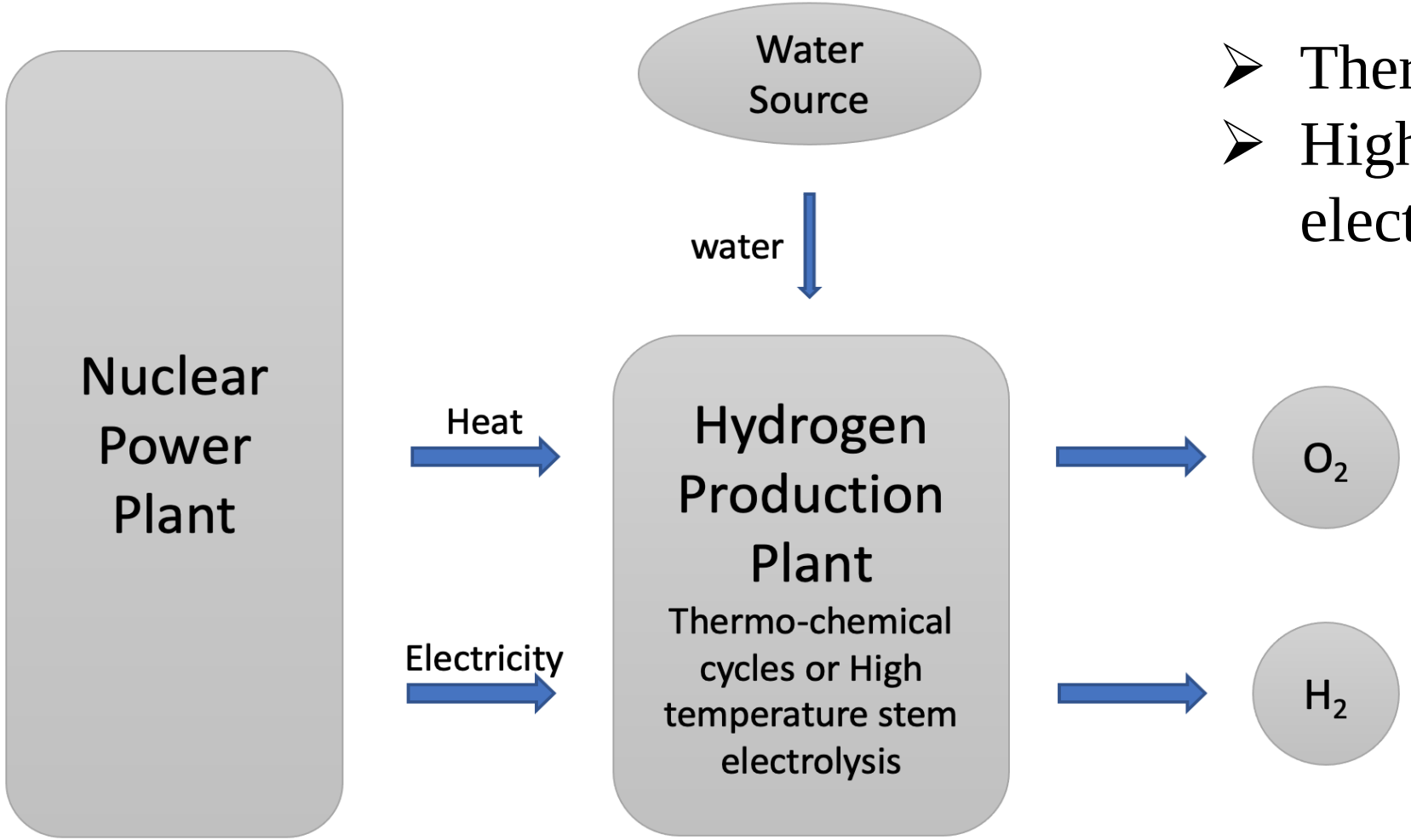


- Thermochemical cycles
- High temperature steam electrolysis

# Prototypic iPWR-type SMR / Thermodynamic Side

- The most suitable SMR for industrial application in terms of licensing.

| Parameters | |
|---|---|
| Live steam flow [kg/s] | 71.3 |
| Turbine inlet temperature [ºC] | 255 |
| Turbine inlet pressure [MPa] | 3.1 |
| Condenser pressure [MPa] | 0.0063 |
| Exit steam quality [%] | 80.6 |
| | |
| Nuclear heat input [kW] | 159975 |
| Total heat input [kW] | 159975 |
| Net electric power [kW] | 45005 |
| Net electric efficiency [%] | 28.14 |

**Table 1**: Technical data of the prototypic Integral PWR SMR type used similar to.

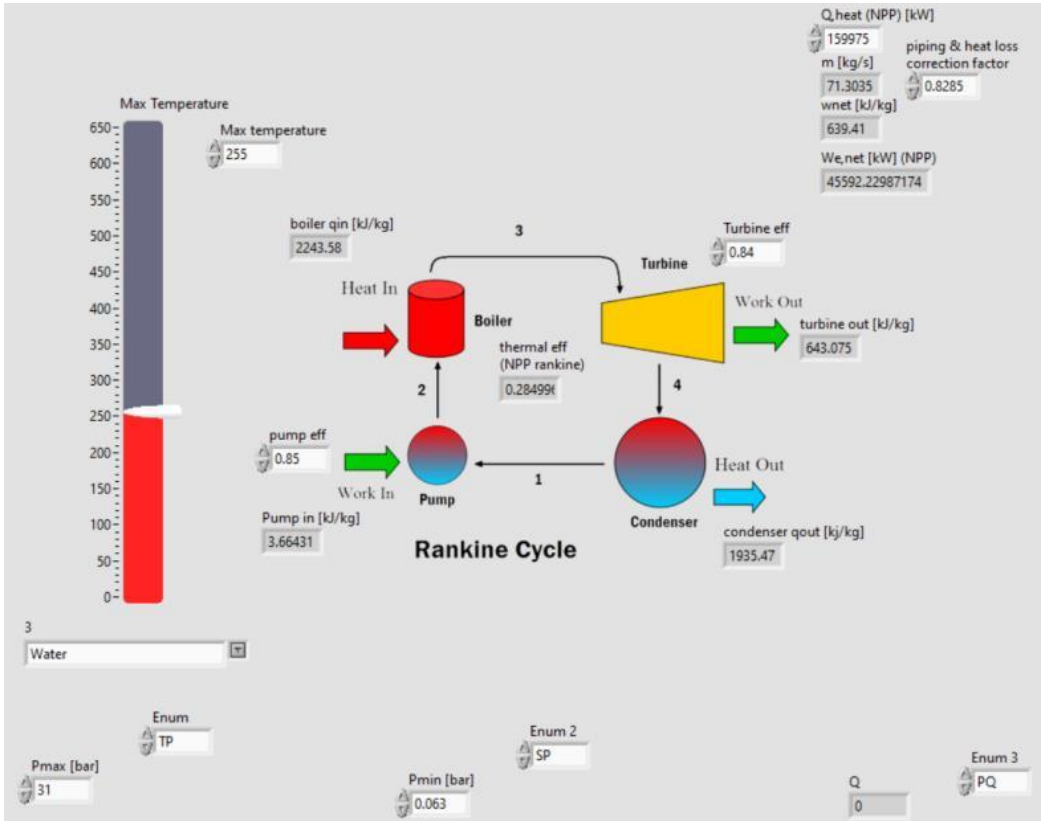


System level model of a iPWR type SMR with prototypic **Rankine energy** conversion cycle, as modeled using **LabVIEW**.

*D. Popov and A. Borissova, "Innovative configuration of a hybrid nuclear-parabolic trough solar power plant," Int. J. Sustain. Energy, vol. 37, no. 7, pp. 616–639, 2018, doi: 10.1080/14786451.2017.1333509*

# Concentrated Solar Power (CSP)

- Produces **heat energy** at **530 $^{0}$C** (thanks to molten salt as a fluid).
- Capable to produce $H_2$.
- Mirrors direct sunlight to a receiver.
- The thermal energy collected in the receiver powers a steam turbine, which provides electricity.

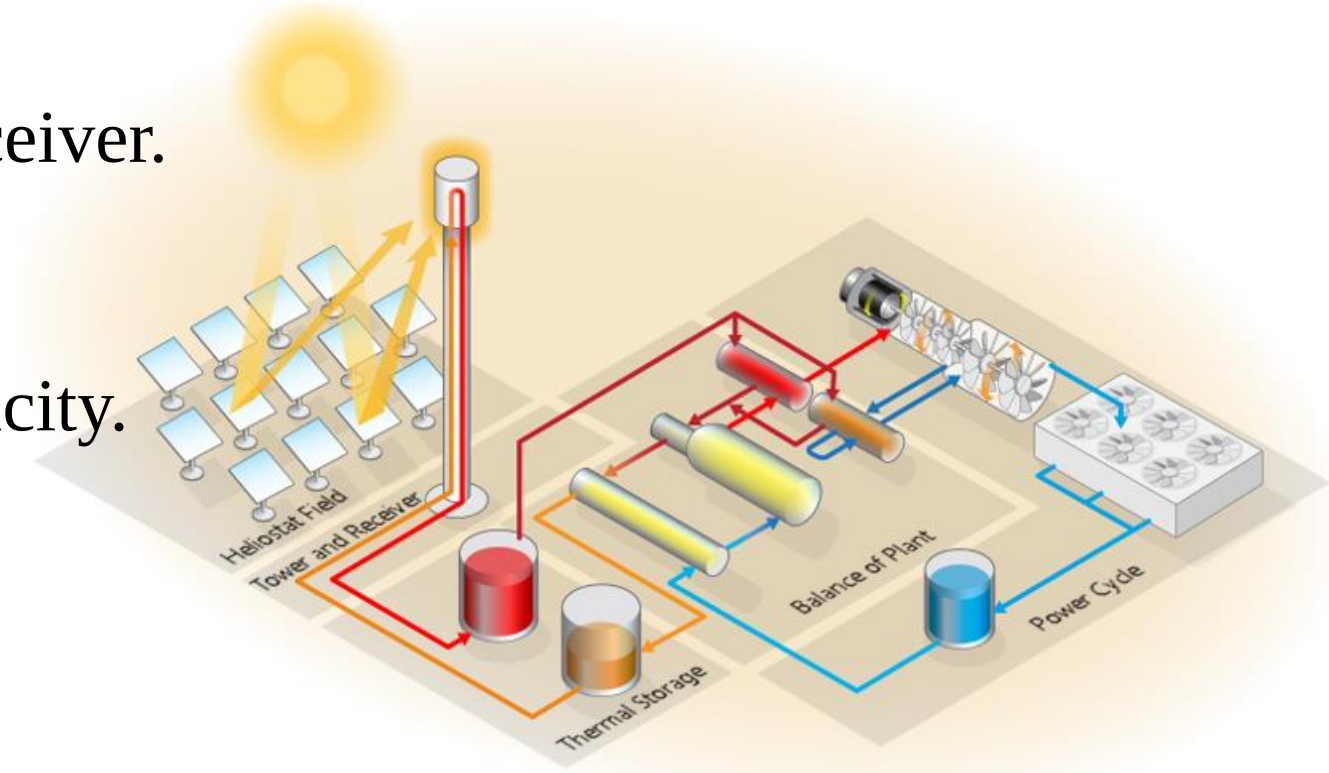


CSP Plant schematic produced by SAM

*Taken from SAM software*

- solar field (heliostats),
- thermal storage,
- power block.

# Concentrated Solar Power (CSP)

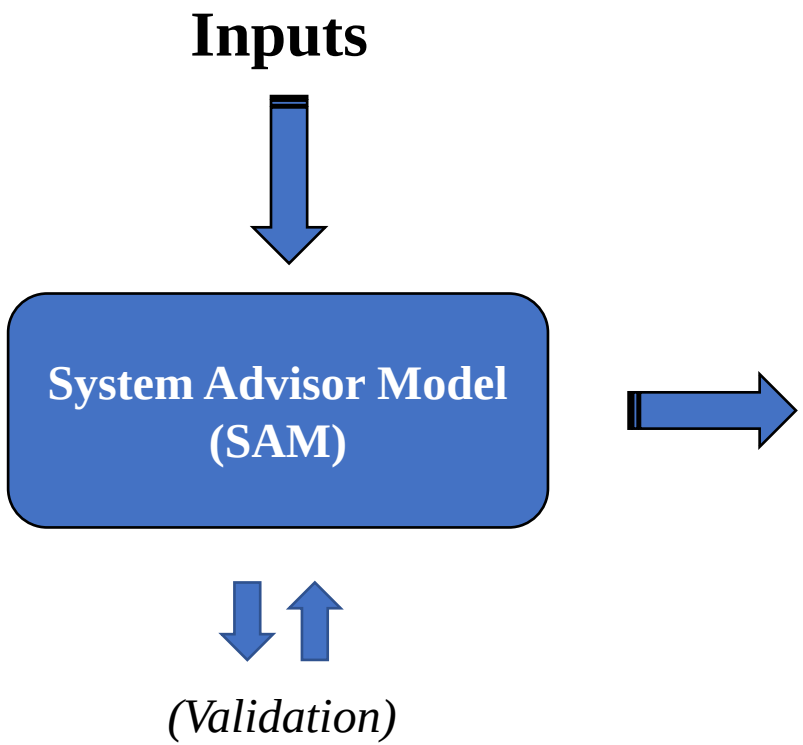


## Outputs

| Total hour | Day | Month | Hour | Electricity to grid \| ($kW_e$) | Electricity from grid \| ($kW_e$) | PC input energy \| ($kW_{th}$) | Net Efficiency |
|---|---|---|---|---|---|---|---|
| 1 | 1 | 1 | 0 | 9983.48 | 0 | 120593 | 0.082 |
| 2 | 1 | 1 | 1 | 34724.6 | 0 | 123414 | 0.281 |
| 3 | 1 | 1 | 2 | 34659.8 | 0 | 123263 | 0.281 |
| : | : | : | : | : | : | : | : |
| 8758 | 31 | 12 | 21 | 44009.3 | 0 | 121110 | 0.363 |
| 8759 | 31 | 12 | 22 | 43921.1 | 0 | 120896 | 0.363 |
| 8760 | 31 | 12 | 23 | 0 | 0 | 60837.1 | 0 |

An indication of one year of hourly based data of CSP (Daggett Barstow, California).

*D. Popov and A. Borissova, "Innovative configuration of a hybrid nuclear-parabolic trough solar power plant," Int. J. Sustain. Energy, vol. 37, no. 7, pp. 616–639, 2018, doi: 10.1080/14786451.2017.1333509*

# Cu-Cl Thermo-chemical $H_2$ Production Cycle

- Thermally separating water into oxygen and hydrogen using clean energy sources that do not emit greenhouse gases.
- Owing to chemical compounds and reactions.
- Requires 200 kJ at **525 $^0$C heat energy**, 25 kJ electrical energy per mol-$H_2$.

*(traditional electrolysis requires **52.4 kJ** heat energy at less than 100 $^0$C, **363.5 kJ** electrical energy per kg-$H_2$)*

- $2CuCl_2(s) + H_2O(g) \rightarrow Cu_2OCl_2(s) + 2HCl(g)$
- $Cu_2OCl_2(s) \rightarrow ½\ \mathbf{O_2(g)} + 2CuCl(l)$
- $2CuCl(aq) + 2HCl(aq) \rightarrow \mathbf{H_2(g)} + 2CuCl_2(aq)$
- $CuCl_2(aq) \rightarrow CuCl_2(s)$

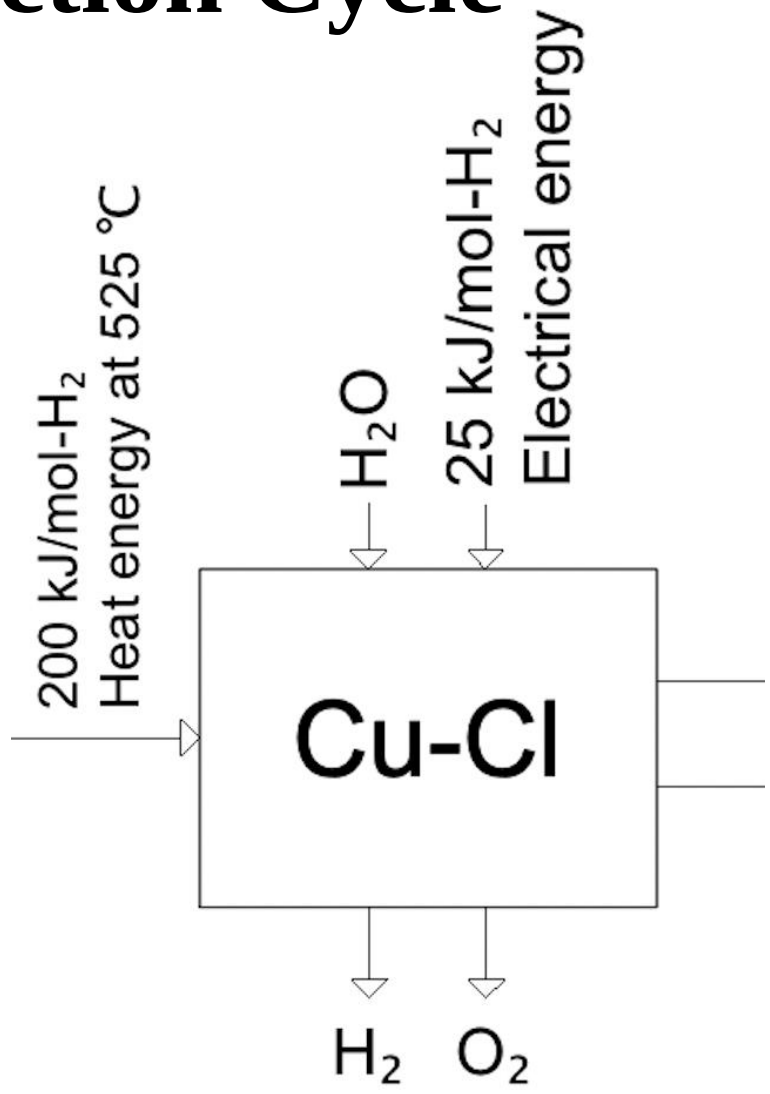


Cu-Cl cycle

# Modelling & Integration of N-RHES

- NPP and CSP produce heat and as Cu-Cl requires more heat energy than electricity. Therefore, all subsystems perform harmonically each other.
- **NPP** and **CSP** each have their **own Rankine power cycle** for energy generation.
- Electricity from NPP to CSP to keep molten-salt in a liquid form

A schematic of NHES.

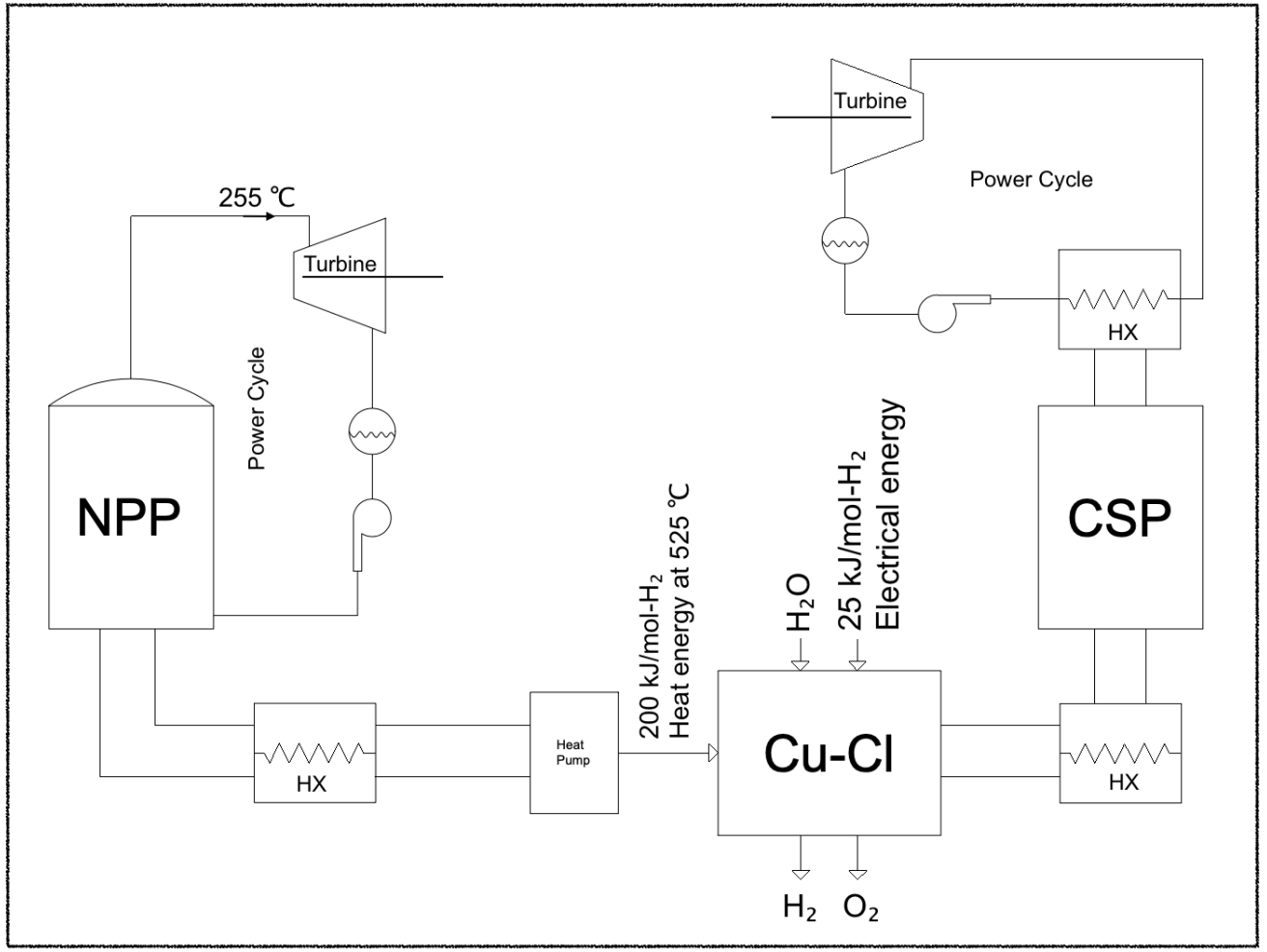

# Modelling & Integration of Nuclear-Renewable Hybrid Energy System (N-RHES)

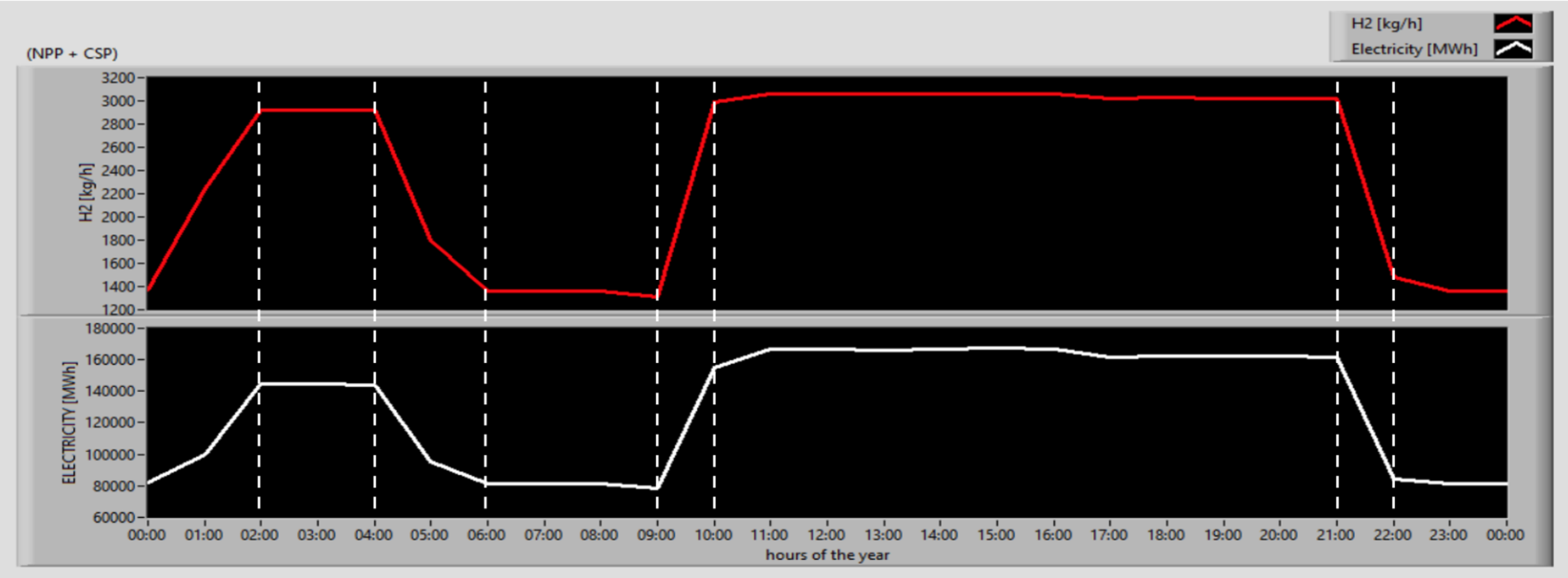


Results from simulation of total hydrogen [kg] and electricity production [MWh] for **24 hour period, from a combined NPP and CSP source.**

- The amount of heat power of **NPP and/or CSP** are defined as a **percentage** to produce hydrogen and the left heat power of NPP and/or CSP is used to produce electricity as shown in the figure.
- By specifying **a date range**, the amount of hydrogen and power produced is calculated and presented individually on the graph, thanks to the code written using **LabVIEW**.

# Modelling & Integration of N-RHES

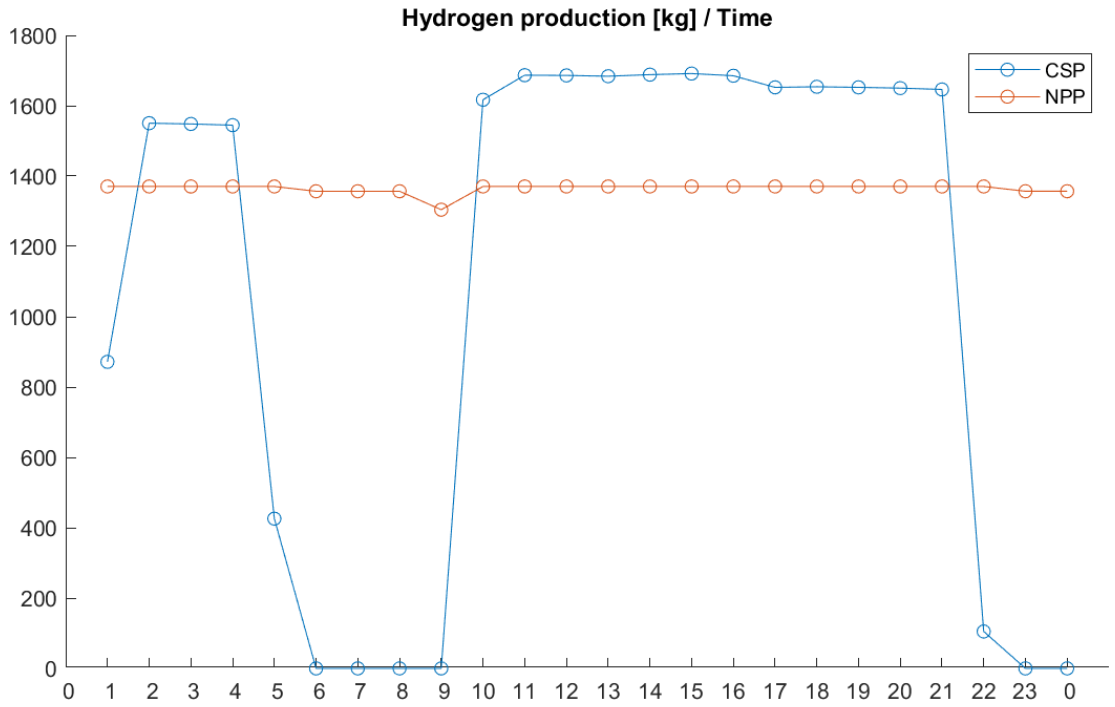


An indication of 24-hour period hydrogen production in kg by employing 50% of NPP and 50% of CSP sources, (January 1st).

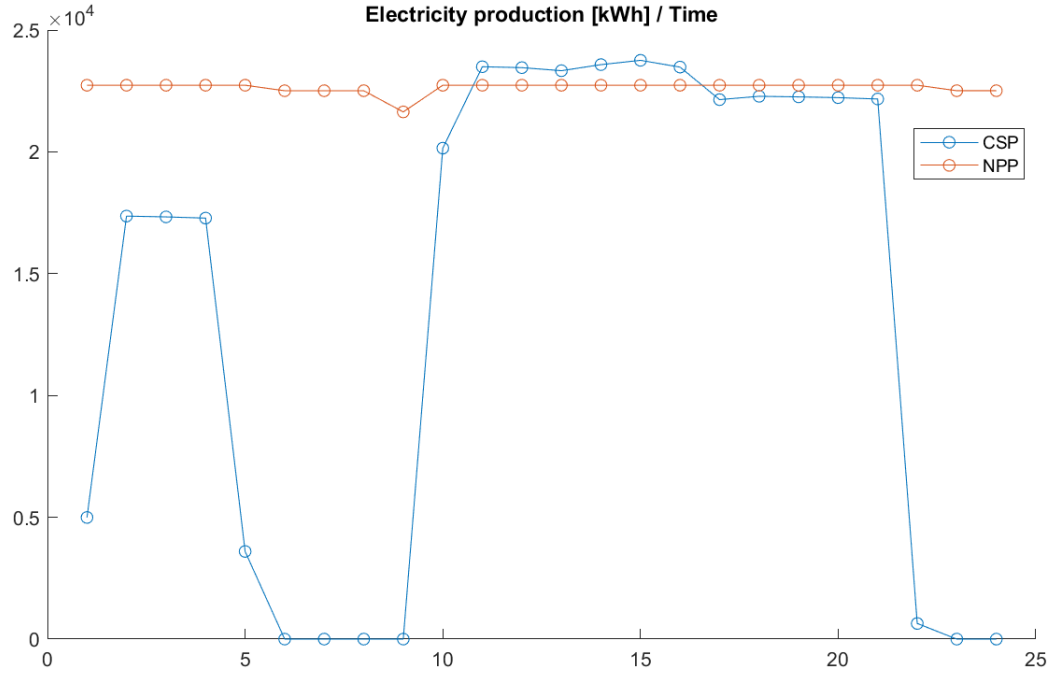


An indication of 24-hour period electricity production in kWh by employing 50% of NPP and 50% of CSP, (January 1st).

# Modelling & Integration of N-RHES

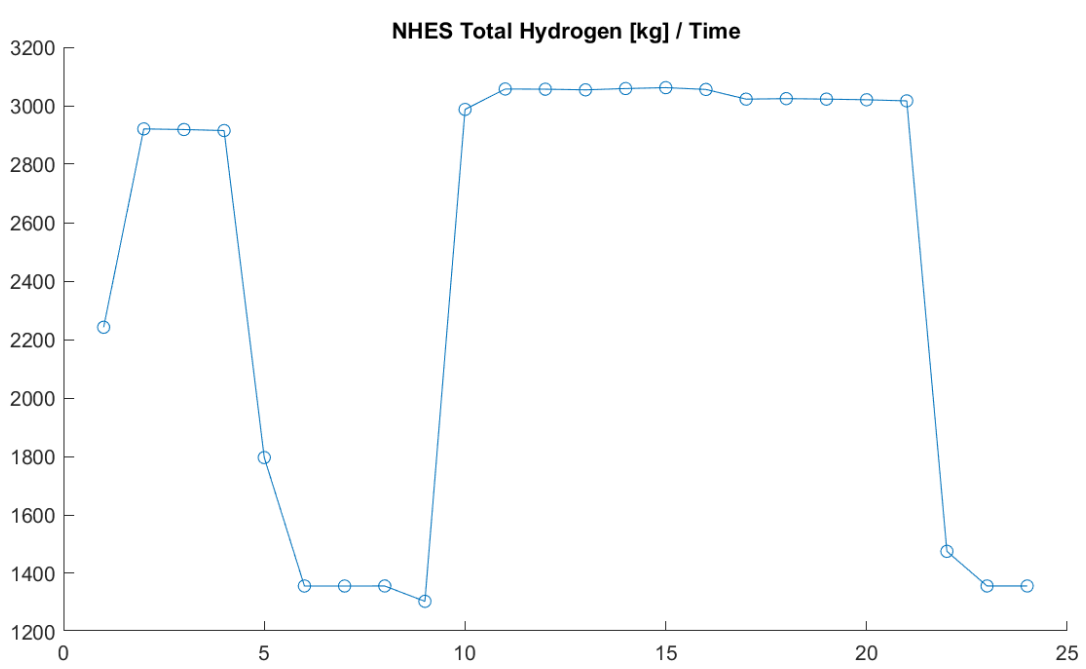


An indication of 24-hour period total hydrogen production in kg by employing 50% of NPP and 50% of CSP sources, (January 1st).

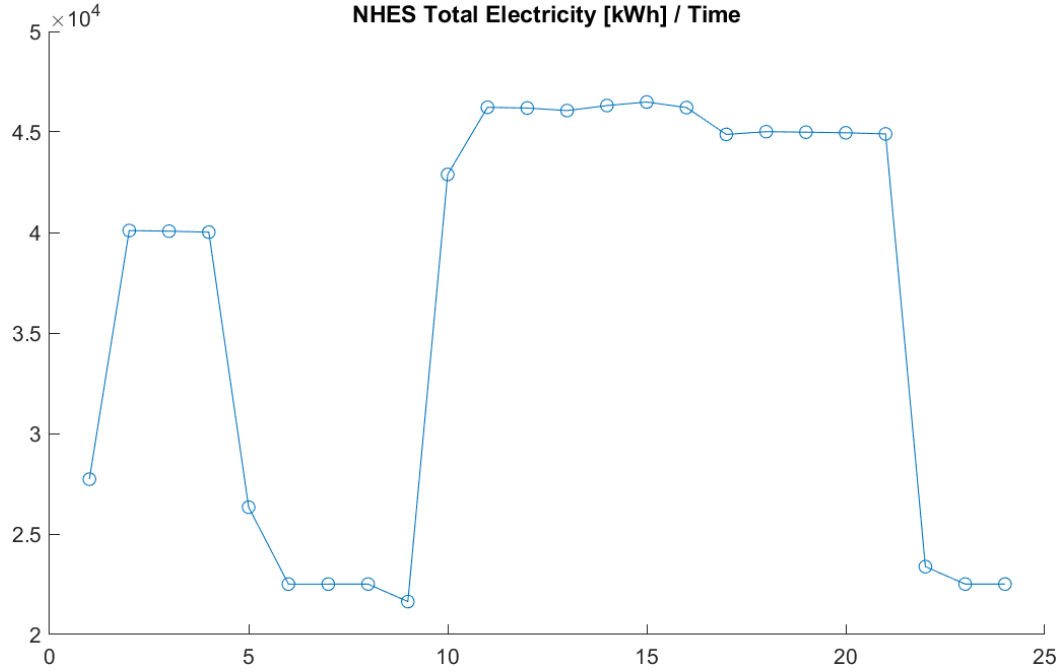


An indication of 24-hour period hydrogen production in kg by employing 50% of NPP and 50% of CSP sources, (January 1st).

# Results / Scenarios (non-optimized)

| | | $H_2$ in kg | | | | | | | |
|---|---|---|---|---|---|---|---|---|---|
| | | **Winter1** | **Winter2** | **Spring1** | **Spring2** | **Summer1** | **Summer2** | **Fall1** | **Fall2** |
| | | *DEC-15 (9.4 °C)* | *FEB-11 (26.7 °C)* | *MAR-11 (13.3 °C)* | *MAY-31 (38.9 °C)* | *JUN-10 (30 °C)* | *JULY-10 (47.8 °C)* | *OCT-26 (18.3 °C)* | *SEP-7 (43.3 °C)* |
| **CSP1** | **25%** | 10331.9 | 14733.2 | 16909.9 | 19728.3 | 17388.7 | 16409.7 | 15115.1 | 4355.77 |
| **NPP1** | **25%** | 16386.2 | 16420.1 | 16440.6 | 16454 | 16417.1 | 16411.4 | 16420.4 | 16312.5 |
| **CSP2** | **50%** | 20663.8 | 29466.4 | 33819.9 | 39456.6 | 34777.4 | 32819.3 | 30230.2 | 8711.53 |
| **NPP2** | **50%** | 32772.5 | 32840.2 | 32881.2 | 32908.1 | 32834.1 | 32822.9 | 32840.8 | 32625.1 |
| **CSP3** | **75%** | 30995.6 | 44199.6 | 50729.8 | 59184.8 | 52166.1 | 49229 | 45345.3 | 13067.3 |
| **NPP3** | **75%** | 49158.7 | 49260.3 | 49321.7 | 49362.1 | 49251.2 | 49234.3 | 49261.1 | 48937.6 |
| **CSP4** | **100%** | 41327.5 | 58932.8 | 67639.7 | 78913.1 | 69554.9 | 65638.6 | 60460.5 | 17423.1 |
| **NPP4** | **100%** | 65545 | 65680.5 | 65762.3 | 65816.2 | 65668.2 | 65645.8 | 65681.5 | 65250.2 |

- Although the NPP's power remains the same, some differences are observed **in the production amount of hydrogen and electricity via NPP**: in fact the NPP meets the CSP required electricity for keeping molten salt in a liquid form and all auxiliary components needed at all times.

- Despite that the **summer2** average outside temperature is more than that of **summer1**, there is a decrease in the production of hydrogen or electricity via CSP in the **summer2**. **Daylight** time in summer2 can be shown as the reason for this situation.

# Results / Scenarios (non-optimized)

| | | Electricity in kWh | | | | | | | |
|---|---|---|---|---|---|---|---|---|---|
| | | **Winter1** | **Winter2** | **Spring1** | **Spring2** | **Summer1** | **Summer2** | **Fall1** | **Fall2** |
| | | *DEC-15 (9.4 °C)* | *FEB-11 (26.7 °C)* | *MAR-11 (13.3 °C)* | *MAY-31 (38.9 °C)* | *JUN-10 (30 °C)* | *JULY-10 (47.8 °C)* | *OCT-26 (18.3 °C)* | *SEP-7 (43.3 °C)* |
| **CSP1** | **75%** | 4.14E+05 | 5.88E+05 | 6.79E+05 | 7.77E+05 | 6.64E+05 | 6.12E+05 | 6.06E+05 | 1.54E+05 |
| **NPP1** | **75%** | 8.17E+05 | 8.19E+05 | 8.20E+05 | 8.21E+05 | 8.19E+05 | 8.19E+05 | 8.19E+05 | 8.14E+05 |
| **CSP2** | **50%** | 2.76E+05 | 3.92E+05 | 4.52E+05 | 5.18E+05 | 4.43E+05 | 4.08E+05 | 4.04E+05 | 1.03E+05 |
| **NPP2** | **50%** | 5.45E+05 | 5.46E+05 | 5.47E+05 | 5.47E+05 | 5.46E+05 | 5.46E+05 | 5.46E+05 | 5.42E+05 |
| **CSP3** | **25%** | 1.38E+05 | 1.96E+05 | 2.26E+05 | 2.59E+05 | 2.21E+05 | 2.04E+05 | 2.02E+05 | 5.14E+04 |
| **NPP3** | **25%** | 2.72E+05 | 2.73E+05 | 2.73E+05 | 2.74E+05 | 2.73E+05 | 2.73E+05 | 2.73E+05 | 2.71E+05 |
| **CSP4** | **100%** | 5.52E+05 | 7.84E+05 | 9.05E+05 | 1.04E+06 | 8.86E+05 | 8.17E+05 | 8.08E+05 | 2.06E+05 |
| **NPP4** | **100%** | 1.09E+06 | 1.09E+06 | 1.09E+06 | 1.09E+06 | 1.09E+06 | 1.09E+06 | 1.09E+06 | 1.08E+06 |

- Considering fall1 and fall2, the decrease in the amount of hydrogen produced by CSP despite the fact that **the temperature in fall2 is higher than that in fall1 is an indication that not only the temperature but also other weather-related parameters play a very important role in the power of the CSP.**

# Results / Seasonal Daily Averages (non-optimized)

(depending on the power of sources)

**Hydrogen Production**

The average daily hydrogen production amounts;

- **In spring**, **almost equal** amounts of hydrogen are produced, although the percentage rates of the sources are **different**.
- However, **in summer**, there is an **increase** in hydrogen production due to the increased energy of CSP.
- **In the winter**, the amount of hydrogen produced by 100% NPP power is lower. **The reason for this is that the CSP's power decreases in the winter, and the NPP provides the electrical energy needed to keep the CSP running.**

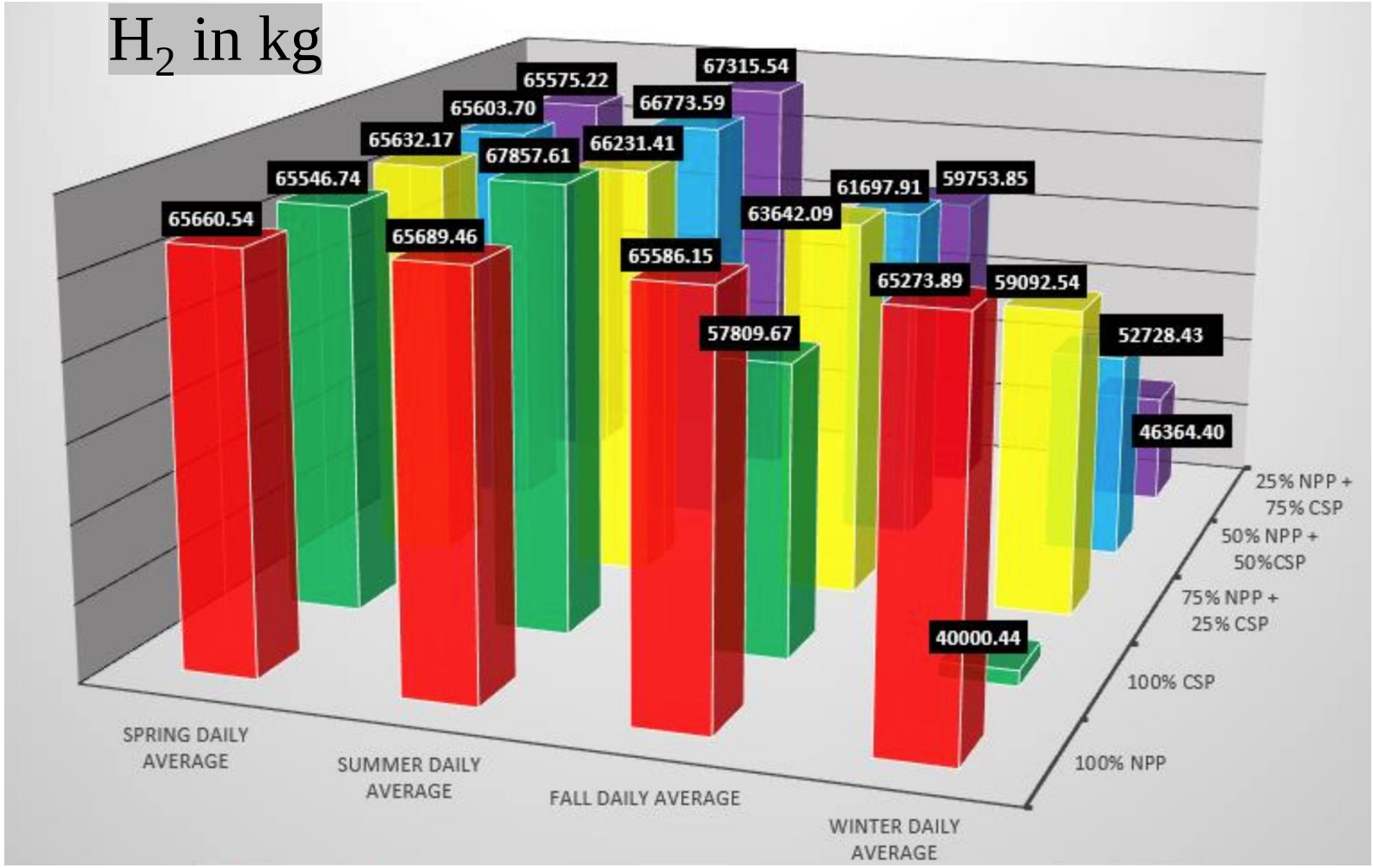


Seasonal comparison of hydrogen production depending on reliance on NPP, CSP or jointly in percentage given.

100% NPP
100% CSP
75% NPP + 25% CSP
50% NPP + 50% CSP
25% NPP + 75% CSP

# Results / Seasonal Daily Averages (non-optimized)

(depending on the power of sources)

**Electricity Production**

- The amount of electricity generated is decreasing in fall and winter. Although the ratio of CSP increases, the amount of electricity produced decreases.

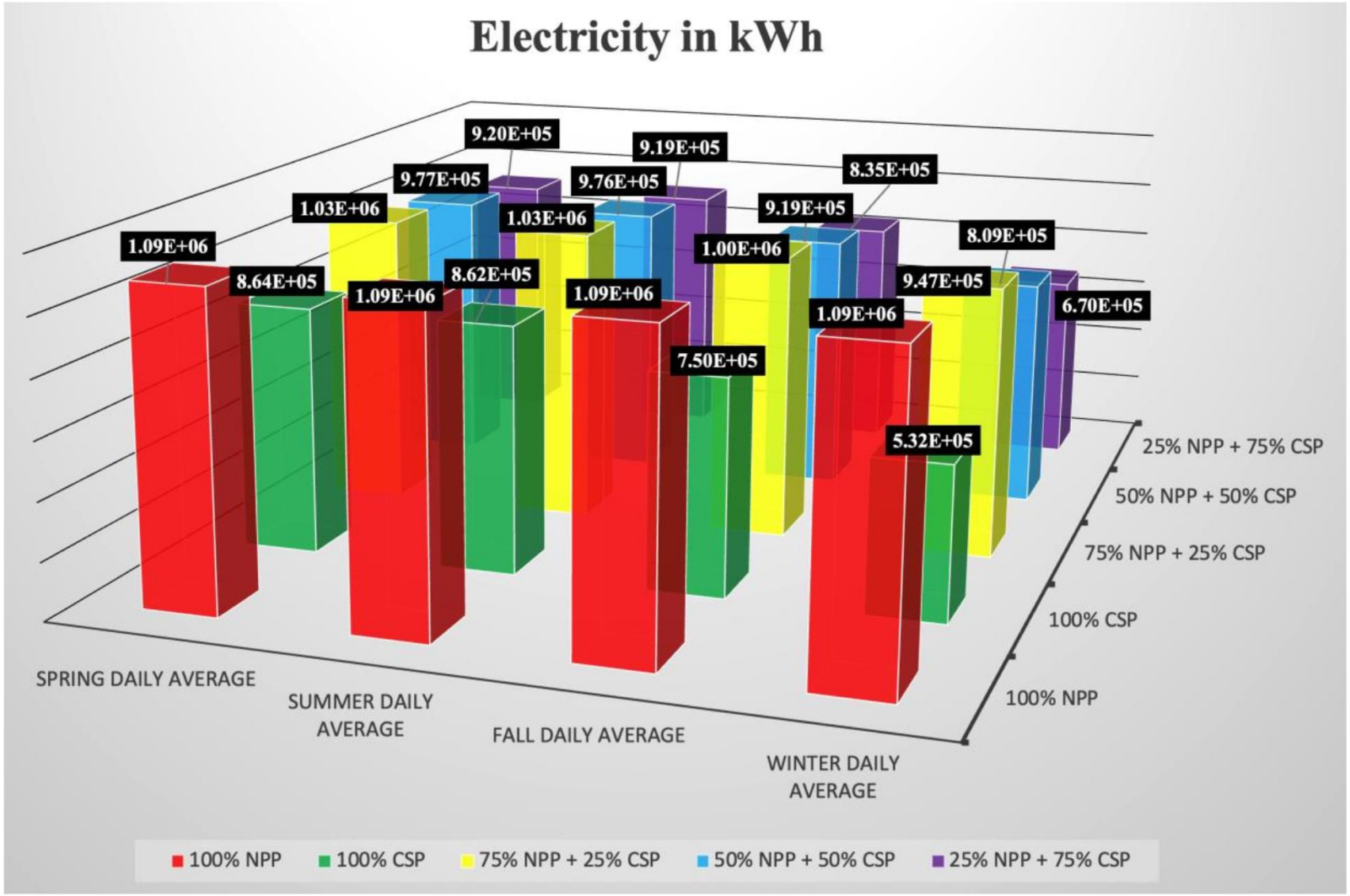


Comparison of electricity production depending on seasonal, and generation source (NPP, CPS or combination).

# Optimization of N-RHES

- Total hydrogen in kg
- Total electricity in kWh

- **Total profit in USD**
- **Total heat equivalent in kJ**

**Multi-objective optimization based on Genetic Algorithm with Pareto Front Principle**

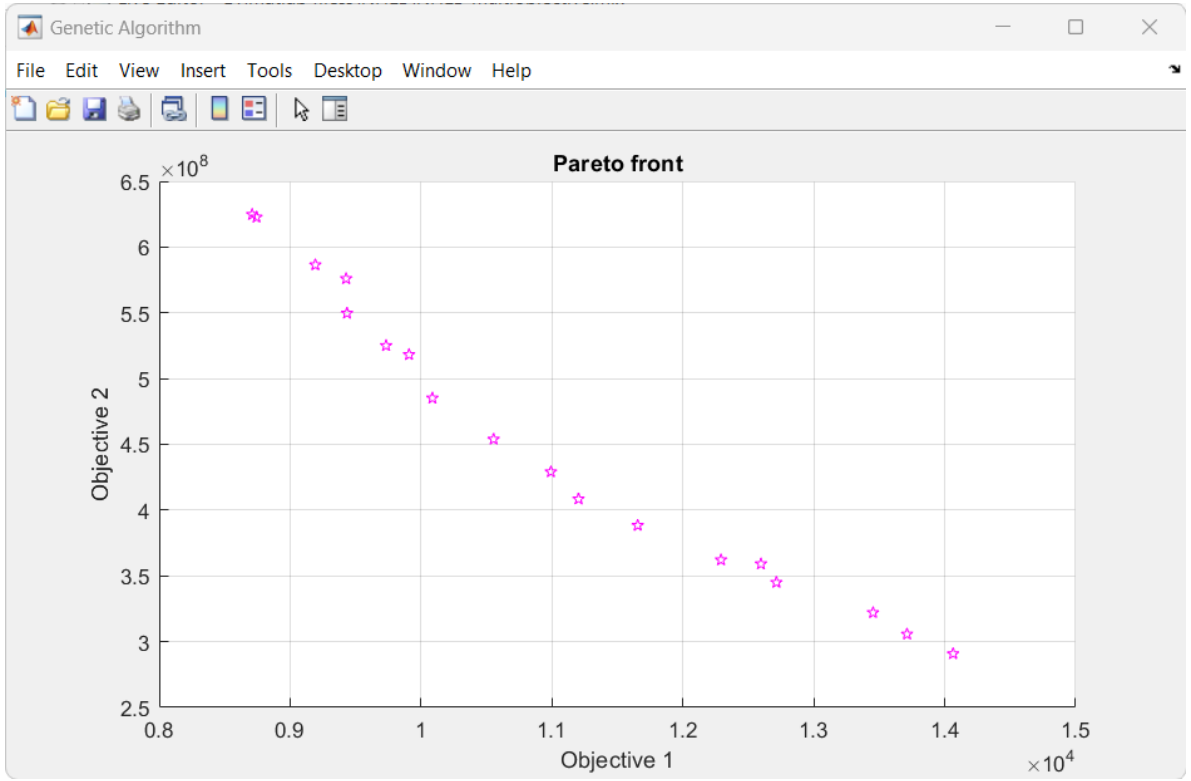


An indication of multi-objective Genetic Algorithm Pareto Front.
*Objective 1: Total profit*
*Objective 2: Total heat equivalent*

*Assuming that 1 kg-$H_2$ = 120.1 MJ heat energy, 1kJ electrical energy = 1 kJ heat energy*

# Price Modelling

- 8760 Hourly Ontario Electricity Price (HOEP) from "www.ieso.ca".

- **Hydrogen Price Modelling;**

  - hydrogen price is between US$ 1.00 and US$ 1.80 per kg-hydrogen,
  - a relationship between hydrogen price and electricity price,
  - From a reference paper (Pinsky, 2020), 1 kg of $H_2$ with electrolysis requires approximately 50 kWh electricity,
  - Therefore, the price of 50 kWh electricity (HOEP) is added to the base price (US$ 1).

  *To calculate a realistic overall $H_2$ price depending on the hours of a day:*

  - If the hour is between **1:00am and 5:00am**, "Hourly Ontario 50 kWh-Electricity Price" is multiplied by the square of "Hourly Ontario 1 kWh Electricity Price".

  - If the hour is **not** between **1:00am and 5:00am**, "Hourly Ontario 50 kWh Electricity Price" is multiplied by "Hourly Ontario 1 kWh Electricity Price".

*Hydrogen Energy Systems, LLC [Internet]. 2022 Nov 1. Available from: https://heshydrogen.com/hydrogen-fuel-cost-vs-gasoline/.*
*R. Pinsky, P. Sabharwall, J. Hartvigsen, and J. O'Brien, "Comparative review of hydrogen production technologies for nuclear hybrid energy systems," Prog. Nucl. Energy, vol. 123, p. 103317, 2020, doi: 10.1016/j.pnucene.2020.103317.*

# Results based on Multi-objective Optimization

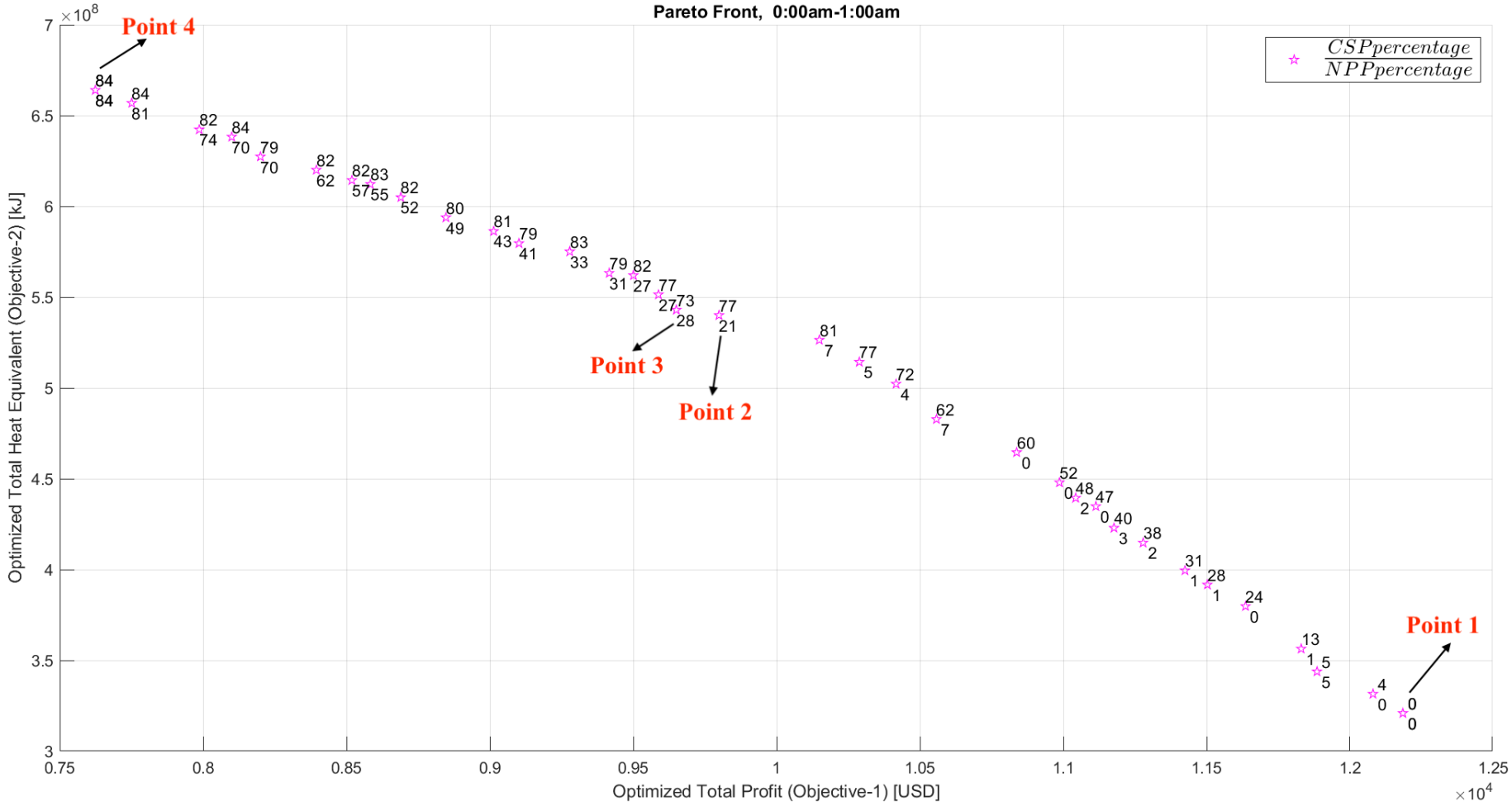


Between point 2 and point 3,
While total heat equivalent amount changes only **0.5%**, the total profit amount changes by **1.5%**.

Applying MOGA for N-RHES **(JUN-15, between 00:00am and 1:00am).**

# Results based on Multi-objective Optimization

| | **Results** / JUN-15, between 00:00am and 1:00am | | | | | |
|---|---|---|---|---|---|---|
| | **Non-Optimized** | **Non-Optimized** | **Optimized Point 1** | **Optimized Point 2** | **Optimized Point 3** | **Optimized Point 4** |
| NPP percentage to produce $H_2$ | 50% | 25% | 0.47% | 21.30% | 28.91% | 84.94% |
| CSP percentage to produce $H_2$ | 50% | 25% | 0.00% | 77.20% | 73.17% | 84.98% |
| Total profit (**Obj.1**) | 9.51E+03 | 1.09E+04 | **1.22E+04** | 9.80E+03 | 9.65E+03 | 7.62E+03 |
| Total heat equivalent (**Obj.2**) | 5.22E+08 | 4.21E+08 | 3.21E+08 | 5.40E+08 | 5.43E+08 | **6.64E+08** |
| Total $H_2$ amount [kg] | 3.02E+03 | 1.51E+03 | 1.28E+01 | 3.13E+03 | 3.20E+03 | 5.13E+03 |
| Total electricity amount [kWh] | 4.45E+04 | 6.67E+04 | 8.87E+04 | 4.57E+04 | 4.40E+04 | 1.34E+04 |

- Between point 2 and point 3,
  While total heat equivalent amount changes only **0.5%**, the total profit amount changes by **1.5%**.

# Results based on Multi-objective Optimization

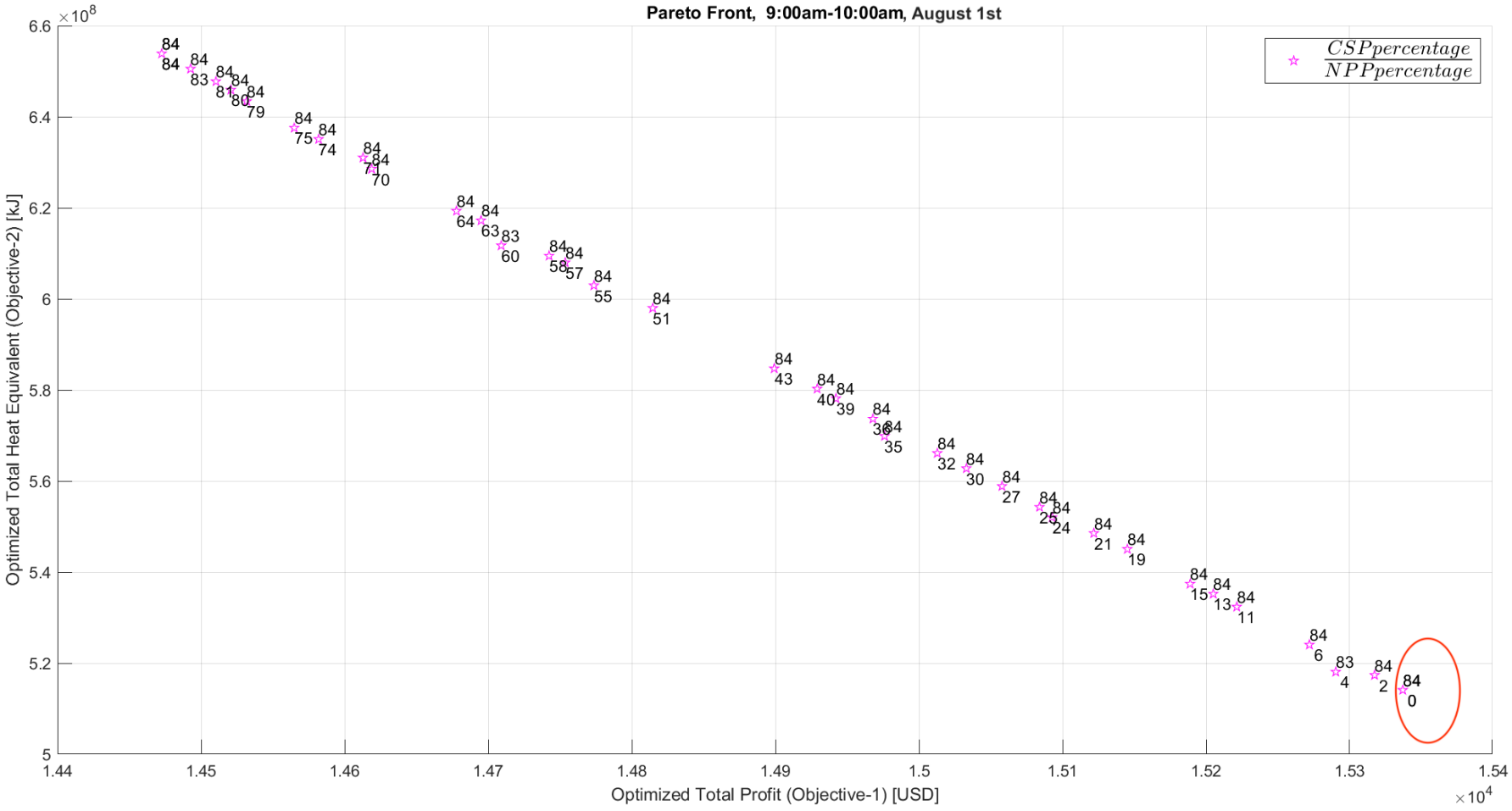


*Another example;*

When max profit is obtained with **0% CSP** and **0% NPP** on June 15,

Max. profit is obtained with **84% CSP** and **0% NPP** on August 1.

An optimized result for **August 1st, 9:00am and 10:00am.**

# Comparative Results

## *Comparative results of non-optimized versus optimized results for one day*

24-hour period starting on August 1st, 00:00am and ending on August 1st, 11:59pm.

| All day, August 1st | | | |
|---|---|---|---|
| **CSP** | **NPP** | **Total Profit** | **Total Heat Equivalent** |
| 50% | 50% | 2.49E+05 | 1.05E+10 |
| 25% | 25% | 2.54E+05 | 8.47E+09 |
| **Optimized** | | 2.72E+05 | 1.33E+10 |

# Total Profit

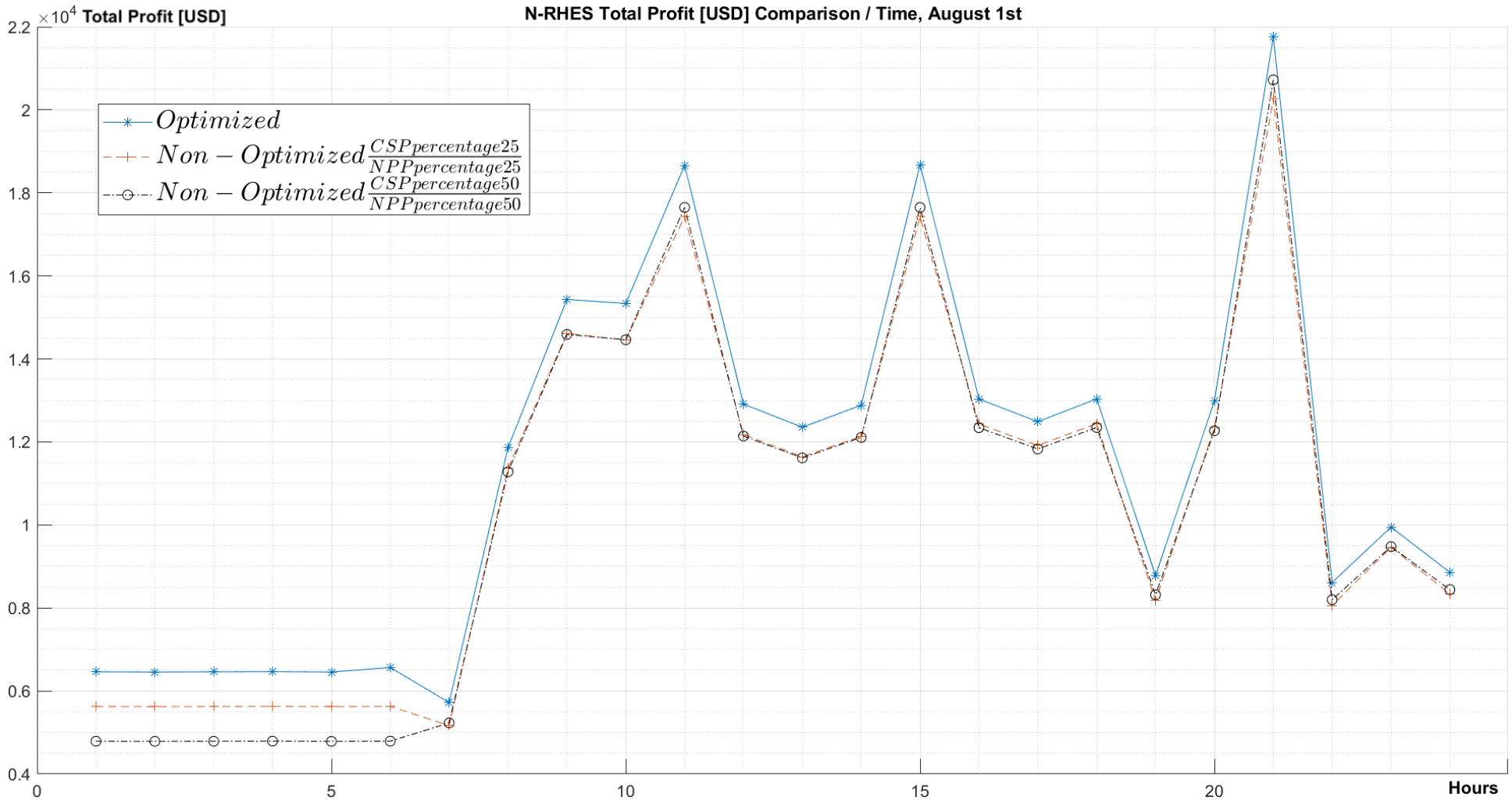


**Total Profit** (objective-1) comparison based on scenarios, **optimized** N-RHES for maximum profit,

**25%NPP-25%CSP** and

**50%NPP-50%CSP** on **August 1st.**

# Production Amounts

*For maximizing profit*

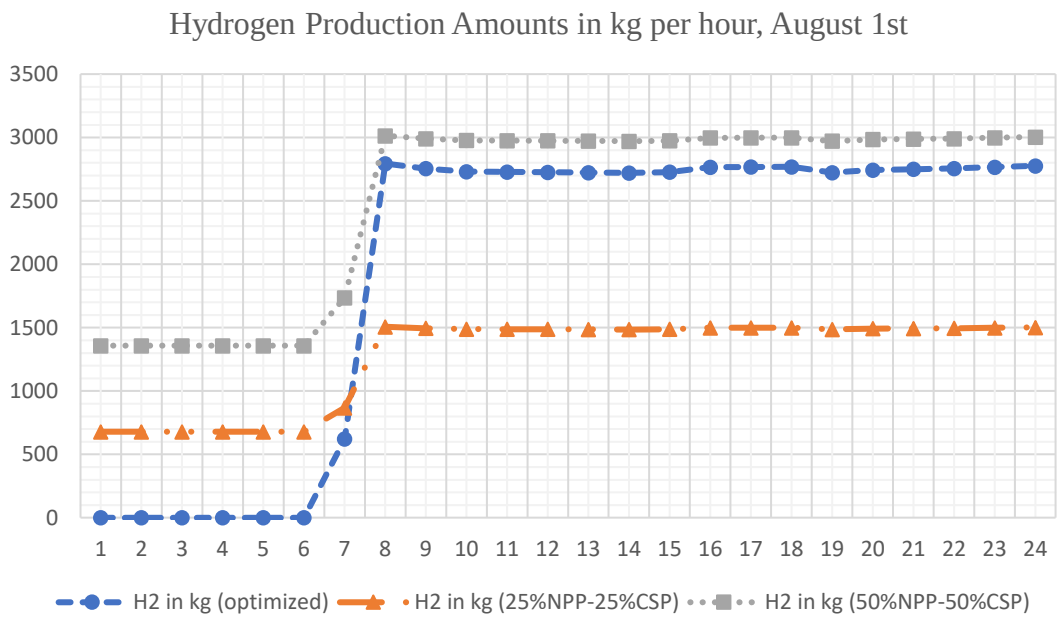


Hydrogen production amounts depending on three scenarios (optimized N-RHES for max. profit, 25%NPP-25%CSP and 50%NPP-50%CSP) on August 1st

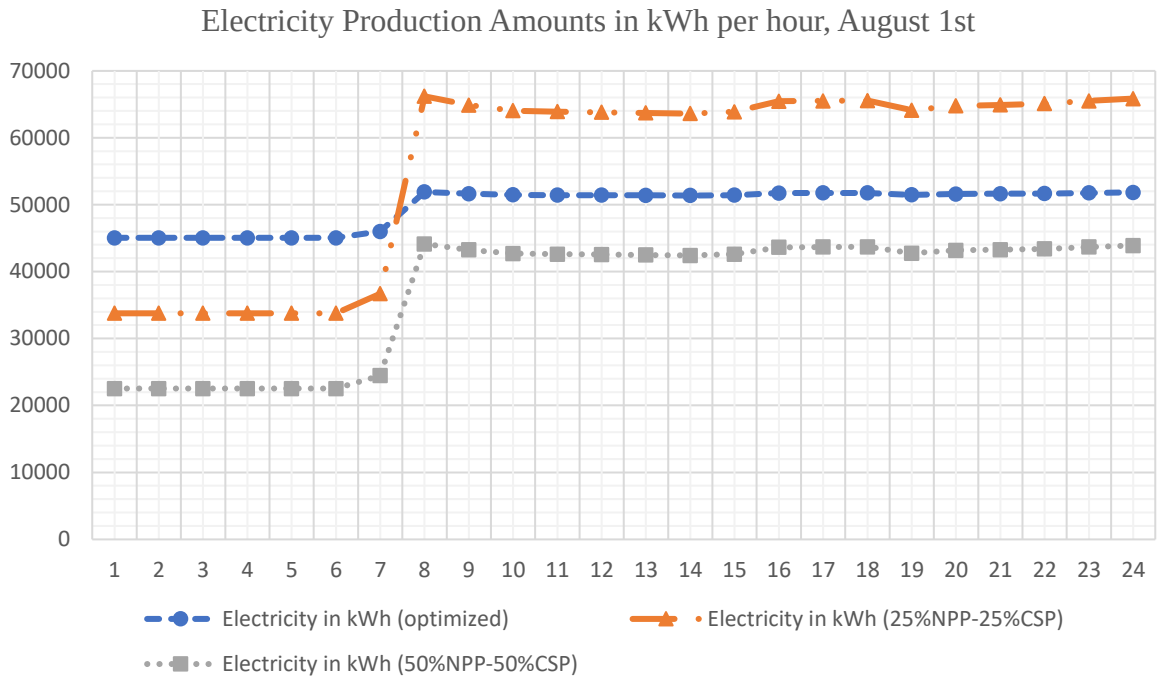


Electricity production amounts depending on three scenarios (optimized N-RHES for max. profit, 25%NPP-25%CSP and 50%NPP-50%CSP) on August 1st

# Total Heat Equivalent

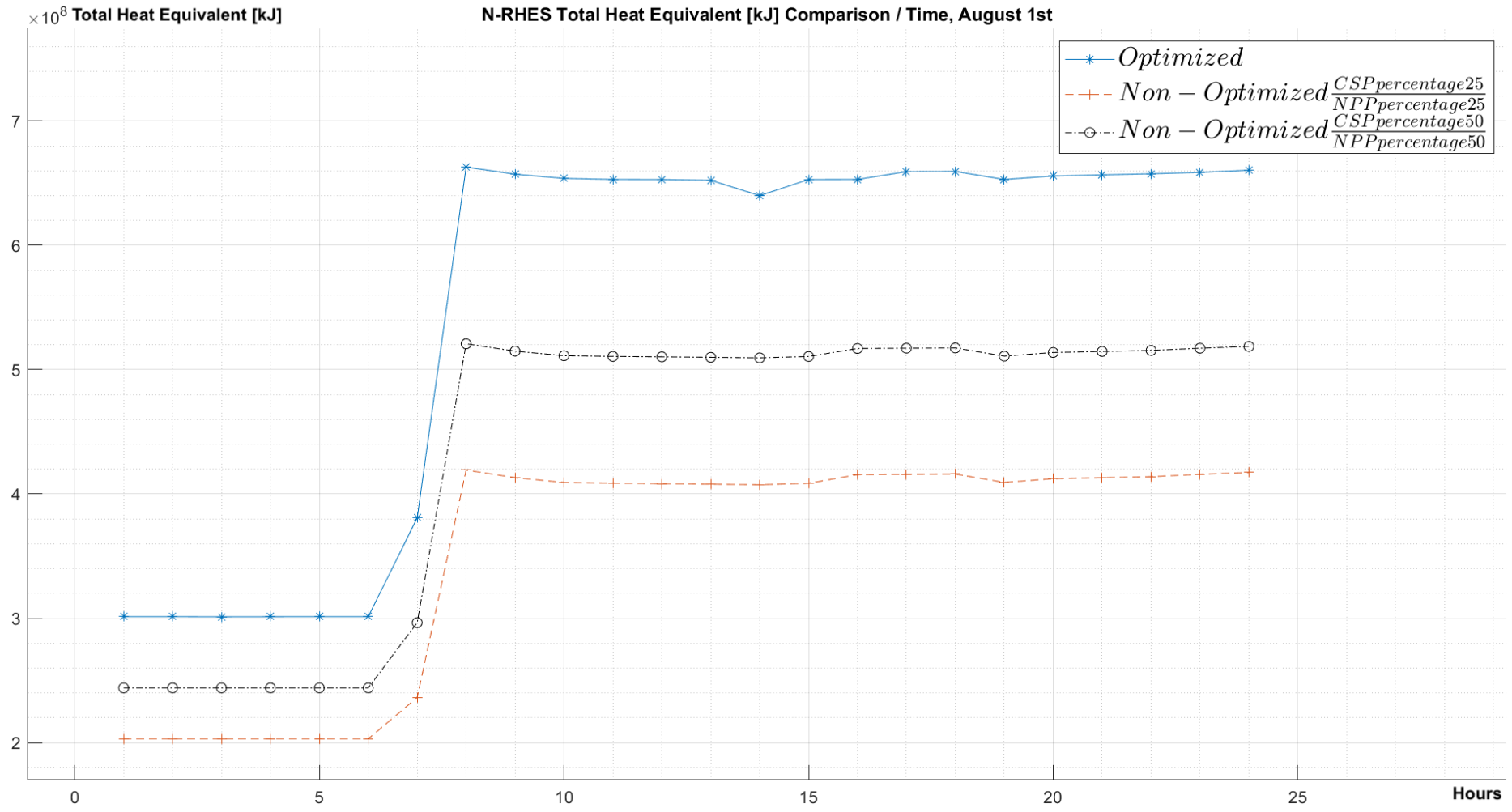


**Total Heat Equivalent** (objective-2) comparison based on scenarios,

**optimized** N-RHES for maximum total heat equivalent,

**25%NPP-25%CSP** and

**50%NPP-50%CSP**

**on August 1st.**

# Consideration of NPP Electricity Requirement

- For 100% full power operation, the electricity requirement (the unit service load) from the grid is around **6%** of the reactor full power capacity (total MWe).

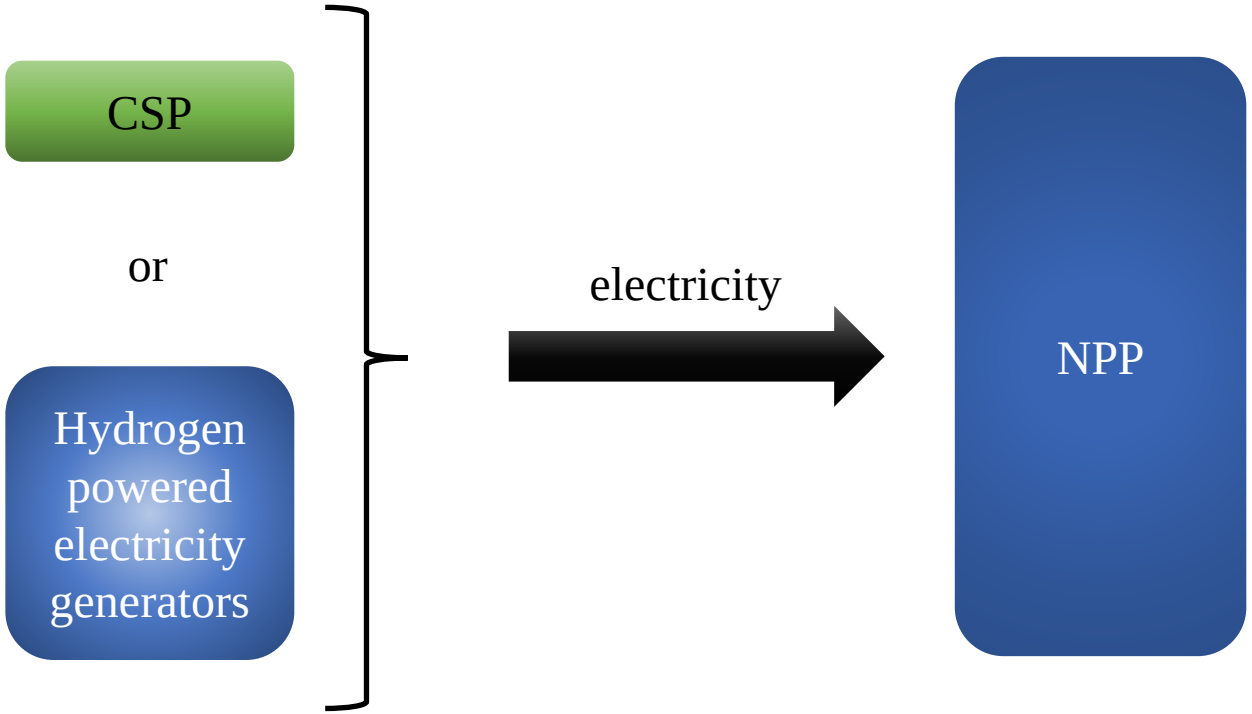


- **Hydrogen powered generators** perform with a **~60%** energy conversion from hydrogen heat energy (120.1 $MJ_{th}$ /1kg-$H_2$) to electrical energy (72.06 $MJ_e$ /1kg-$H_2$)
- **1kg-$H_2$ is equal to 20.01 $kWh_e$.**

*S. Ali, "Regarding approximate electricity requirements in a nuclear generating station itself", private communication, November 2022.*

*Stern, A. G. (2018). A new sustainable hydrogen clean energy paradigm. International Journal of Hydrogen Energy, 43(9), 4244–4255. doi:10.1016/j.ijhydene.2017.12.180.*

# Consideration of NPP Electricity Requirement

Hourly required $H_2$ amount to meet NPP electricity demand on August 1st.

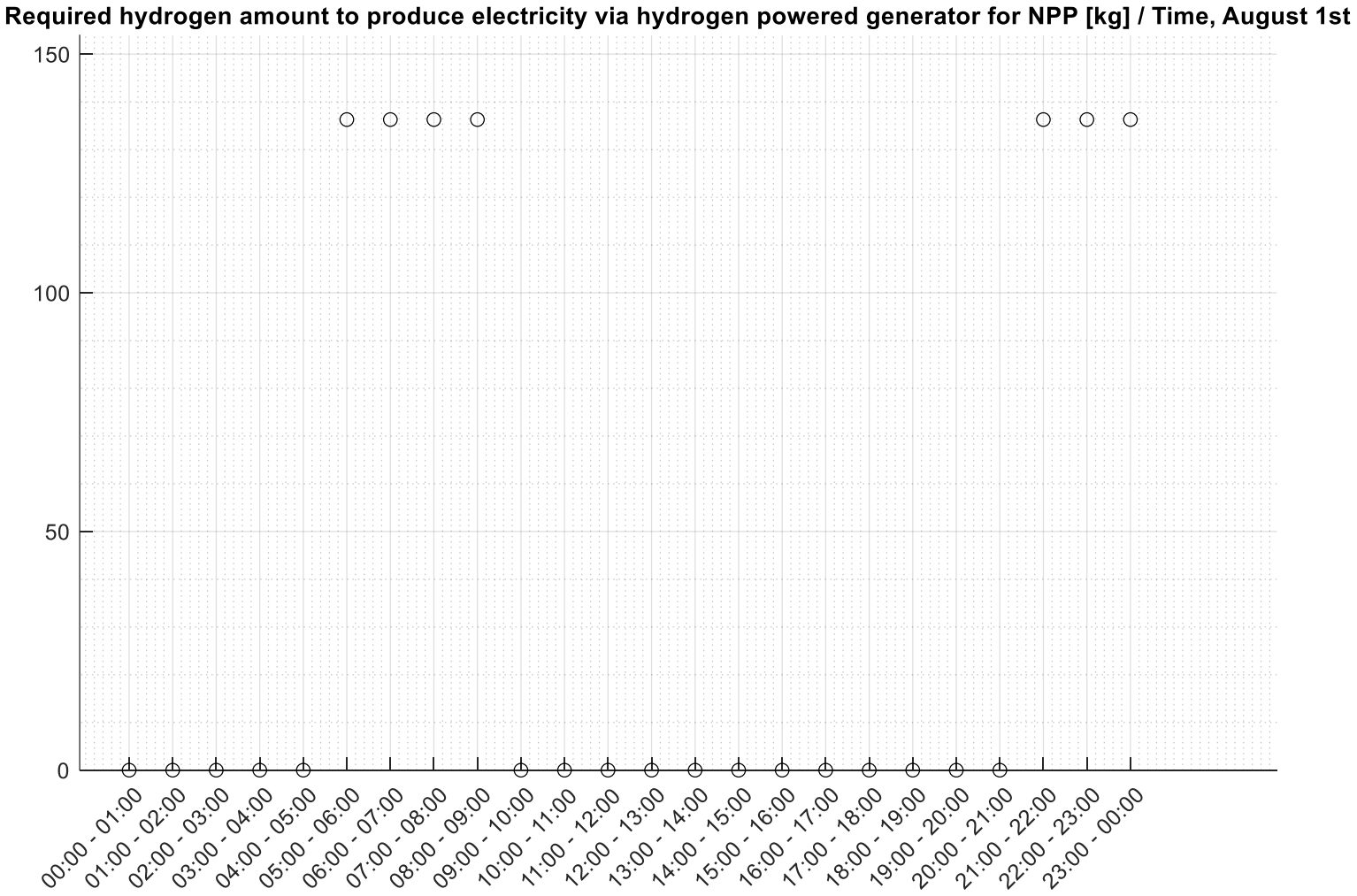


- 136.29 kg-$H_2$ per hour.
- Totally 954 kg-$H_2$ on August 1st.
- If no CSP power, 3271 kg-$H_2$.

# Consideration of SMR Safety-in-design

- Provided that SMRs are co-located with a **renewable** plant and/or a **hydrogen plant** until there is (nuclear and related) regulatory change in terms of the emergency planning zone (EPZ) [132], which is required for all nuclear power plants, **Canadian Nuclear Safety Commission** (CNSC) (US, or national) **regulations will take precedence**.
- The **important** point on SMR safety-in-design is **the time evolution** of the accident, after the accident or event initiation. The time response, say **1 hour, 2, 4, 8, 24, or 48 hours after event start**, is crucial and connected to the **safety-in-design of the SMR** at the level of the (nuclear; SMR) safety system. Safety must always be upheld even if the SMR is connected to a **renewable energy** or **hydrogen production** facility. The safety of the SMR must not be compromised by any disruption to the **hydrogen** or **renewable energy plant.** These **time "slots"** are therefore related to safety-in-design and must be taken into account as a design variable and parameter. **Assuming that anything lasting more than 4 hours will need reactor shutdown**, it is divided into two categories: **under 4 hours and over 4 hours.**
- In terms of safety-in-design, the elapsed period after accident onset is thus generally linked to the SMR's design.

# Calculation for NPP Electricity Requirement

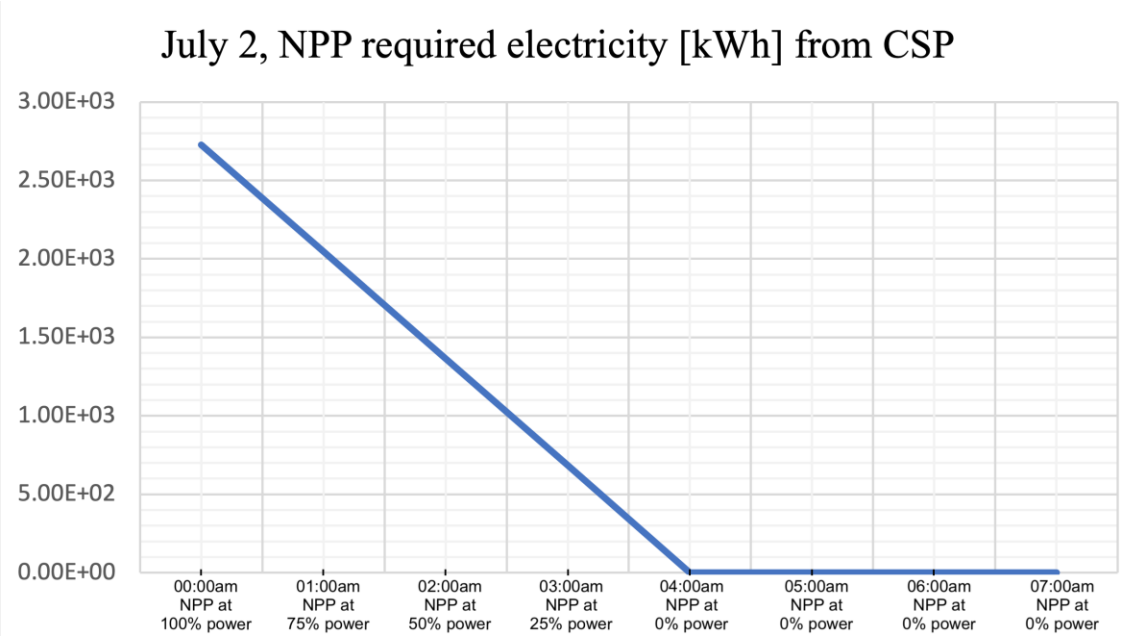


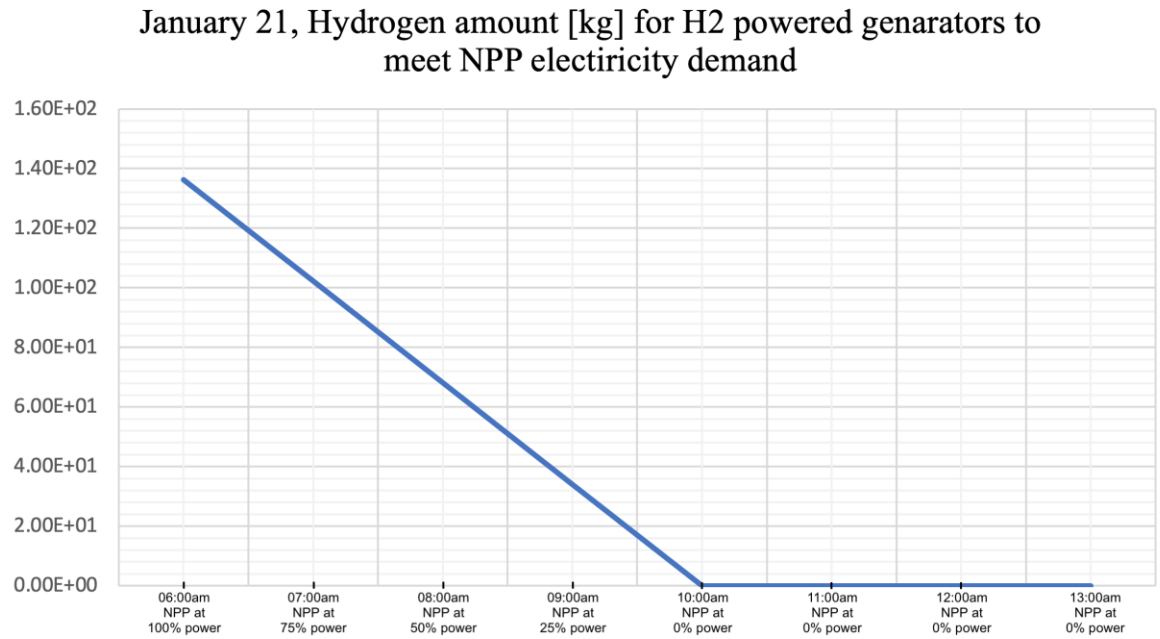


NPP electricity requirement while NPP power decreases from 100% to 0% in 4 hours.

# Consideration of SMR Safety-in-design

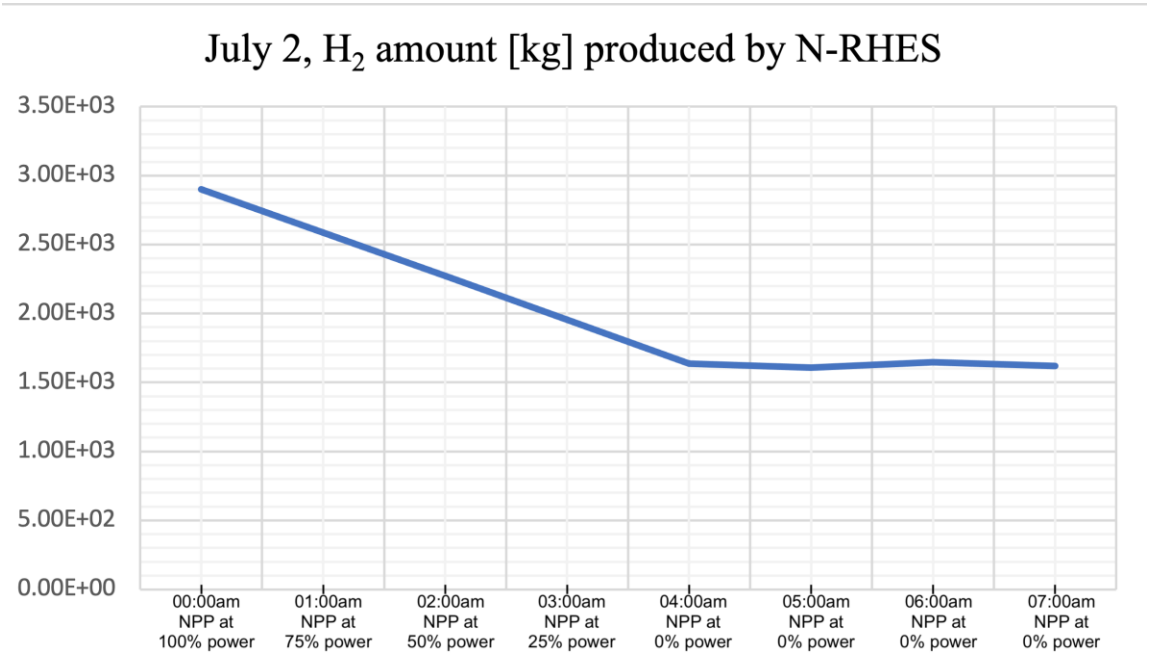


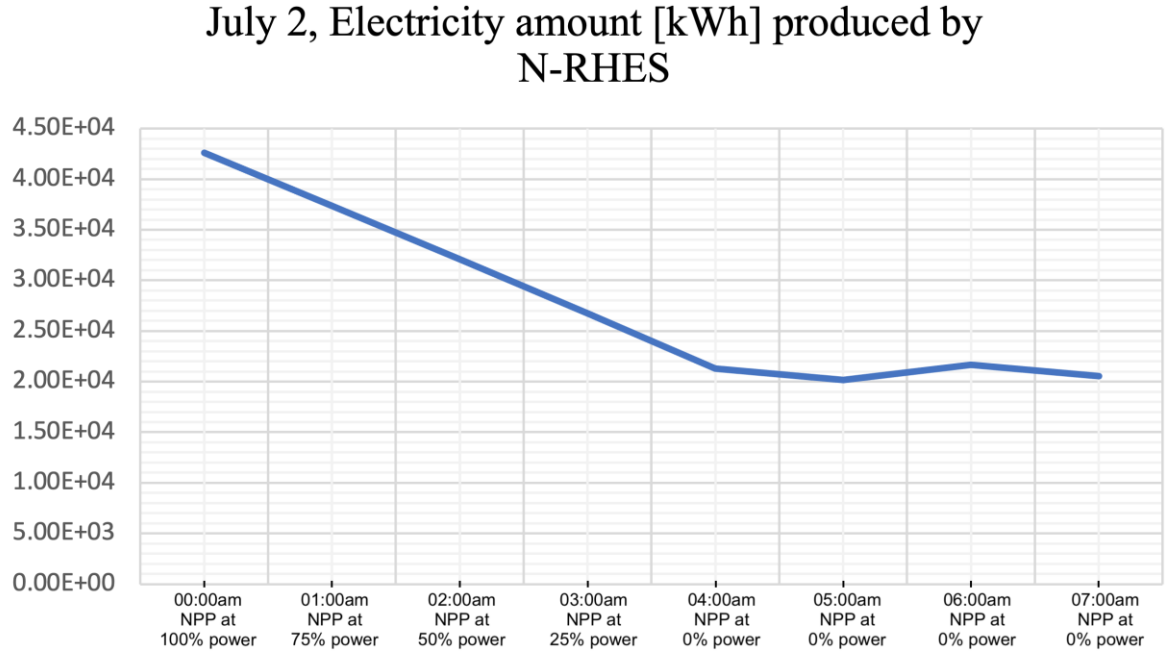


Hydrogen and Electricity productions amount while NPP power decreases from 100% to 0% in 4 hours.

# Conclusions

- If the electrical energy is not needed, N-RHES can produce hydrogen instead of producing electricity. Therefore, NPP can be performed always at maximum power.

- 8760 hourly based data is taken from SAM to written to an Excel file. Then, these are transferred to LabVIEW and MATLAB software to process, which is necessary to calculate hourly based results of hydrogen and electricity productions and optimization as well.

- N-RHES produces clean hydrogen via Cu-Cl thermochemical cycle which requires more heat energy than electrical energy. Which is more efficient due to the less energy conversion as there is less energy conversation from heat to electrical energy.

- When CSP requires electrical energy from the grid to keep its main cycle fluid (molten-salt) in a liquid form, the N-RHES is capable to meet the energy requirement of CSP via NPP.

- By using multi-objective optimization approach, **two objectives**, maximizing total profit and maximizing total heat equivalent, are optimized. According to objectives, better results are obtained and explained in this research.

# Conclusions

- Some scenarios results based on power percentages of NPP and CSP to produce hydrogen and/or electricity are pointed out to be able see hydrogen and electricity production amounts in different weather conditions.

- With Genetic Algorithm method on MATLAB the hybrid energy system is optimized in terms of total profit as an objective-1 and total heat equivalent as an objective-2 . **The reason why GAs are selected in this research is that GAs analyze the all population of solutions simultaneously and thus do not get stuck with the local best solutions.**

- Comparative results, non-optimized versus optimized, are shown. By applying multi-objective optimization to achieve preferred objective in this study.

- Finally, this N-RHES is considered in terms of safety-in-design. Important time slots after an event are given. Thus, after an event, hydrogen and electricity productions and how to meet NPP electricity demand via CSP or hydrogen powered electricity generators are pointed out in this thesis.

# Thank you for listening!

**Questions?**

OntarioTech
Energy Systems
& Nuclear Science

# References


*IEA, "The Future of Hydrogen," 2019. Accessed: Nov. 21, 2021. [Online]. Available: https://www.iea.org/reports/the-future-of-hydrogen.*

*M. Ciftcioglu, F. Genco, A. Tokuhiro, "Optimized Clean Hydrogen Production using Nuclear Small Modular Reactors and Renewable Energy Sources: a Review," Serial | Major Trends in Energy Policy and Nuclear Power, atw, Vol. 67, pp 16-30, 2022.*

*D. Popov and A. Borissova, "Innovative configuration of a hybrid nuclear-parabolic trough solar power plant," Int. J. Sustain. Energy, vol. 37, no. 7, pp. 616–639, 2018, doi: 10.1080/14786451.2017.1333509*

*R. Pinsky, P. Sabharwall, J. Hartvigsen, and J. O'Brien, "Comparative review of hydrogen production technologies for nuclear hybrid energy systems," Prog. Nucl. Energy, vol. 123, p. 103317, 2020, doi: 10.1016/j.pnucene.2020.103317.*

*Hydrogen Energy Systems, LLC [Internet]. 2022 Nov 1. Available from: https://heshydrogen.com/hydrogen-fuel-cost-vs-gasoline/.*

*S. Ali, "Regarding approximate electricity requirements in a nuclear generating station itself", private communication, November 2022.*

*Stern, A. G. (2018). A new sustainable hydrogen clean energy paradigm. International Journal of Hydrogen Energy, 43(9), 4244–4255. doi:10.1016/j.ijhydene.2017.12.180.*

# Total Heat Equivalent

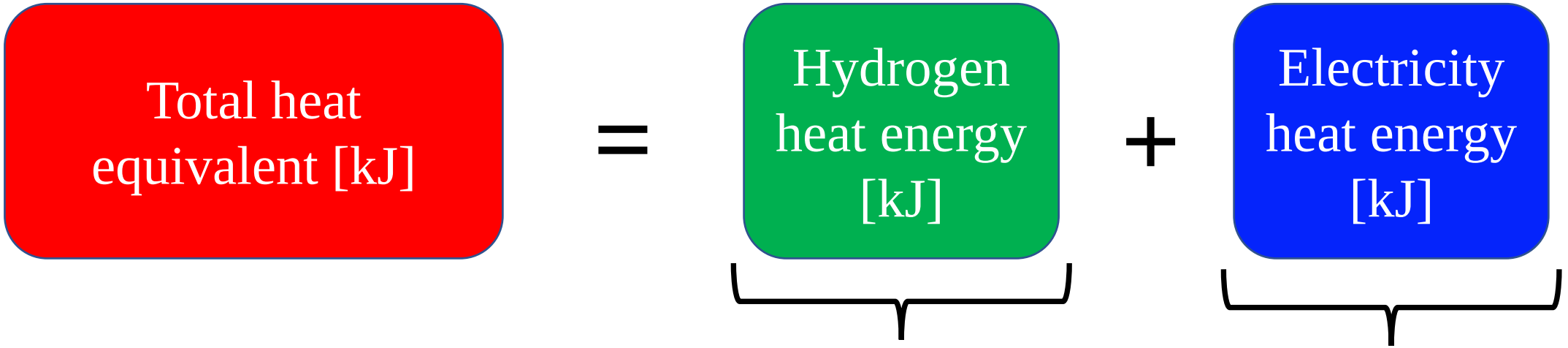


Total heat equivalent [kJ] = 120.1 $kJ_{th}$ / 1kg-$H_2$ + 1 $kJ_{th}$ / 1 $kJ_e$

# CSP Inputs

| Power Block Parameters | |
|---|---|
| Net electric power attributed to solar heat (kW) | 47922 |
| Turbine inlet pressure (Bar) | 100 |
| Condenser pressure (Bar) | 0.085 |
| Solar heat input required (kW) | 117685 |
| Solar heat to electricity efficiency (%) | 40.72 |
| **Thermal Energy Storage Parameters** | |
| Hours of storage (h) | 15 |
| Nominal storage capacity (MWh) | 1765.3 |
| Nominal storage tank discharge flow rate (kg/s) | 265.1 |
| Nominal hot tank temperature (°C) | 565 |
| Nominal cold tank temperature (°C) | 270 |
| Mass of stored fluid (tonne) | 14177 |
| Storage volume ($m^3$) | 8202 |
| Storage tank height (m) | 9.796 |
| Storage tank diameter (m) | 32.65 |
| **Solar Field Parameters** | |
| Field Configuration | Circular Surround |
| Design point DNI ($kW/m^2$) | 0.915 |
| Solar multiple | 2.5 |
| Solar heat generation required (kW) | 294220 |
| Overall corrected collector efficiency (%) | 56.49 |
| Field Incident thermal power (kW) | 520822.3 |
| Reflective area in solar field ($m^2$) | 569043 |
| Reflective area per heliostat ($m^2$) | 44.59 |
| Number of heliostats | 12760 |
| Tower structure height (m) | 136.1 |
| Tower inner diameter (m) | 11.22 |
| Receiver height (m) | 13.59 |
| Receiver diameter (m) | 10.2 |
| Receiver face area ($m^2$) | 435.5 |
| Distance from tower base to outermost mirror on North side (m) | 1021.1 |
| Distance from tower base to innermost mirrors | 102.1 |
| Heliostat field land area ($m^2$) | 2775818 |

| Location: Daggett Barstow, California | |
|---|---|
| Altitude | 586m |
| Latitude | 34.85 °N |
| Longitude | -116.8 °E |
| Time zone | GMT -8 |
| Annual DNI | 7.46 $kWh/(m^2.day)$ |
| Design point DNI | 0.915 $kW/m^2$ |

# System Advisor Model (SAM)

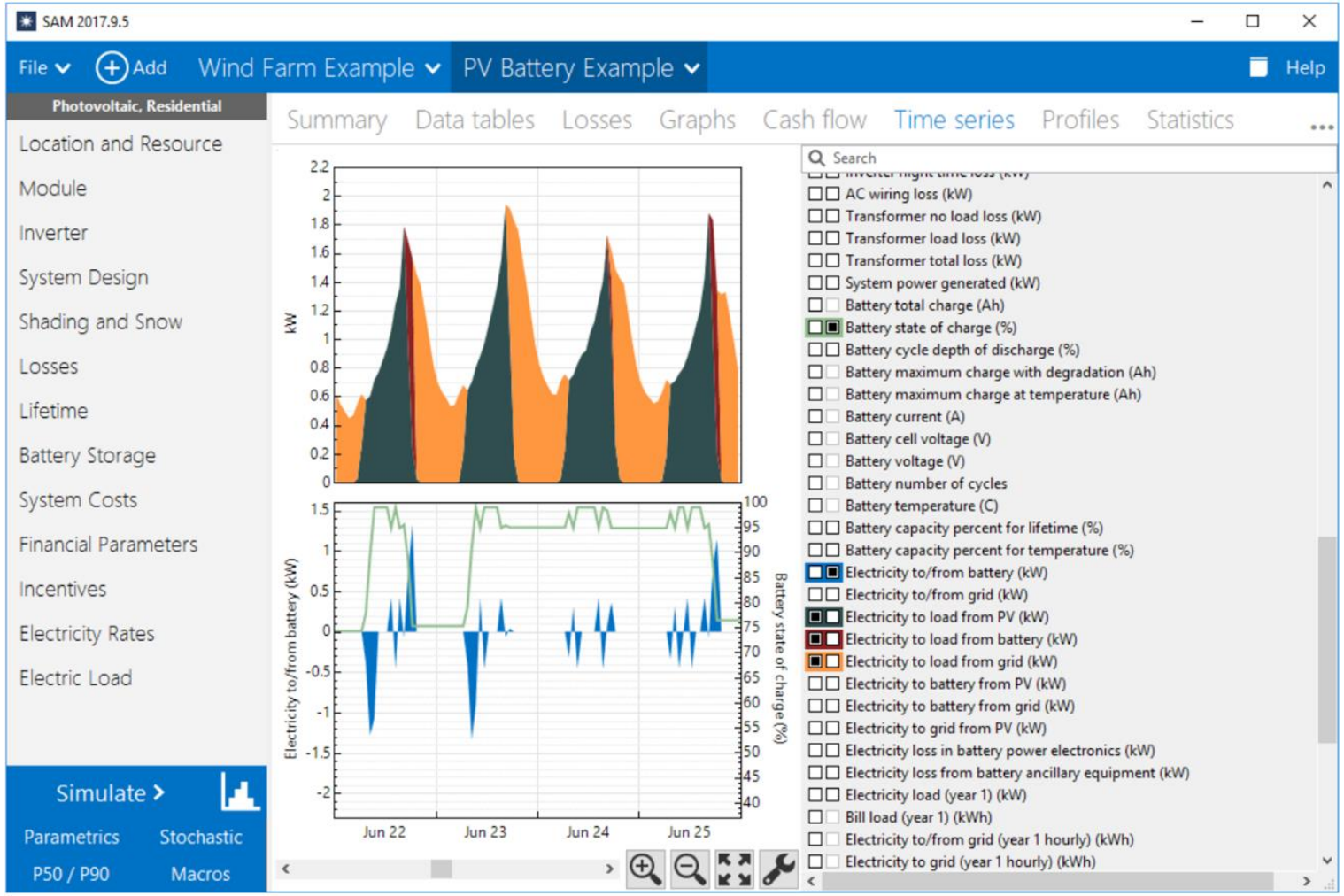

# SMRs for non-electric applications

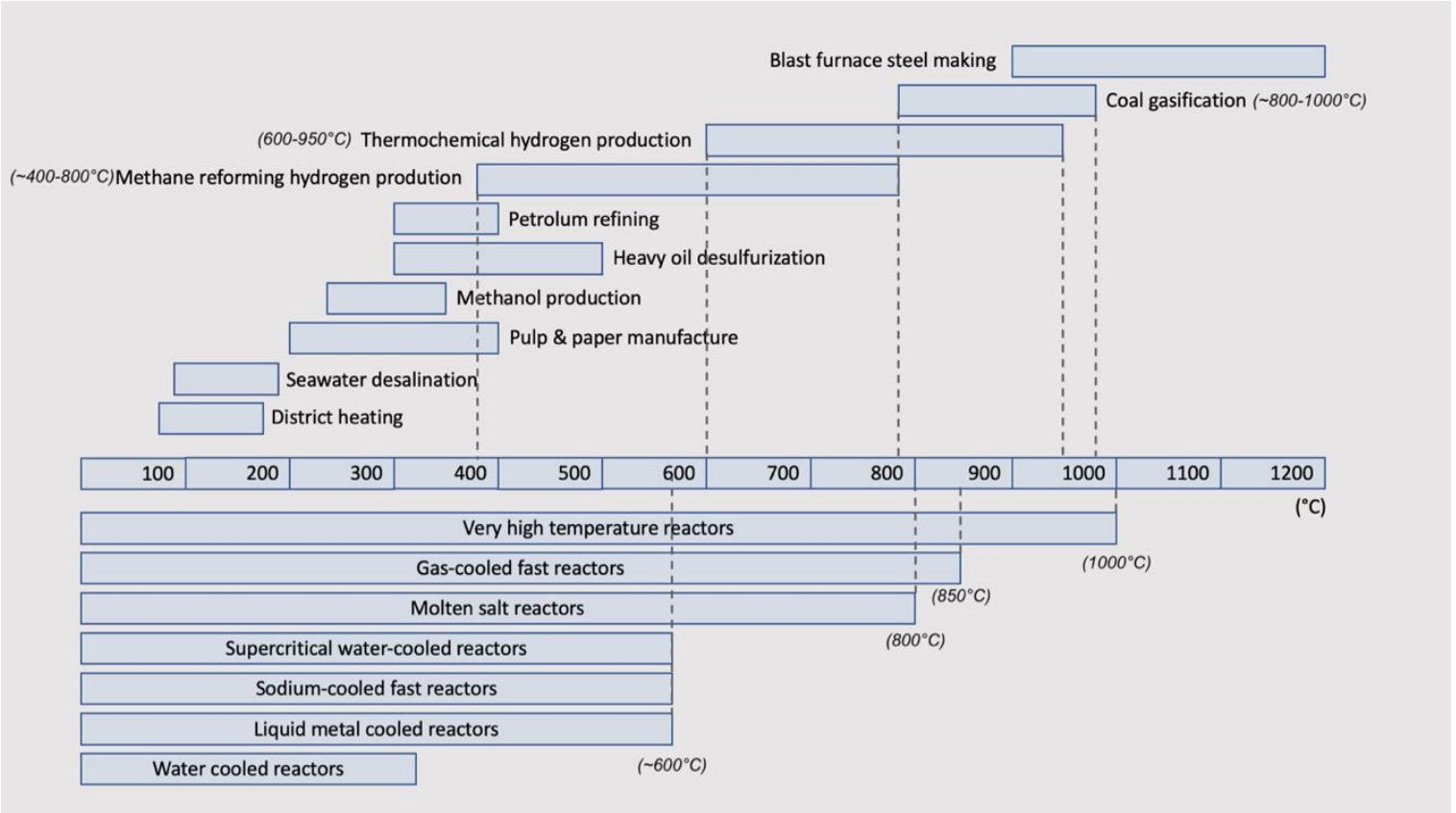

# Traditional Electrolysis

| Parameters | | Inputs (/kg $H_2$) | | Outputs (/kg $H_2$) | |
|---|---|---|---|---|---|
| $T_{max}$ (°C) | 60 | Electricity (MJ) | 180 | $H_2$ | 1 |
| Pressure (MPa) | 0.1 | Heat (MJ) | 26.2 | $O_2$ | 8 |
| TRL | 9 | Water (kg) | 11.5 | $CO_2$ | 0 |
| $H_2$ Yield eff. (HHV)** | 29.8 | | | Production cost* | $US 5.92 |
| *Production cost (est. $US 2019). | | | | | |
| **Assuming a power cycle conversion efficiency of 40%. (HHV: Higher heating value) | | | | | |

# Comparison of Cu-Cl, S-I, HTE

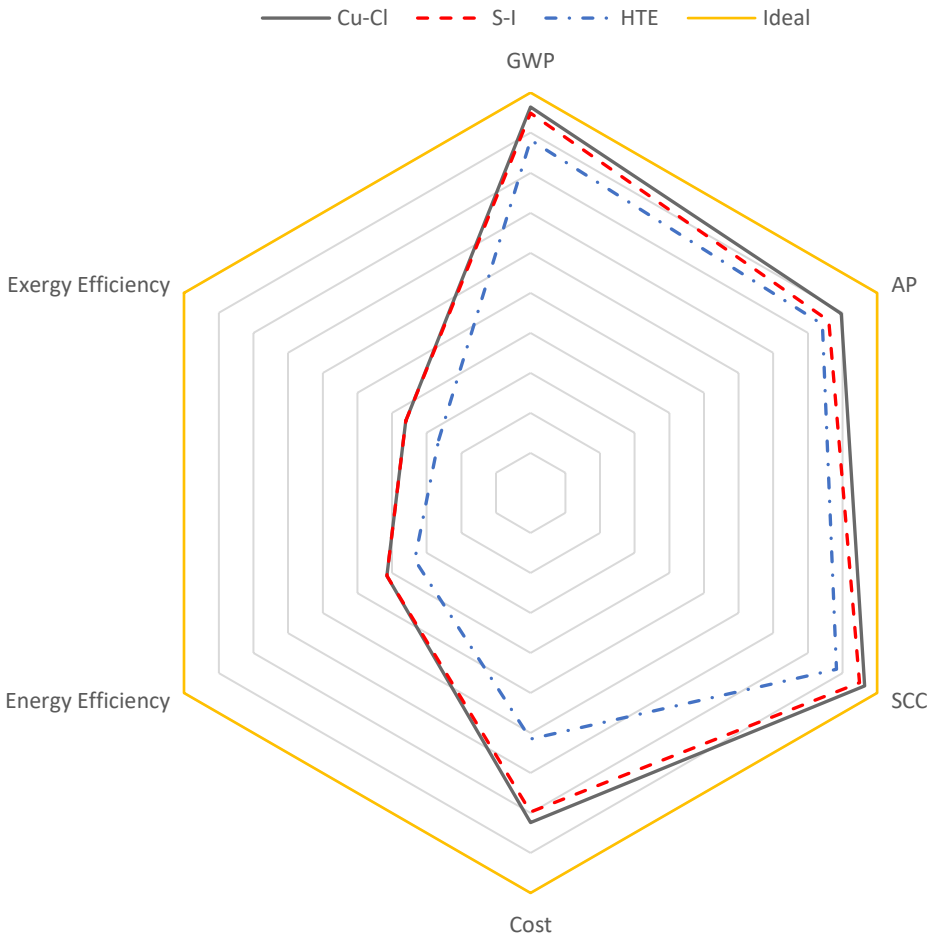

# TRL

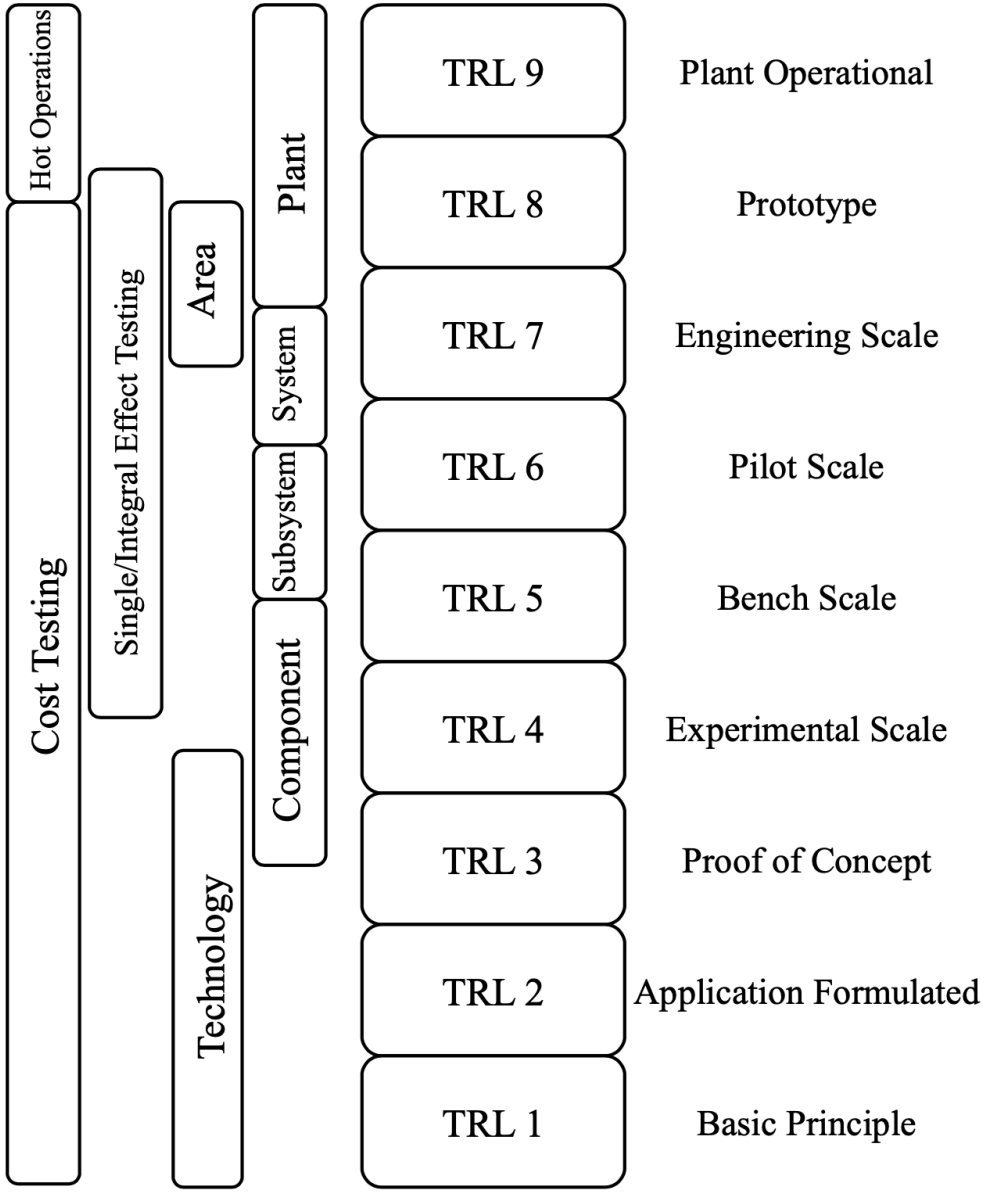
Hot Operations
Cost Testing
Single/Integral Effect Testing
Area
Technology
Plant
System
Subsystem
Component
TRL 9
Plant Operational
TRL 8
Prototype
TRL 7
Engineering Scale
TRL 6
Pilot Scale
TRL 5
Bench Scale
TRL 4
Experimental Scale
TRL 3
Proof of Concept
TRL 2
Application Formulated
TRL 1
Basic Principle

# TRL

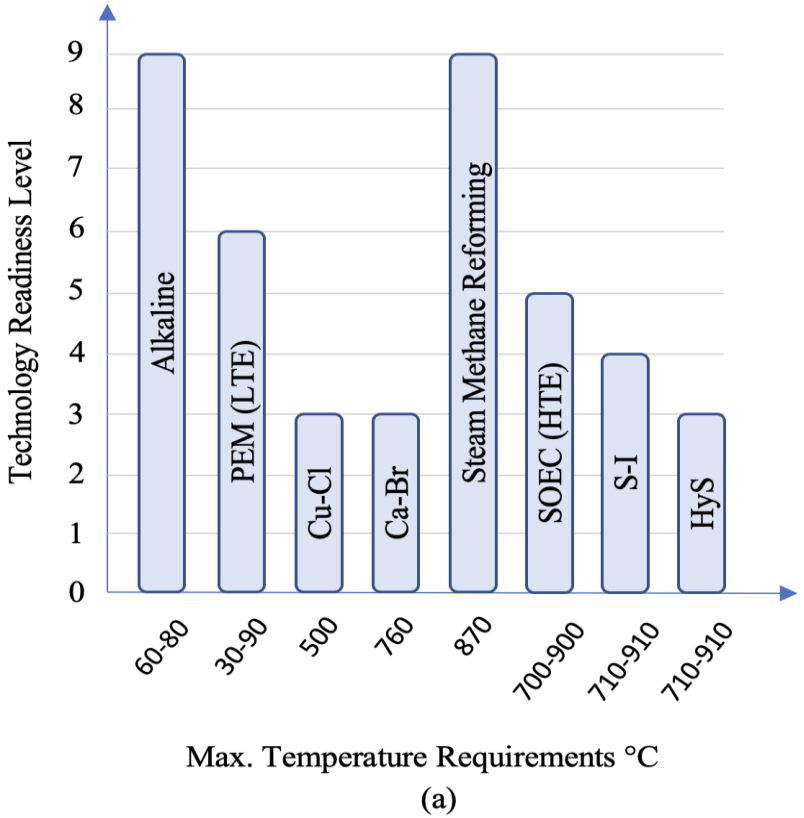
Technology Readiness Level
0
1
2
3
4
5
6
7
8
9
Alkaline
PEM (LTE)
Cu-Cl
Ca-Br
Steam Methane Reforming
SOEC (HTE)
S-I
HyS
60-80
30-90
500
760
870
700-900
710-910
710-910
Max. Temperature Requirements °C
(a)

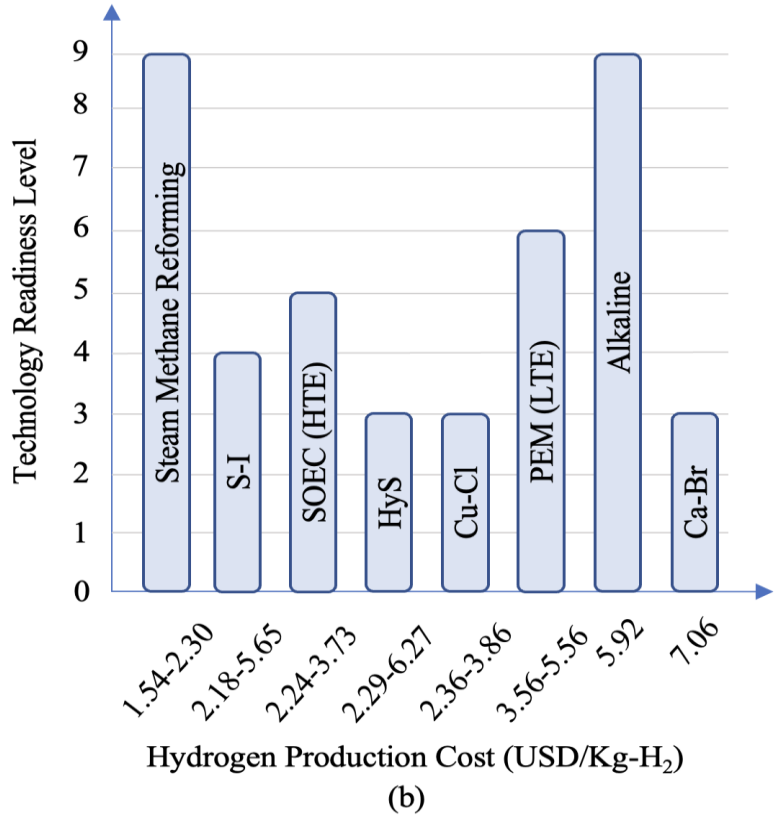
Technology Readiness Level
0
1
2
3
4
5
6
7
8
9
Steam Methane Reforming
S-I
SOEC (HTE)
HyS
Cu-Cl
PEM (LTE)
Alkaline
Ca-Br
1.54-2.30
2.18-5.65
2.24-3.73
2.29-6.27
2.36-3.86
3.56-5.56
5.92
7.06
Hydrogen Production Cost (USD/Kg-H2)
(b)

# Heat pump

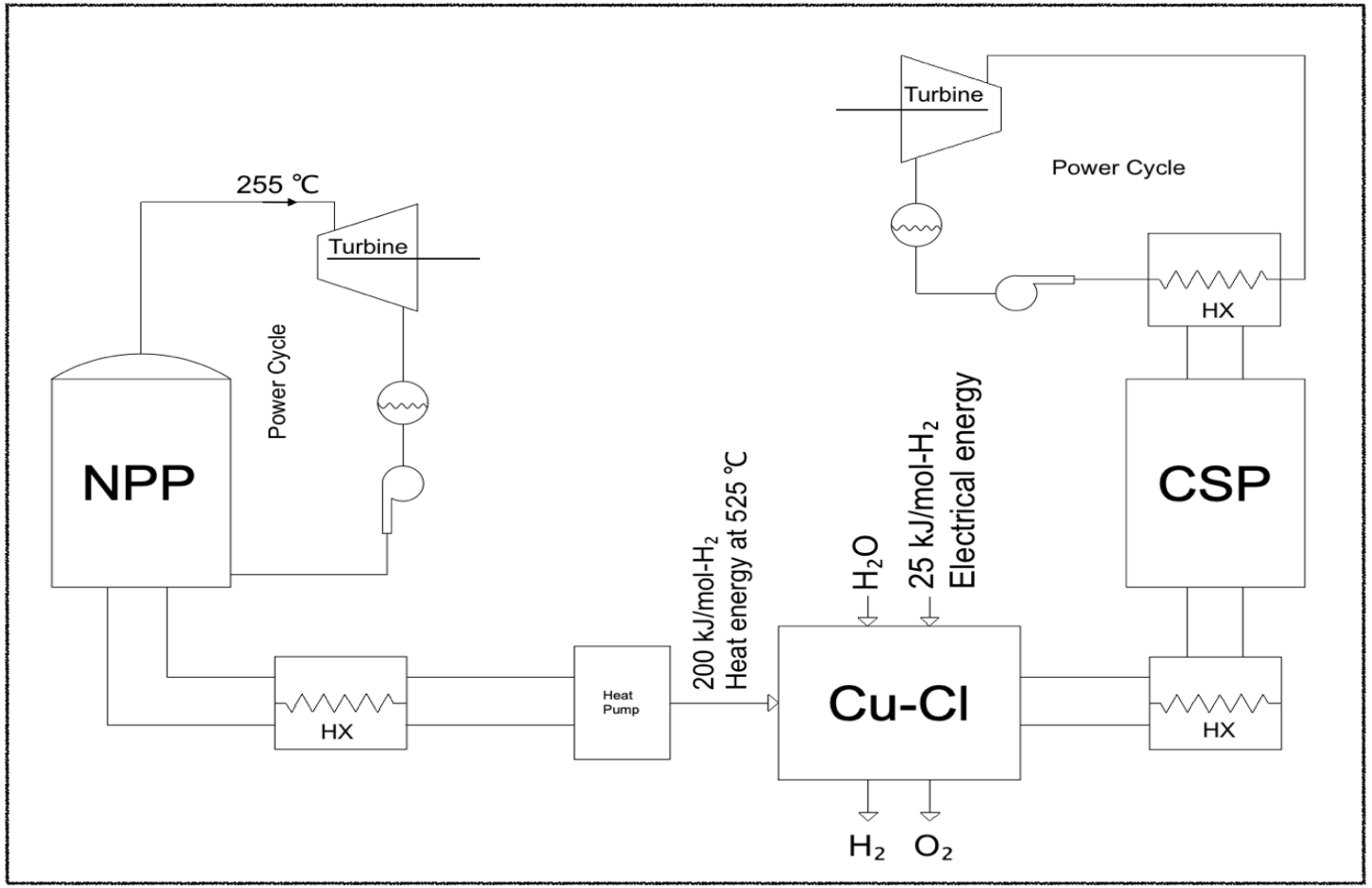


An **ideal reversible thermochemical** heat pump is utilized to raise the temperature of the fluid leaving the NPP, which is at 255°C, as the Cu-Cl cycle needs heat energy at a temperature of roughly 525°C. The reference heat pump calls **for 0.4235 kJ of heat energy to enhance the fluid's temperature by 1°C**. In this N-RHES, the needed heat energy for the pump is provided by the NPP. The reversible thermochemical heat pump does not require any electricity.

*El-Emam, R. S., Dincer, I., & Zamfirescu, C. (2019). Enhanced CANDU reactor with heat-upgrading hybrid chemical-mechanical heat pump for combined power and hydrogen production. International Journal of Hydrogen Energy. doi:10.1016/j.ijhydene.2019.06.181.*

# What I learned

- What exactly is the meaning of being academician.
- How to prepare a scientific paper.
- Courses
  - Neu-Fuzzy Method in Nuclear Applications
  - Nuclear Concepts
  - Nuclear Power Systems…
- Simulations and modelling of systems on MATLAB, LabVIEW.
- Multi-objective Optimization.
- How to think in a scientific way…

# Contribution to the literature

- Hydrogen production via NPP and CSP with Cu-Cl
- NPP and CSP electricity demands can be met each other
- Optimization, Multi-objective optimization
- Safety-in-design